State of California

California Natural Resources Agency

DEPARTMENT OF WATER RESOURCES

Methodology for Flow and Salinity Estimates in the Sacramento-San Joaquin Delta and Suisun Marsh

**35th Annual Progress Report to the
State Water Resources Control Board in
Accordance with Water Right Decisions 1484 and 1641**

June 2014

Edmund G. Brown Jr.

Governor

State of California

John Laird

Secretary for Natural Resources

California Natural Resources Agency

Mark W. Cowin

Director

Department of Water Resources

Foreword

This is the 35th annual progress report of the California Department of Water Resources' San Francisco Bay-Delta Evaluation Program, which is carried out by the Delta Modeling Section. This report is submitted annually by the section to the California State Water Resources Control Board pursuant to its Water Right Decision 1485, Term 9, which is still active pursuant to its Water Right Decision 1641, Term 8.

This report documents progress in the development and enhancement of the Bay-Delta Office's Delta Modeling Section's computer models and reports the latest findings of studies conducted as part of the program. This report was compiled under the direction of Tara Smith, program manager for the Bay-Delta Evaluation Program.

Online versions of previous annual progress reports are available at:

http://baydeltaoffice.water.ca.gov/modeling/deltamodeling/annualreports.cfm.

For more information contact:
Tara Smith
Chief, Delta Modeling Section,
Bay-Delta Office,
California Department of Water Resources
tara@water.ca.gov
(916) 653-9885

State of California
Edmund G. Brown Jr., Governor

California Natural Resources Agency
John Laird, Secretary for Natural Resources

Department of Water Resources
Mark W. Cowin, Director

Laura King Moon, Chief Deputy Director

Office of the Chief Counsel Cathy Crothers	Public Affairs Office Nancy Vogel, Ass't Dir.	Internal Audit Office Jeff Ingles
Office of Workforce Equality Stephanie Varrelman	Policy Advisor Waiman Yip	Legislative Affairs Office Kasey Schimke, Ass't Dir.

Deputy Directors

Vacant **Delta and Statewide Water Management**
Assistant to Deputy Director: J Gleim

Gary Bardini **Integrated Water Management**
Assistant to Deputy Director: C Brown; Assistant Deputy Director J Andrew

Carl Torgersen **State Water Project**
Assistant to Deputy Director: D Adachi, P Lecocq, and D Uding; Assistant Deputy Director: M Anderson

John Pacheco, acting **California Energy Resources Scheduling**

Kathie Kishaba **Business Operations**
Assistant to Deputy Director: J Cole

Bay Delta Office
Paul A. Marshall, Chief

Modeling Support Branch
Francis Chung, Chief

Delta Modeling Section
Tara Smith, Chief

Edited by:
Min Yu, Bay Delta Office
Ralph Finch, Bay Delta Office

Chapter 1 and Chapter 3 Authors
Lianwu Liu and **Prabhjot Sandhu**

Chapter 2 Author
Ralph Finch

Chapter 4 Authors
En-Ching Hsu, **Eli Ateljevich** and **Prabhjot Sandhu**

Chapter 5 Authors
Yu Zhou and **Bob Suits**

Chapter 6 Author
Tara Smith

Chapter 7 Authors
Eli Ateljevich, **Kijin Nam**, **Y. Joseph Zhang**, **Rueen-fang Wang**, and **Qiang Shu**

Editorial review, graphics, and report production
Under direction of Supervisor of Technical Publications Patricia Cornelius
Research Writers

Frank Keeley	Charlie Olivares	Carole Rains
William O'Daly	Jeff Woled	

Table of Contents

Figures

**Chapter 5.   Automation of Spatial Map with Temporal Data from DSM2-QUAL
                Output using ArcGIS**..**5-1**

Chapter 6.   Delta Modeling for Emergency Drought Barriers **6-1**

Tables

Preface

Chapter 1 Channel Volume Correction in DSM2-Qual Version 8.1

DSM2-Qual calculates volume of a channel by starting with the initial channel volumes read from the DSM2-Hydro tidefile at the beginning of a run , and then using flows from the Hydro tidefile to calculate the volume into or out of a channel at every time step. This calculation determines the water volume left in the channels (represented by parcels). The channel volumes at other time steps are available in the Hydro tidefile but not used.

This method would be accurate if water mass balances in channels are perfect. However, when there are water mass balance errors in Hydro, the errors will accumulate in Qual. In rare situations, the errors may accumulate significantly and stop Qual from running. This chapter describes a correction procedure that has been added to Qual and tested for accuracy.

Chapter 2 Quantitative Calibration of DSM2

For the first time in its use, DSM2, the 1D hydrodynamic and water quality simulation model of the Sacramento-San Joaquin Delta, is being calibrated in a quantitative manner with mathematically-based techniques. This chapter describes the background, motivation, goals, and status of the project, as well as preliminary findings.

Chapter 3 DSM2 Version 8.1 Time Step Sensitivity Test

This chapter gives the update on DSM2 version 8.1.2 time step sensitivity test results. The sensitivity tests are important because relatively small changes in time steps should not result in large changes in water quality results. If there are large differences in results due to differences in time step size, this reflects a problem in the model's ability to converge. Time steps for Hydro (the DSM2 hydrodynamic module), the tidefile (output from Hydro), and Qual (the DSM2 water quality module) have been tested. Sensitivity tests were done to evaluate the effects of different time steps on simulated EC. These results suggest DSM2 converges well. Time steps for the version 8.1 (v8.1) calibration were chosen based on these results.

Chapter 4 DSM2-GTM

DWR's Delta Modeling Section is developing a new DSM2 transport module, the General Transport Model (GTM). The mesh for GTM is fixed (Eulerian) rather than moving with flow (Lagrangian), and this should make it easier to interact with other models, georeferenced data and visualization as well as to couple to Hydro. It is also based on a more flexible software framework that is easier to adapt to new groupings of constituents -- mercury and sediment are of particular interest. The algorithm is a second order upwind solver developed in a prior collaboration with UC Davis with low numerical diffusion and an elaborate verification framework covering tough problems.

This chapter describes some of the practical issues of embedding such a model in a looped network or in a DSM2 grid with many intermediate junctions (nodes) along a single physical channel reach. We demonstrate the effect the DSM2-Qual schema can have on numerical diffusion, and make some preliminary comparisons with DSM2-Qual on advection problems in which GTM appears to be less diffusive in more complex flow fields or on more intricate grids.

Chapter 5 Automation of Spatial Map with Temporal Data from DSM2-QUAL Output using ArcGIS

This chapter presents a new post-processing tool for DSM2-QUAL output which enables generation of ArcGIS geo-referenced contour maps and time-varying animations to visualize water quality distributions in the Sacramento-San Joaquin Delta area.

Chapter 6 Delta Modeling for Emergency Drought Barriers

This chapter is a summary of work and documentation completed by several staff members from the Department of Water Resources' Bay-Delta Office and the Division of Operations and Maintenance. It summarizes the modeling processes used to determine the potential water quality and water supply impacts of Rock Barriers in Sutter Slough, Steamboat Slough, and False River.

Chapter 7 Bay-Delta SELFE Calibration Overview

The Delta Modeling Section and Virginia Institute of Marine Sciences are completing an initial calibration of the semi-implicit Eulerian-Lagrangian finite element (SELFE) 2-D/3-D model on the Bay-Delta domain. This chapter describes the project scope and the SELFE model and also gives some preliminary results representative of the forthcoming calibration document. SELFE is open source, uses a second-generation semi-implicit algorithm and has been used in a variety of cross-scale contexts on estuary problems around the world. Results for the Bay-Delta suggest the model is able to accurately reproduce the most important transport processes in this domain. Greater emphasis will now be placed on usability and applications, although the chapter also identifies areas of uncertainty or potential improvement.

Chapter 1.   Channel Volume Correction in DSM2-Qual Version 8.1

1.1 Introduction

DSM2-Qual (Qual) calculates the volume of a channel by starting with the initial channel volumes read from the DSM2-Hydro (Hydro) tidefile at the beginning of a run, and then using flows from the Hydro tidefile to calculate the volume into or out of a channel at every time step. This calculation determines the water volume left in the channels (represented by parcels). The channel volumes at other time steps are available in the Hydro tidefile but not used.

This method would be accurate if water mass balances in channels are perfect. However, when there are water mass balance errors in Hydro, the errors will accumulate in Qual. In rare situations the errors may accumulate significantly and stop Qual from running. This chapter describes a correction procedure that has been added to Qual and tested for accuracy.

1.2 Description and Testing Scenarios

The mass balance problem was encountered when a large tidally operated gate was added to a channel for a DSM2 study (i.e., a gate was added at Turner Cut near the San Joaquin River). Whenever the gate was opened, it caused flow fluctuations and mass balance errors in Hydro. When running Qual later, the error accumulated until the total parcel volume in channel 172 was 0. Qual stopped running with a "0 parcels in channel" message.

A correction procedure is added in Qual: after each time step, the total parcel volume in each channel is calculated using the channel's inflows and outflows, and comparing it to the channel volume found in the tidefile ($average\ channel\ cross\ sectional\ area \cdot channel\ length$). The volume difference is added to a parcel in the middle of the channel[1]. By handling it this way, the total parcel volume errors in channels will not accumulate, and volumes calculated by determining inflows and outflows to the channel will always be consistent with the channel volume in the tidefile. This will avoid the 0 parcel problem and ensure Qual to run without errors.

This modification was tested for accuracy. The following two setups were run from 1974 to 1984 (before a "0 parcels in channel" crash occurred) with both the original v8.1 and the modified v8.1 with channel volume corrections:

1. Original setup: original Turner Cut gate with 15 minute time step for Hydro. Flow fluctuates at channel 172 are shown in Figure 1-1 (blue line). Volume balances in some channels (including 172) are bad and cause the 0 parcel problem in channel 172.

---

[1] Originally the concentration of this parcel was also recalculated to conserve constituent mass, but we found it was not necessary, considering the changes in one time step are so small and the concentration recalculation may be problematic for nutrient models.

2. Refined setup: Turner Cut gate coefficients changed to 0.5 to remove flow fluctuations at channel 172 (red line in Figure1-1). Volume balance is much better. Flow in the channel is not restricted by the gate coefficient change.

Figure 1-1 Simulated Flow at Turner Cut Gate before (blue) and after (red) Coefficient Change
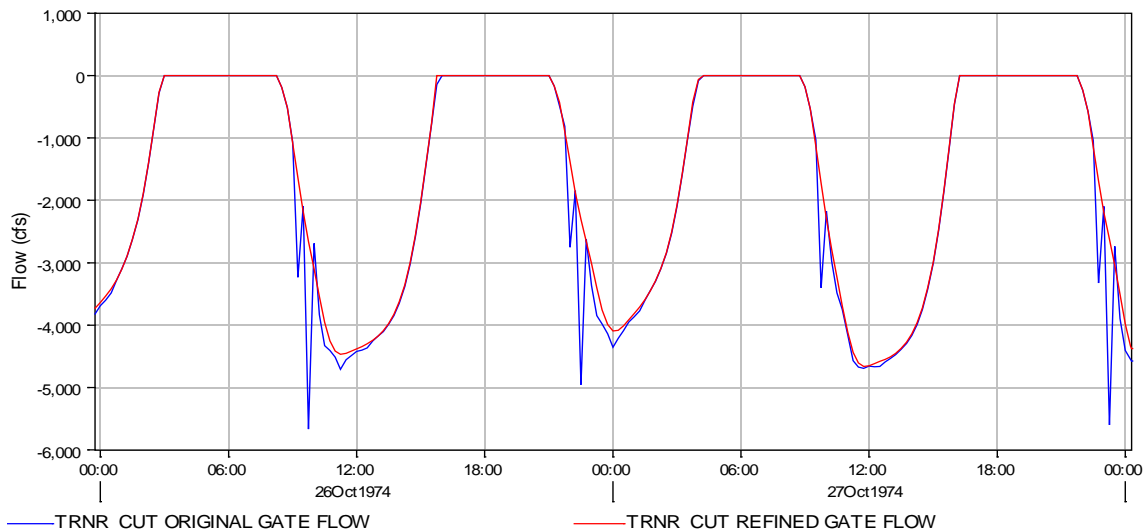
For all four runs, electrical conductivity (EC) results were practically identical at key stations: RSAC081, RSAN007, RSAN018, ROLD024, and Clifton Court Forebay. The maximum difference between using the original v8.1 and v8.1 with volume correction was 0.05% at ROLD024 (Figure 1-2 and 1-3) with the original gate setup.

Volumetric fingerprinting[2] results are shown in Figures 1-4 and 1-5. With the original gate setup, the volume correction tended to make the volumetric fingerprinting slightly worse (i.e., the error was less than 0.01% as shown in Figure 1-4). The reason for such an error is because the volume correction is artificially adding (or removing) a small amount of water into a channel, which is not counted as an initial boundary condition. This additional amount of water would be spread out to other channels with time and cause some error in the volumetric fingerprinting. However, this error is quite negligible in this case.

With gate coefficients changed to 0.5, most flow fluctuations were eliminated and the mass balance was much improved. The volume correction did not cause any difference in volumetric fingerprinting results (see red and green lines overlapping in Figure 1-5). Also, we noticed in this figure that sometimes the total volume deviates from 100%. This is due to the fact that a very small amount of water is from the water originally in the Delta.

---

[2] Fingerprinting is a methodology for running DSM2 to determine sources of water or constituents at specified locations. Volumetric fingerprinting determines the portion of the volume of water contributed from each source at a specified location and time.

Figure 1-2 Simulated EC at Old River at Bacon Island (ROLD024)

——ROLD024 ORIGINAL SETUP BY V8.1 EC
——ROLD024 ORIGINAL SETUP BY V8.1 WITH CHANNEL VOL CORRECTION EC
——ROLD024 REFINED SETUP BY V8.1 EC
——ROLD024 REFINED SETUP BY V8.1 WITH CHANNEL VOL CORRECTION EC
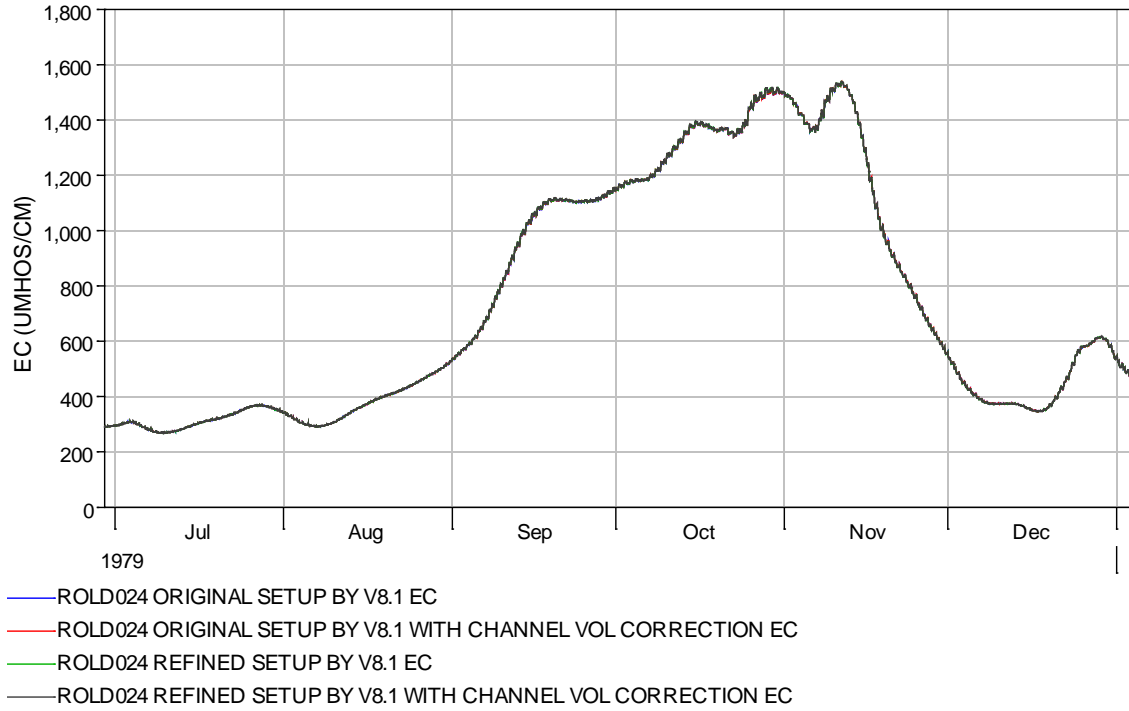
Figure 1-3 Regression Analysis of Simulated EC at Old River at Bacon Island (ROLD024)

$y = 1.0005x$
$R^2 = 1$

○ ROLD024 EC
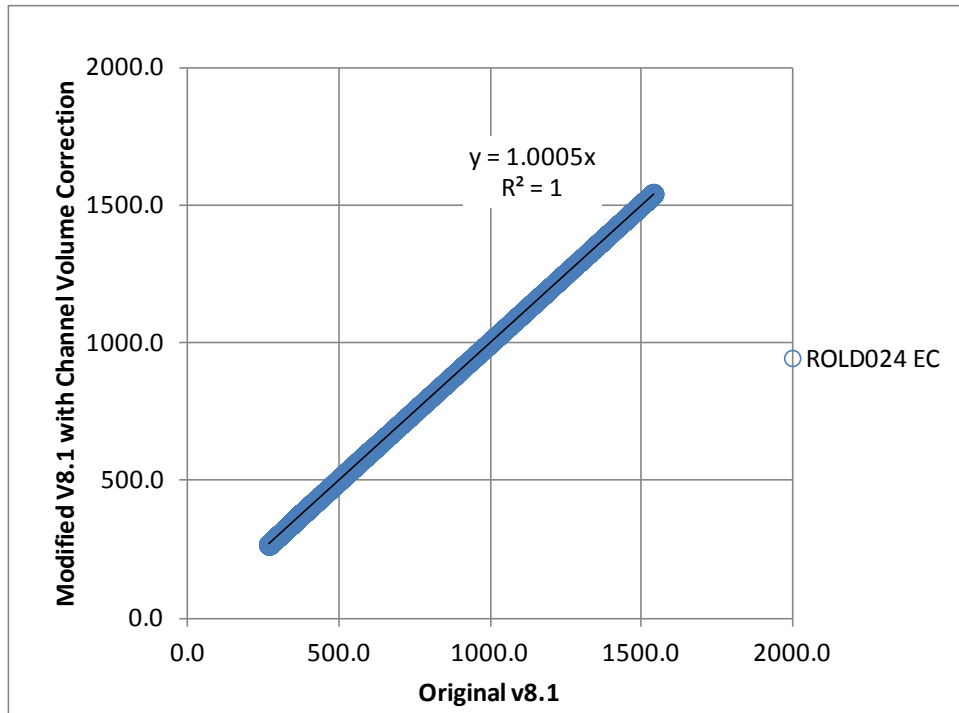
Figure 1-4 Volumetric Fingerprinting at Clifton Court Forebay with Original Setup

— CLIFTON_COURT ORIGINAL SETUP BY V8.0.4 UNIT
— CLIFTON_COURT ORIGINAL SETUP BY V8.1 UNIT
— CLIFTON_COURT ORIGINAL SETUP BY V8.1 WITH CHANNEL VOL CORRECTION UNIT
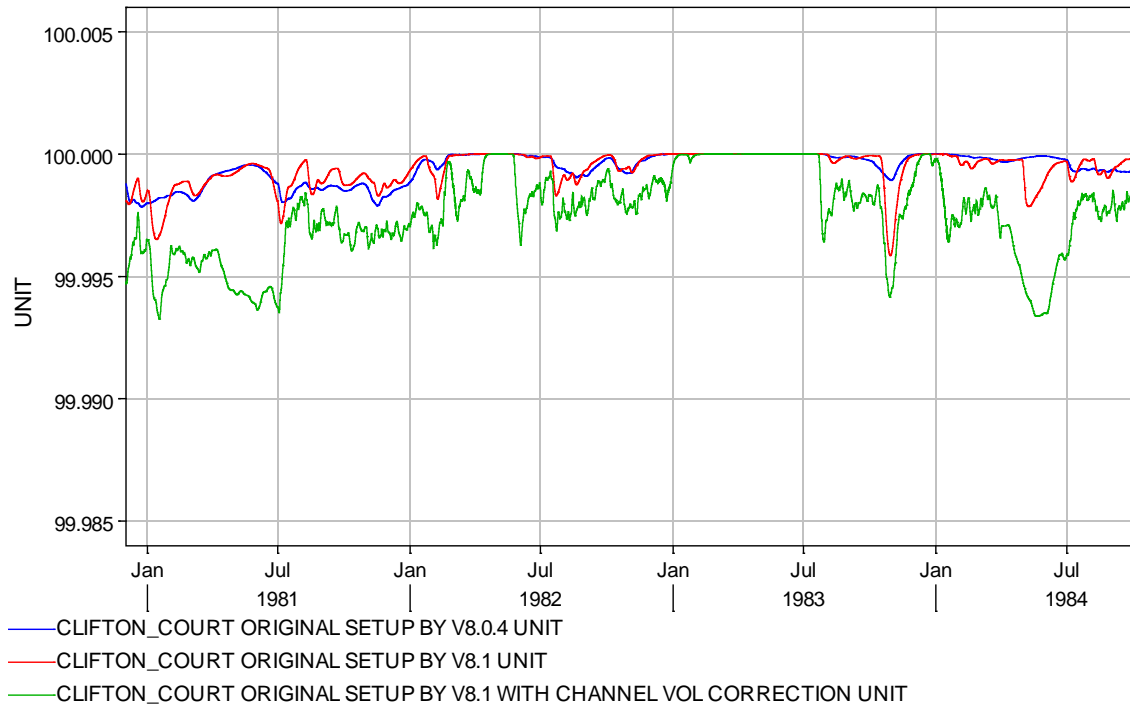
Figure 1-5 Volumetric Fingerprinting at Clifton Court Forebay with Gate Coefficients 0.5

— CLIFTON_COURT REFINED SETUP BY V8.0.4 UNIT
— CLIFTON_COURT REFINED SETUP BY V8.1 UNIT
— CLIFTON_COURT REFINED SETUP BY V8.1 WITH CHANNEL VOL CORRECTION UNIT
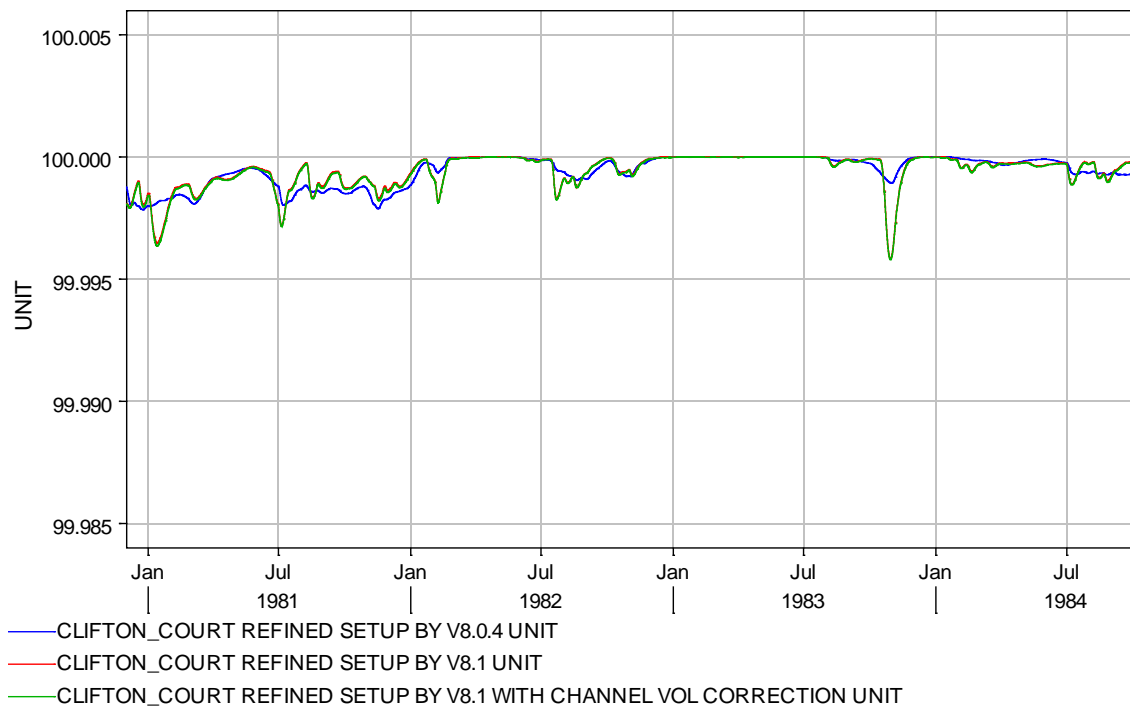
1.3 Summary

A channel volume correction procedure has been added in v8.1. EC results were practically identical for all the runs. While large fluctuating flows occurred with the original gate setup, the volume correction has kept Qual running with some negligible error in volumetric fingerprinting runs. Under the refined setup, the simulated flows were much better and there was no difference in volumetric fingerprinting results.

A new message alert was added to warn users for accumulated volume balance errors at the end of a Qual run. Detailed channel volume balance errors for each channel are listed in the end of the output file (*.qof). By setting the value of `checkdata` to `True`, Qual will check the channel volume balance before making the full run.

Chapter 2.   Quantitative Calibration of DSM2

2.1 Summary

For the first time in its use, DSM2, the 1D hydrodynamic and water quality simulation model of the Sacramento-San Joaquin Delta, is being calibrated in a quantitative manner with mathematically-based techniques. This chapter describes the background, motivation, goals, and status of the project, as well as preliminary findings.

2.2 Background

Calibration, as used with physically-based numerical models, is the process of comparing model output with observed data; changing appropriate parameters in the model; running the model with the new parameter values and comparing again; and repeating until the discrepancy between observed and computed data is considered acceptable and the model "calibrated."

In the past, Delta models, including DSM2, have been calibrated with traditional methods, using only channel friction (Manning's N) values and dispersion coefficients as calibration parameters. (Liu & Sandhu, 2012). The traditional approach implicitly assumes that other inputs are either perfect (and therefore their values should not change), or that adding more parameters would render an already complex process nearly impossible to perform by hand.

The traditional approach also assumes, in the case of DSM2, that each channel's calibration parameter (friction or dispersion coefficient) is independent of other channels. This leads to an ill-posed system which is simplified by ad hoc grouping of parameters (all friction parameters of channels in a group are adjusted by the same value or percent). The comparison-adjustment cycle is usually done manually, perhaps using automatically prepared graphs of observed and computed values, which is time-consuming and subjective.

Poor data resulting in uncertain modeling of Delta agricultural diversions and drainage remains as a problem and certainly affects our ability to develop a calibrated model. Until considerably more accurate estimates are available (unlikely in the near future for drainage flows and qualities), they are legitimate candidates for calibration parameters. However, to add these to a traditional manual calibration would overburden an already difficult process.

2.3 Motivation

The traditional calibration process, using little automation, is lengthy, labor-intensive, and subjective. It is not repeatable: two independent people or groups performing a calibration of the same model with the

same observed data will surely arrive at fairly different parameter values. And the traditional process is not quantifiable: there are no practical ways of calculating and comparing parameter sensitivity and robustness of the final parameter value set; we do not know how good the "final" calibration really is, and there are no estimates of error ranges in the production model.

A mathematically-based calibration, on the other hand, reduces or eliminates the shortcomings of the traditional calibration. Adding more calibration parameters candidates to the process results only in longer computer time, not greater conceptual difficulty, as with a manual calibration. Its big disadvantage is the requirement to make far more model runs than in the traditional method. But since the runs can be made in parallel, with a network of fast multi-core desktop computers (which the Delta Modeling Section possesses), this potential disadvantage does not exist. It is not only desirable but now entirely practical to abandon the traditional approach to calibration of DSM2 and adopt a modern procedure.

2.4 Goals

We have several goals with this project:
- To test the chosen software, described below, to see if it is ready, or can be made ready, to run with DSM2 and its input/output files.
- To develop pre- and post-processors at DWR to streamline and automate the process of preparing input files necessary for the chosen calibration software.
- To examine the sensitivity of various parameters, including non-traditional parameters, on DSM2 output.
- To calibrate DSM2 with only channel Manning's N and dispersion coefficients as parameters and compare with a traditional (manual) calibration to see what improvement, if any, a quantitative calibration can offer over a manual calibration.
- To calibrate DSM2 with new bathymetry, new estimates for Delta consumptive use, and additional calibration parameters such as agricultural drainage flows and water qualities, for use as a production calibration for DSM2 studies.

2.5 PEST Overview

The parameter estimation (PEST) software package (S.S. Papadopulos & Associates, 2014) was chosen to calibrate DSM2 after a lengthy search through academic literature and the Internet. Coincidently it has already been used in the Modeling Support Branch to calibrate the Integrated Water Flow Model groundwater model.

The best description of PEST comes from its manual (Doherty, 2010):

> *The purpose of PEST…is to assist in data interpretation, model calibration and predictive analysis. Where model parameters and/or excitations need to be adjusted until model-generated numbers fit a set of observations as closely as possible…PEST should be able to do the job. PEST will adjust model parameters and/or excitations until the fit between model outputs and laboratory or field observations is optimized in the weighted least squares sense. Where parameter values inferred through this process are nonunique, PEST will analyze the repercussions of this nonuniqueness on predictions made by the model…a model*

does not have to be recast as a subroutine and recompiled before it can be used within a parameter estimation process.

Several compelling features of PEST are noted:
- Mature methodology and software. The methods used are described in peer-reviewed literature as well as readily available "gray literature," that is, institutional documents such as USGS reports. The software has been used for years, it is actively supported and is continuously updated.
- The method includes regularization (Doherty, 2010):
  - *In its broadest sense, "regularization" is a term used to describe the process whereby a large number of parameters can be simultaneously estimated without incurring the numerical instability that normally accompanies parameter nonuniqueness. Numerical stability is normally achieved through the provision of "supplementary information" to the parameter estimation process. Such supplementary information" often takes the form of preferred values for parameters, or for relationships between parameters.*
- In other words, PEST can be easily set up to eliminate unimportant parameters and not allow the remaining parameter values to zoom off to extreme limits.
- In predictive analysis mode, PEST will estimate the error involved in the accepted calibration. Thus, for the first time, we should be able to estimate error limits in studies using DSM2.

2.6 Connection to DSM2

PEST must be able to start the forward model in batch (unattended) mode, read all the model output as text files, and adjust parameters and create new text input files for the model. DSM2 is nearly ideal for these broad requirements, with the exception of its output, which is in the form of HEC-DSS files. To deal with the DSS-text file issue, its post-processor is used immediately after every DSM2 run, to convert the necessary DSS model timeseries to text files (described below).

The individual DSM2 (Hydro and Qual) runs are typically one year in length, which takes only a few minutes to process on a modern desktop computer. However, because hundreds or thousands of runs are done for a single calibration run, it is necessary to parallelize the runs, that is, run them simultaneously. We use HTCondor (University of Wisconsin-Madison, 2014), developed and maintained by the University of Wisconsin, to conveniently queue, run, and manage several dozen simultaneous runs on the network of multi-core desktop machines in the Delta Modeling Section.

The creation of the several input files and scripts necessary to run DSM2 under HTCondor and PEST was automated. The principle script file, PEST_Create_Files.py, is written in Python and creates several other files (Figure 2-1).

Figure 2-1 **Initialization Files Block Diagram**

PEST Files

DSM2.pst control file and PEST template files.

DSM2_run4Genie.bat

Windows batch file that creates runtime directory, copies DSM2 input files, finalizes HTCondor submit file; starts PEST executables and HTCondor slaves.

PEST_Create_Files.py

User sets basic calibration variables; creates PEST, runtime, and HTCondor files.

dsm2run.bat

Windows batch file that is run by PEST and in turn runs a pre-processor; DSM2 Hydro and Qual in desired time period; traps runtime errors; runs post-processor.

PEST_pre_DSM2Run.py

Pre-processor before DSM2 runs to update DSM2 parameter values from PEST coefficient files.

PEST_post_DSM2Run.py

Writes DSM2 DSS output to text file; creates necessary PEST instruction files.

Once PEST_Create_Files.py is run, a calibration run is started by running the Windows batch file DSM2_run4Genie.bat. This creates a unique directory for the calibration run, copies DSM2 executables and input files and modifies the appropriate files for the calibration, finalizes the HTCondor submit file, and starts the Genie runtime manager, the PEST program, and a few dozen batch programs under HTCondor which run pre- and post-processors for DSM2 and the DSM2 programs Hydro and Qual (Figure 2-2).

Figure 2-2 Calibration Preparation and Start Block Diagram

DSM2_run4Genie.bat

Windows batch file that creates runtime directory, copies DSM2 input files, finalizes HTCondor submit file; starts PEST executables and HTCondor slaves.

Runtime Directory

Directory contains all necessary DSM2 files modified for particular calibration run under HTCondor.

HTCondor Submit File

The final submit file for running all DSM2 parameter runs under HTCondor on the Delta Modeling Section's networked computers.

An actual calibration process (Figure 2-3) consists of:
- Genie, the PEST++ run manager, which communicates between PEST++ and the many PEST++ slave jobs running on multiple-core desktop computers under HTCondor on the local network;
- PEST++, which implements the mathematical theory behind the PEST concept and controls the numerical calibration procedure;
- dsm2run.bat, which runs a pre-processor, DSM2 Hydro and Qual, and a post-processor, and traps runtime errors. If desired, errors can simply trigger the return of DSM2 baserun results, which causes PEST to think that particular parameter value does not affect DSM2 results. Otherwise, an error fails the calibration run.

Figure 2-3 Calibration Run Block Diagram

Calibration Run Process

- Submit many dsm2run.bat jobs to HTCondor.
- Start Genie (PEST run manager) in new console window.
- Start PEST++ (PEST main program) in new console window.

dsm2run.bat
(run on multiple cores/machines)

- Run PEST_pre_DSM2Run.py to prepare DICU and channel cross-section parameters.
- Run Hydro and Qual, catch errors and either fail run or return base results.
- Run PEST_post_DSM2Run.py to copy DSM2 output from DSS file to text file.

2.7 Traditional and Non-Traditional Potential Parameters

In past calibrations of DSM2 and other Delta models, only channel roughness (Manning's N value) and dispersion coefficients have been adjusted to improve model output fit to observed data. However, all inputs have some unknown error associated with them so all inputs should be candidates for calibration. Using an automated calibration procedure lets us add additional parameters with little extra effort, and the quantitative nature of the PEST procedure allows us to compare all parameter groups easily for their sensitivity, that is, their effect on improvement of calibration fit.

Therefore, in addition to Manning's N and dispersion coefficient values, we are also including:
- DICU (Delta Island Consumptive Use) diversion flows, return drainage flows, and return flow water quality;
- Reservoir and gate flow coefficients;
- Channel bathymetry, in the form of changes to either cross-sectional layer width or elevation, which in turn affects area and hydraulic radius;
- Channel lengths.

The last potential parameter may seem uncalled for. It is fairly easy to accurately measure the actual streamflow length for each DSM2 channel using ArcMap or other geo-referenced tools. However, a few channels in DSM2 represent complex braided channels in the real Delta. Figure 2-4 shows an example, where the green channel is a line representation of DSM2 channel 313; the dark blue line is a nominal channel centerline, which length will be used by DSM2; and the pale blue lines the map representation of the actual Delta channels. These complex channels may benefit from the use of an adjusted channel length.

Figure 2-4 DSM2 Channel 313

2.8 Status and Preliminary Findings

As of this writing, we have confirmed that DSM2 is a suitable candidate for calibration using PEST. Nearly all of the setup is automated with Python and Windows Batch programs[3], and some analysis is automated with Gawk programs to read and reformat PEST output to a style convenient for Excel and ArcMap. Statistical analysis is performed by the contractor using R programs.

To simplify the initial calibration we are not formally introducing new parameters yet (though they have all been tested), nor has new bathymetry or DICU replacements been used. Instead, we are calibrating only with Manning's N and dispersion coefficients in each channel, with existing bathymetry and DICU values. In addition to being a simple initial case, this will let us compare the quantitative calibration with the traditional manual calibration.

So far we have made the following informal findings:
- Manning's N is the dominant parameter. DSM2 output is much more sensitive to Manning's than to dispersion coefficients, agricultural diversions and drainages, and most channel bathymetry changes.
- It is easy to gain significant improvement in the RMS error using only Manning's N during the calibration period (summer 2009). However, using the modified parameters in the validation period (summer 2002) shows only slight improvement. We speculate this could be
  - the calibration and validation periods are too far apart, reflecting changes to the Delta, or
  - the calibration is calibrating to noise in the observed data which is different or absent in the validation period.
  - We expect to resolve this in future work.
- It is desirable to highly automate the entire process, as it then becomes almost trivial to try different numerical experiments. Incremental computing power comes at essentially zero cost so a highly automated process reduces elapsed time to only the parallel running time of DSM2.

2.9 Sensitivity Maps

We find it desirable to display several items of information in a dynamic map of the Delta. ArcMap, an ESRI GIS product, was used for this.

Figure 2-5 shows an example sensitivity map of Manning's N values in channels in the western Delta. Lighter green indicates less sensitive, darker green, more sensitive. In other words, a dark green channel's Manning's N value is a more powerful calibration "knob" than a light green channel. Circles (solid or rings) mark observation stations that are not used in the calibration; Pushpins indicate stations which have data that are used.

It is interesting to note some general patterns. Most Montezuma Slough channels are moderately sensitive except for channel 515. Other Suisun Marsh channels have little effect on Delta output. Channels which represent bays and are "dead ends" (e.g. channels 572, 573, 574, and 575) are less important than channels in the main river and that convey flow.

---

[3] To be sure, the various scripts comprising the automation should be rewritten to modern programming standards.

Further inland (Figure 2-6) we see similar sensitivity among channels with little variance from channel to channel. In this map we have placed DSM2 agricultural nodes, colored according to their sensitivity to DICU diversion flow: pink is relatively insensitive, red is relatively sensitive. Here we see some groups forming. For instance, a few nodes in Old River and the South Delta show high sensitivity, and one node adjacent to Discovery Bay (198) shows very high sensitivity compared to its neighbors.

Another way of viewing calibration parameters is showing their final value compared to their starting value. Figure 2-7 is similar to Figure 2-6 except the nodes are now colored according to their final calibration adjustment coefficient for diversion flows. This adjustment coefficient ranges from about 0.5 (bright red), indicating half the pre-calibration diversion flow, to about 1.5 (bright green), indicating 50% more diversion flow. This gives us a direction to the sensitivity—whether a particular parameter is adjusting up or down from its initial value. PEST has just been modified to incorporate both sensitivity and direction in a single value, so future displays will require only one map to show both types of information.

Figure 2-5 West Delta Sensitivity Map
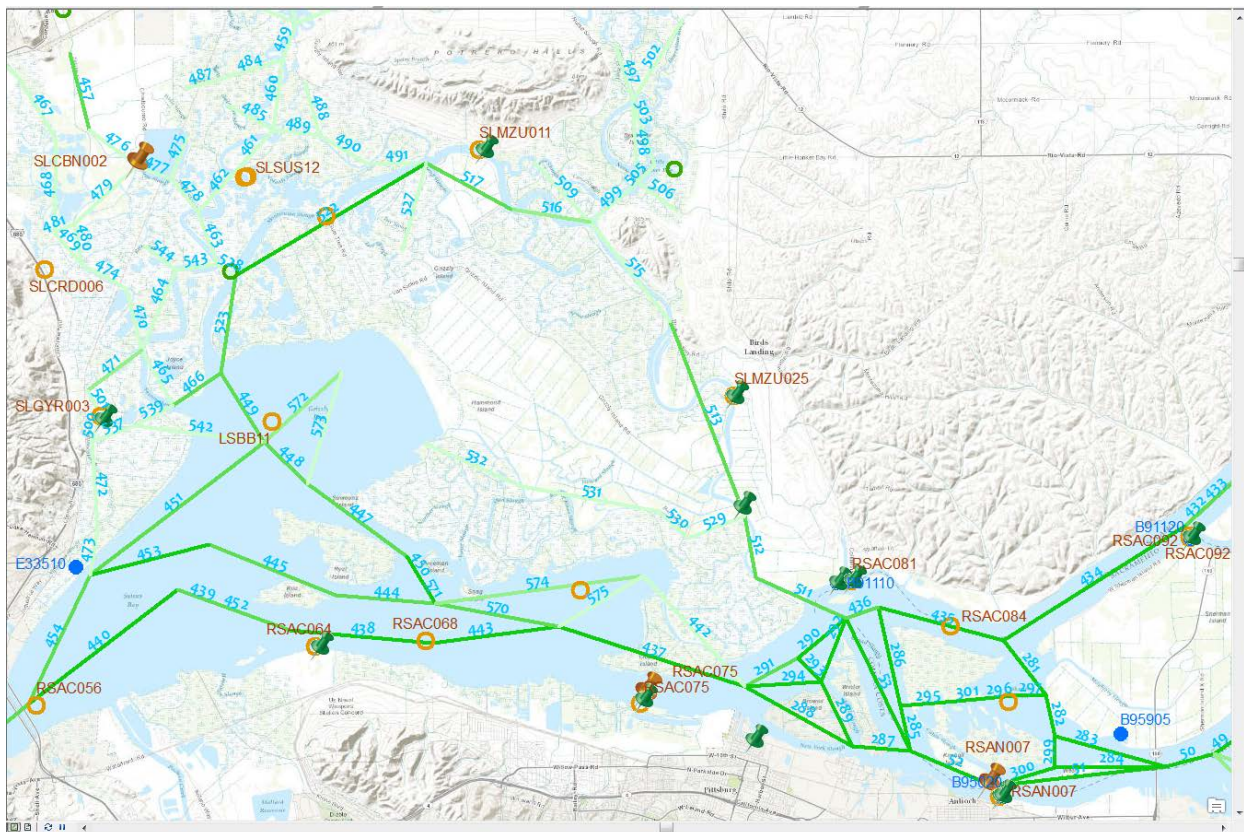
Figure 2-6 South Delta Sensitivity Map
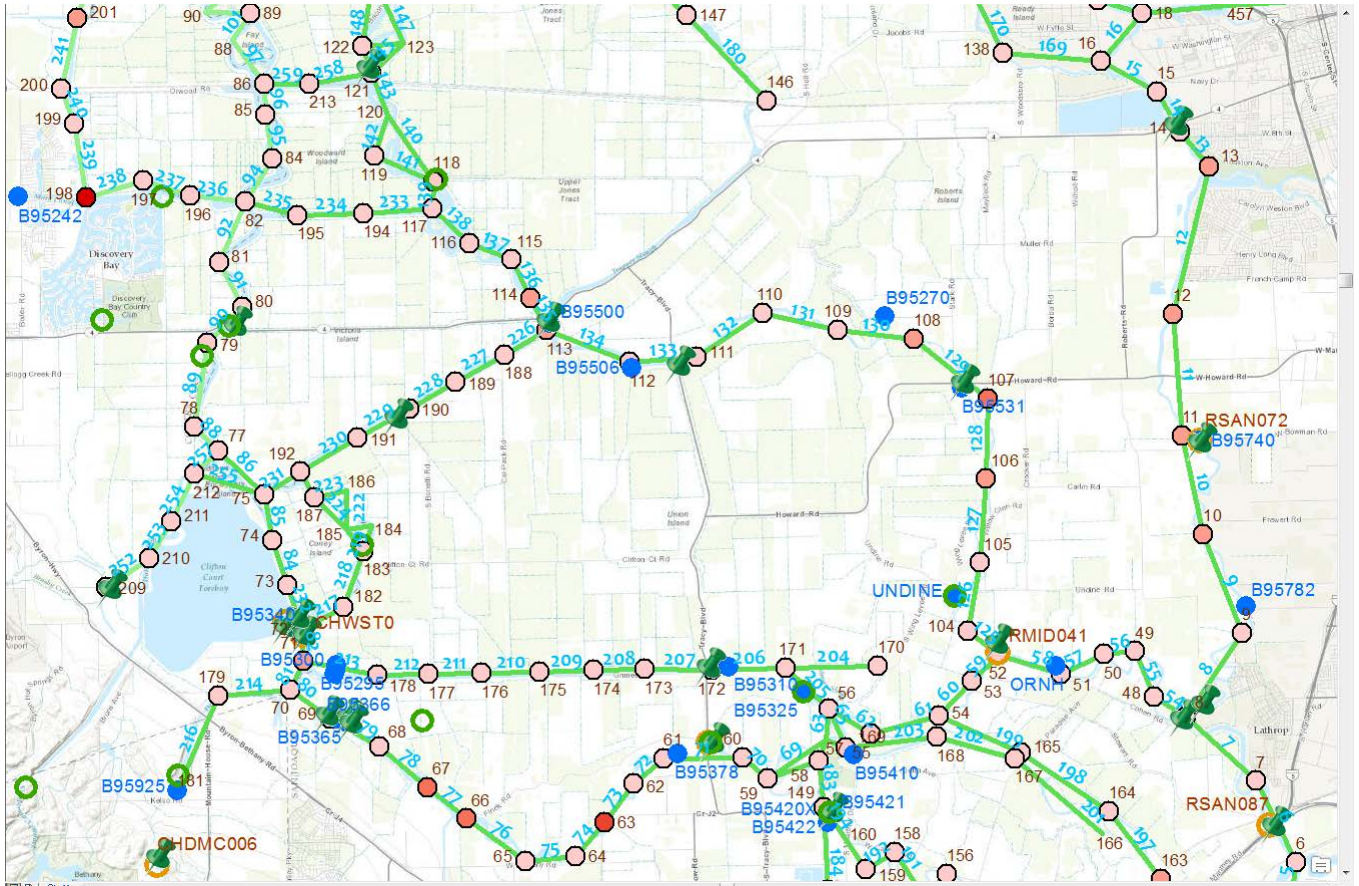
Figure 2-7 South Delta Final Value Map
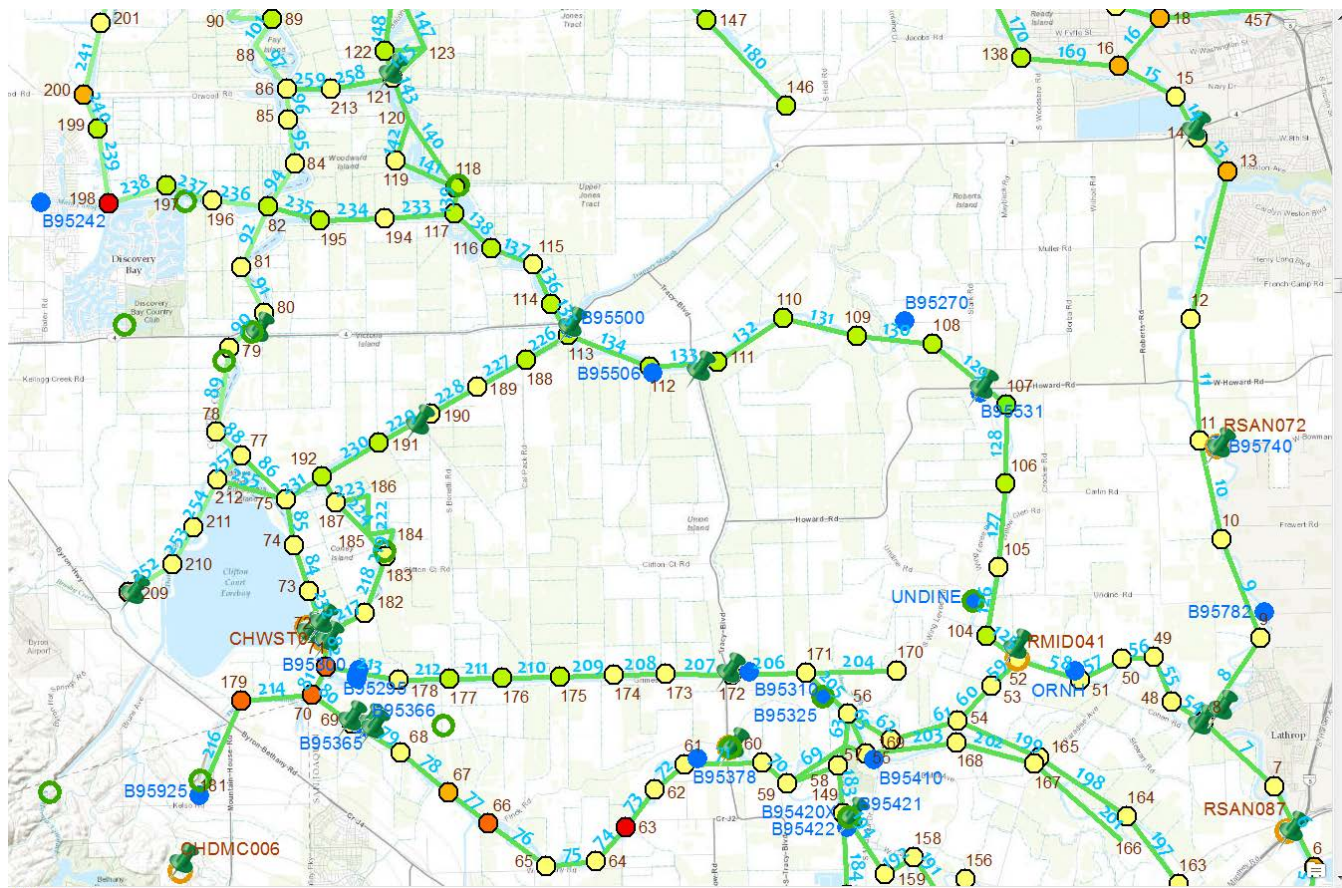
2.10 Future Directions

2.10.1 Working with more PEST Features

At this time we have used no more than half, and probably less, of PEST's many calibration features. While not all features are necessary or even desirable for the DSM2 calibration, a number are, and will be tested with DSM2. We wish to achieve a fairly standard method of calibrating DSM2 in the future, having tried all relevant PEST features and kept the most useful ones without creating an overly complex calibration process.

We have barely touched the possibilities for post-calibration analysis. In addition to visual displays using ArcMap, the consultant has extensive experience and a collection of R programs for performing statistical analyses of calibration results, as well as a recently developed system for displaying comparison data online via a web browser. We expect to use these much more in coming months.

2.10.2 Using better Bathymetry and Delta Evapotranspiration of Applied Water (DETAW)

Known improvements for DSM2 are its channel bathymetry and estimates of channel diversions, drainage return flows, and return flow water quality.

A separate effort (Wang & Ateljevich, 2012) has developed good quality bathymetric digital elevation maps (DEMs) of the Delta. Concurrent with the calibration project, another project with a GIS contractor is developing a modern, GIS-based cross-section development and editing program for use with DSM2. This project should be finished before the calibration project and will be used with the bathymetry DEMs to develop new cross sections for DSM2.

Much better ET estimates for the Delta have been developed (DiGiorgio, 2009); (Kadir, 2006). They will be incorporated for the final calibration of DSM2.

2.11 Acknowledgments

This work would not be possible without a contract with S. S. Papadopulos & Associates (SSP&A), funded by the State Water Project and supported and approved by Tara Smith (Chief, Delta Modeling Section), Dr. Francis Chung (Chief, Modeling Support Branch) and Kathy Kelly (former Chief, Bay-Delta Office). Matt Tonkin, President of SSP&A is the principle contractor and developed many of the theoretical methods and implementations in software. Chris Muffels of SSP&A developed the Genie run manager.

2.12 References

DiGiorgio, C. L. (2009, June). Chapter 2 Data Quality Associated with EC Values in the DICU Model. *Methodology for Flow and Salinity Estimates in the Sacramento-San Joaquin Delta and Suisun Marsh, 30th Annual Progress Report.*

Doherty, J. (2010). PEST; Model-Independent Parameter Estimation. *5th*.

Kadir, T. (2006, October). Estimates for Consumptive Water Demands in the Delta using DETAW. *Methodology for Flow and Salinity Estimates in the Sacramento-San Joaquin Delta and Suisun Marsh, 27th Annual Progress Report.*

Liu, L., & Sandhu, N. (2012). DSM2 Version 8.1 Recalibration. *Methodology for Flow and Salinity Estimates in the Sacramento-San Joaquin Delta and Suisun Marsh*, p. Chapter 3.

S.S. Papadopulos & Associates. (2014). *PEST*. Retrieved April 2014, from S.S. Papadopulos & Associates, Inc.: http://www.sspa.com/software/pest.html

University of Wisconsin-Madison. (2014). *HTCondor*. Retrieved April 2014, from Department of Computer Sciences, University of Wisconsin-Madison: http://research.cs.wisc.edu/htcondor/

Wang, R.-F., & Ateljevich, E. (2012, June). Chapter 6 A Continuous Surface Elevation Map for Modeling. *Methodology for Flow and Salinity Estimates in the Sacramento-San Joaquin Delta, 33rd Annual Progress Report.*

Chapter 3.   DSM2 Version 8.1 Time Step Sensitivity Test

3.1 Introduction

This chapter gives the update on DSM2 version 8.1.2 time step sensitivity test results. The sensitivity tests are important because relatively small changes in time steps should not result in large changes in water quality results. If there are large differences in results due to differences in time step size, this reflects a problem in the model's ability to converge. Time steps for Hydro (the DSM2 hydrodynamic module), the tidefile (output from Hydro), and Qual (the DSM2 water quality module) have been tested. Sensitivity tests were done to evaluate the effects of different time steps on simulated EC. These results suggest DSM2 converges well. Time steps for the v8.1 calibration were chosen based on these results.

3.2 Testing Scenarios and Result Analysis

The historical run setup was used for all the test runs. The simulation period was from June 1, 2006, to June 1, 2008. The two-year time period is long enough to provide representative data for comparing the results.

3.3 Test for Qual Time Step Sensitivity

For Qual, four time steps of 15, 5, 3 and 1 minutes were tested. In all these simulations, Hydro was run at a 5-minute time step and the tidefile was output at 15-minute time steps. The EC results were tidally filtered and compared. Results at a few representative key stations are shown here in the following figures. The key stations are Clifton Court Forebay (CLIFTON_COURT), Old River at Bacon Island (ROLD024), San Joaquin River at Jersey Point (RSAN018), and Stockton Ship Channel (RSAN058) (Figures 3-1 to 3-4).

The output results show that the model converges well. The difference between time steps of 15 minutes and 5 minutes is around 1% for Clifton Court Forebay and Old River at Bacon Island (Figures 3-5 and 3-6). In each of these two figures, the top part shows comparison and the difference in values, and the bottom part shows the difference in percentage. The difference in simulated results between time steps of 5 minutes and 3 minutes is less than 1% (Figures 3-7 and 3-8). The difference between time steps of 3 minutes and 1 minute is less than 0.4% (Figures 3-9 and 3-10).

Figure 3-1 Qual Time Step Sensitivity at Clifton Court Forebay

CLIFTON_COURT TIDALLY_FILTERED_15MIN EC
CLIFTON_COURT TIDALLY_FILTERED_5MIN EC
CLIFTON_COURT TIDALLY_FILTERED_3MIN EC
CLIFTON_COURT TIDALLY_FILTERED_1MIN EC
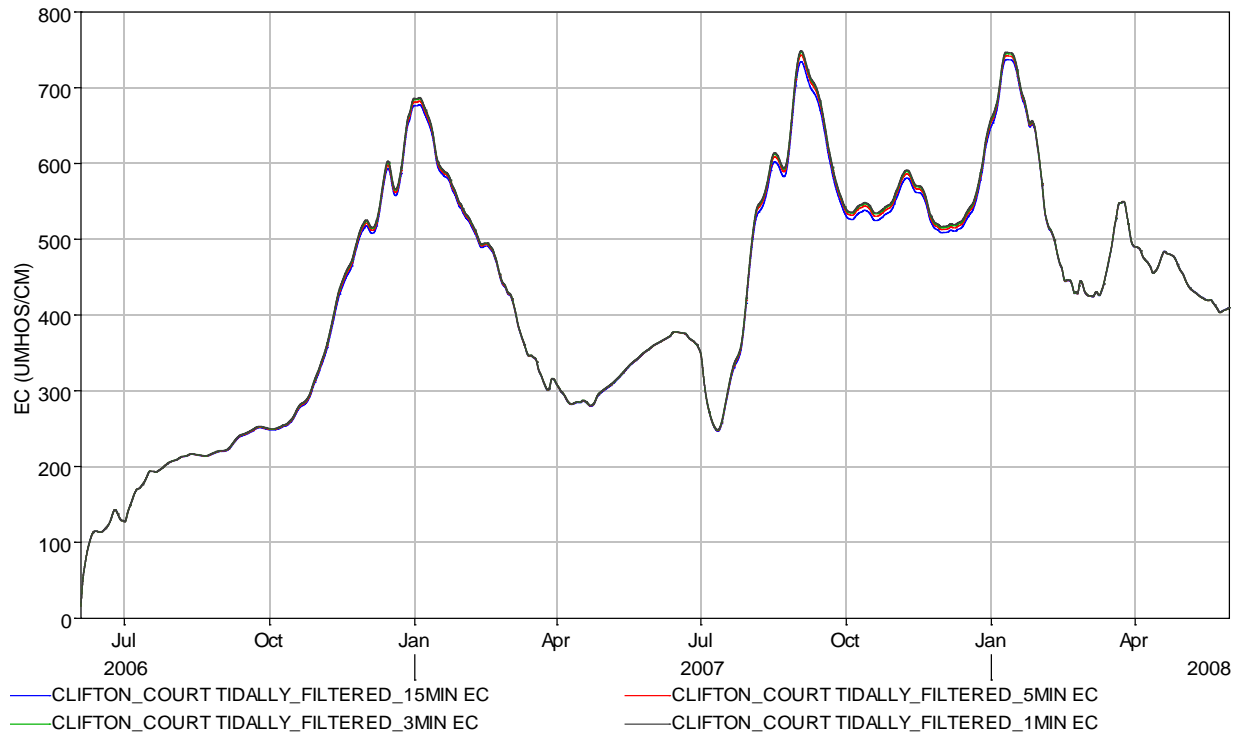
Figure 3-2 Qual Time Step Sensitivity at Bacon Island (ROLD024)

ROLD024 TIDALLY_FILTERED_15MIN EC
ROLD024 TIDALLY_FILTERED_5MIN EC
ROLD024 TIDALLY_FILTERED_3MIN EC
ROLD024 TIDALLY_FILTERED_1MIN EC
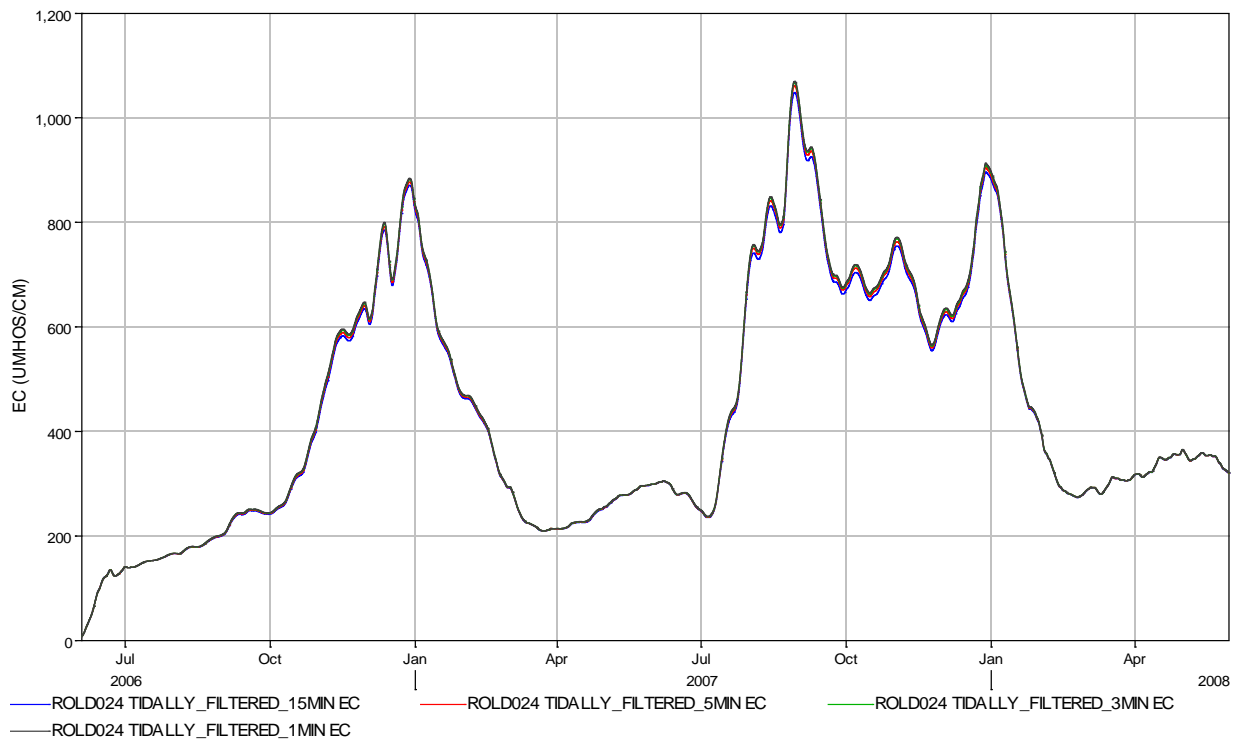
Figure 3-3 Qual Time Step Sensitivity at Jersey Point (RSAN018)
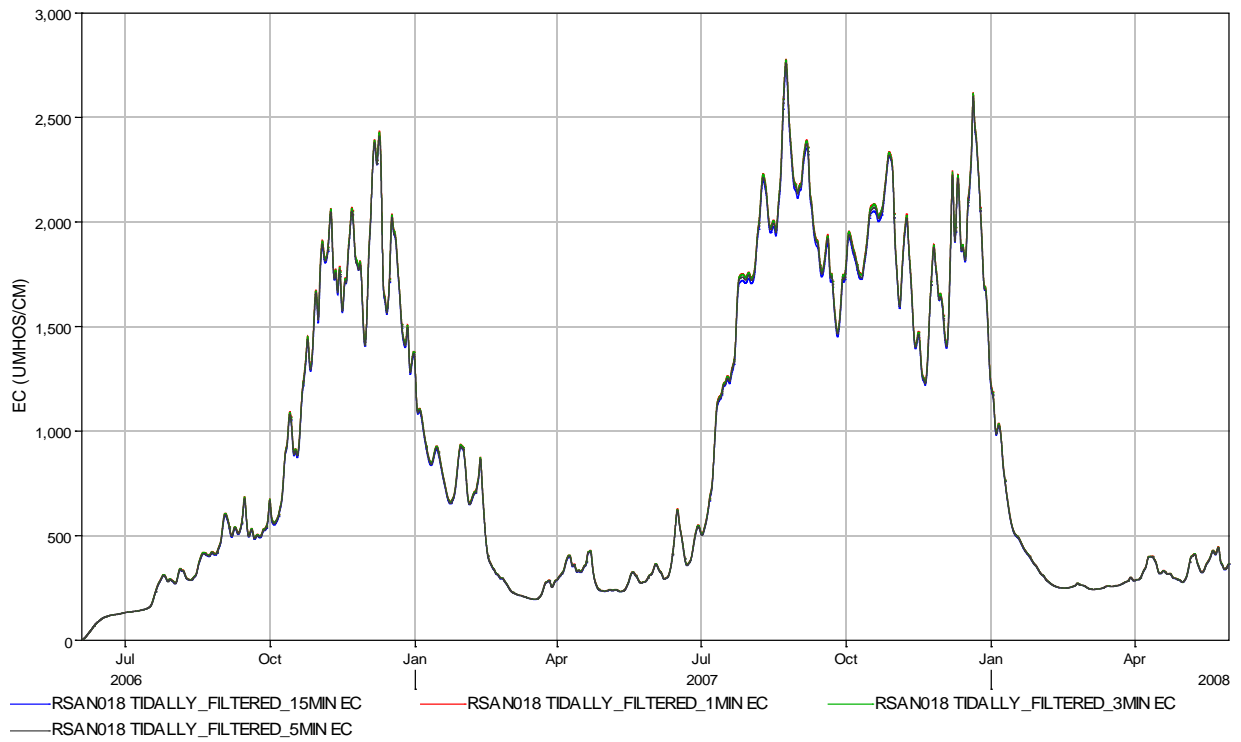
Figure 3-4 Qual Time Step Sensitivity at Stockton Ship Canal (RSAN058)
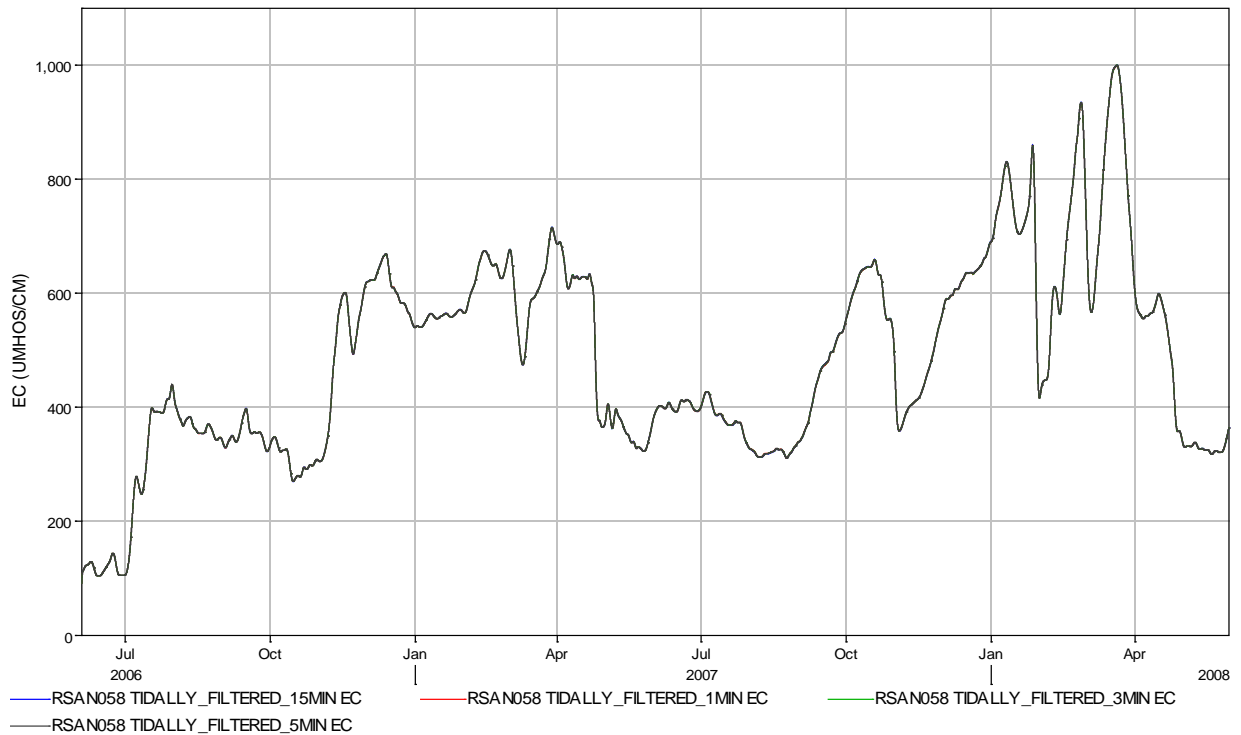
**Figure 3-5 Comparison of Simulated EC with Time Steps
of 15 Minutes and 5 Minutes at Clifton Court Forebay**

CLIFTON_COURT DIFFERENCE_TIDALLY_FILTERED EC
CLIFTON_COURT TIDALLY_FILTERED_15MIN EC
CLIFTON_COURT TIDALLY_FILTERED_5MIN EC
CLIFTON_COURT PERCENTDIFF_TIDALLY_FILTERED_ EC
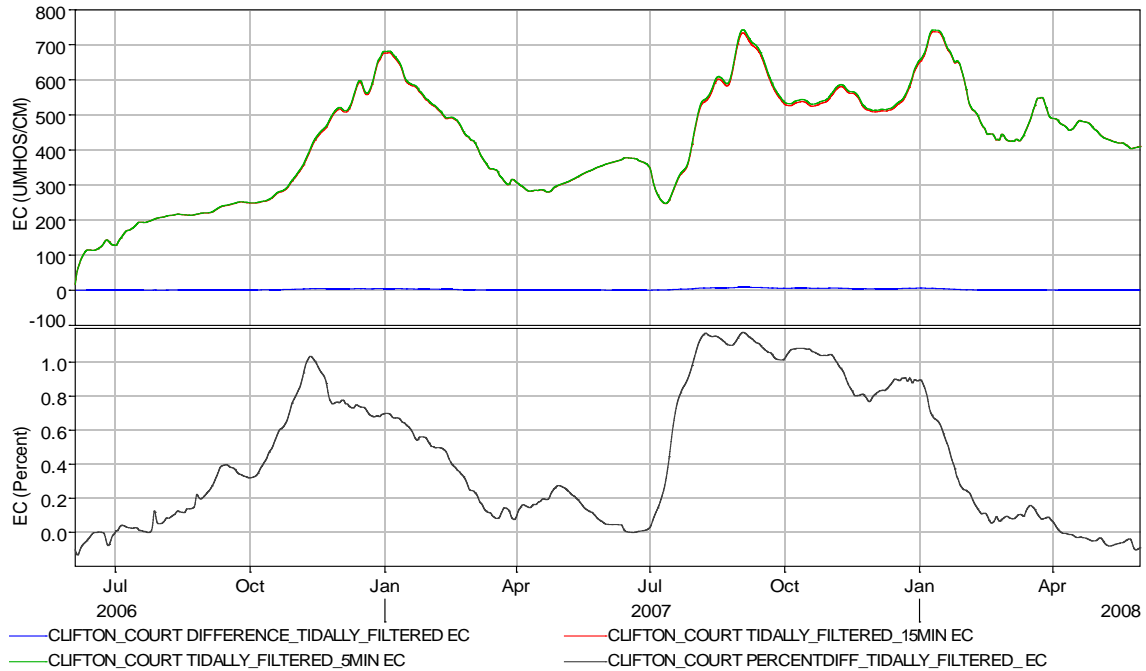
**Figure 3-6 Comparison of Simulated EC with Time Steps
of 15 Minutes and 5 Minutes at Bacon Island**

ROLD024 DIFFERENCE_TIDALLY_FILTERED EC
ROLD024 TIDALLY_FILTERED_15MIN EC
ROLD024 TIDALLY_FILTERED_5MIN EC
ROLD024 PERCENTDIFF_TIDALLY_FILTERED_ EC
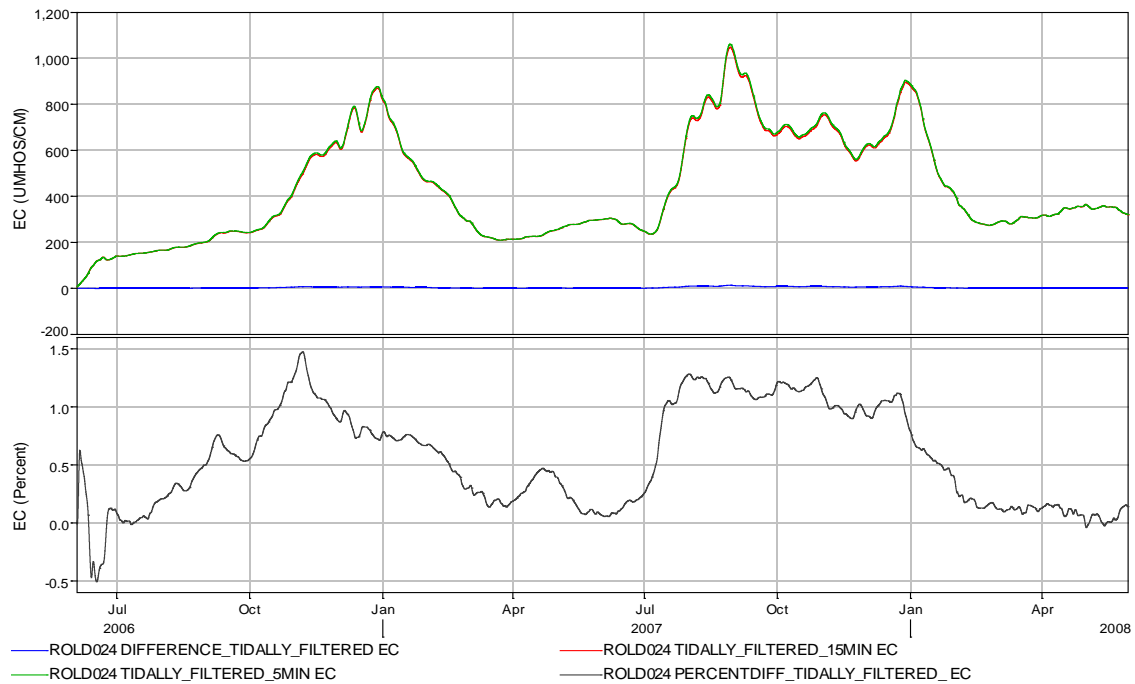
**Figure 3-7 Comparison of Simulated EC with Time Steps
of 5 Minutes and 3 Minutes at Clifton Court Forebay**
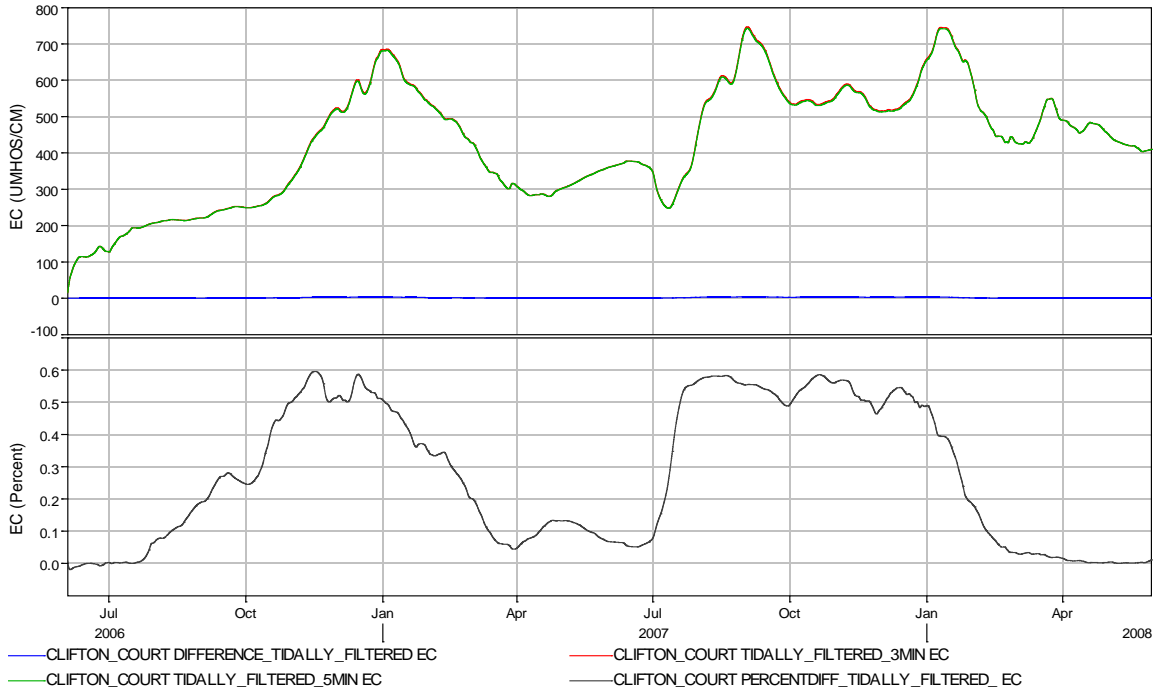
**Figure 3-8 Comparison of Simulated EC with Time Steps
of 5 Minutes and 3 Minutes at Bacon Island**
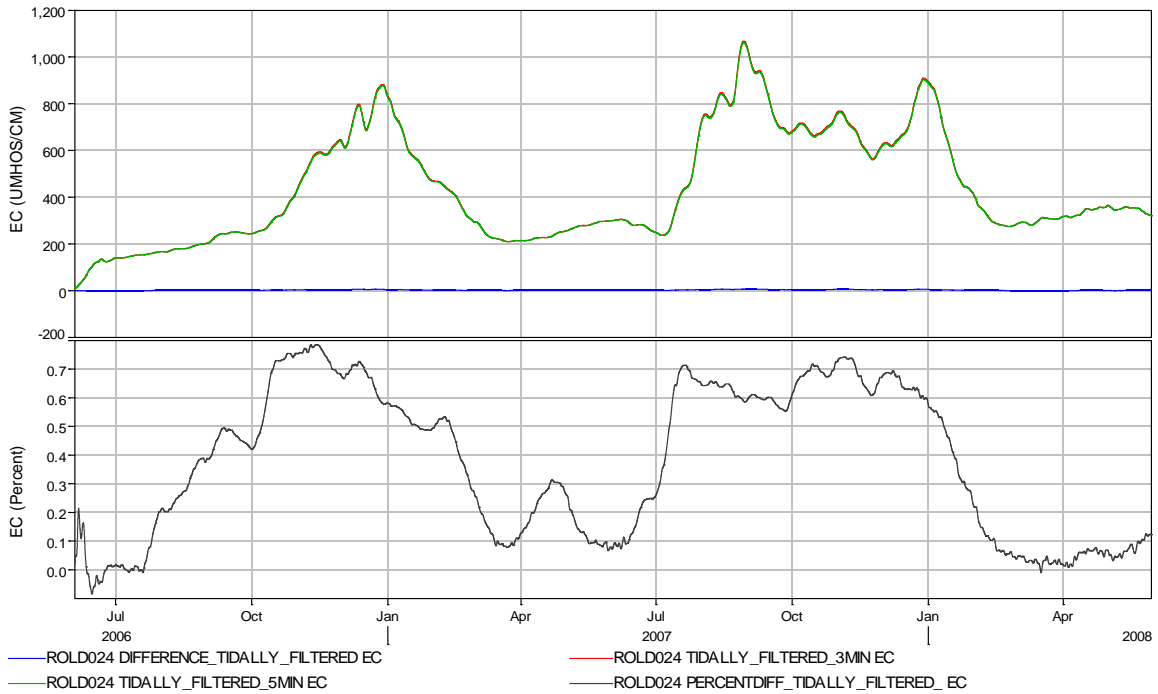
**Figure 3-9 Comparison of Simulated EC with Time Steps
of 3 Minutes and 1 Minute at Clifton Court Forebay**

——— CLIFTON_COURT DIFFERENCE_TIDALLY_FILTERED EC   ——— CLIFTON_COURT TIDALLY_FILTERED_3MIN EC
——— CLIFTON_COURT TIDALLY_FILTERED_1MIN EC   ——— CLIFTON_COURT PERCENTDIFF_TIDALLY_FILTERED_ EC
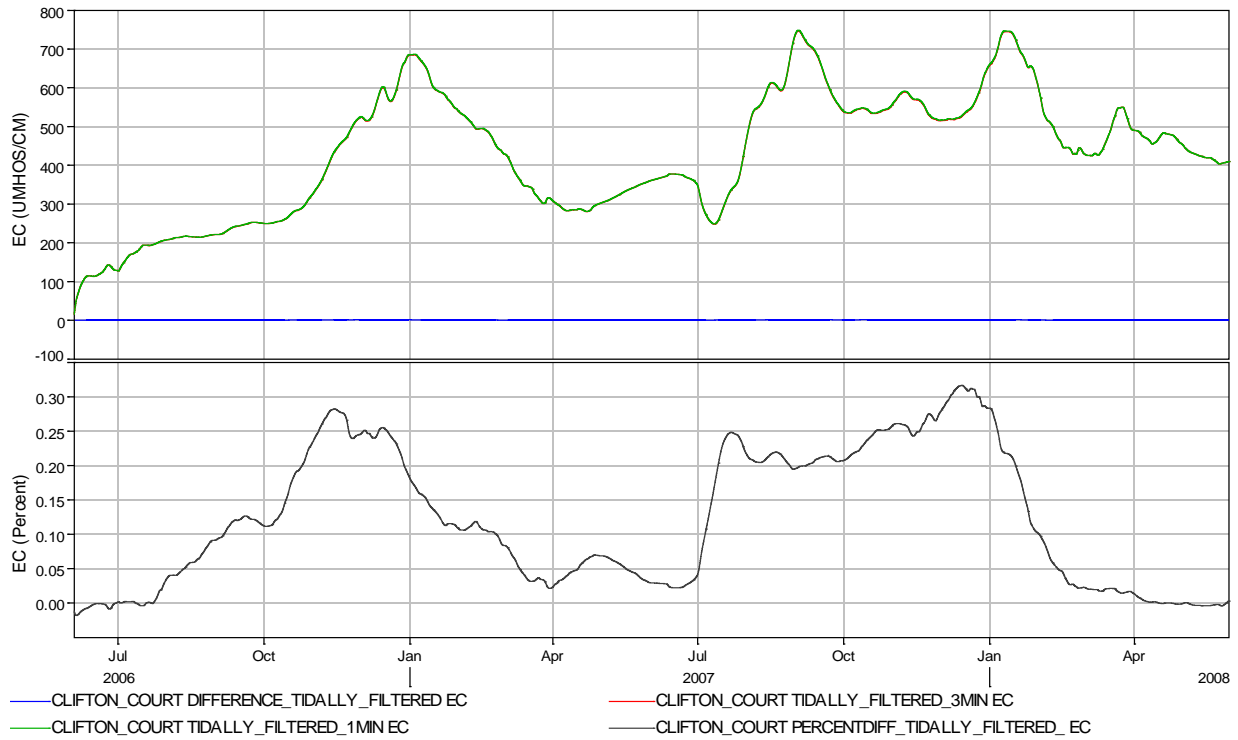
**Figure 3-10 Comparison of Simulated EC with Time Steps
of 3 Minutes and 1 Minute at Bacon Island**

——— ROLD024 DIFFERENCE_TIDALLY_FILTERED EC   ——— ROLD024 TIDALLY_FILTERED_3MIN EC
——— ROLD024 TIDALLY_FILTERED_1MIN EC   ——— ROLD024 PERCENTDIFF_TIDALLY_FILTERED_ EC
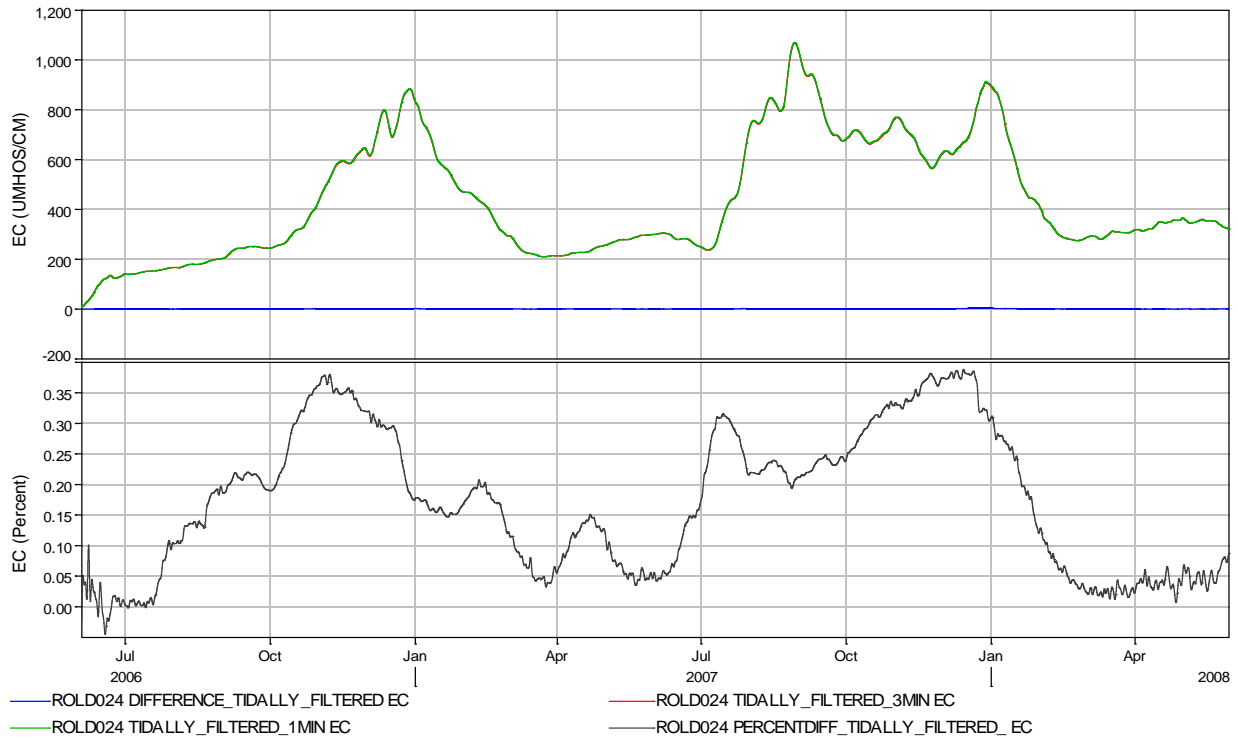
3.4 Test for Tidefile Time Steps

The four time steps compared for the tidefile were 1 hour, 30 minutes, 15 minutes, and 5 minutes. To be consistent, all Hydro and Qual runs used the same 5-minute time step. For 30, 15, and 5 minutes, the results show good convergence (Figures 3-11 to 3-14). The difference in output results between the 30-minute and 15-minute time steps is within 1% (Figures 3-17 and 3-18). The difference in output results between the 1-hour and 30-minute time steps is around 3% to 4% (Figures 3-15 and 3- 16). This further proves that using 1-hour time step for tidefile would not be ideal.

Furthermore, for a 16-year run, the size of the tidefile is about 4 GB for the 30-minute interval versus 8 GB for the 15-minute interval. Thus, for striking a practical balance between accuracy and disk space, we recommend using the 30-minute interval.

Figure 3-11 Tidefile Time Step Sensitivity at Clifton Court Forebay
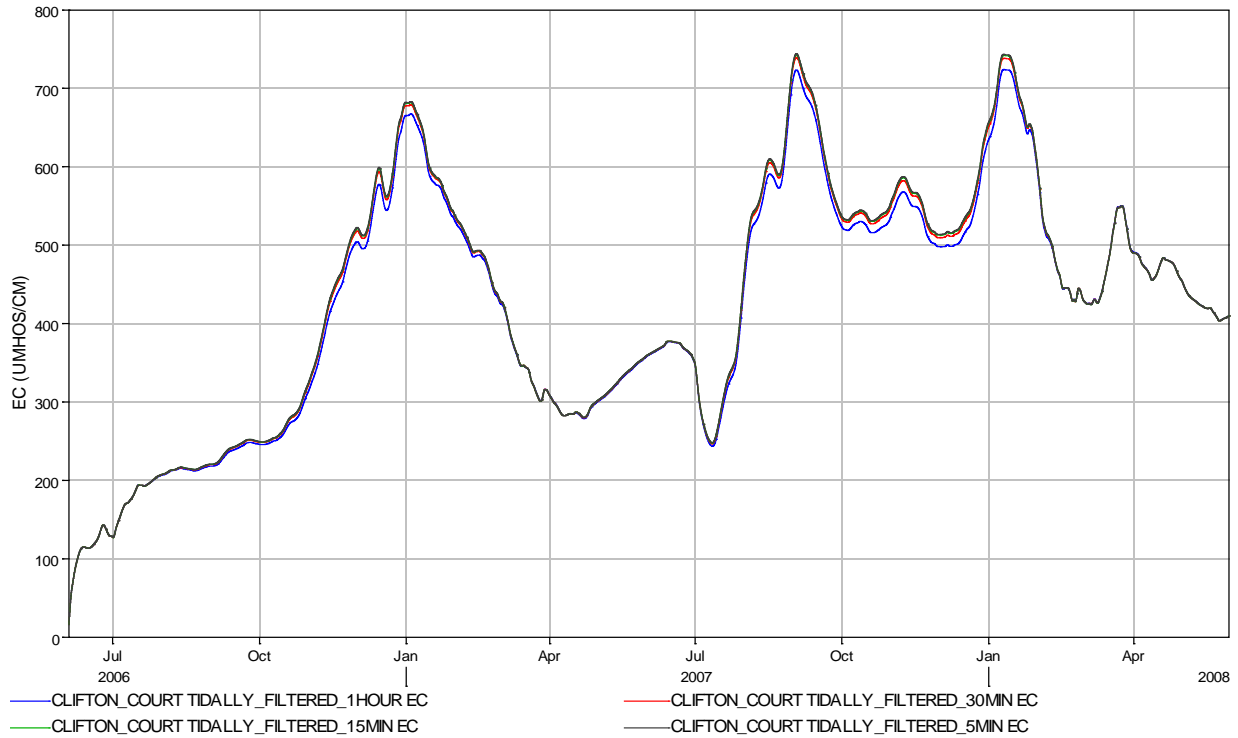
Figure 3-12 Tidefile Time Step Sensitivity at Bacon Island
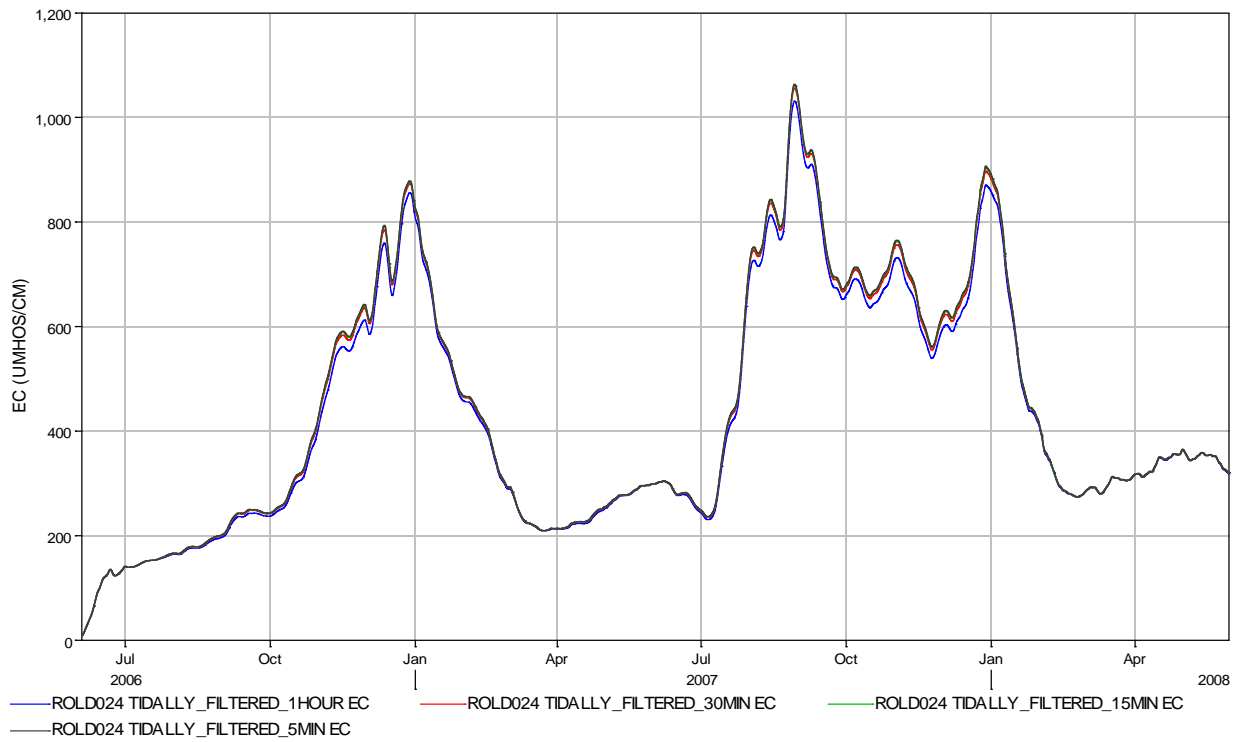
Figure 3-13 Tidefile Time Step Sensitivity at Jersey Point
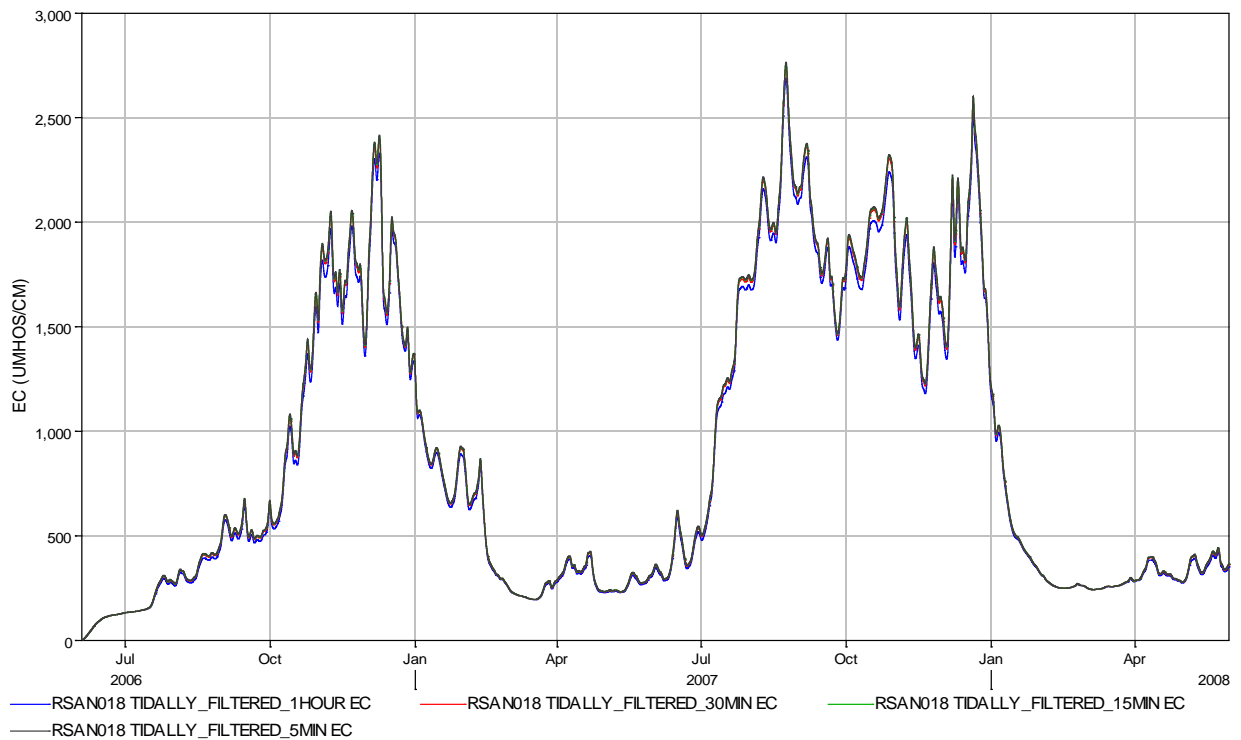
Figure 3-14 Tidefile Time Step Sensitivity at Antioch
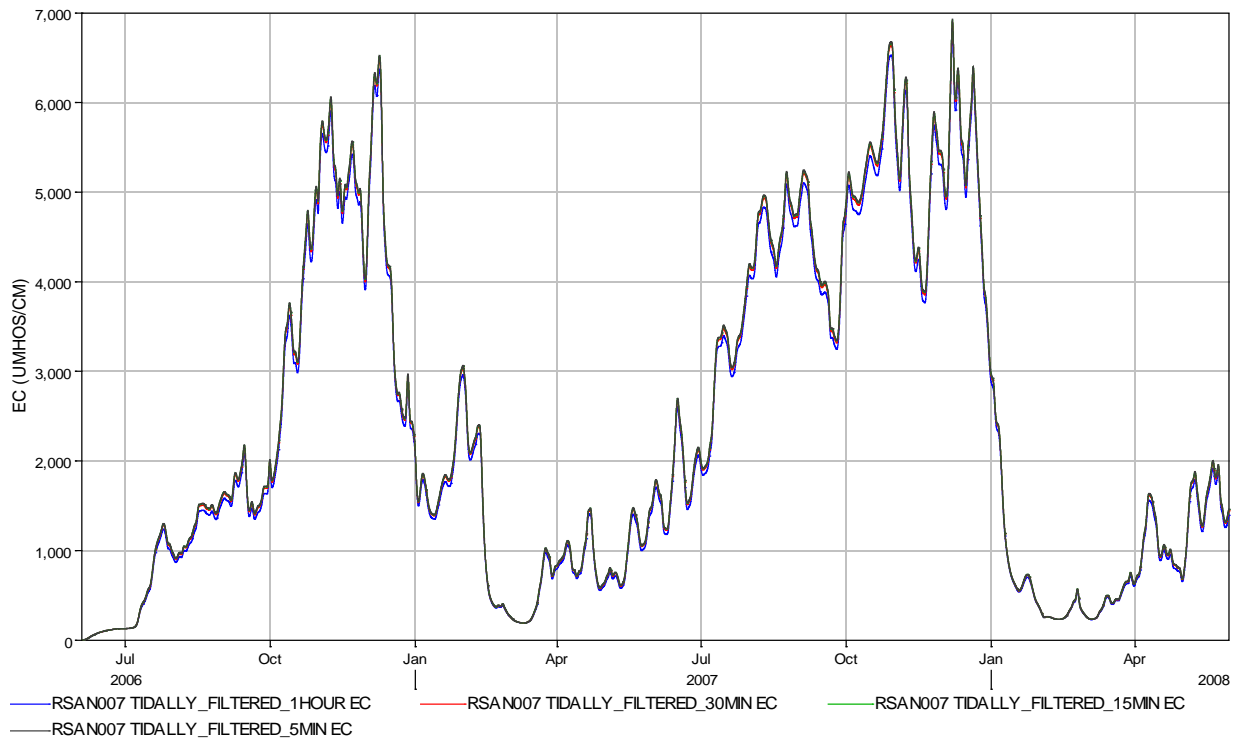
Figure 3-15 Comparison of EC results with 1 Hour and 30 Minute Tidefiles at Clifton Court Forebay
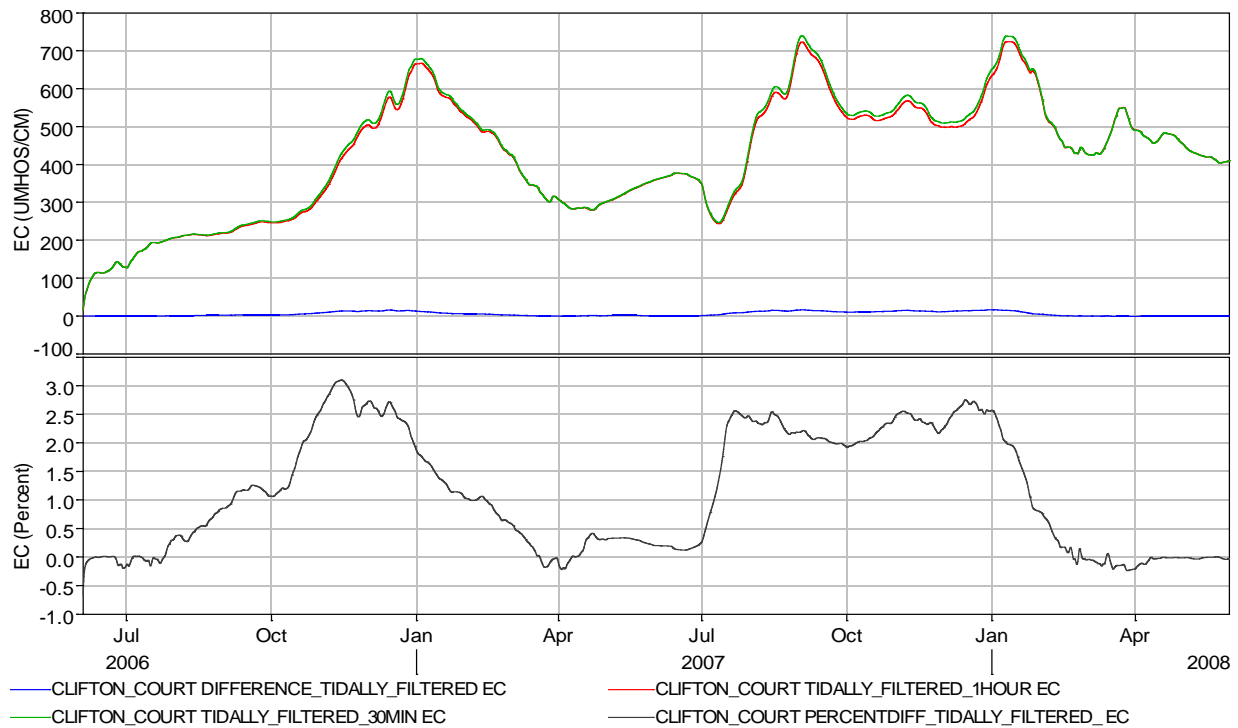
Figure 3-16 Comparison of EC Results with Time Steps of 1 Hour and 30 Minute Tidefiles at Bacon Island
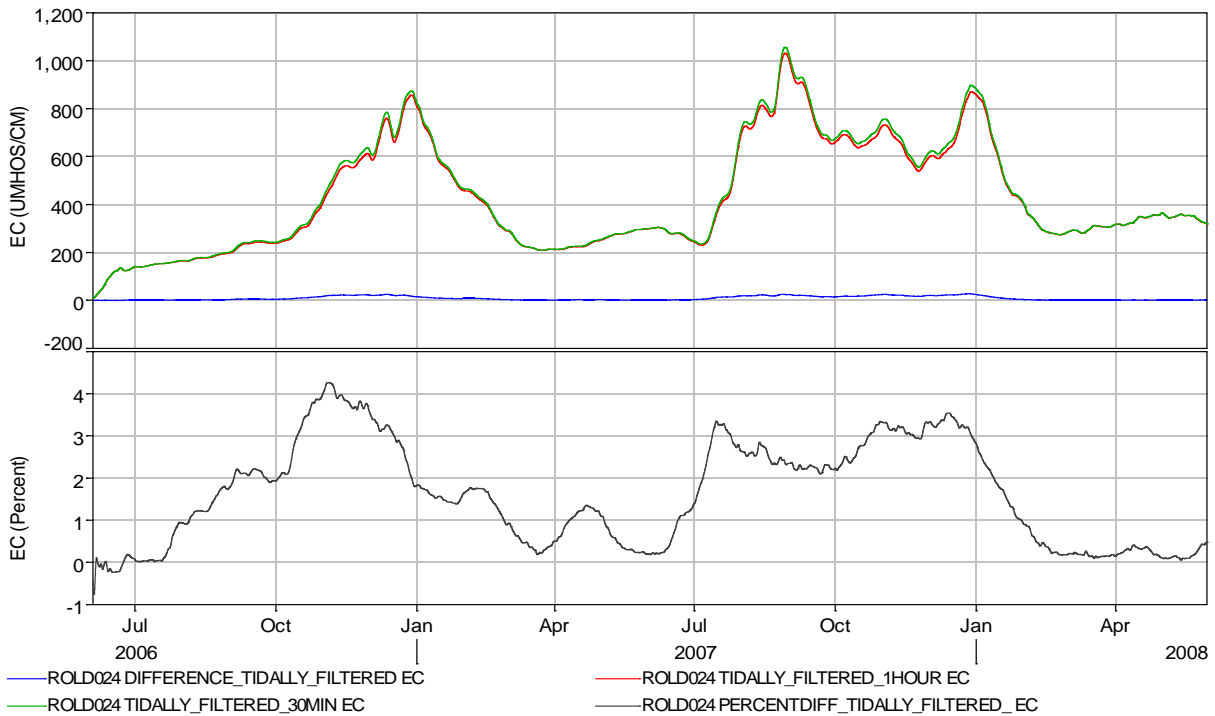
Figure 3-17 Comparison of EC Results with 30 Minute and 15 Minute Tidefiles at Clifton Court Forebay
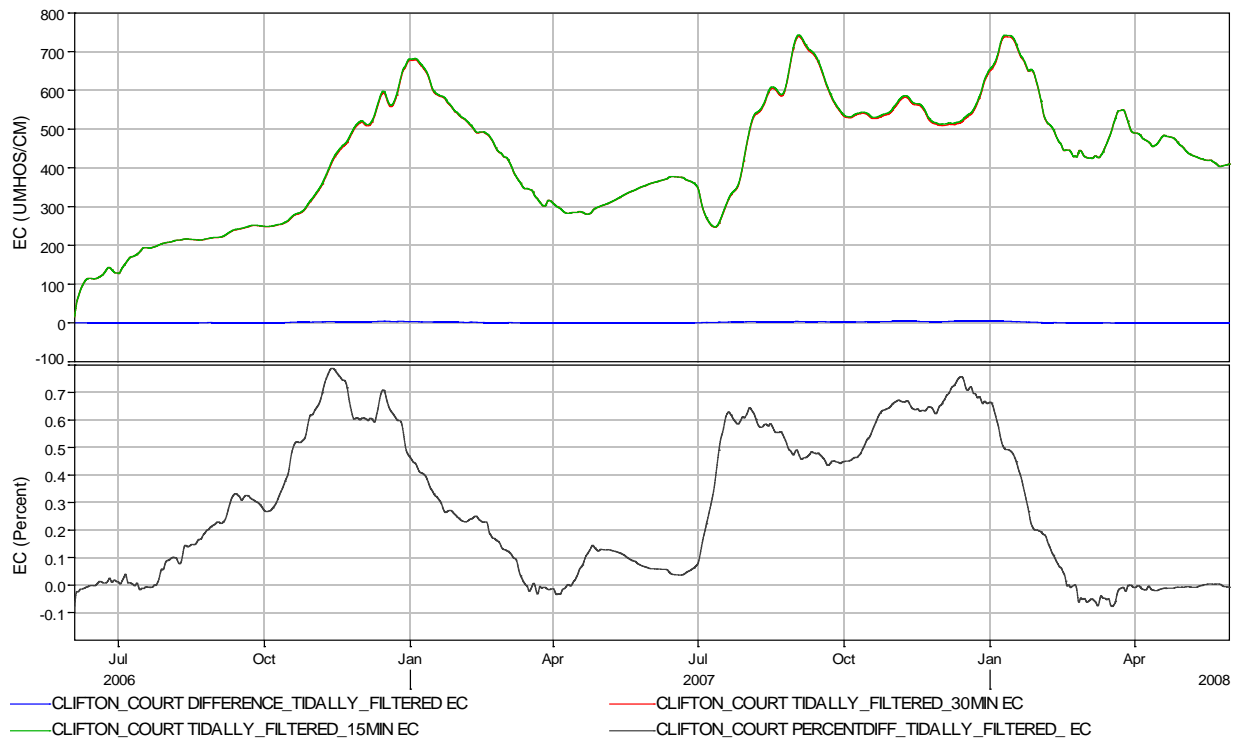
Figure 3-18 Comparison of EC Results with 30 Minute and 15 Minute Tidefiles at Bacon Island
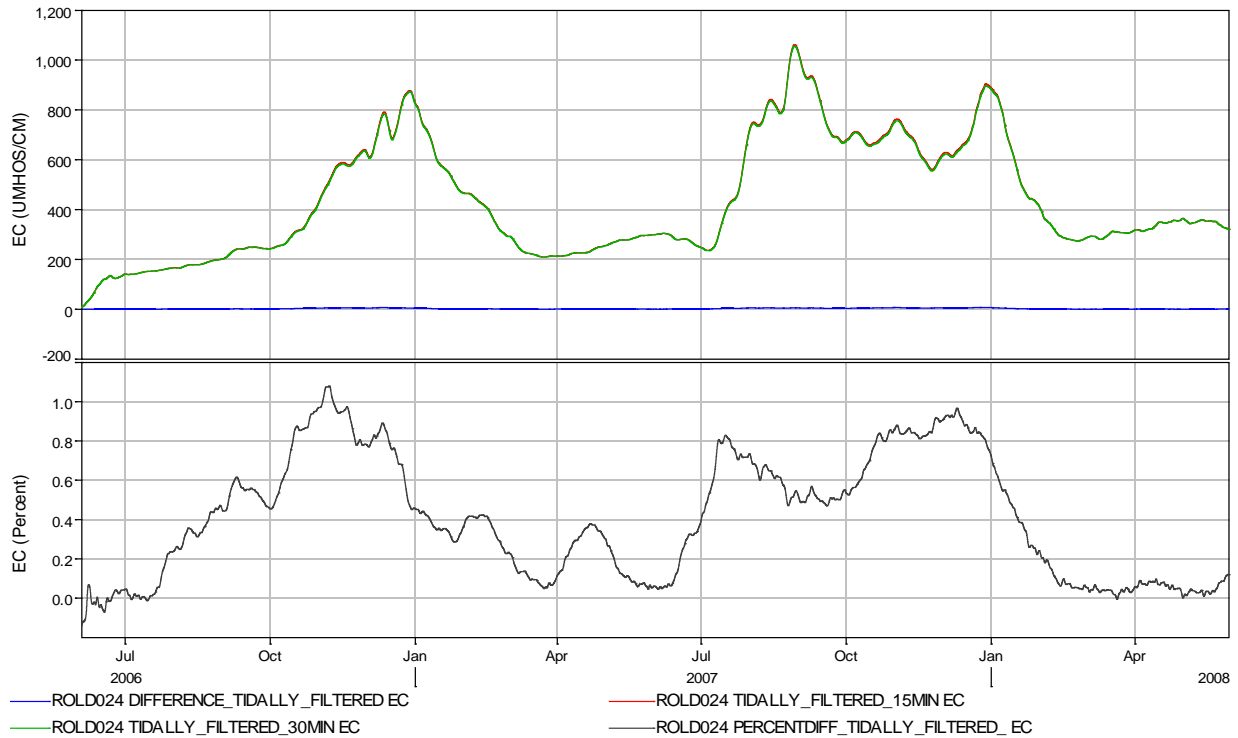
3.5 Test for Hydro Time Steps

Three Hydro time steps of 15, 5 and 3 minutes were tested. For all simulations, the tidefile was generated at 15-minute intervals; Qual used a 5-minute time step. The simulated EC at a few key stations (CLIFTON_COURT, ROLD024, RSAN018, and RSAN007) are plotted in Figure 3-19 through Figure 3-22. The maximum difference in EC results between the 15-minute and 5-minute time steps is less than 2%. The maximum difference in EC results between the 5-minute and 3-minute time steps is around 0.3% (see Figures 3-23 and 3-24).

Figure 3-19 Comparison of EC with 15 Minute and 5 Minute Hydro Time Steps at Clifton Court Forebay
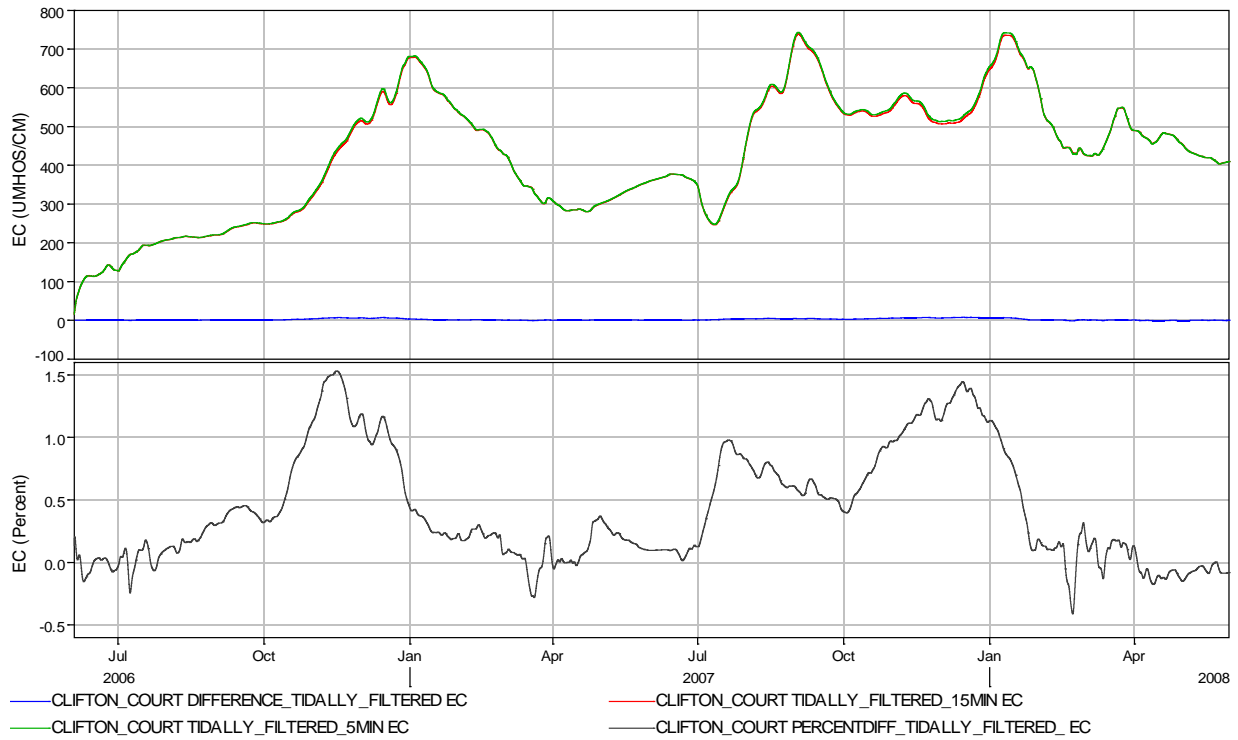
Figure 3-20 Comparison of EC with 15 Minute and 5 Minute Hydro Time Steps at Bacon Island
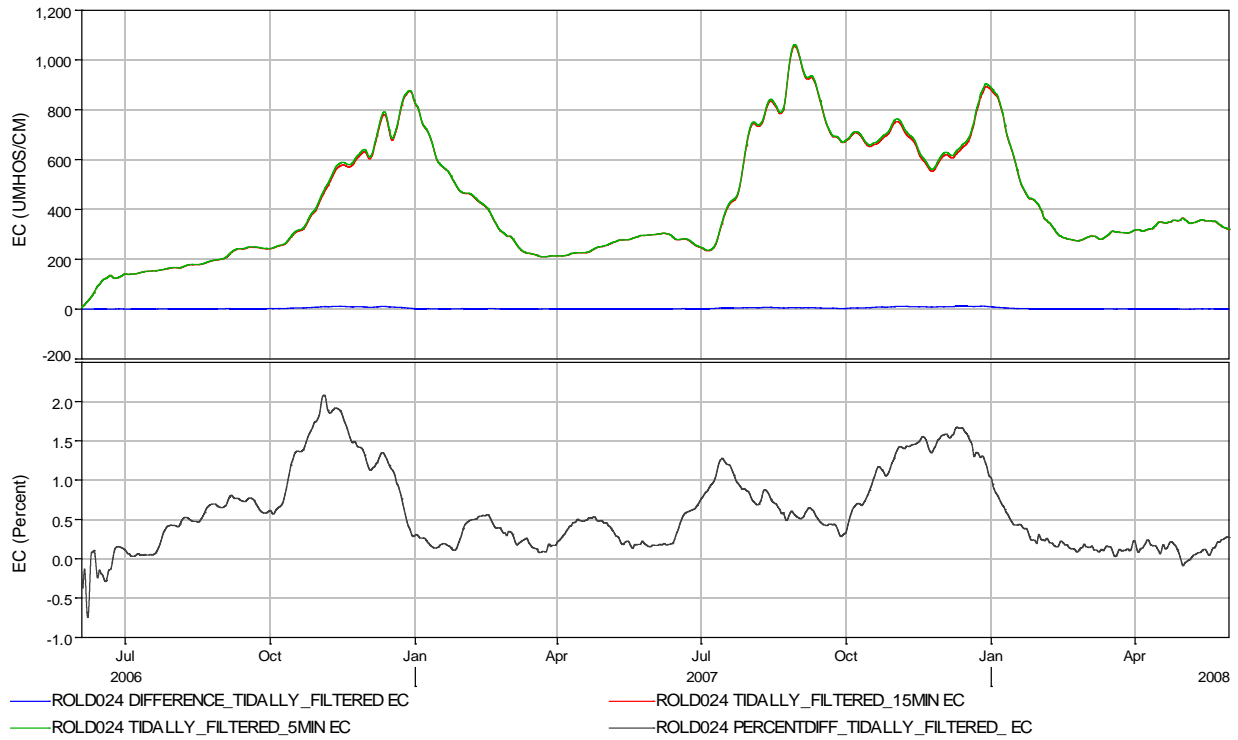
Figure 3-21 Comparison of EC with 15 Minute and 5 Minute Hydro Time Steps at Jersey Point

RSAN018 DIFFERENCE_TIDALLY_FILTERED EC
RSAN018 TIDALLY_FILTERED_15MIN EC
RSAN018 TIDALLY_FILTERED_5MIN EC
RSAN018 PERCENTDIFF_TIDALLY_FILTERED_ EC
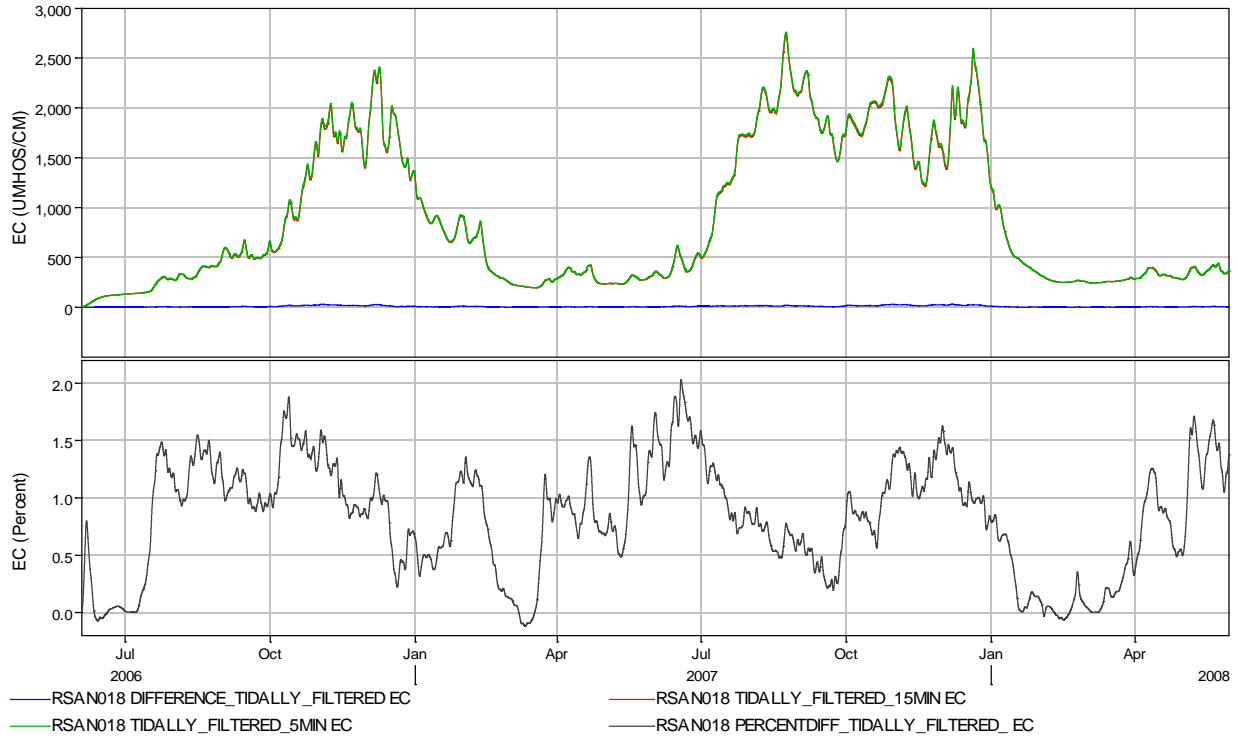
Figure 3-22 Comparison of EC with 15 Minute and 5 Minute Hydro Time Steps at Antioch

RSAN007 DIFFERENCE_TIDALLY_FILTERED EC
RSAN007 TIDALLY_FILTERED_15MIN EC
RSAN007 TIDALLY_FILTERED_5MIN EC
RSAN007 PERCENTDIFF_TIDALLY_FILTERED_ EC
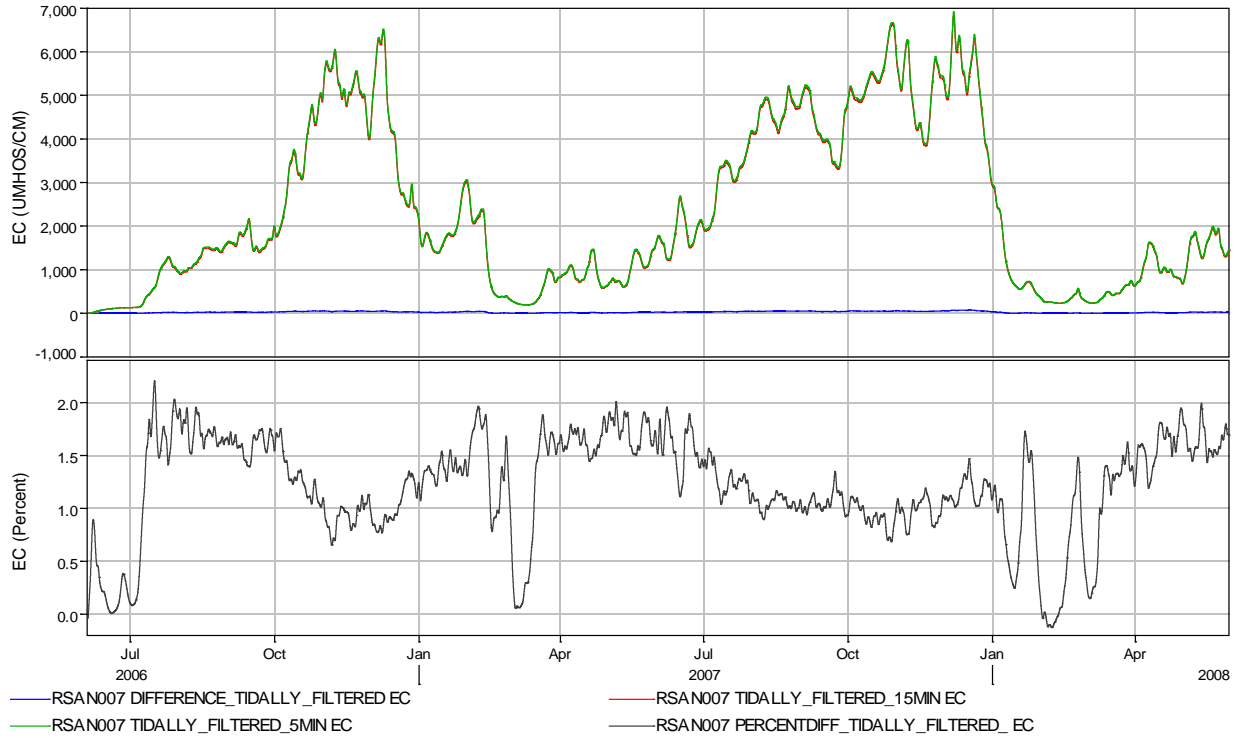
Figure 3-23 Comparison of EC with 5 Minute and 3 Minute Hydro Time Steps at Clifton Court Forebay

— CLIFTON_COURT DIFFERENCE_TIDALLY_FILTERED EC — CLIFTON_COURT TIDALLY_FILTERED_3MIN EC
— CLIFTON_COURT TIDALLY_FILTERED_5MIN EC — CLIFTON_COURT PERCENTDIFF_TIDALLY_FILTERED_ EC
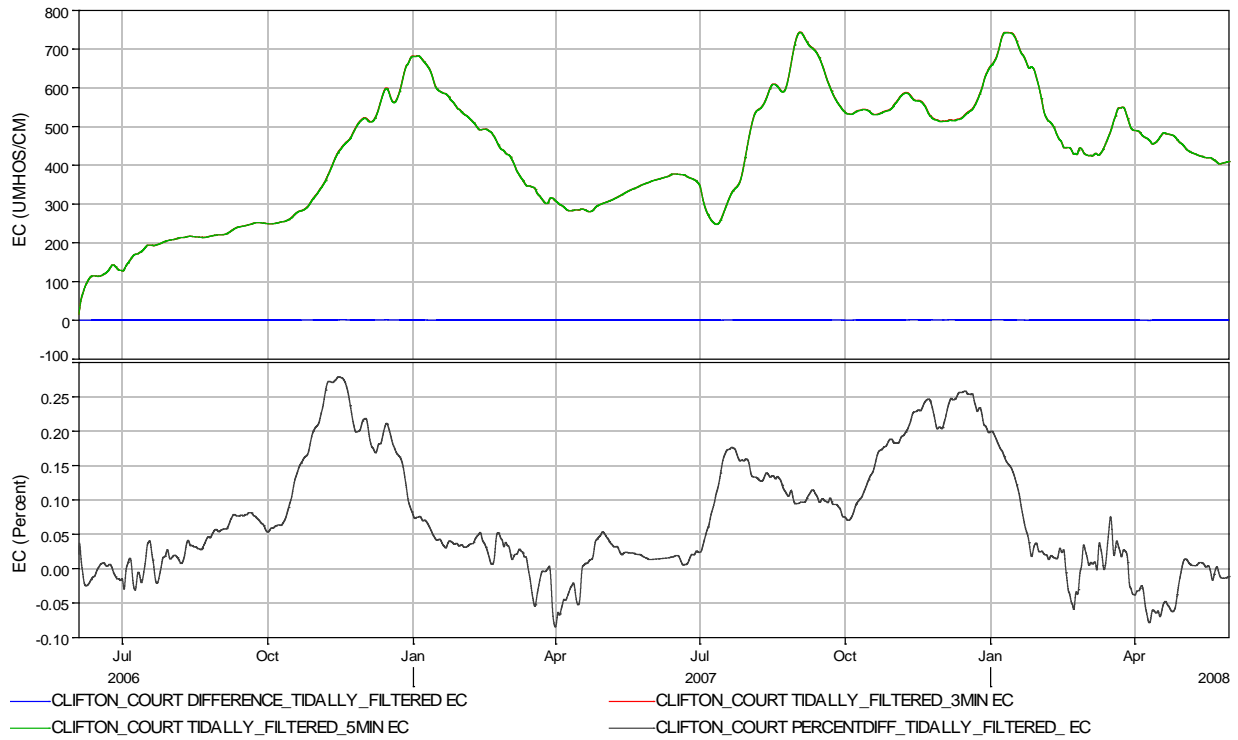
Figure 3-24 Comparison of EC with 5 Minute and 3 Minute Hydro Time Steps at Bacon Island

— ROLD024 DIFFERENCE_TIDALLY_FILTERED EC — ROLD024 TIDALLY_FILTERED_3MIN EC
— ROLD024 TIDALLY_FILTERED_5MIN EC — ROLD024 PERCENTDIFF_TIDALLY_FILTERED_ EC
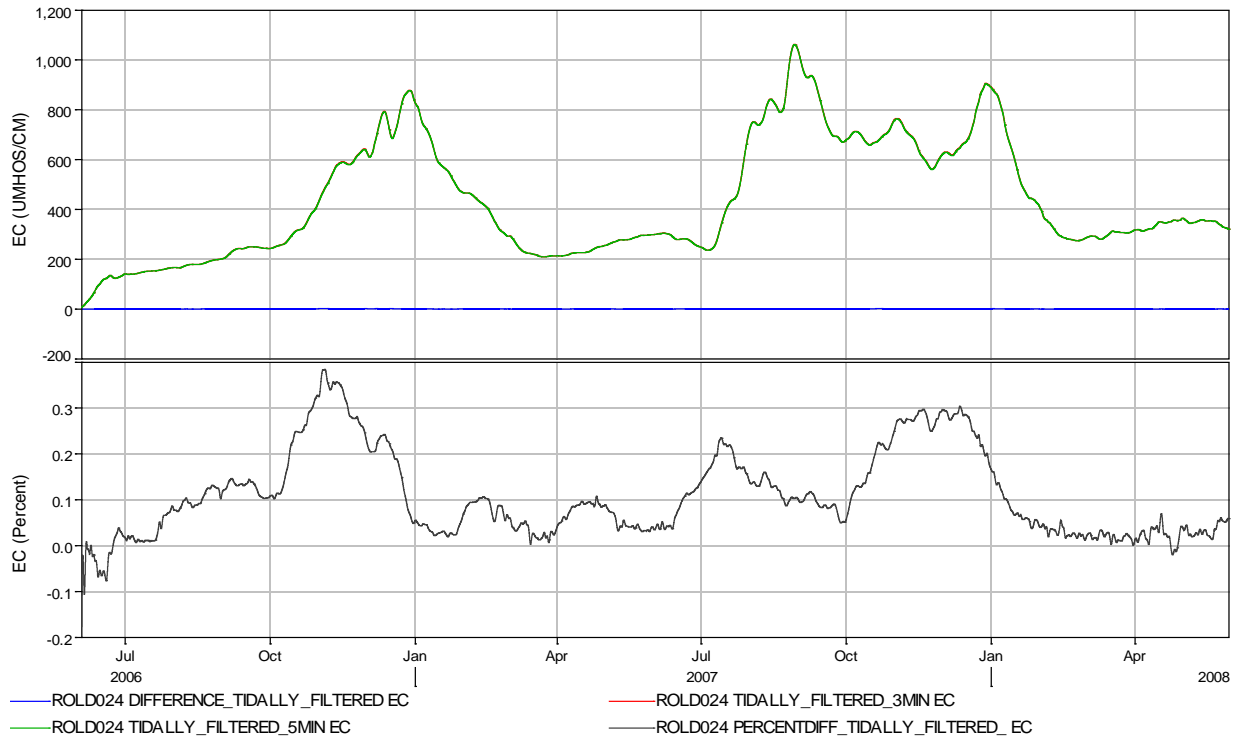
3.6 Comparing Time Step Combinations for Hydro, Tidefile, and Qual

The two most preferred time step combinations are compared. One combination uses time steps of 15, 30, and 15 (15/30/15) minutes for Hydro, the tidefile, and Qual (Hydro/tidefile/Qual), respectively. The other combinations uses time steps of 5, 15, and 5 minutes for Hydro/tidefile/Qual. The results show the difference in EC is around 4% at key stations (see Figures 3-25 through 3-28). The difference can be made up with calibration parameters, e.g. dispersion coefficient. The time steps chosen for the calibration were 15/30/15 minutes for Hydro/tidefile/Qual. For better accuracy, 5/15/5 minutes for Hydro/Tidefile/Qual could be used; however, that would result in a doubling of run time and doubling of the tidefile size.

Figure 3-25 **Comparison of EC Results at Antioch (RSAN007)**
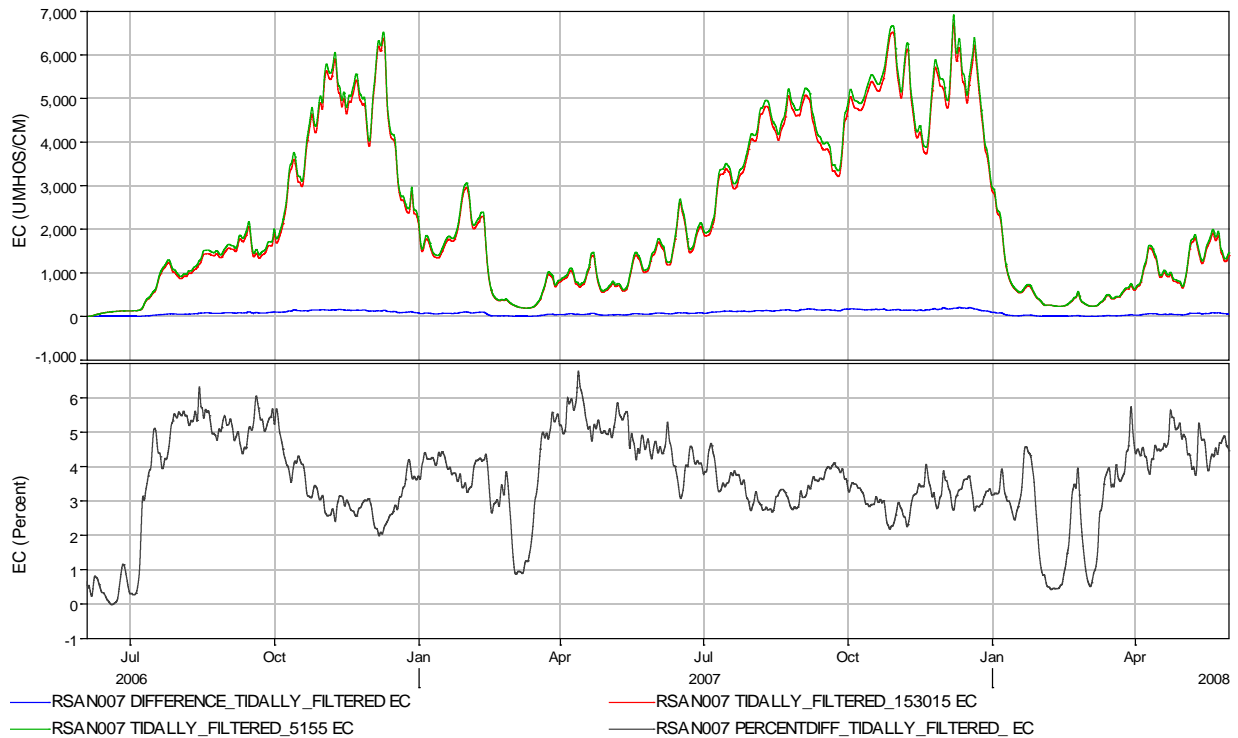
Figure 3-26 Comparison of EC Results at Jersey Point
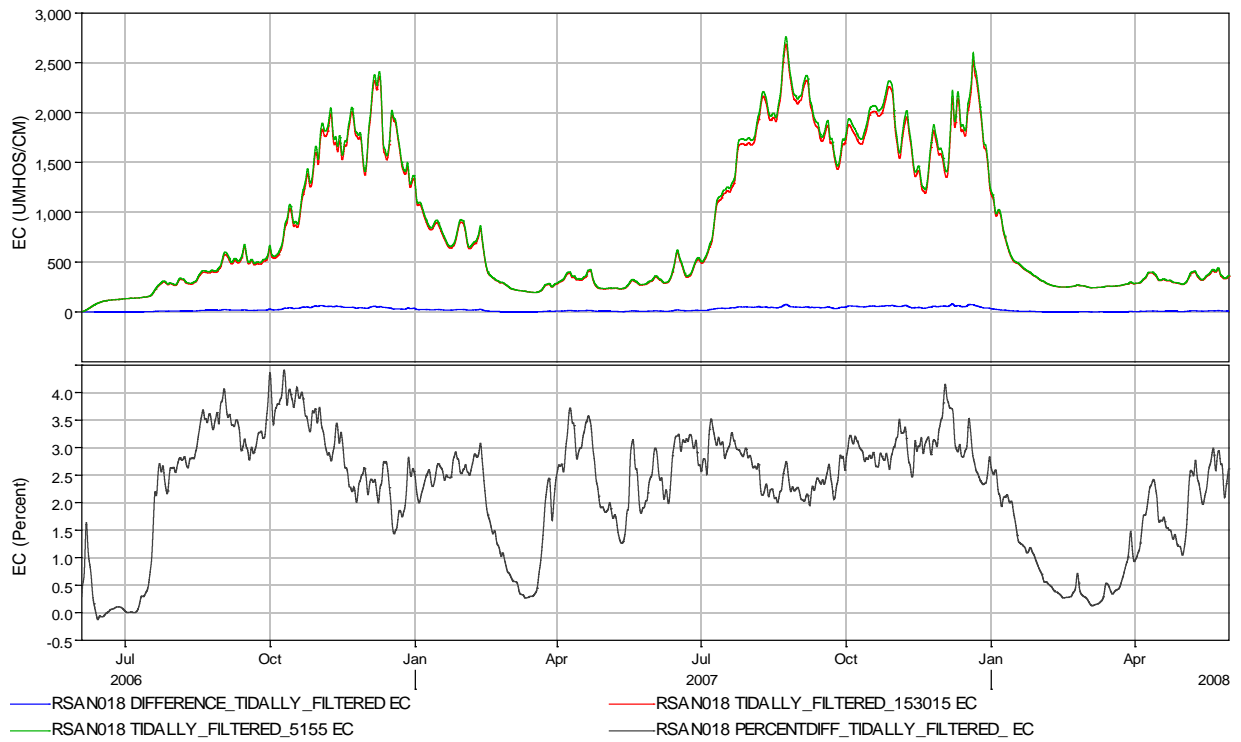
Figure 3-27 Comparison of EC Results at Bacon Island
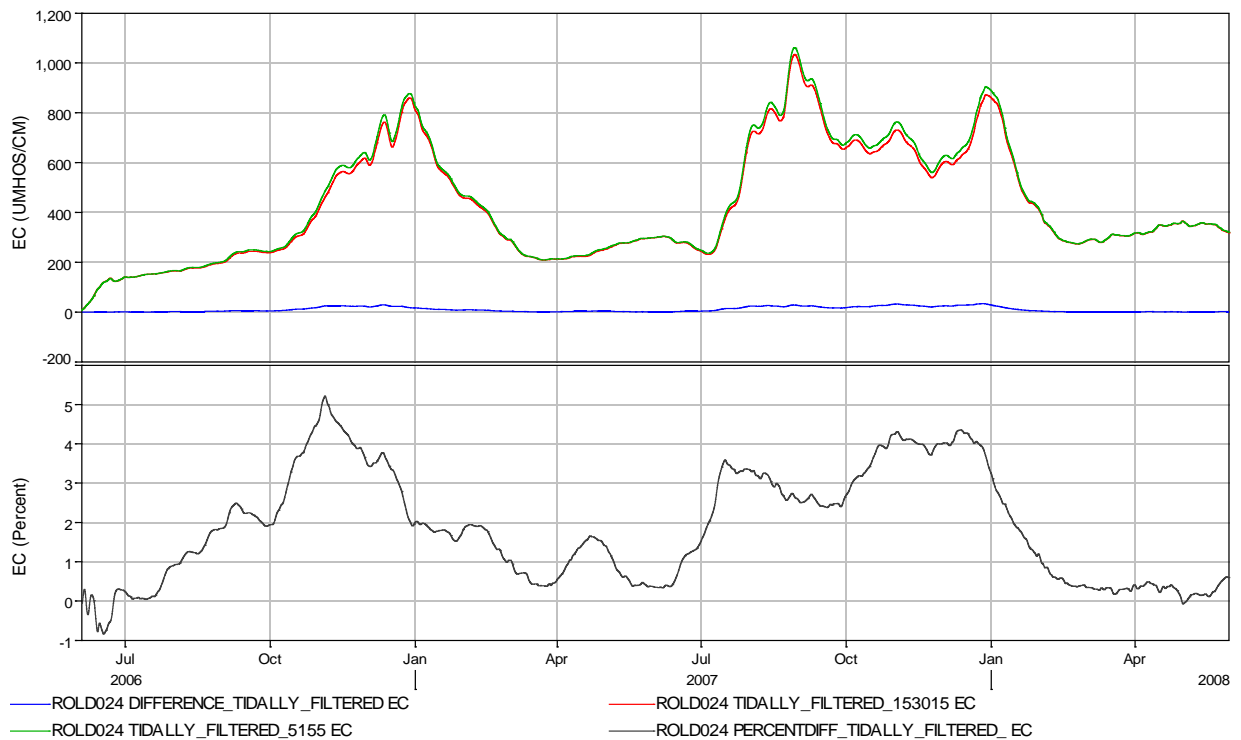
Figure 3-28 Comparison of EC Results at Clifton Court Forebay

CLIFTON_COURT DIFFERENCE_TIDALLY_FILTERED EC
CLIFTON_COURT TIDALLY_FILTERED_5155 EC
CLIFTON_COURT TIDALLY_FILTERED_153015 EC
CLIFTON_COURT PERCENTDIFF_TIDALLY_FILTERED_ EC
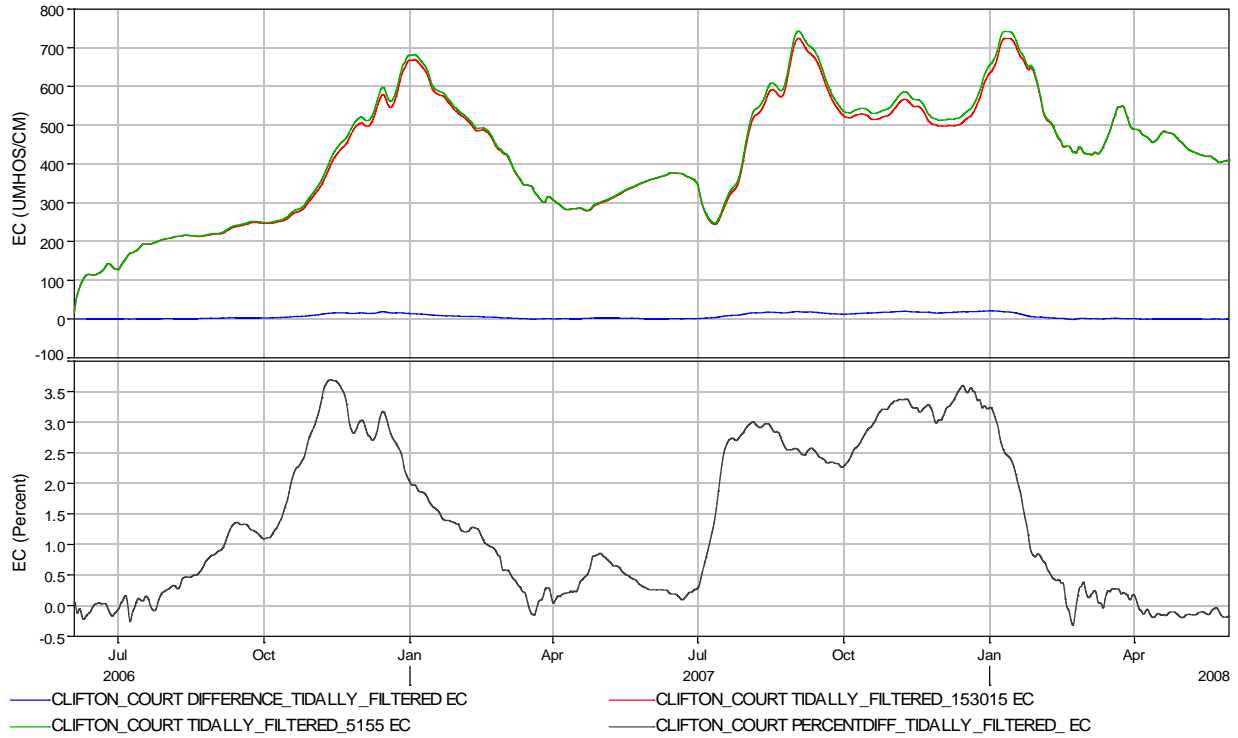
3.7 Summary

The sensitivity tests were done in terms of reviewing the effects of time steps on simulated EC. The time steps chosen for the calibration were 15, 30 and 15 minutes for Hydro, the tidefile and Qual, respectively. For Hydro, the difference in EC results between 15-minute and 5-minute time steps is less than 2%. For the tidefile, the difference in EC results between 30-minute and 15-minute time steps is less than 1%. For Qual, the difference in EC results between 15-minute and 5-minute time steps is about 1%. With the longer time step combinations, running a typical 16-year planning study consumes about 1 hour of CPU time on a 3.2 GHz desktop computer.

Chapter 4.   DSM2-GTM

4.1 Introduction

DWR's Delta Modeling Section is developing a new DSM2 transport module, the General Transport Model (GTM). The mesh for GTM is fixed (Eulerian) rather than moving with flow (Lagrangian). This should make it easier to interact with other models, georeferenced data, and visualization, as well as to couple to Hydro. It is also based on a more flexible software framework that is easier to adapt to new groupings of constituents. Mercury and sediment are of particular interest. The algorithm is a second order upwind solver developed in a prior collaboration with UC Davis with low numerical diffusion and an elaborate verification framework covering tough problems. This chapter describes some of the practical issues of embedding such a model in a looped network or in a DSM2 grid with many intermediate junctions (nodes) along a single physical channel reach. We demonstrate the effect the DSM2-Qual schema can have on numerical diffusion, and make some preliminary comparisons with DSM2-Qual on advection problems in which GTM appears to be less diffusive in more complex flow fields or on more intricate grids.

4.2 Eulerian versus Lagrangian Frames of Reference

Eulerian and Lagrangian frames of reference are two fundamental ways of thinking about and measuring transport processes, each with its advantages and disadvantages. The Eulerian frame of reference can be visualized as sitting on the bank of a river and watching the water passing that fixed location. A typical Eulerian transport model has a fixed spatial grid that is updated by defining fluxes between cells. The accuracy of the flux approximation usually drives the accuracy of the overall scheme. The simplest schemes are plagued by numerical diffusion (a tendency for a plume to spread out) and although this is a solved problem at this point, the better schemes have only become ubiquitous within the last 15 years. Multidimensional models often use Eulerian or hybrid approaches.

A Lagrangian frame of reference can be visualized as sitting in a boat and drifting down a river. In fluid dynamics, a Lagrangian model follows individual fluid parcels as they move through space and time. Figure 4-1, bottom, shows a "train" of particles moving from left to right with local flow. One parcel is created on the left and others exit on the right. The number of parcels in a channel depends on the length of the channel, local velocity, and tidal excursion. As few as one parcel can occupy a channel, but a more typical number is 30 to 50. In theory, Lagrangian schemes are immune to numerical diffusion, an advantage that has been known since the time of Fischer (1979), although, as we shall see, the practical implementation (junctions, output retrieval) leads to some inaccuracy.

Perhaps the greater issue with a Lagrangian model comes from trying to relate it to an Eulerian world – exporting data to a Geographical Information System (GIS), or creating an animation. It is possible to economically track parcels based on volumetric calculations by estimating when parcels pass tracking points and junctions. In Qual's predecessor, the Branched Lagrangian Transport Model (BLTM), tracking points were also used as locations to inject a more detailed flow field without triggering mixing (which occurs at junctions). Example tracking points are shown in the bottom of Figure 4-1. For reasons that hark back to computational and memory limitations, DSM2 does not exploit the idea of interior tracking points within a channel.

Figure 4-1 Illustration of Eulerian versus Lagrangian Frame of Reference
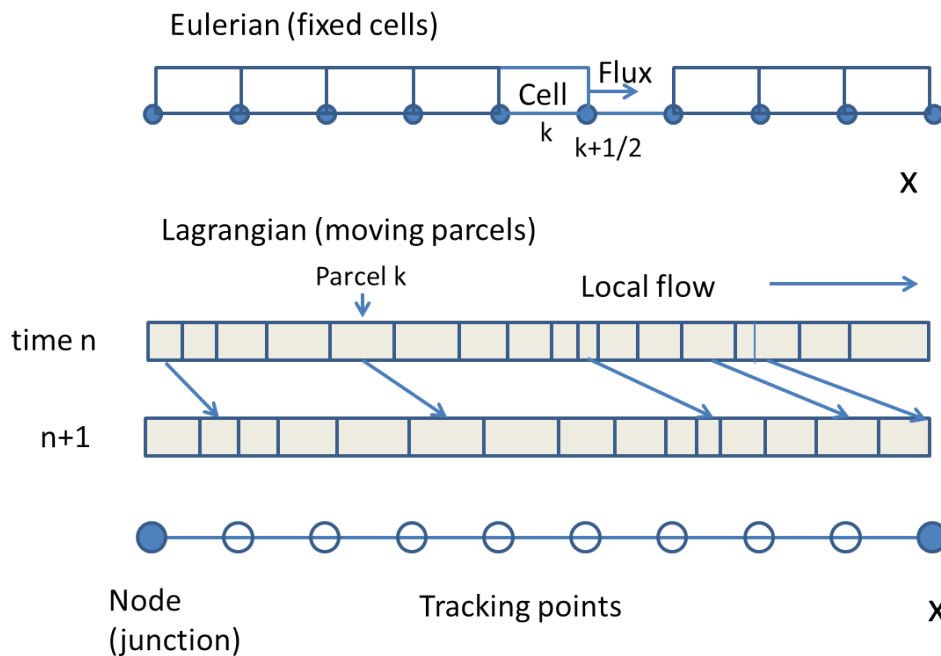
4.3 DSM2-Qual and the Branched Lagrangian Transport Model (BLTM)

DSM2-Qual is based on the BLTM. The original transport code was developed by Harvey Jobson (USGS) and adapted to the Delta by DWR staff (Annual Report, 1998). DSM2-Qual has been widely used to simulate water quality in the Sacramento-San Joaquin Delta. Besides conservative constituents (e.g. EC), DSM2-Qual models the dispersion and kinetics of a fixed selection of non-conservative constituents, including dissolved oxygen, carbonaceous biochemical oxygen demand, phytoplankton, organic nitrogen, ammonia nitrogen, nitrite nitrogen, organic phosphorus, dissolved phosphorus, total dissolved solids, and temperature. The conceptual and functional descriptions of the constituent reactions are based generally on QUAL2E (Brown and Barnwell, 1987). See Jobson and Scoellhamer (1987) for a description of the Lagrangian formulation which provides the basic framework for DSM2-Qual.

As its name implies, a key practical feature of the BLTM design is the accommodation of a branching or looping channel structure. This is an important feature when modeling the Delta. In BLTM, parcels entering a channel junction are blended before being sent on into outgoing channels. This blending is an appropriate treatment for nodes that represent real junctions and confluences, such as node 113 at the junction of Middle River and Victoria Canal in Figure 4-2.

In DSM2-Qual, intermediate nodes along a single physical reach (such as nodes 104-112 on Middle River in Figure 4-2) are also treated as BLTM junctions, and parcels passing them are therefore mixed as well. The design imposes the following tradeoff between the accuracy of the flow field and the accuracy of the transport algorithm:
- Flows are delivered from Hydro to Qual only at the upstream and downstream end of each channel, next to map nodes. Thus, in order to deliver sufficient flow detail, more nodes are required.

- Nodes are treated by DSM2-Qual as BLTM junctions, therefore causing mixing of parcels at fairly regular Eulerian intervals and inducing numerical diffusion.

The dense spacing of map nodes was further cemented into practice by the way agricultural (DICU) mass sources and sinks are input, which is only allowed at map nodes. Although we will not pursue the idea further for DSM2-Qual, some of the design could be improved upon by eliminating the large number of intermediate nodes and treating them as tracking points, leaving longer uninterrupted reaches of Lagrangian transport.

Figure 4-2 DSM2 Map Showing Node and Channels for a Region near Clifton Court
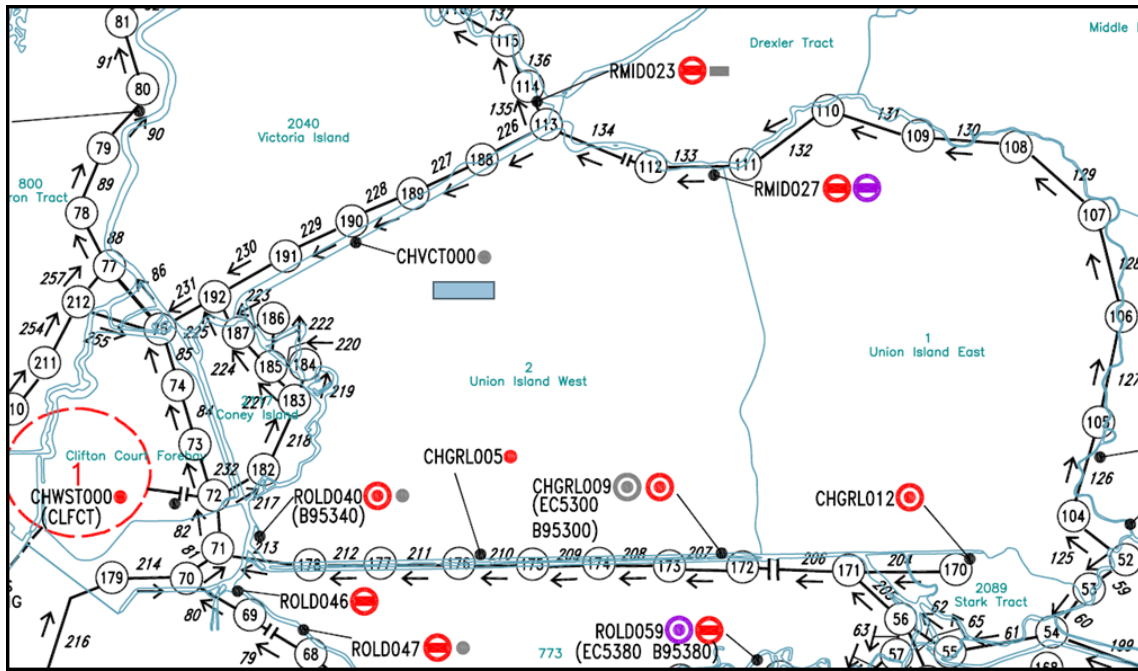
4.4 GTM: An Eulerian One-Dimensional Transport Model

4.4.1 Project Introduction

In a collaborative project with UC Davis, Ateljevich et al. (2011) developed a second order upwind one dimensional Eulerian model of advection, dispersion and reactions or sources. The advective-diffusive part of model describes basic conservative transport, and the generalized reaction term can be tailored to non-conservative water quality kinetics including sediment transport.

In conservative form, the equations read:

$$\frac{\partial\big(A(x,t)C(x,t)\big)}{\partial t} + \frac{\partial\big(A(x,t)C(x,t)u(x,t)\big)}{\partial x} = \frac{\partial}{\partial x}\left(A(x,t)K(x,t)\frac{\partial C(x,t)}{\partial x}\right) + R(x,t,C(x,t)) \qquad \text{Eq. 4-1}$$

Time evolution   Advection   Dispersion   Source/Reaction

where x is the distance, t is time, A is the wetted area, C is the scalar concentration, u is the mean flow velocity, K is the longitudinal dispersion coefficient, and R is the source term (deposition, erosion, lateral inflow, and other forms of sources and sinks). Eq. 4-1 describes the mass conservation of a pollutant in dissolved phase, or suspended sediment away from the streambed.

An operator splitting approach was adopted for the solution, meaning that the advection, dispersion, and reaction processes are integrated sequentially in a specially orchestrated predictor-corrector sequence. The nature of the problem and the importance of the conservation of mass strongly suggested employing a finite volume method (FVM). The algorithms employed for GTM include a second-order two-step unwinding method with van Leer flux limiter for advection.

A software testing framework was also developed for verifying the required accuracy of this solver over an incrementally more complex set of 1-D flows, geometry, spatially varying mixing parameters and combinations of operators. Our testing objective was to verify second-order (or close) accurate scheme in both time and space on nonlinear problems, allowing for some loss of accuracy for problems with more involved boundary conditions or over complex geometry.

Prior work focused on a single-channel, with speculative software "hooks" where the algorithm had to be patched together for use in a network. Much additional work was needed to make the algorithm workable for production modeling in the Delta, including the provision of a flow field from DSM2-Hydro, specification of the behavior at junctions and connection to the DSM2 input system. These topics are sketched below.

4.4.2 Flow and Geometry Transfer from DSM2-Hydro

GTM was designed so that the provision of the flow field and geometry is a swappable role that is not connected to any particular model or input system. We had three different sources in mind:
- Tests, where the flow field can be written as a software function.
- Stored output from DMS2 Hydro using a *tidefile.*
- Direct connection (*in-line)* interaction with Hydro to facilitate longitudinal density effects on momentum and operating rules based on water quality.

Figure 4-3 Illustration of DSM2 Nodes and DSM2-Hydro Computational Points
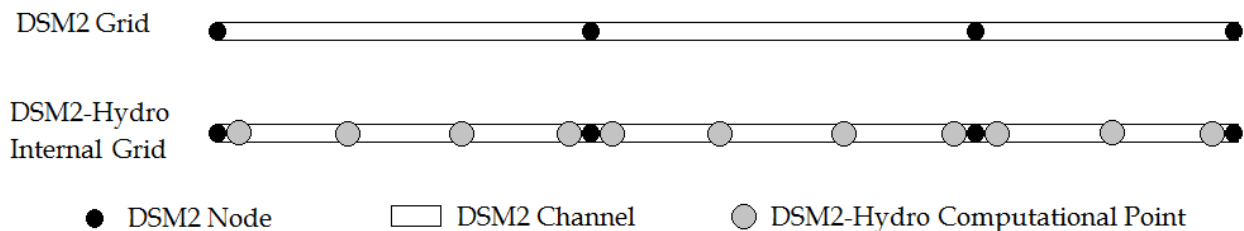
DSM2-Hydro computes hydrodynamics at computational points spaced more densely than the nodes on a DSM2 map (Figure 4-3). By default, the model only writes out hydrodynamics results at the upstream and downstream end of each channel. We have already remarked this imposes an awkward tradeoff in DSM2-Qual between the accuracy of the flow field and that of the transport algorithm, so we now write out and utilize data at every DSM2-Hydro computation point.

In the present project, the tidefile is being expanded to allow a lossless representation in both time and space, without transformation. Tidefile flows in the current DSM2-Hydro are *theta averaged*, a sort of lopsided time average that is related to DSM2-Hydro's stability criterion and sense of mass conservation, but otherwise not particularly desirable or intuitive. These averaged flows cannot be inverted to recover the original instantaneous flows so the new hydro tidefile will only store ordinary instantaneous flow. In terms of memory use, the additional spatial detail represents a 30% to 50% increase in the amount of stored data. The extra space may be recouped to some extent by removing redundant information. For instance, DSM2-Hydro outputs both stage and flow area, but flow area and other geometric quantities can be calculated readily from stage or water surface elevation provided the relevant lookup tables are also included.

Finally, the spatial resolution of GTM is much finer (usually by a power of 2, such as 8 or 16) than that of DSM2-Hydro. Even with a lossless transfer the flow field provided by hydro is incompletely specified and requires interpolation. Our approach starts by interpolating water surface elevation. The area is then calculated based on geometry and water surface. Once area is determined for all grids, flow is obtained by satisfying conservation of mass marching forward in time. A small discrepancy can develop between the flows thus calculated and the value at the next hydro time step, and the residual is redistributed. The accuracy of the scheme is still being evaluated.

4.4.3 Network Considerations

As in the case of DSM2-Qual, an important implementation detail for GTM in the Sacramento-San Joaquin Delta is the method to treat junctions and flow over a network.

Our compatibility conditions at nodes differentiate between true junctions at the confluence of two or more channels (Figure 4-4a) and intermediate nodes along channels (4-4b). Both the advection and dispersion schemes span intermediate nodes without interruption except for the introduction of lateral agricultural sources. Because adjoining channels do not have exactly the same mesh spacing (dx), some modification was required to accommodate discrete changes in the discretization that occur across nodes. The model does not attempt to calculate concentration gradients (ie, it drops from second to first order accuracy) near multi-channel junctions. Incoming water to the junction is completely mixed before being sent on to outgoing channels.

Figure 4-4 Representation of (a) "True Junction" (Node 3) and (b) a String of Intermediate Nodes along a Single Reach
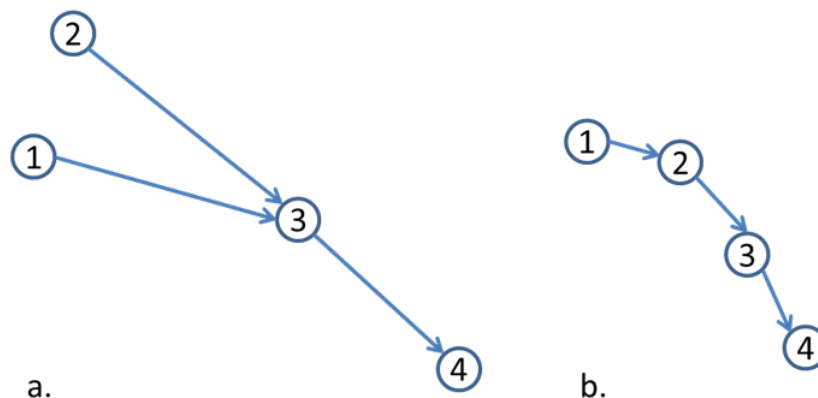
All these treatments are simple. We found it difficult to engineer simple compatibility conditions at these junctions that would work over a broad class of flows, salinity gradients, channel sizes and configurations. We also wished to avoid additional inputs and ad hoc decision making (e.g. to specify the "main channel").

4.5 Other GTM Code Design and DSM2 Integration Considerations

In connecting GTM to DSM2-Hydro, much of the effort has been spent on input and output (I/O) system design, temporal and spatial interpolation, testing, modifications for boundaries, junctions, and reservoirs. A few items are mentioned here that we believe are of interest even in the prototype stage.

4.5.1 User Input and Output

GTM uses the same common DSM2 code for reading and processing data such as the channel network and boundary data. The input system is based on a text reader using keywords that will seem familiar to users of DSM2-Qual. GTM reads in time-varying data from HDF5[4] and HEC-DSS[5]. A few minor additions and modifications have been made, for instance to specify the nominal cell size of the transport model (dx).

GTM will use HDF5 for model output to write the model state at specified intervals in space and time. There will be separate post-processing tools to take care of requests for output in other formats (HEC-DSS or text) at specific locations and for the creation of restart files.

4.5.2 Multiple Interactive Constituents

This transport model has been designed to allow multiple constituents moving at the same time. GTM simulates advection-diffusion, relegating the reactions between constituents to external modules using a design that facilitates synergy between components. The external modules in development include a sediment, dissolved oxygen, temperature, and mercury cycling module.

4.5.3 Courant-Friedrichs-Lewy (CFL) Condition and Subcycling

In transport problems, the CFL condition describes the time step required for stability while solving for advection. For a one-dimensional problem, the CFL condition has the following form:

$$CFL = \frac{u\Delta t}{\Delta x} \leq C_{max}$$

Eq. 4-2

where u is the magnitude of the velocity, Δt is the time step, Δx is the space interval and C_{max} depends on the method used to solve the discretized equation, such as whether the method is explicit or implicit. Typically C_{max}=1 for an explicit solver, which amounts to a fairly mild restriction.

In intuitive terms, the CFL condition for our algorithm says that fluid may not be transported by the mean velocity more than one GTM computational cell in one time step. Since the possibility of this happening somewhere over a large channel network is common and hard to anticipate, most practical models that use explicit time stepping (including the community multidimensional models such as UnTRIM, RMA, SUNTANS, and SELFE) generally use subcycling or sub-time steps: the model is specified in terms of a

---

[4] HDF5 is a portable file format with no limit on the number and size of data objects
[5] HEC-DSS is a data storage system developed by the U.S. Army Corps of Engineers Hydrologic Data Center

nominal (usually coarse) step size that is subdivided adaptively in integer fractions to respond to faster flows.

4.5.4 Unit Testing

Ateljevich et al. (2011) already incorporated software quality and algorithm testing for the solver, both to test components of their algorithm and to verify formal convergence properties of GTM. The testing was done with uniform and reversing flow, and synthetic (analytical) tidal flow for single channel problems of increasing complexity in terms of nonlinearity and spatial variation of parameters. For the integration within DSM2, we are introducing tests both of the I/O system and of the solver at the scale of a full channel network, which may have multiple boundaries, junctions, and reservoirs. Many of these tests are practical in nature, for instance, to validate that the algorithm works symmetrically at a flow split. The only test we have added of a numerical nature is one that verifies the advection component of the algorithm for a channel with a transition in spatial step (dx) near the source of a contaminant plume. The original form of the GTM solver did not include variable spatial steps and it is essential for the way we implemented flow on the DSM2 network.

4.6 DSM2-GTM Test Cases and Results Comparison to DSM2-Qual

We designed a number of simple test cases to evaluate the behavior of GTM over a network and code correctness. In addition, a comparison with DSM2-Qual was of great interest. The hydrodynamics state for these cases are obtained from a DSM2-Hydro tidefile, appropriately formatted for each of the two transport models.

4.6.1 Advection in Uniform Flow along a Reach

The first case is steady, uniform, frictionless flow on a single reach with intermediate nodes. The mesh in this case is a straight long reach with 21 intermediate nodes from the beginning to the end (Figure 4-5). The spacing for those nodes is 5,000 ft. The upstream boundary condition is a uniform flow of 20,000 cfs and the downstream boundary condition is a fixed water elevation 20 ft. The channel area is 20,000 ft^2 over the full reach, yielding a uniform velocity of 1 ft/s. The hydrodynamics were simulated with DSM2-Hydro and verified to reach a steady state. The output was stored in Hydro tidefile, which contains 15-minute flows, water surface time series data and channel geometries.

A triangle shape of initial concentration with a peak of 500 (nominal units) was specified in the middle of the entire network. One ancillary reason for specifying intermediate nodes (besides our interest in their influence) is that DSM2-Qual only allows users to specify constant initial conditions for each channel – there is no control at the parcel level. This means that when we specify an initial condition, it is only correct up to a step-wise representation – a significant impediment to verification work.

Figure 4-5 Test Case for a Single Reach with Intermediate Nodes with Upstream Uniform Flow and Given Initial Concentration in the Middle of Reach
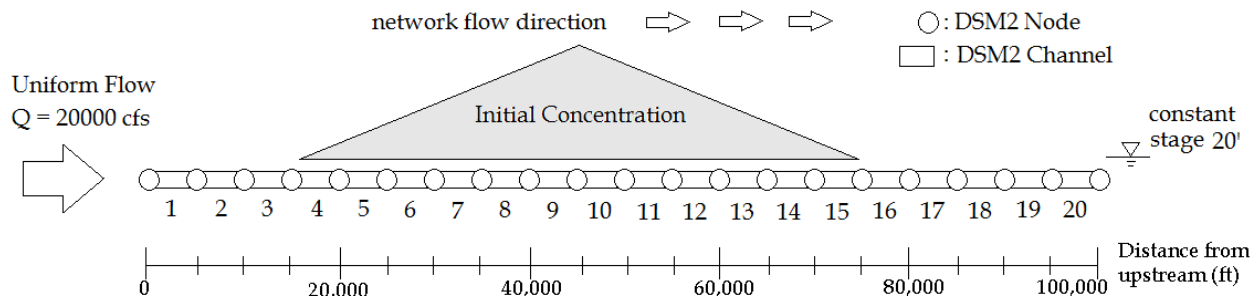
The result from DSM2-Qual is shown in Figure 4-6. The abrupt transitions come from the coarse assignment of initial concentration. Otherwise, the model exhibits the diffusion-free behavior expected of a Lagrangian model in simple flow – the plume keeps its amplitude and shape as it moves down the channel. The result from DSM2-GTM is shown in Figure 4-7 with dx=625 ft, and Figure 4-8 with the number of cells doubled so dx=312.5 ft. There is about a 4% peak reduction when dx=625 ft and the shape is preserved nearly perfectly when dx=312.5 ft. The time steps for the cases of dx=625 ft and dx=312.5 ft are 450 seconds and 225 seconds, respectively, and that makes CFL number 0.72.

Figure 4-6 Results of DSM2-Qual for Advection in Uniform Flow along a Single Reach with Given Initial Concentration in the Middle of Reach
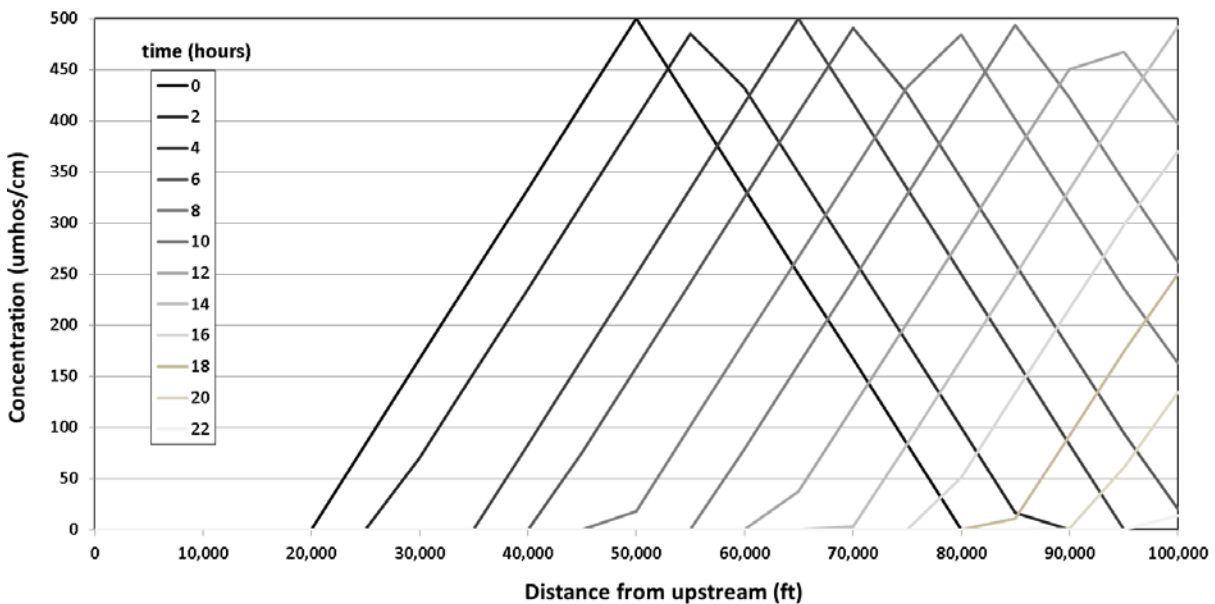
Figure 4-7 Results of DSM2-GTM for Advection in Uniform Flow along a Single Reach with Given Initial Concentration in the Middle of Reach (dx=625 ft)
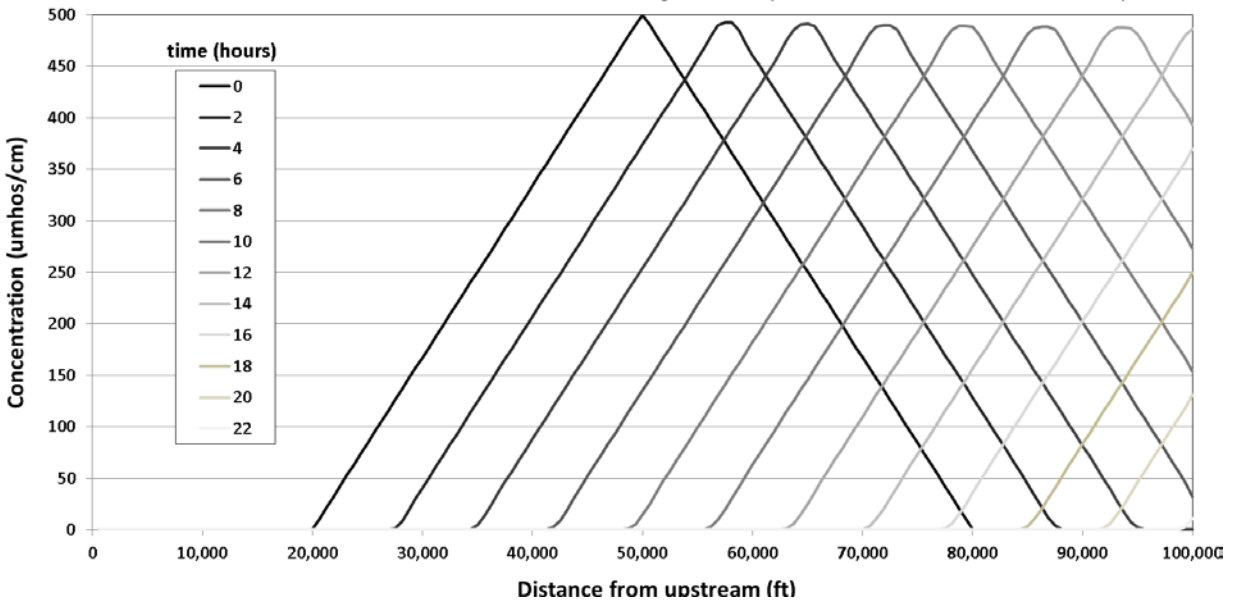
Note: dx=625 ft., dt=450 sec., CFL=0.72

Figure 4-8 Results of DSM2-GTM for Advection in Uniform Flow along a Single Reach with Given Initial Concentration in the Middle of Reach (dx=312.5 ft)
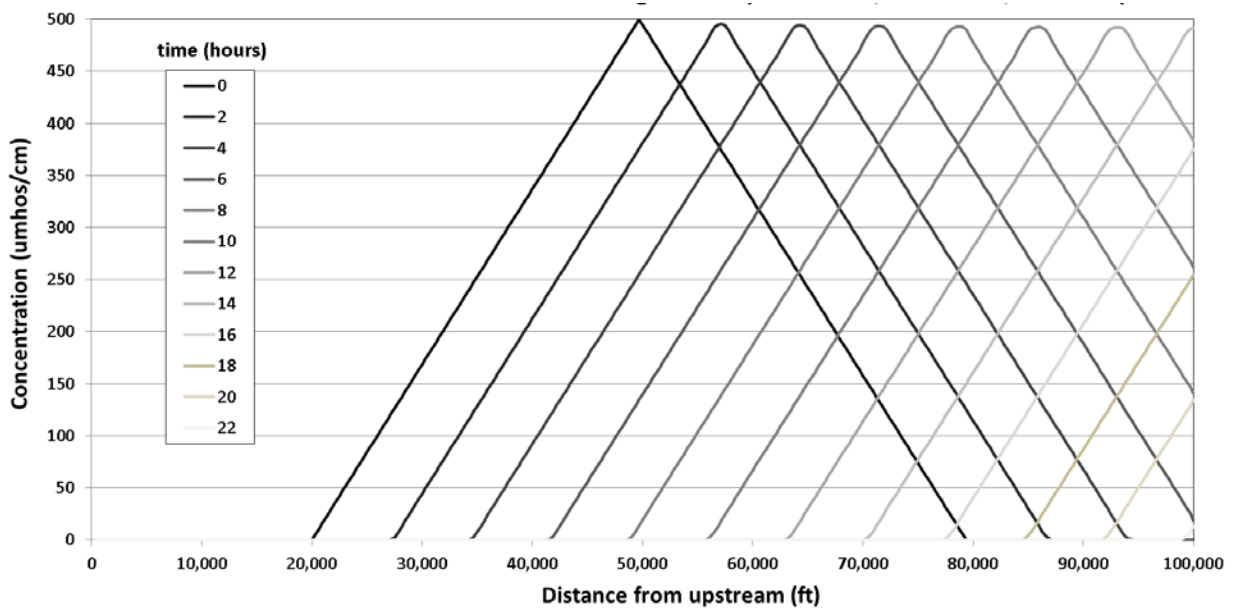
Note: dx=312.5 ft., de=225 sec., CFL=0.72

4.6.2 Advection in Oscillating Flow along a Reach

Our second test investigates the response to a sloshing tidal-like flow in the same channel system as the previous test. We assign zero inflow from upstream and 12-hour sinusoidal oscillation as the downstream stage boundary (Figure 4-9). The hydrodynamics is simulated with DSM2-Hydro until a periodic steady state is observed and the output is stored in Hydro tidefile at a 15-minutes time interval for input to DSM2-Qual and DSM2-GTM. The initial condition is as before but located slightly farther away from the downstream boundary.

Figure 4-9 Test Case for Advection in Oscillating Flow along a Reach with Given Initial Condition
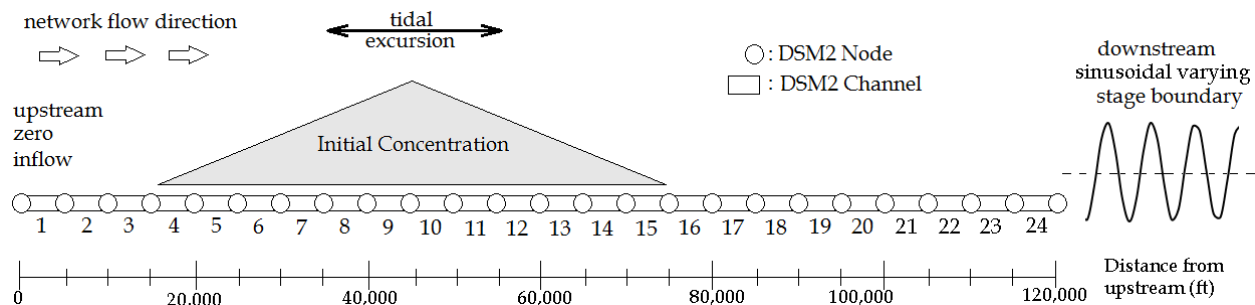
The tidal excursion in this problem is approximately 20,000 feet. Solutions to closed basin problems are usually standing waves with uniform phase over the whole channel, so that after each 12-hour semidiurnal cycle, we expect the plume will return to its initial location. The result from DSM2-Qual is shown in Figure 4-10. After 12 days, the plume still centers on initial location but the peak is reduced by around 9%, which is still a remarkable achievement in this tough test. After one year (Figure 4-11), the amplitude of the plume is deteriorated to half and the location is shifted quite a bit.

The result from DSM2-GTM using the same tidal forcing is shown in Figure 4-12 and Figure 4-13. The peak of the plume reduces around 6% after 12 days of simulation. After one year of simulation, the amplitude remains at 75% value with no significant spatial shift and a slowdown in numerical diffusion.

Figure 4-10 Results of DSM2-Qual for Advection in Oscillating Flow along a Reach after 12 Days of Simulation
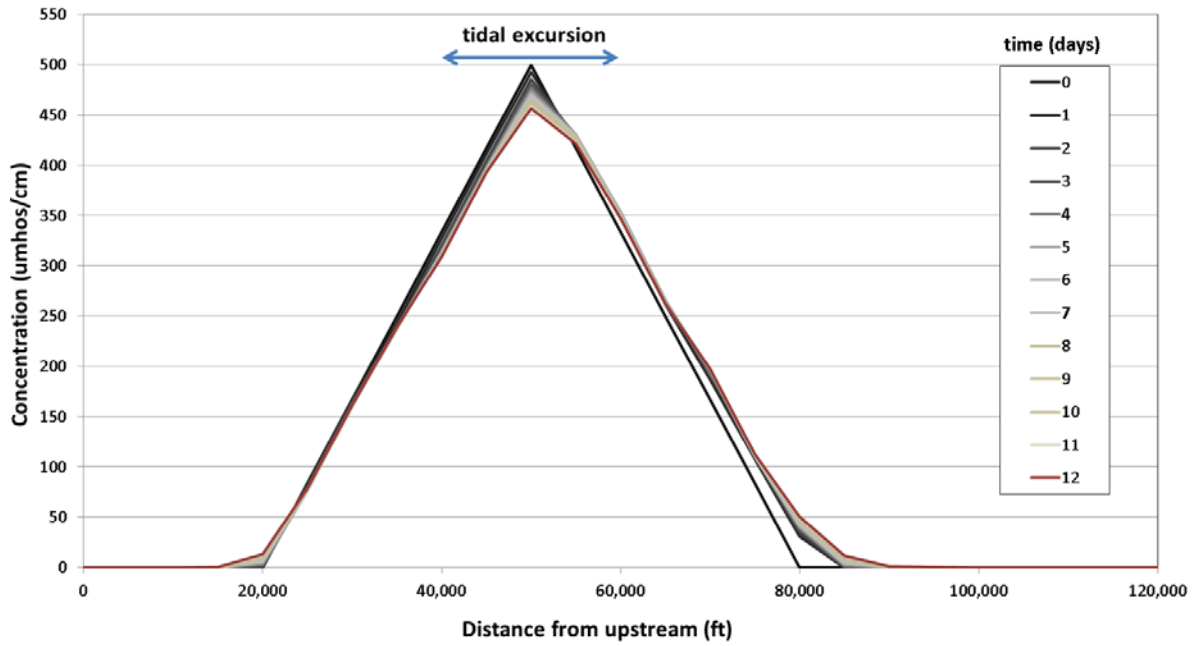
Figure 4-11 Results of DSM2-Qual for Advection in Oscillating Flow along a Reach after One Year of Simulation
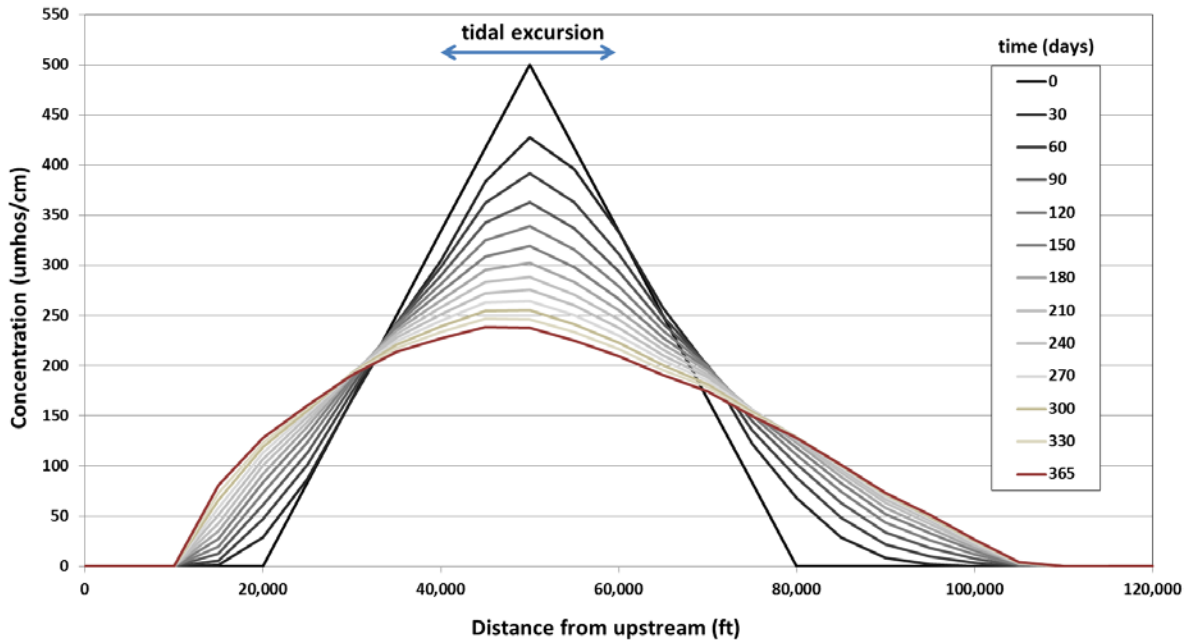
Figure 4-12 Results of DSM2-GTM for Advection in Oscillating Flow along a Reach after 12 Days of Simulation
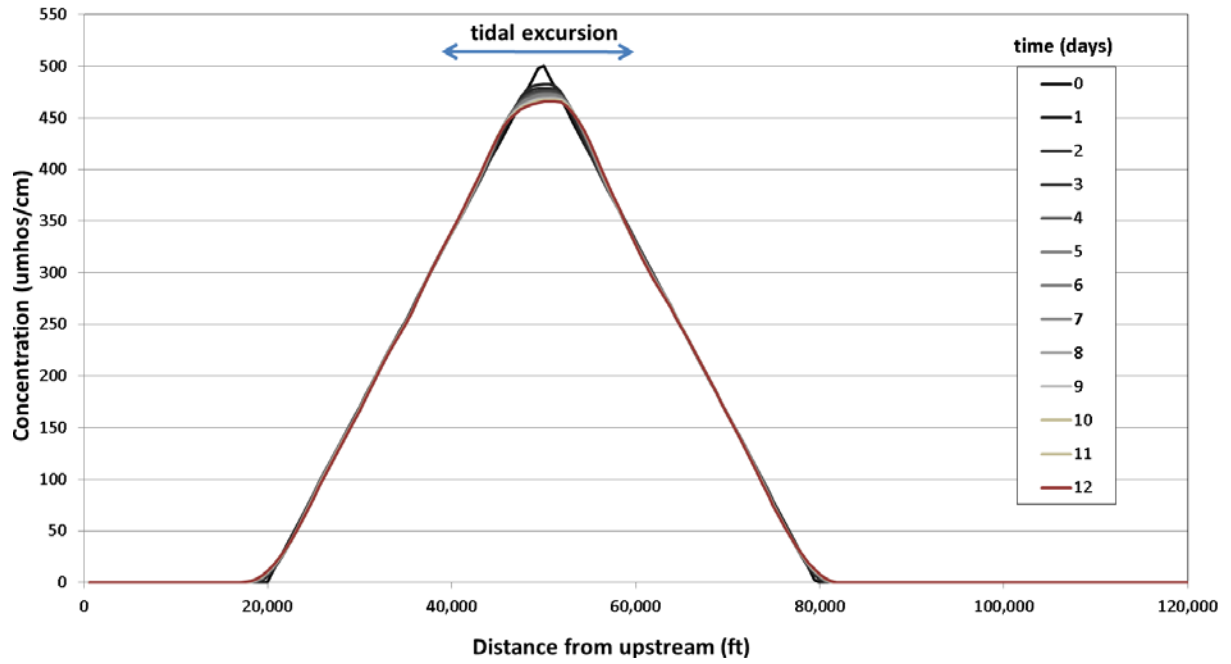
Note: dx=625 ft., dt=180 sec., CFL<0.9

Figure 4-13 Results of DSM2-GTM for Advection in Oscillating Flow along a Reach after One Year of Simulation
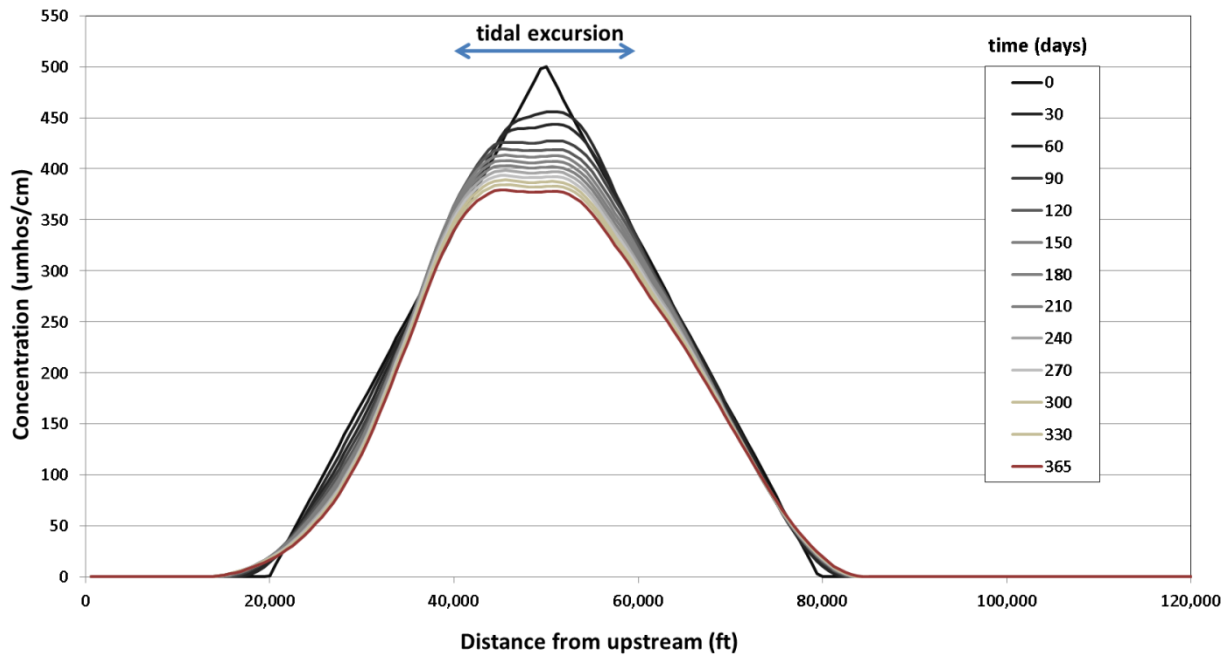
Note: dx=625 ft., dt=180 sec., CFL<0.9

Figure 4-14 Results of DSM2-Qual for Advection in Uniform Flow along a Reach with Given Concentration Boundary Condition
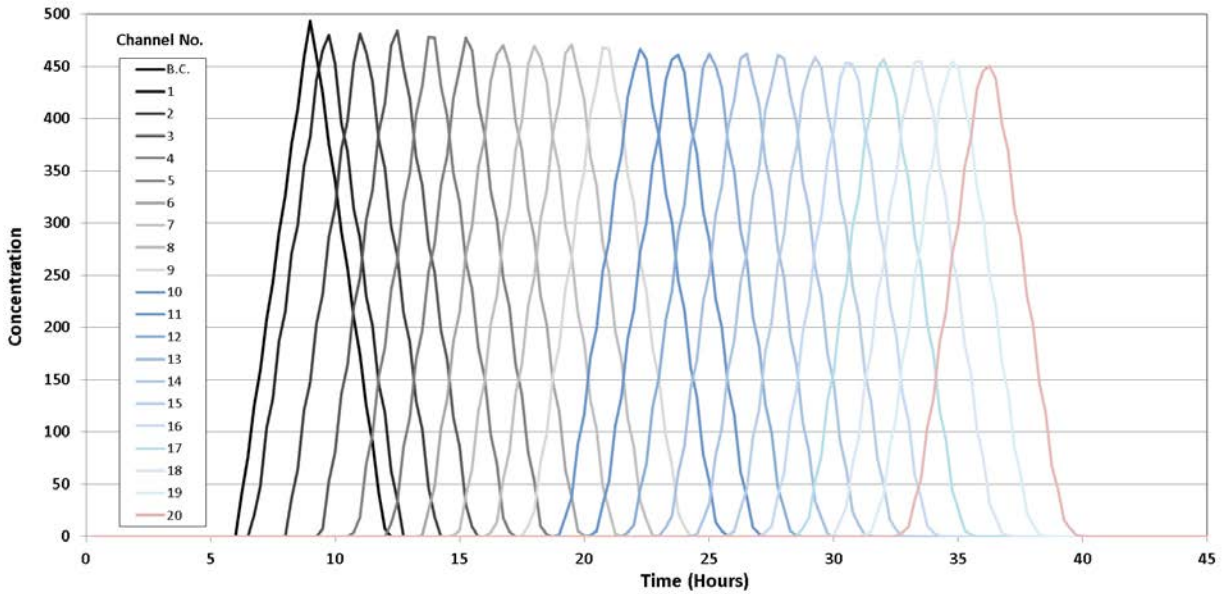
Figure 4-15 Results of DSM2-GTM for Advection in Uniform Flow along a Reach with Given Concentration Boundary Condition
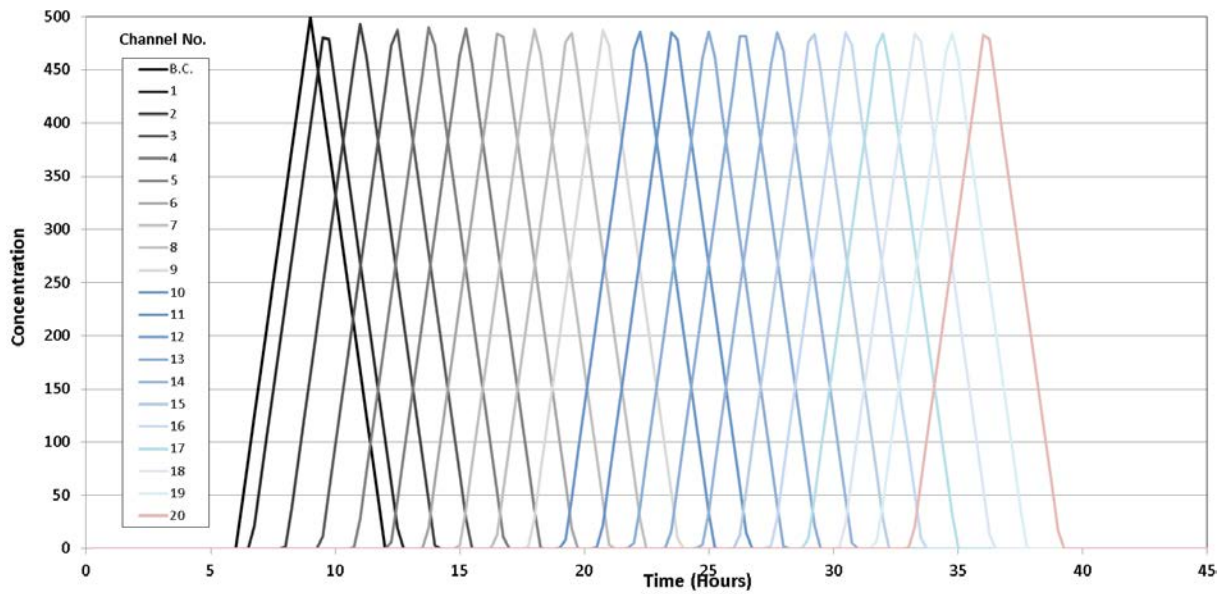
Note: dx=312.5 ft., dt=5 min., CFL=0.96

4.6.3 Advection in Uniform Flow along a Reach with Junctions

In the next test, we compare flow in a single channel to an equivalent problem around a flow split involving several junctions. For the single channel base case, the network is the same as we have used

before (Figure 4-5). Instead of using an initial concentration, we assign zero initial concentration and a time varying boundary condition that produces the same triangular shaped plume with a peak of 500 (nominal units) entering at the upstream boundary. The concentration at each channel over time is shown in Figure 4-14 and Figure 4-15. This gives us a baseline to see the impacts that are introduced by junctions.

Next, we insert a diamond shaped flow divide into the middle of the long channel, creating two divergent and two convergent junctions (Figure 4-16). The problem is otherwise the same as before, with the plume traversing from left to right.

**Figure 4-16 Test Case Design for Junctions with Upstream
Uniform Flow and Concentration Boundary Condition**
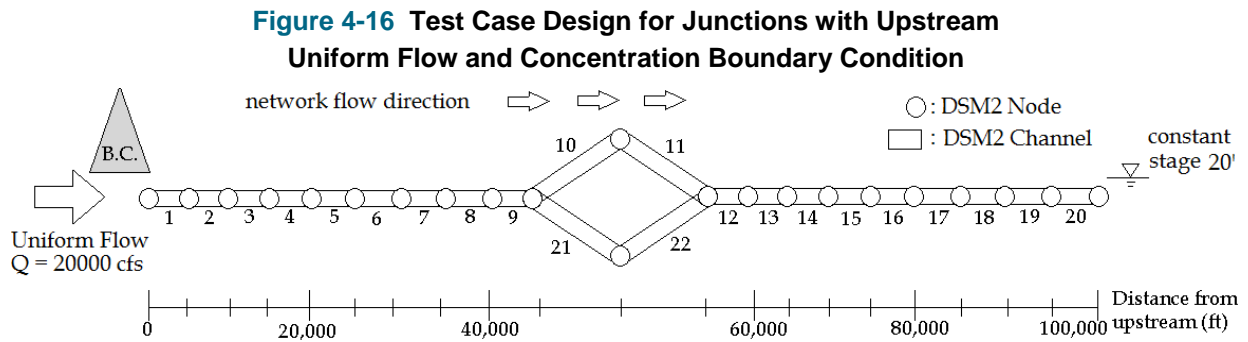
The results from DSM2-Qual and DSM2-GTM are shown in Figure 4-17 and Figure 4-18, respectively. Both of them exhibit good symmetry of transport around the flow divide, with similar concentration for Channels 10 and 21 and for Channels 11 and 22. The large number of nodes introduces visible numerical diffusion into both models, but in different ways. In DSM2-Qual, the attenuation is gradual, reaching 10% by the time flow exits the flow split. The reason for this is that all nodes and junctions are detrimental in Qual, so the flow split is not really a novel feature in terms of error. In DSM2-GTM, we have eliminated a lot of the numerical error at intermediate nodes, so extra attenuation is attributable specifically to the flow splits. The peak drops by 8% which is 3% more than the case without junctions.

Figure 4-17 Results of DSM2-Qual for Advection in Uniform Flow along a Reach with Junctions
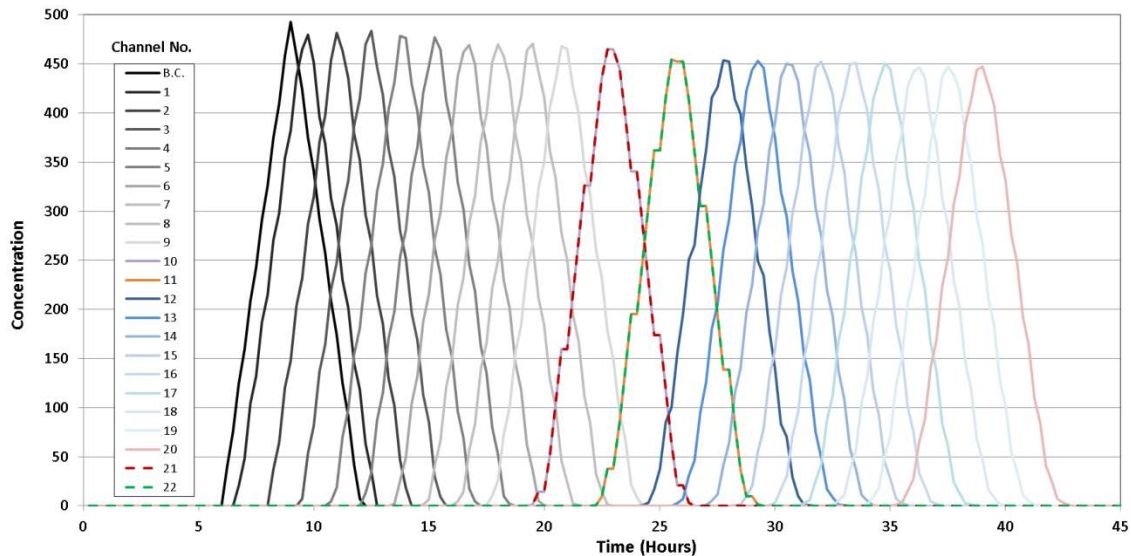
**Figure 4-18 Results of DSM2-GTM for Advection in Uniform Flow
along a Reach with Junctions**
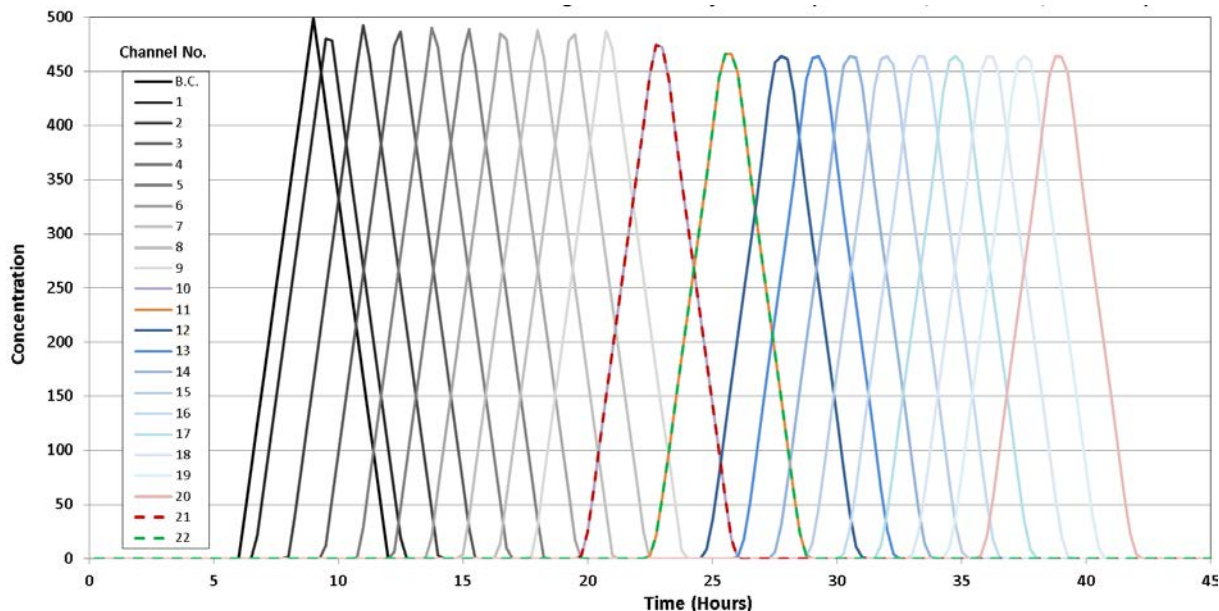
4.6.4 Diffusion and Reaction Tests

The diffusion and reaction components were developed collaboratively with UC Davis and unit tested by Ateljevich et al. (2011) on single channel cases including interaction with advection with time-varying boundaries (which tend to be difficult problems to solve accurately with operator splitting). We have implemented diffusion in the context of DSM2 and network flow, but verified only qualitatively that diffusion works as intended. We are still actively working on compatibility conditions at nodes.

The reaction component solver has also been tested in prior work on complex cases, including stiff reactions and interaction with advection and boundaries. The solver has been connected to GTM, but again like diffusion it has not been extensively tested in the context of a channel network.

4.7 DSM2-GTM Advection Test for a Delta-like Network and Comparison to DSM2-Qual

As a larger scale system test including network geometry, input time series and the Eulerian scheme over the network, we use a simplified synthetic hydrodynamic forcing over the entire Delta.

The DSM2 grid for the Sacramento-San Joaquin Delta is shown in Figure 4-19. The red dots represent DSM2 nodes; blue lines in between are DSM2 channels. Observed 15 minutes historical inflows from February 1, 1998, to March 30, 1998, are imposed at Sacramento, Yolo, Cosumnes, Mokelumne, Calaveras, and Vernalis. Historical water levels are imposed at Martinez. A triangle-shaped boundary concentration with a peak of 500 umhos/cm and 6-hour span is specified at Sacramento and zero initial concentration is specified across the entire grid. Hence, the problem has tidal character as far as the flow field but the tracer being modeled is not similar to salt in that it propagates from the upstream boundary.

The results from DSM2-Qual and DSM2-GTM are shown in Figure 4-20 and Figure 4-12, respectively. In both cases the plume is considerably diluted as it makes its way downstream, a phenomenon that is certainly influenced both by tidal mixing and numerical diffusion. Travel time and the modes of the plumes coincide reasonably well at many stations, with disagreement growing with travel time. Overall, the GTM result is the less attenuated one at most sites, but this generalization is not universal.

Figure 4-19 Test Case for Delta-like Grid with Observed Inflows and Tidal Stage at Martinez
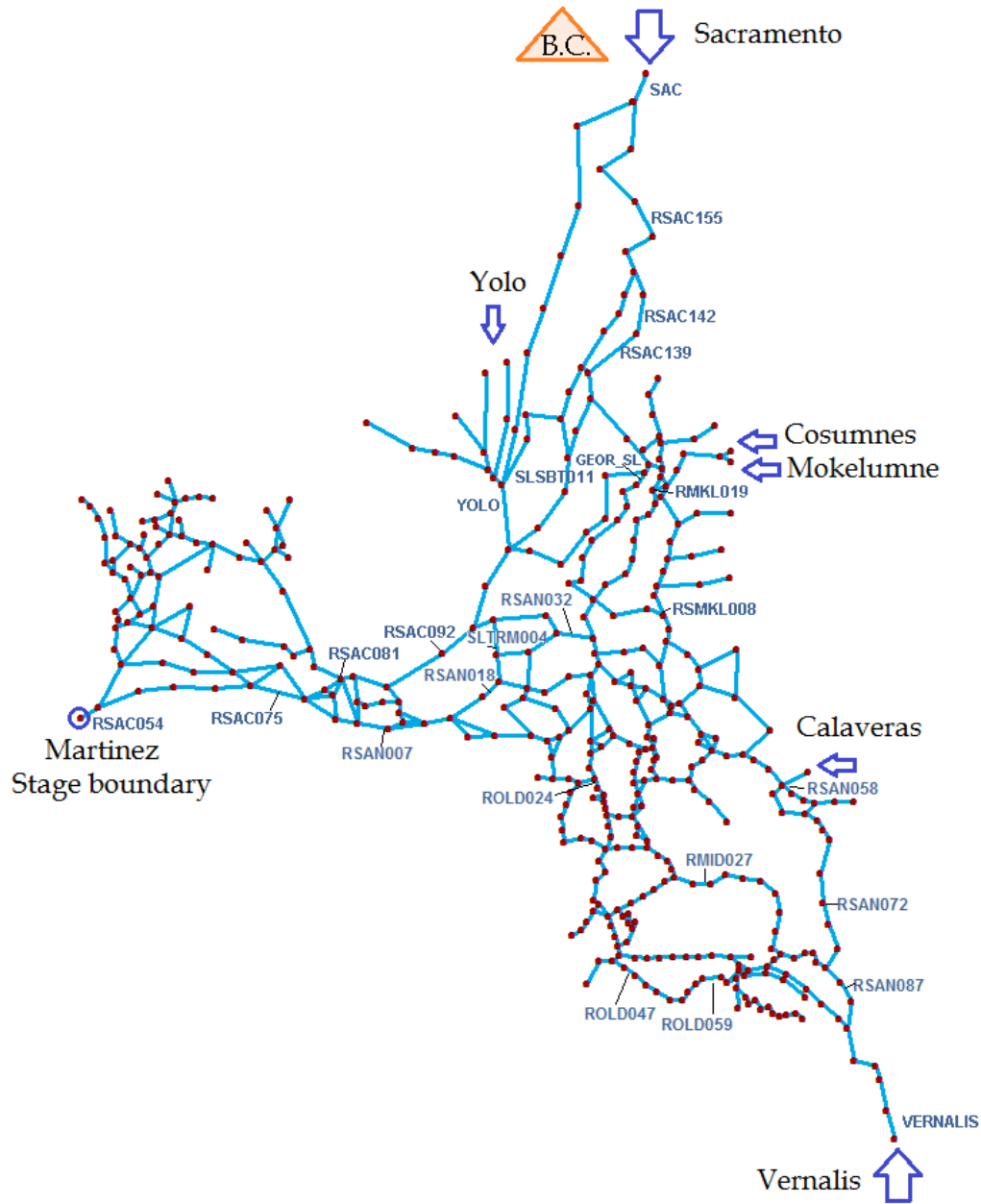
name	location	name	location
SAC	Sacrmaneto River upstream	SLTRM004	San Joaquin River at Three Mile Slough
RSAC155	Sacramento River at Freeport	RSAC092	Emmaton
RSAC142	Sacramento River at Hood	RSAC081	Collinsville
RSAC139	Sacramento River at Green's Landing	RSAC075	Mallard Island
SLSBT011	Steamboat Slough	RSAC054	Martinez
GEORG_SL	Georgiana Slough	RSAN032	San Andreas Landing
RMKL019	North Fork Mokelumne River	RSAN018	Jersey Point
YOLO	Yolo Bypass	RSAN007	San Joaquin River at Antioch
RSMKL008	South Fork Mokelumne at Staten Island		

Figure 4-20 Results of DSM2-Qual for Entire Delta with Observed Inflows and Stage at Martinez
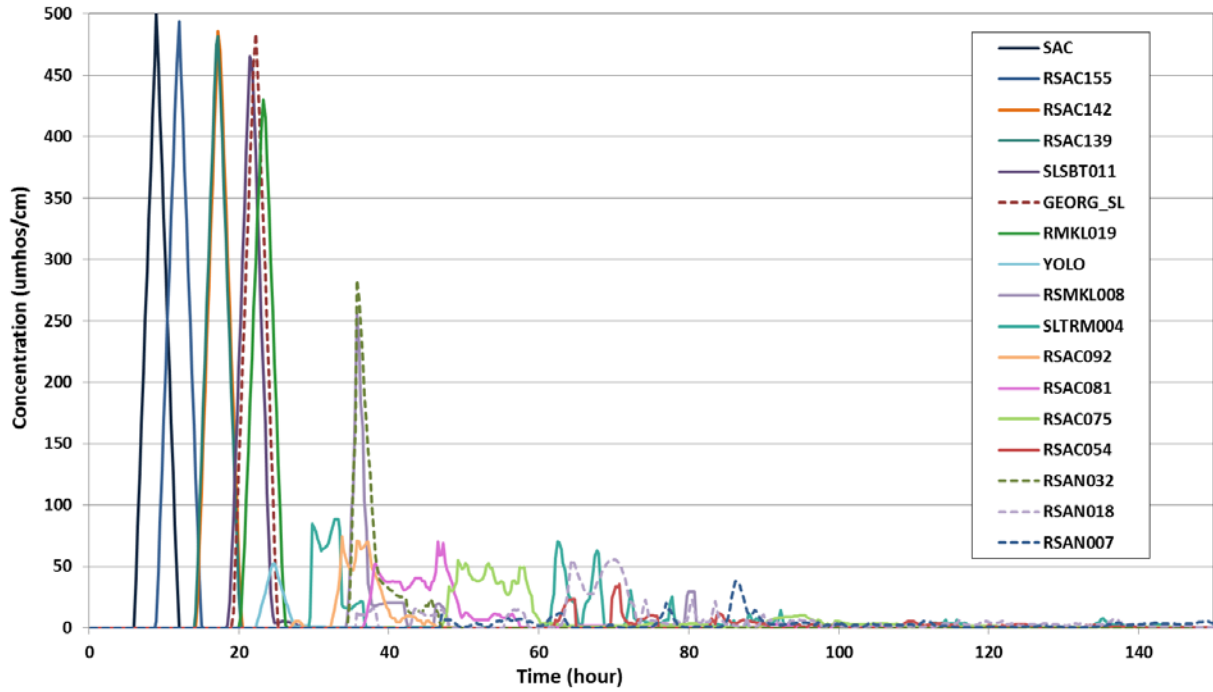
Figure 4-21 Results of DSM2-GTM for Entire Delta with Observed Inflows and Stage at Martinez
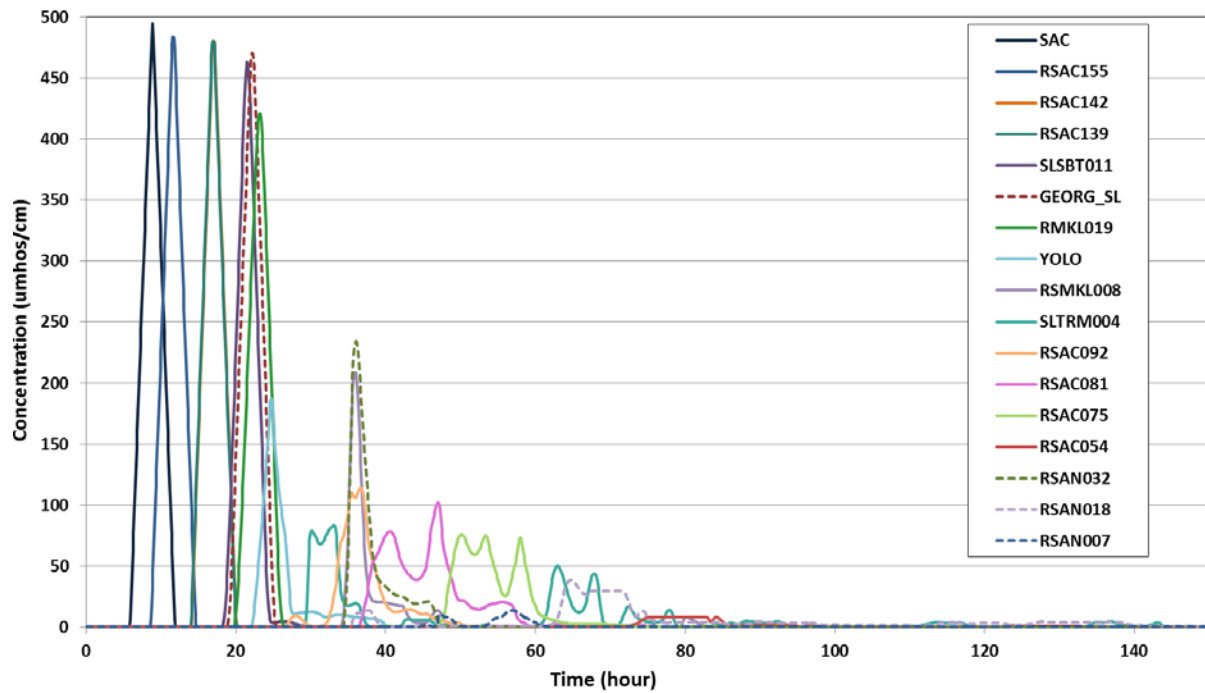
4.8 Summary

1. DSM2-GTM accomplishments thus far include integration of GTM into DSM2, accommodating special features (boundaries, junctions, etc.), and successful simulation of advection over a full Delta using a full cycle of DSM2-Hydro and DSM2-GTM.
2. Test results indicate GTM simulates transport well for either uniform or tidal flow. Eulerian spatial referencing offers convenience and extensibility.
3. The computational code in GTM has been verified rigorously in a repeatable framework.
4. Tests indicate DSM2-Qual exhibits significant numerical dispersion when a plume travels through a reach with many intermediate nodes, yet an artificial tradeoff exists whereby such intermediate nodes are required for flow field accuracy. DSM2-GTM is less impacted by such nodes.
5. We have implemented diffusion and generic reactions in GTM. These processes have been thoroughly tested in prior work, including some thorny operator splitting issues associated with boundaries.
6. Preliminary results for a Delta-scale problem without reservoirs indicate GTM is comparable to DSM2-Qual in performance and gives reasonable results.
7. Simultaneous, ongoing work is being conducted on coupled mercury and sediment interaction.

4.9 Acknowledgements

We want to acknowledge Fabian Bombardelli and Kaveh Zamani from UC Davis for their roles in the initial development of the GTM solver and testing system. We thank Ralph Finch and Lianwu Liu for their helpful descriptions of aspects of DSM2-Hydro and DSM2-Qual.

4.10 References

Ateljevich, E., Anderson, J., Zamani, K. and Bombardelli, F.A. (2011). Using Software Quality and Algorithm Testing to Verify a One-dimensional Transport Model. Methodology for Flow and Salinity Estimates in the Sacramento-San Joaquin Delta and Suisun Marsh, 32th Annual Progress Report.

Bay-Delta Office, California Department of Water Resources (1998). DSM2 Qual. Methodology for Flow and Salinity Estimates in the Sacramento-San Joaquin Delta and Suisun Marsh, 19th Annual Progress Report, Chapter 3.

Bay-Delta Office, California Department of Water Resources (1998). DSM2 Input and Output. Methodology for Flow and Salinity Estimates in the Sacramento-San Joaquin Delta and Suisun Marsh, 19th Annual Progress Report, Chapter 5.

Browns, L.C. and Barnwell, T.O. (1987). The Enhanced Stream Water Quality Models QUAL2E and QUAL2E-UNCAS: Documentation and Users Manual. U.S. EPA, Athens, Georgia, EPA 600/3-87/007.

Colella, P., Puckett, E. G. (1998). Modern Numerical Methods for Fluid Flow, UC Davis Class Note.

Fischer, H.B., List, E.T., Imberger, J. and Brooks, N.H. (1979). Mixing in Inland and Coastal Waters. Academic Press, New York.

Jobson, H.E., and Schoellhamer, D.H. (1987). Users Manual for a Branched Lagrangian Transport Model. U.S. Geological Survey, Water Resources Investigation Report 87-4163.

Jobson, H.E. (1997). Enhancements to the branched Lagrangian Transport Modeling System. U.S. Geological Survey, Water Resources Investigations Report 97-4050.

Liu, L., Ateljevich, E., Sandhu, P. (2012).Improved Geometry Interpolation in DSM2-Hydro. Methodology for Flow and Salinity Estimates in the Sacramento-San Joaquin Delta and Suisun Marsh, 33th Annual Progress Report.

Saltzman, J. (1994). An Unsplit 3D Upwind Method for Hyperbolic Conservation Laws. Journal of Computational Physics, Vol. 115, pp. 153-168.

Van Leer, B. (1997). Towards the Ultimate Conservative Difference Scheme, IV. A New Approach to Numerical Convection. Journal of Computational Physics, Vol. 23, pp. 276-299.

Chapter 5.   Automation of Spatial Map with Temporal Data from DSM2-QUAL Output using ArcGIS

5.1 Introduction

This chapter presents a new post-processing tool for DSM2-QUAL output which enables generation of ArcGIS geo-referenced contour maps and time-varying animations to visualize water quality distributions in the Sacramento-San Joaquin Delta area.

5.2 Methodology

DSM2-QUAL output includes a DSS[6] time series for specified locations in the Delta. The new tool extracts simulated water quality data throughout the Delta, couples with geo-referenced coordinates, and interpolates the data to create continuous contour maps. The tool then generates animations or user-specified sets of static contours for comparing simulated scenarios. This process is shown in Figure 5-1.

Figure 5-1 Flow Chart of Methodology

---
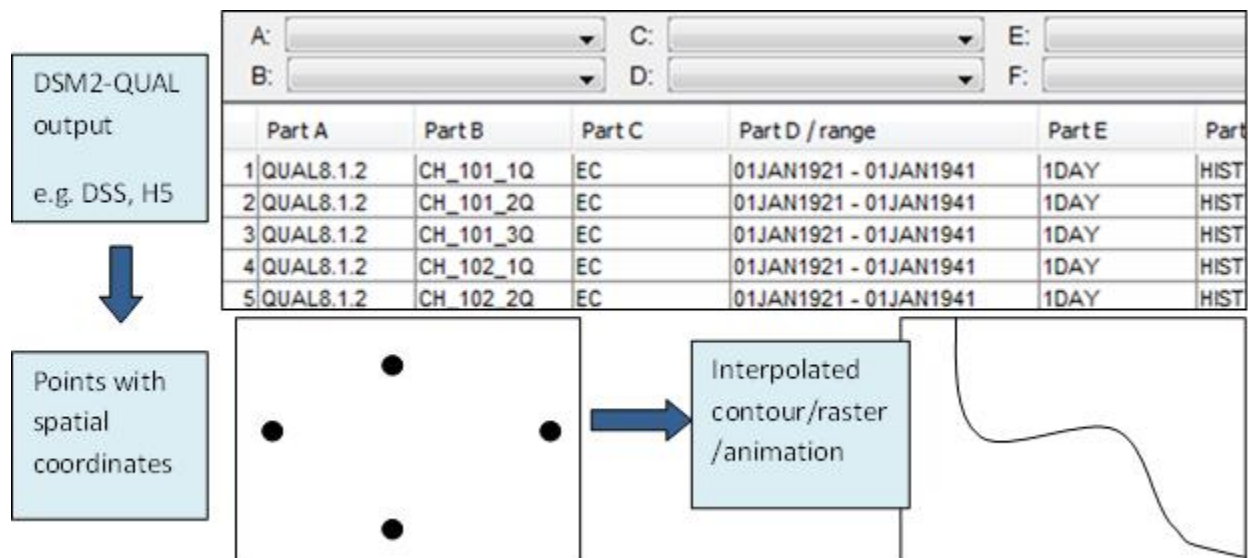
[6] U.S. Army Corps of Engineers Hydrologic Engineering Center Data Storage System (HEC-DSS) is a file type/database that stores scientific information.

5.2.1 Spatial Network of the Delta

In order to generate a meaningful continuous surface map, a geo-referenced fine grid network of DSM2-Qual output locations was developed based on the standard DSM2 Delta grid. This network uses locations in DSM2 channels rather than nodes to avoid situations in which multiple channels converge at one node. Figure 5-2 (a) shows an example of where Channels 374, 364, 347, 348 could have different water quality values approaching node 271.

The proposed network is three times denser than the DSM2 standard Delta grid in order to accommodate the situation when adjacent channels are close to each other in DSM2, a 1-dimensional model. Figure 5-2 (b) shows Channel 426 and 370 are very close, yet water in the channels originates from different sources. These channels' water quality values should be interpolated based on their upstream and downstream channels, not from their parallel neighbors, no matter how close they are.

Figure 5-2 **Examples of DSM2 Grid**
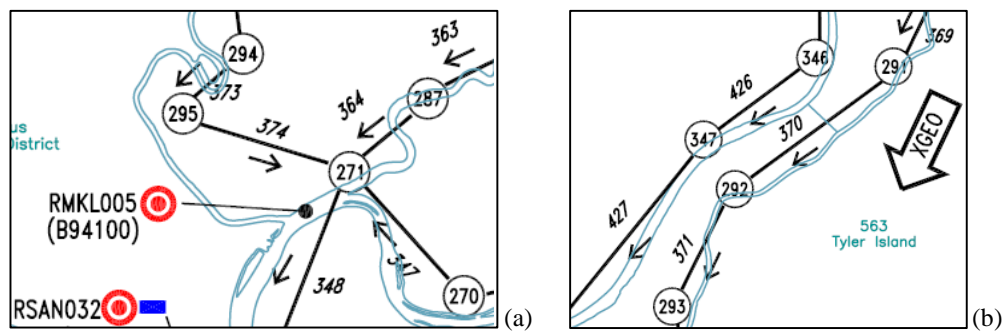
The process then established a Delta network template with 1,551 points from 517 DSM2 Delta channels, the points being located at one-fourth, one-half, and three-fourths of the channel lengths. All the network points were coupled with their longitudinal and latitude (X, Y) coordinates, in the spatial reference of NAD_1983_UTM_Zone_10N (Figure 5-3 and Figure 5-4 (a)).

5.2.2 Temporal Data Extraction and Conversion

The tool enables users to easily investigate the spatial distribution of Delta water quality at user-specified dates for multiple DSM2 simulations.

The simulated water quality data are first extracted from DSM2-QUAL output DSS file, converted to a 2-D data matrix in a text file, then imported into ArcGIS to create a point feature layer. Vtools[7] was used in this process. Figure 5-3 shows the attribute table of an imported point group in ArcGIS.

---

[7] Python library of DSS manipulation developed by DWR's Bay-Delta Office

Figure 5-3 Sample ArcGIS Point Feature Coupled with XY Coordinates, and Temporal EC Data

OBJECTID *	chan	pos	x_utm83	y_utm83	ec220903	ec230831	ec240828	ec250906	ec260827
1	1	ch_1_2q	652934	4172956.1	811.1	800.9	1254.5	1188.5	1264.7
2	2	ch_2_2q	652358.2	4175095.8	811.1	800.9	1251.5	1189.3	1320.6
3	3	ch_3_2q	651119.9	4176021.1	811	800	1286.3	1185.3	1338
4	4	ch_4_2q	649789.4	4177816.7	811	800	1341.9	1156.3	1335.6
5	5	ch_5_2q	649700.1	4180660.5	811	799.9	1338.1	1030.2	1324.2
6	6	ch_6_2q	649407.1	4182886.5	812	799.7	1290.3	1019.7	1302.2
7	7	ch_7_2q	648143.8	4184494.4	823.5	796.2	1297.5	1080.4	1214.4
8	8	ch_8_2q	648008.8	4186110.6	831.4	779.7	1384.2	1107.5	1101.8
9	9	ch_9_2q	648239.7	4188170	825.2	771.2	1584.5	1075.8	986.8

5.2.3 GIS Spatial Interpolation

The spatial analyst function "kriging'" of ArcGIS is used to create interpolated raster images. Kriging is an advanced geostatistical procedure that generates an estimated surface from a scattered set of points with z-values. It is based on statistical models that include autocorrelation, that is, the statistical relationships among the measured points. (How Kriging works, Kriging in Geostatistical Analyst).

The spatial analyst function 'contour list' is then used to create specified contours from the interpolated raster images (How Contouring works). Users are able to specify any data ranges (e.g. EC levels of 2,640 us/cm or 75% volume water from Sacramento River).

Figure 5-4 Interpolation of ArcGIS to Generate Contours and Colored Raster from Geo-Referenced Points

(a) EC distribution   (b) Interpolated raster   (c) Contours
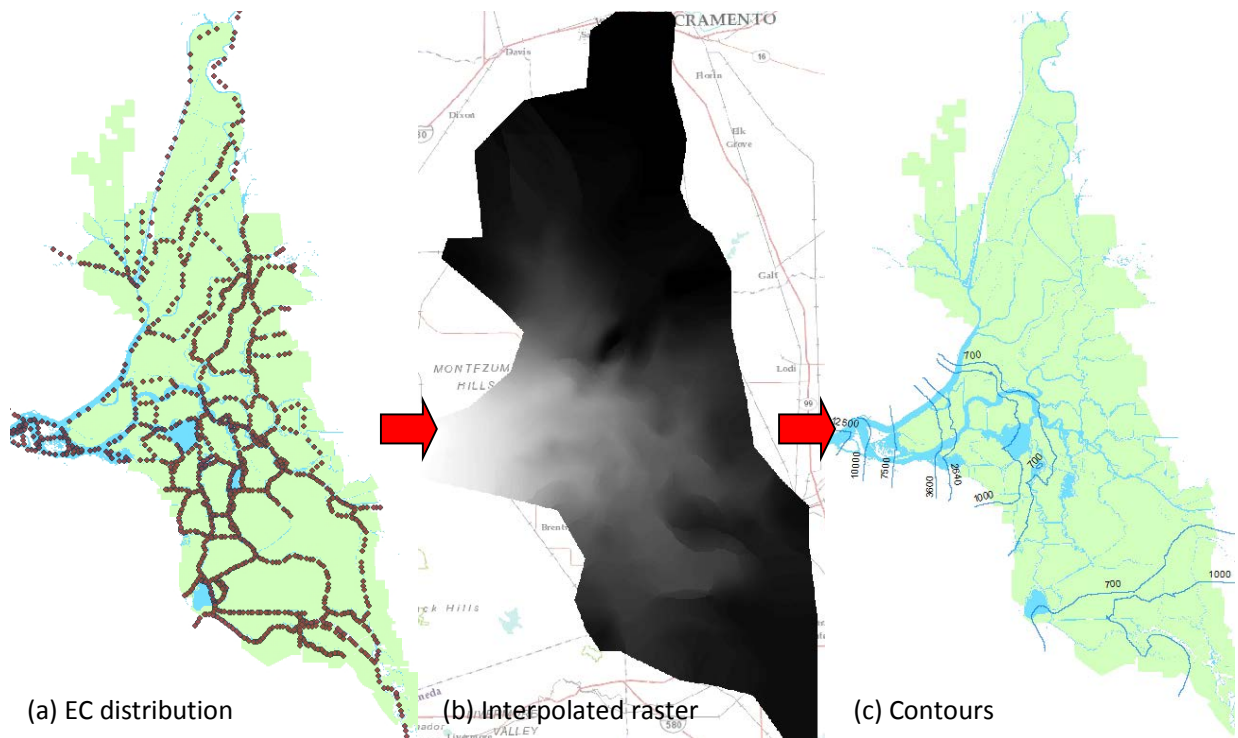
5.2.4 GIS Visualization of Temporal Data

ArcGIS 10 and higher versions have a "time-enable" feature, which can visualize data changes over time in ArcMap. For the two types of map objects, ArcGIS has different ways to process:

- Contours (vector maps) are combined into a summarized polylines feature (Figure 5-5)
- Raster images (color band maps) are combined into a mosaic dataset (Figure 5-6).

Figure 5-5 Sample GIS Vector Feature with Extracted Contours from Specified Times
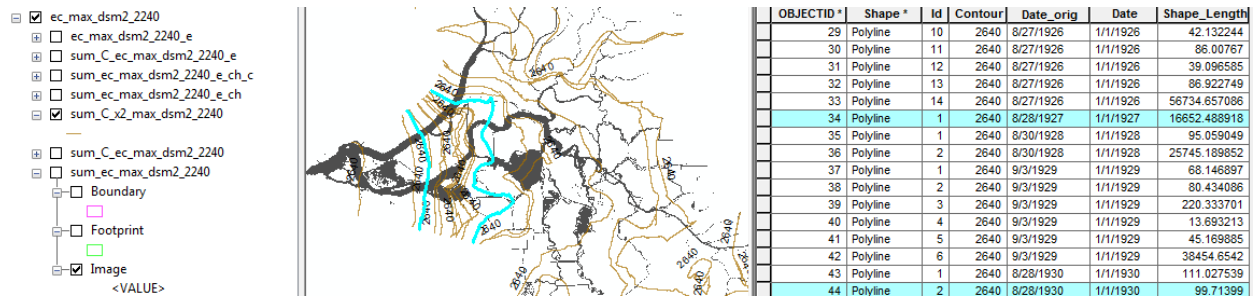
The new tool described in this chapter utilizes Python scripts to automate assignment of time features to the generated maps and combine them into user defined groups, in the format of geodatabase provided by ArcCatalog. Time Property Tab and Time Slider are used to control, display, and export the designed temporal maps.

Figure 5-6 Sample GIS Mosaic Feature with Extracted Raster Images from Specified Times
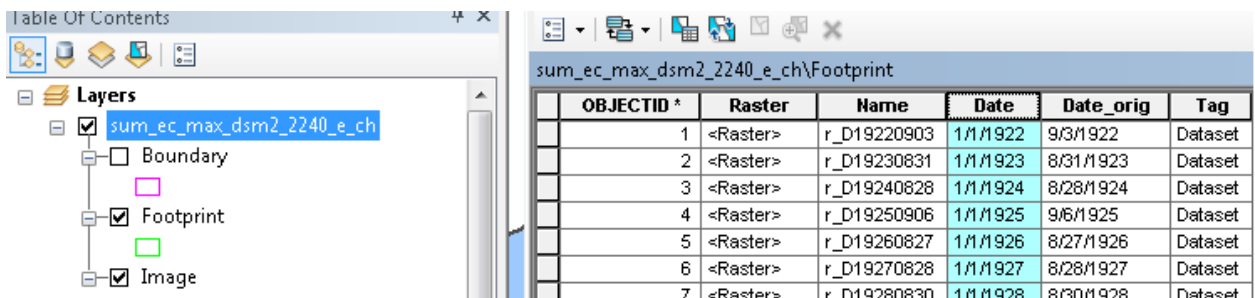
5.3 Sample Applications

The tool has been used to help analysis of possible 2014 drought scenarios. It was applied to the water quality output from simulations of various 2014 drought forecasts and historic drought events pre- and post-SWP installation and operation. In particular, the periods of 1976-2012 and 1922-1940 were studied. Detailed maps and animations of the corresponding outputs have been placed on DWR Portal online folder at: http://baydeltaoffice.water.ca.gov/downloads/DSM2_Users_Group/DSM2_QUAL_spatial/

Figure 5-7 Sample Presentations of the Areal Distribution of Water Quality in the Delta

(a) EC distribution in channels   (b) EC affected regions   (c) volumetric fingerprint
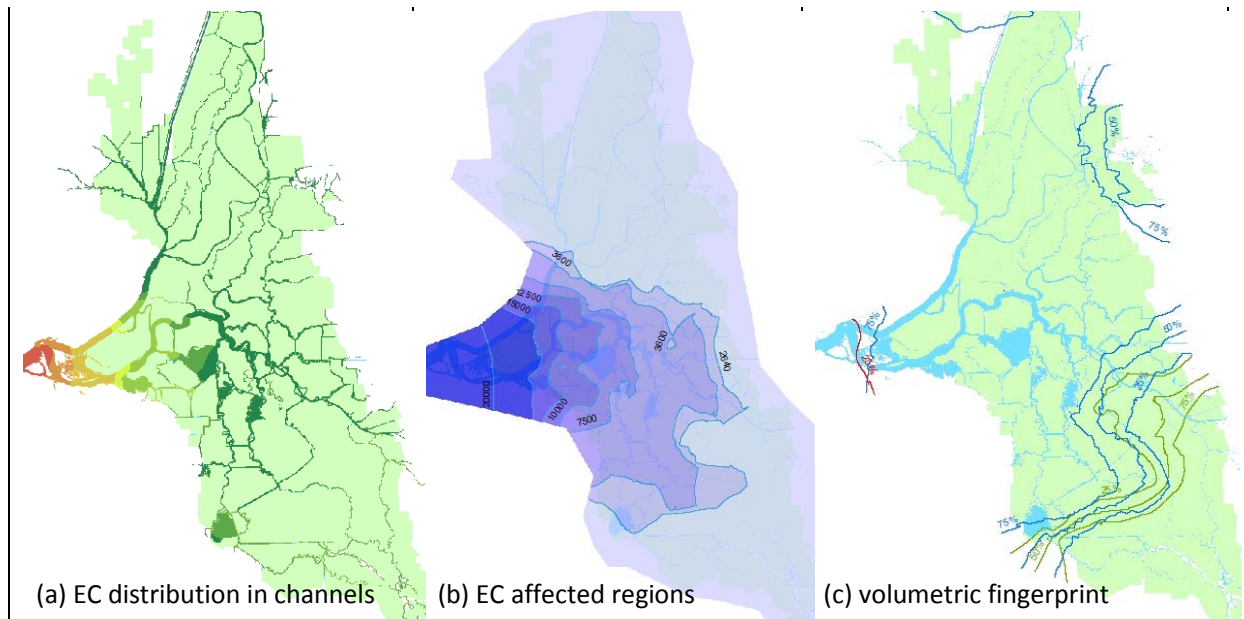
5.3.1 Water Quality

The major application of the designed tool is to display the spatial distribution of Delta water quality. Salinity (in terms of EC) is a key parameter. Figure 5-7 (a) shows a typical way of presenting the EC distribution within Delta channels, with colors red to green, to display salinity level from high to low. Figure 5- 7 (b) shows another way of presenting EC, based on the new tool.

5.3.2 Fingerprint of Water Volume and Constituents

DSM2-Qual can generate constituent and volume fingerprints which show the contribution of various sources in the Delta (Anderson, 2002). The new tool can also display the distribution of different sources of water or constituent in various combinations. Figure 5-7 (c) provides a sample contour map with a volumetric fingerprint from sources of Martinez (red contours), the Sacramento River (blue contours), and the San Joaquin River (green contours), with their respective contributions of 25%, 50%, and 75%.

5.3.3 Other Functions Extensions

ArcGIS provides a powerful and well-established platform to spatially analyze DSM2-Qual output, such as comparing different scenarios, comparing to other geo-referenced data such as observed data, spatial analysis, etc.

Figure 5-8 (a) displays the comparison of maximum yearly X2 intrusion of some historical drought years, as well as the recent 20 years and 2 forecast scenarios in 2014. Figure 5-8 (b) displays the comparison of Delta islands acreage affected by yearly maximum salinity intrusion for the periods of 1991-2009 (after project) and 1922-1940 (pre-project).

**Figure 5-8 Sample Map of Maximum Salinity Intrusions
of Different Drought Years Using DSM2 Simulation**
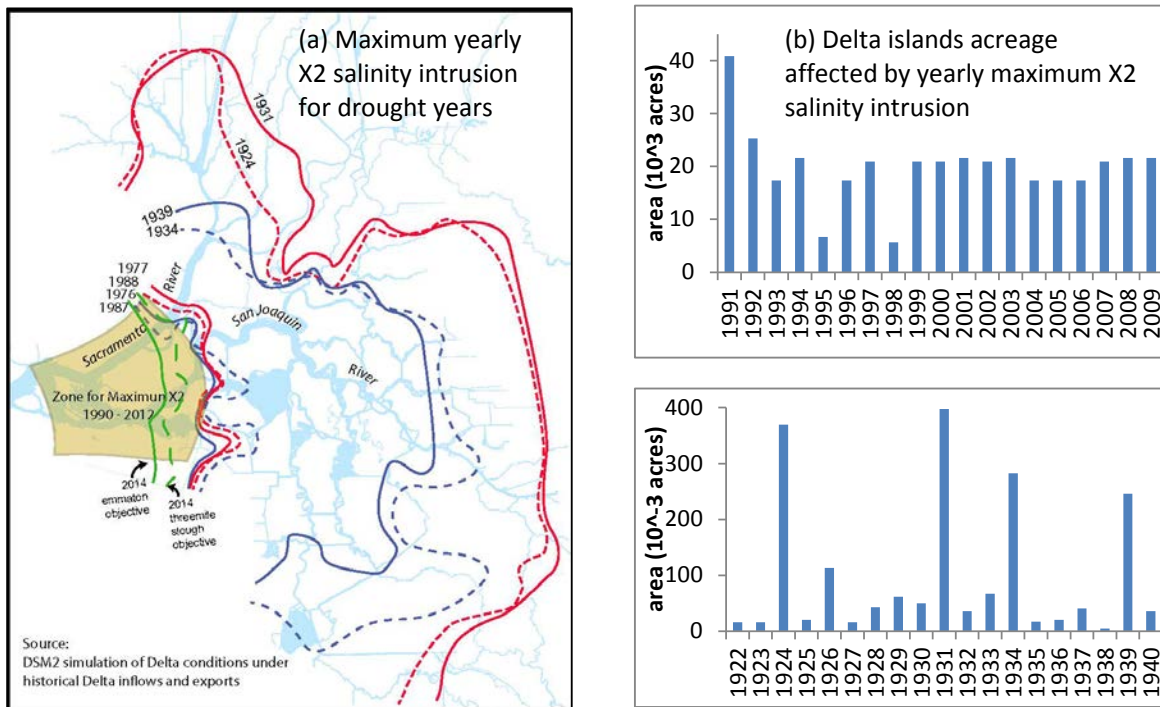
5.4 Summary and Future Work

A new tool uses ArcGIS, Python scripts, and DSM2-QUAL output to generate static or dynamic Delta-wide contours of DSM2-generated water quality parameters. This tool can help users:

- directly investigate the distribution of water quality in the Delta,
- better visualize model output for specified time period,
- identify the areal extent of the Delta affected by changes in water quality due to changes in hydrology, Delta geometry, or barrier installation and operation,
- compare scenarios or different years from another perspective, and
- validate the water quality model from another perspective, particularly under low Delta outflow conditions.

Future work will use geo-referenced Delta agriculture diversion locations in order to refine estimation of impact to Delta agriculture under significant salinity intrusion.

5.5 Acknowledgements

Lan Liang provided important help in the study and report revision.

5.6 Reference

Anderson, J. (2002). Chapter 14, DSM2 Fingerprint Methodology. *Methodology for Flow and Salinity Estimates in the Sacramento-San Joaquin Delta and Suisun Marsh, 23rd Annual Progress Report.*

How Contouring works. (n.d.). Retrieved from ArcGIS Help 10.1:
http://resources.arcgis.com/en/help/main/10.1/index.html#/How_Contouring_works/009z000000
vq000000/

How Kriging works. (n.d.). Retrieved from ArcGIS Help 10.1:
http://resources.arcgis.com/en/help/main/10.1/index.html#//009z00000076000000

Kriging in Geostatistical Analyst. (n.d.). Retrieved from ArcGIS Help 10.1:
http://resources.arcgis.com/en/help/main/10.1/index.html#//003100000032000000

Chapter 6. Delta Modeling for Emergency Drought Barriers

The National Weather Service reported that in California, 2013 was the driest calendar year on record. By mid-January 2014, very little precipitation had occurred across California. The statewide precipitation value was 0.10 inches (with an average January experiencing around 3 inches of rain). Reservoir storage levels, shown in Figure 6-1 for January 15, were well below the historical average for that day.

Figure 6-1 DWR's California Data Exchange Center Reservoir Storage Graph January 15, 2014
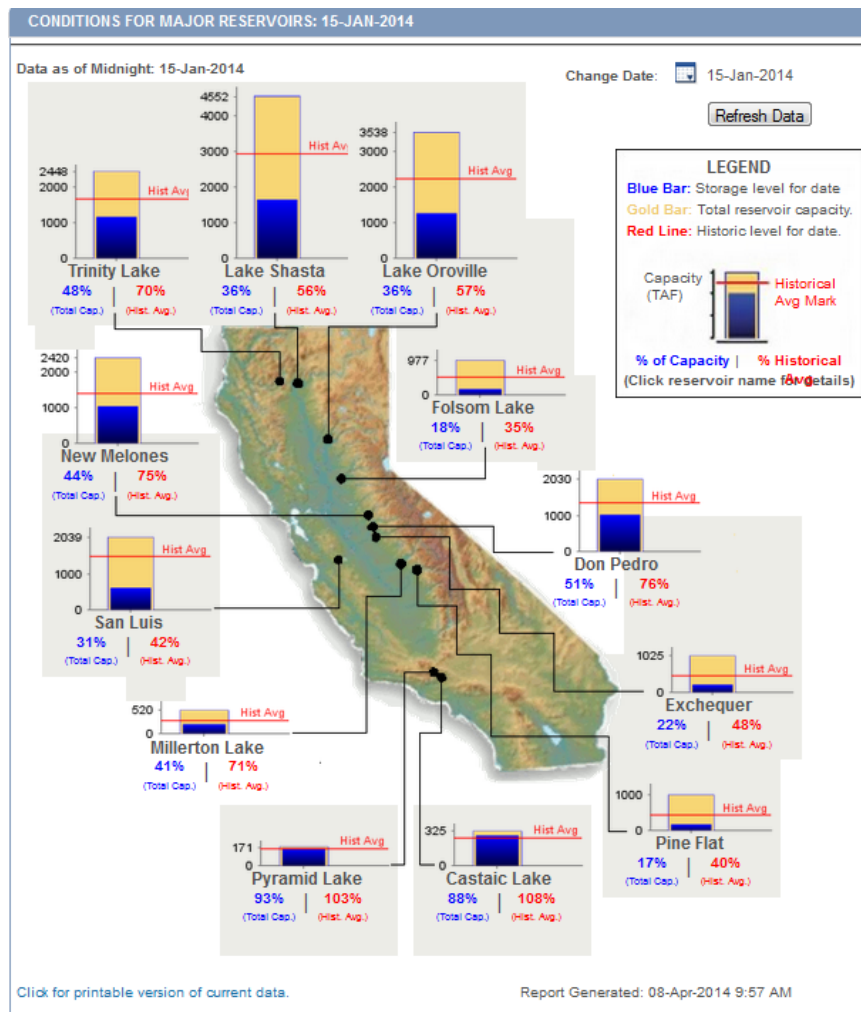
Discussions began on whether emergency rock barriers, similar to those installed in 1976-1977, should be installed in the Delta to minimize the salinity intrusion from San Francisco Bay into the Delta and help meet the State Water Resources Control Board (SWRCB) D-1641 water quality objectives. In this

chapter, these rock barriers are referred to as "emergency barriers." This chapter discusses the modeling approaches that were taken to:

- evaluate the drought's impacts on water quality in the Delta, if another dry year occurs,
- review and analyze salinity modeling results (DSM2 and SELFE) due to the installation of the rock barriers,
- analyze water level, flow and velocity impacts of installing the barriers, and
- analyze water savings (water that would remain in reservoirs instead of being released to reduce salinity intrusion) that potentially could occur with installation of the barriers.

6.1 Summary of Emergency Barrier Work Completed

This chapter is a summary of work and documentation completed by several staff members from the Department of Water Resources' (DWR's) Bay-Delta Office, and Operations and Maintenance office. Some work from Resource Management Associates is also presented. As both an acknowledgement of their hard work and contributions, and as a reference for where to find more complete data or documentation, Table 6-1 lists Delta emergency barrier related work performed and the staff associated with that work. The remainder of this report provides an overview of these emergency barrier analyses.

Table 6-1   DSM2 and SELFE Emergency Barrier Drought Modeling Tasks and Contacts

Work/Task	Name(s)	DWR Office/Division
Delta Coordinated Operations (DCO) Modeling	Amritpal Sandhu, Tracy Pettit	Operations and Maintenance
Modeling for 2009 Emergency Barriers Report	Subir Saha	Bay-Delta Office
DSM2 Forecasts – DCO Minimum Releases, Early February Forecast	Bryant Giorgi, James Edwards, Dan Yamanaka, Tracy Hinojosa	Operations and Maintenance
DSM2 Forecasts – DCO Minimum Releases, Early February Forecast With and Without Barriers	Siqing Liu	Bay-Delta Office
Delta Island Consumptive Use	Lan Liang, Bob Suits	Bay-Delta Office
Flow balance on South Delta Area	Aaron Miller, Ming-Yen Tu	Operations and Maintenance, Bay Delta Office
Net Delta Outflow Analysis using USGS Flow Stations	Rueen-Fang Wang, Eli Ateljevich	Bay-Delta Office
DSM2 Forecasts – DCO Minimum Releases, February 20 Forecast With and Without Barriers	Siqing Liu	Bay-Delta Office
DSM2 Forecasts – DCO Meet Delta Water Quality Objectives Until Storage Water is Unavailable, February 20 Forecast	Bryant Giorgi	Operations and Maintenance
DSM2 Quality Assurance/Quality Control and Analysis of RMA, DSM2 and SELFE Result Differences	Nicky Sandhu, Bob Suits, Eli Ateljevich	Bay-Delta Office
Historical Data Analysis	Bob Suits, Joey Zhou	Bay-Delta Office
DSM2 Forecast, March 21 Forecast With and Without Barriers	Siqing Liu	Bay-Delta Office

Table 6-1 **DSM2 and SELFE Emergency Barrier Drought Modeling Tasks and Contacts (Cont.)**

Work/Task	Name(s)	DWR Office/Division
SELFE Simulation using March 21st Forecast	Eli Ateljevich, Kijin Nam, Rueen-Fang Wang, Inez Ferreira, Jon Shu	Bay-Delta Office
SELFE Animations	Jon Shu	Bay-Delta Office
Full Delta Graphics Tool Modification	Subir Saha	Bay-Delta Office
Specific Location Graphics Tools	Ming-Yen Tu	Bay-Delta Office
Presentation Graphics	Jamie Anderson	Bay-Delta Office
Water Cost Savings Analysis	Eli Ateljevich	Bay-Delta Office
RMA Bay-Delta Forecasts	John DeGeorge, Richard Rachiele, Stacie Grinbergs	Resource Management Associates, Inc

6.2 Modeling Process

6.2.1 Data Analysis and Modeling Process to Determine Potential Salinity Impacts

In analyzing potential salinity intrusion into the Delta, we used historical observed data and computer modeling of forecasted conditions. The modeling process is shown in Figure 6-2.

The Delta models that we used in this analysis were Delta Simulation Model 2 (DSM2) and the Bay-Delta Semi-implicit Eulerian Lagrangian Finite Element (SELFE) model (Ateljevich 2014). DSM2 is a one-dimensional, physically-based model that assumes flows are moving either upstream or downstream in a channel. In SELFE, the direction and magnitude of flow can also change across the channel or down the water column. DSM2 runs much faster than SELFE and requires less input data, but SELFE has a greater resolution.

We chose to use forecasted flow conditions under a dry (90%) hydrology to get a better understanding of what we might expect under a worst-case scenario. Fortunately, DSM2 and its input had been set up and streamlined to do longer term forecasts as part of the DWR's Municipal Water Quality Investigations Program. As a result, we did not have to spend a lot of time setting up and testing the simulations.

We then compared the modeling results to what happened historically in dry years. In a recent project for the State Water Contractors and the San Luis and Delta Mendota Water Authority, staff from Tetra Tech compiled western Delta historical salinity data, from various historical sources, from 1921 to 2012 (Roy, 2012). DWR staff then ran DSM2 for that period. (DSM2 had been run from the mid-1970's onward, but had never been used to simulate earlier historical conditions.)

One of the other areas that we focused on in doing the analysis was the in-Delta diversions and returns. These values are calculated using the Delta Island Consumptive Use (DICU) model. There has not been a good way to validate these values Delta-wide, and in a dry year the quantities of water involved are commensurate with total outflow; thus, a relatively small difference in these consumptive use estimates in a dry year can have significant impacts on salinity intrusion. This will be further discussed later in the chapter.

Figure 6-2 Modeling Process
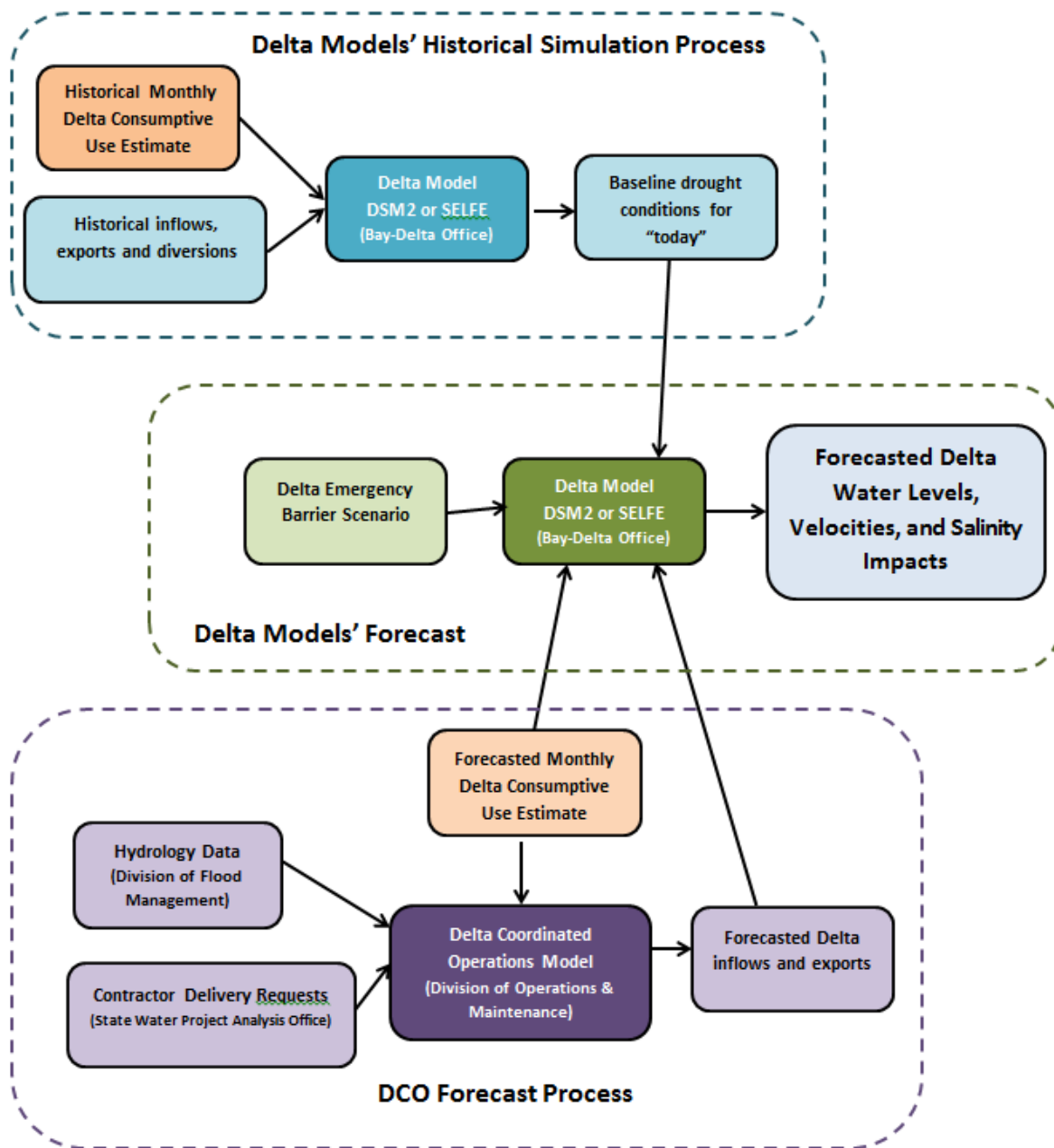
6.2.2 Forecasted Inflows, Diversions, Consumptive Use and Exports

To model the Delta flows, water levels, and salinity, Delta models such as DSM2 and SELFE need boundary inflows, exports, diversions, consumptive use diversions and returns, water levels, and salinity. For inflows to and exports from the Delta, the models use forecasted flows extracted from the Delta Coordinated Operations (DCO) studies that DWR's Division of Operation and Maintenance (O&M) conducts to determine State Water Project allocations (Figure 6-2). DCO studies incorporate hydrology data (developed by the Flood Management Division), contractor delivery requests (compiled by State

Water Project Analysis Office), and regulatory and court restrictions on exports. The DCO allocation forecasts that we used for this analysis assumed a 90% hydrology. A 90% hydrology is one that assumes, based on historical statistics, only one in ten years would be drier than this forecast. The models also use observed historical data up until the forecast period begins.

There were three forecast periods that were used to evaluate the need for barriers, early February, February 21, and March 20. Each forecast incorporated the historical precipitation up until the forecast began. The first Delta forecast that was evaluated was an early February forecast (before the February 9 storm). The flows produced by the DCO model that were used for the first forecasts represented a minimum releases assumption. These minimum releases met upstream flow requirements but did not attempt to meet the D-1641 water quality objectives in the Delta. Even without releasing flows to meet the D-1641 water quality objectives, Shasta, Oroville, and Folsom reservoirs were forecasted to be at very low storage levels by August.

The first DSM2 forecasts, run by O&M staff using the early February DCO forecast, showed that DSM2 was underestimating the historical salinity at D-1641 water quality objective locations in the Delta. One of the potential errors in input was determined to be consumptive use during the February time period. Typically, during February, consumptive use is estimated to be very small, assuming that there recently has been some precipitation (Mahadevan, 1995). However, because the winter of 2013-2014 was very dry, the consumptive use values were adjusted to reflect a higher consumptive use. This higher consumptive use was designated "Run 3" and represented a consumptive use approximately 700 cfs more than the dry year historical estimate that had been previously used. The higher consumptive use scenario also assumed no precipitation and a high evapotranspiration rate.

Table 6-1 Dry Historical and High Estimated Delta Consumptive Use (Run 3)

	Consumptive Use Estimate			Consumptive Use Estimate	
	Dry Historical (cfs)	Run3 (cfs)		Dry Historical (cfs)	Run3 (cfs)
January	304	1008	July	4302	5106
February	1274	1998	August	2788	3577
March	2052	2829	September	1589	2353
April	2272	3059	October	1250	1967
May	2899	3691	November	1025	1731
June	3936	4740	December	1000	1707

6.3 Review of Documents on Salinity Impacts of Barriers in Droughts

To investigate potential sites for barriers, we examined historical drought barrier installation and reviewed results from other studies investigating the placement of barriers to improve water quality in the central Delta. The report that provided the most useful information was the Draft Delta Drought Emergency Barrier Report completed by DWR in April 2009 (DWR 2009). In that report, several alternatives for barrier installation impacts on salinity were investigated. Phase 1 was the identification of alternatives where a fairly comprehensive list of barrier salinity impacts were evaluated. The locations are shown by the red rectangles in Figure 6-3 and Figure 6-4. The effectiveness of the alternatives was measured by looking at the percentage reduction in EC at SWP and CVP export locations between each barrier alternative and the base condition (no project). The analysis was conducted for the July through

November period using 2001 and 2002 hydrology (dry years) and using DSM2 for the modeling analysis. If the reduction in EC was less than 5% it was not included in the Phase 2 analysis. The black X's show the barrier locations that did not provide a 5% or better reduction.

Figure 6-3 **Barrier Locations - Phase 1, 2009 Emergency Barriers Report Map 1**
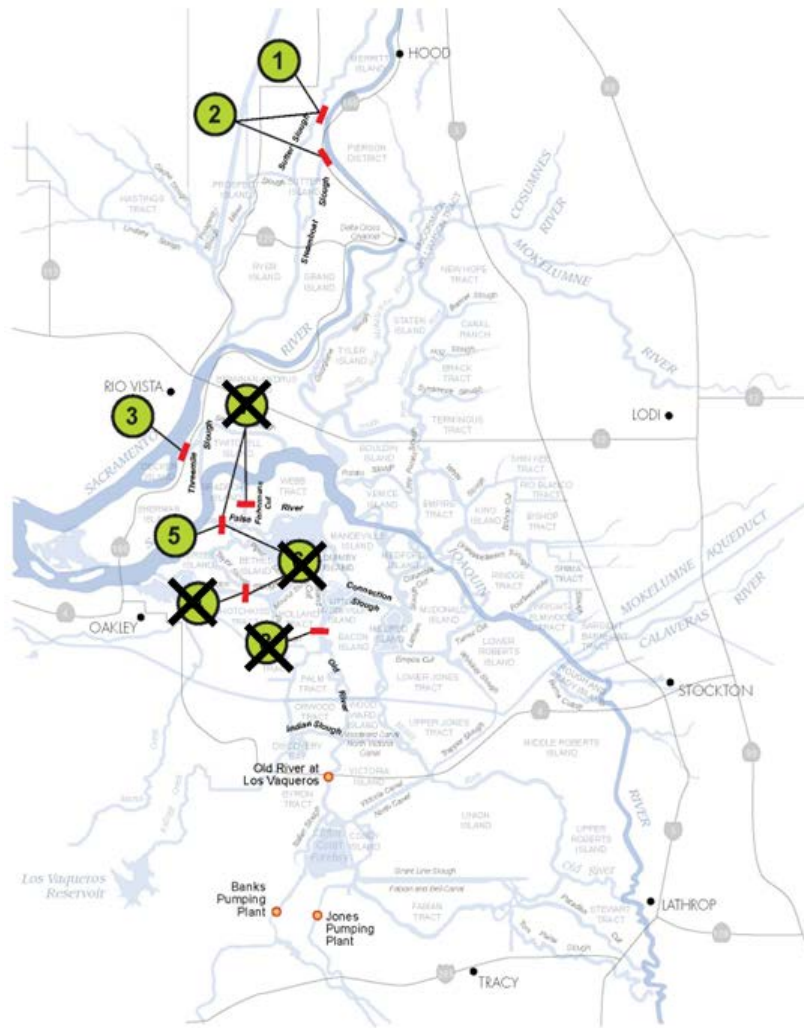
Figure 6-4 Barrier Locations - Phase 1, 2009 Emergency Barriers Report Map 2
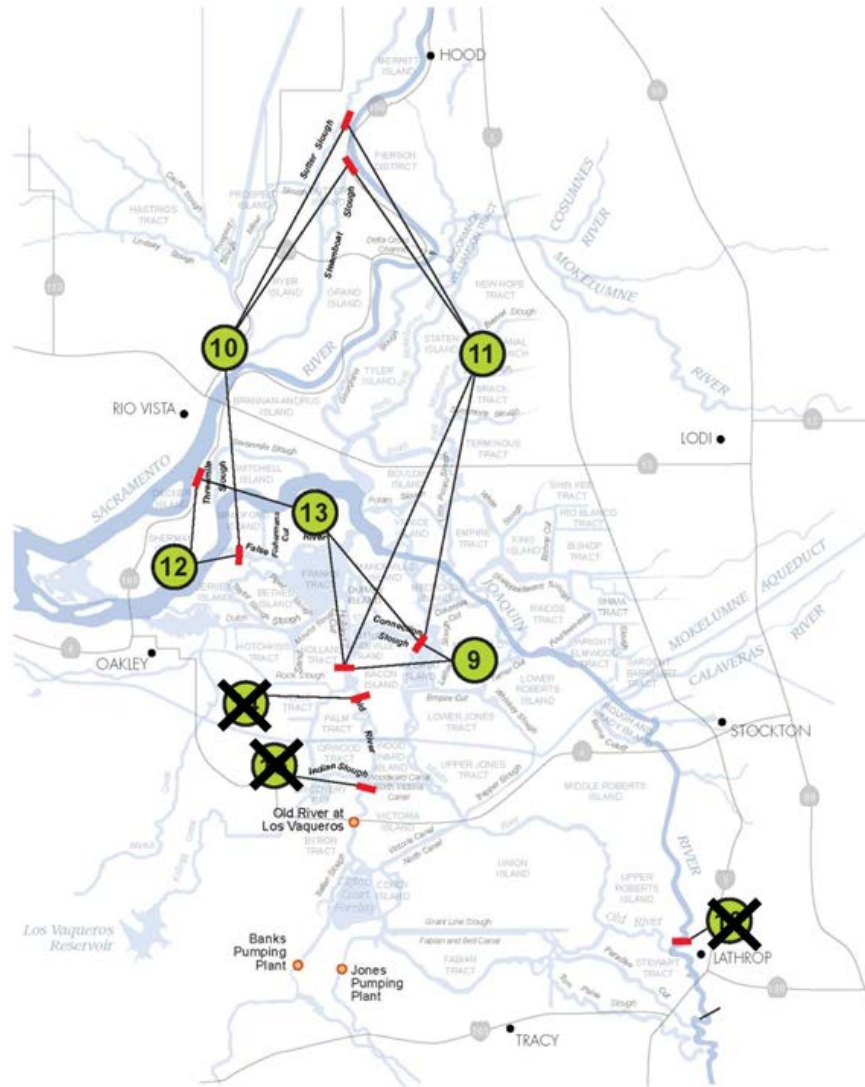
Figure 6-5 shows the barrier locations for the Phase 2 analysis. The Phase 2 alternatives were modeled and analyzed using DSM2 for the July through November historical period of the three years, 2007 to 2009.

6.3.1 Checking if DSM2 Forecast Results Matched Conclusions of 2009 Emergency Barriers Report

DSM2 was run with each of the proposed barrier locations shown in Figure 6-5. The Three Mile Slough barrier and any combination of barriers with Three Mile Slough were dropped from consideration because that barrier/gate must be operable to be effective. Three Mile Slough, with its high tidal flows and velocities, could not reasonably be constructed in time to help reduce pumping salinities. As a result, the barrier locations that were evaluated for impacts were Sutter Slough, Steamboat Slough, False River, and Two Gate (Connection Slough and Old River). Reductions in salinity for the combinations of Sutter, Steamboat and Two Gate versus Sutter Steamboat, and False River were very similar with the former

combination resulting is slightly better EC. However, the Two Gate configuration was dropped in favor of the Sutter, Steamboat and False River configuration for reasons not related to salinity modeling.

Figure 6-5 **Location of Barriers and Average Electrical Conductivity Reduction at Banks Pumping Plant - Phase 2, 2009 Emergency Barriers Report**
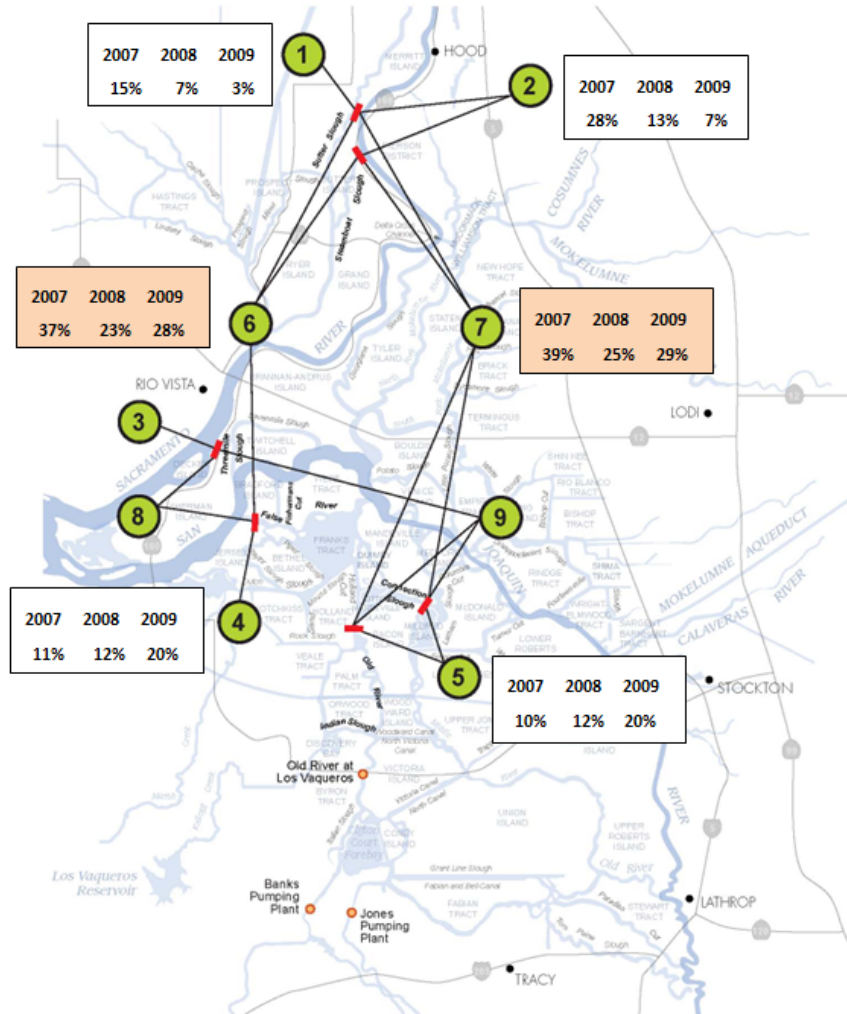
Figures 6-6 and 6-7 show the flow boundary conditions for DSM2 for the early February forecast. Inflows and export values were given by the DCO model. Consumptive use was the very high consumptive use (Run 3) mentioned earlier, and the net Delta outflow was calculated by adding all inflows and subtracting exports and diversions. For this simulation, net Delta outflow drops to less than 3000 cfs in February and drops to less than 1000 cfs in August before rising again to more than 3000 cfs in September.

Figure 6-6 Early February 2014 Forecasted Inflows and Net Delta Outflow
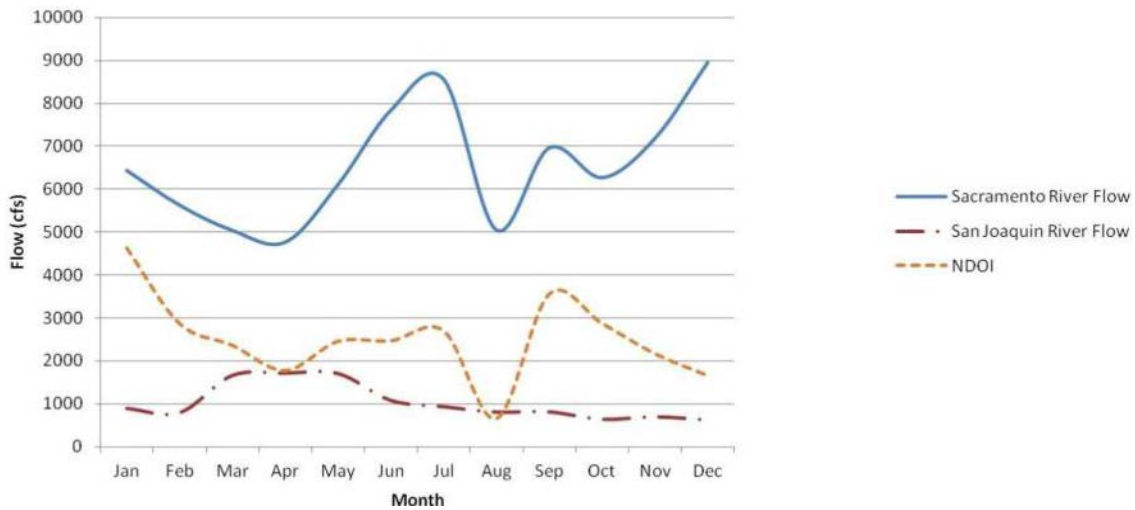
Figure 6-7 Early February 2014 Forecasted Exports and Diversions
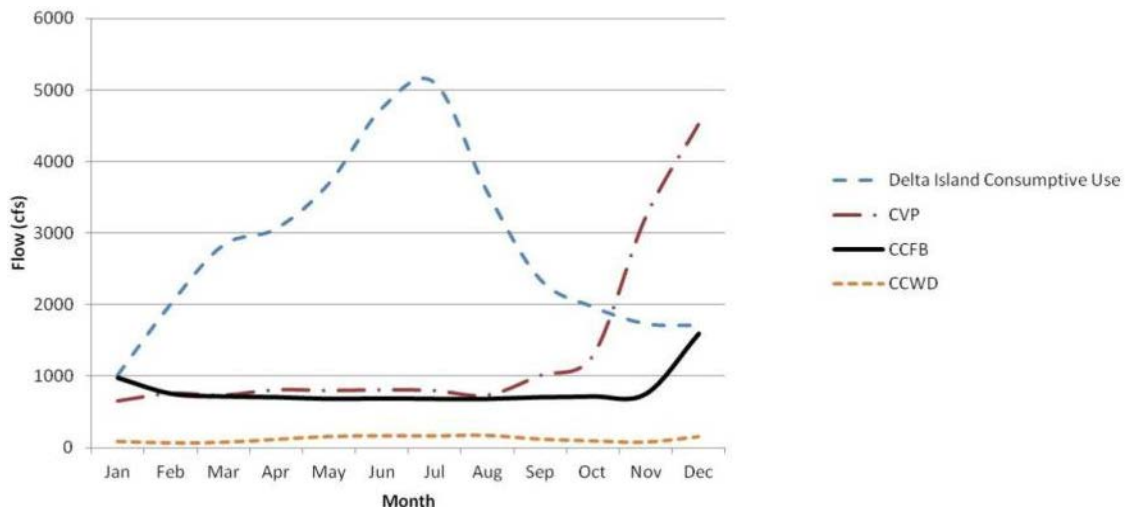
Figures 6-8 and 6-9 show the impacts of the individual barriers and combined barriers for Clifton Court Forebay and Emmaton. The selection of installing the barriers on April 1 in the model was arbitrary and a starting point for evaluating the impacts of the barriers. In 2009 (Figure 6-5), the Sutter Slough barrier provided a 3% reduction in EC at Clifton Court Forebay. These simulations checked, among other things, that the installation of a Sutter Slough barrier would provide a significant reduction in salinity in the central/south Delta. The simulations, not surprisingly, indicated that there would be degradation in EC along the Sacramento River at Emmaton and Rio Vista due primarily to the Sutter and Steamboat Slough barriers.

Figure 6-8 Early February 2014 Forecast

With and Without Barriers - Clifton Court Forebay EC
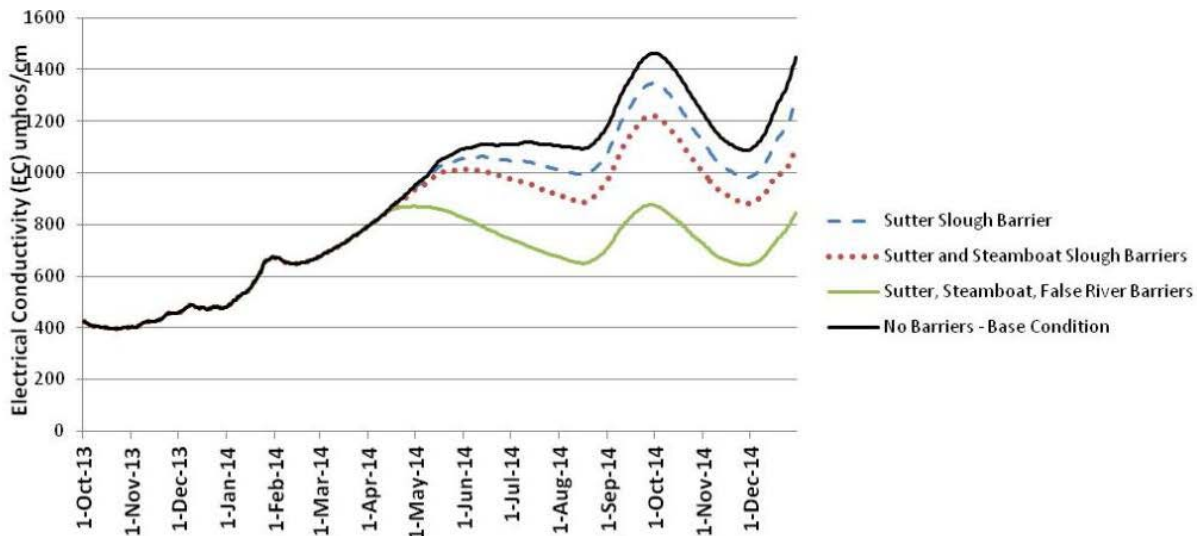
Figure 6-9 Early February 2014 Forecast With and Without Barriers - Emmaton EC

6.4 February 20 and March 21 Forecasts

6.4.1 Evolving Objectives for Studies

Early on, the goal for the barriers was to reduce the EC in the Delta so that most of the D-1641 water quality standards could be met given that a limited amount of water was available for release to help prevent salinity intrusion. Early forecasts, including the February 20 forecast, indicated that if the reservoirs were operated so that all of the water quality objectives were met, then by midsummer there would not be enough water to release to prevent salinity from intruding, resulting in large increases in EC throughout most of the Delta.

Later forecasts that included historical precipitation prior to March 21 had enough reservoirs storage to meet the 1000 EC or 250 CL objectives through August. The available storage in Oroville, Shasta and Folsom barely touched Power Pool levels in the March 21 forecast. DWR currently cannot release water below Power Pool.

After the March 21 forecast, the goal for the barriers was to see if the reservoirs could release less water and still meet most of the objectives. This saved water could be released later in the year or next year if dry conditions persisted. Additional model simulations were performed to determine the water cost or savings.

The sections below describe a few of the simulations completed to evaluate the effectiveness of the barriers for water quality, velocities and water levels. Although the initial focus was on water quality

when choosing the barrier locations, other hydrodynamic impacts needed to be evaluated. A summary of that work is also presented below.

6.4.2 Delta Island Consumptive Use Estimates

As stated earlier, Delta Island consumptive use was an important input into the Delta models. This section describes some of the different consumptive use values used in the various forecasts. Figure 6-10 shows a comparison between Run 3, DCO CU, DICU drought year average consumptive use, and DICU average consumptive use.

Figure 6-10 Monthly Consumptive Use Values Used in DSM2 Simulations
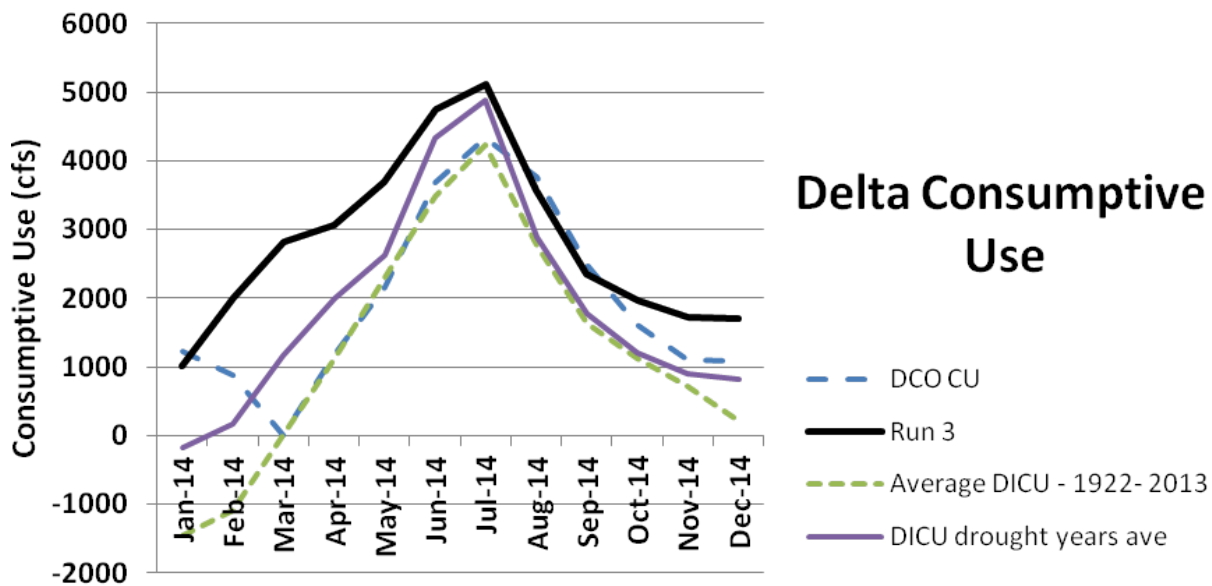
For the early February forecast, before the February 9 storm, the very high consumptive use values, Run 3, were used as input into the model. The February 20 forecast also used the Run 3 consumptive use values for the minimum release simulations. There were also simulations that investigated impacts with other consumptive use levels including a no diversions and no drainage scenario. For the forecasts that looked at meeting water quality objectives until storage water was not available, DSM2 also was run using the consumptive use in the DCO model (DCO CU). In both cases, where Run 3 and DCO CU were used as input, there was not enough storage water to meet water quality objectives in the Delta for the February 20 forecast. For the March 21 forecast, the DCO CU was used as input to the DSM2 simulations. Because of the additional rain that had occurred during February and March, the lower consumptive use values seemed to be a better estimate than the previous Run 3 values.

6.4.3 February 20 Forecast

6.4.3.1 February 20 Forecast Assumptions

The assumptions for the February 20 forecasts are the following:
- The DSM2 simulations used as their input, output from the February 20 DCO forecast by DWR's Operations and Maintenance. The forecast assumes a 90% historical hydrology. Two types of forecasts were analyzed. The first was a minimum releases forecast where water is released over

time but does not meet the D-1641 water quality objectives. In the second forecast type, water was released to meet the D-1641 water quality objectives until there was not water available to release.

- Three different operations of the Delta Cross Channel were evaluated:
  - Delta Cross Channel operated to D-1641,
  - Delta Cross Channel operated diurnally through May 22,
  - and Delta Cross Channel open.
- The high consumptive use, Run 3, was used as input to DSM2. No consumptive use and the DCO consumptive use was also used as input for some of the simulations.
- The temporary barriers in Grant Line Canal, Old River at Tracy, and at the head of Old River were installed at the end of March for the simulations.
- Separate simulations were made evaluating the salinity impacts of installing the emergency barriers on April 1, May 1, and June 1.

Figures 6-11 and 6-12 show the forecasted inflows, net Delta Outflow, exports, and the high Run 3 consumptive use values used as input to DSM2.

Figure 6-11 February 20, 2014 Forecasted Inflows and Net Delta Outflow
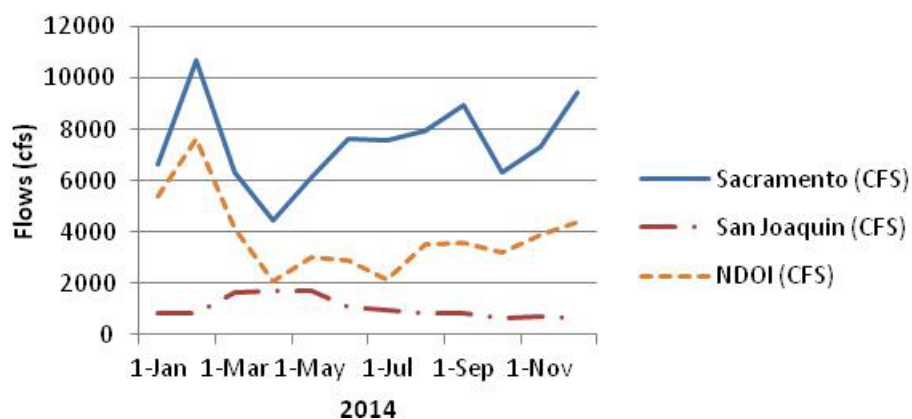
Figure 6-12 February 20, 2014 Forecasted Exports and Diversions
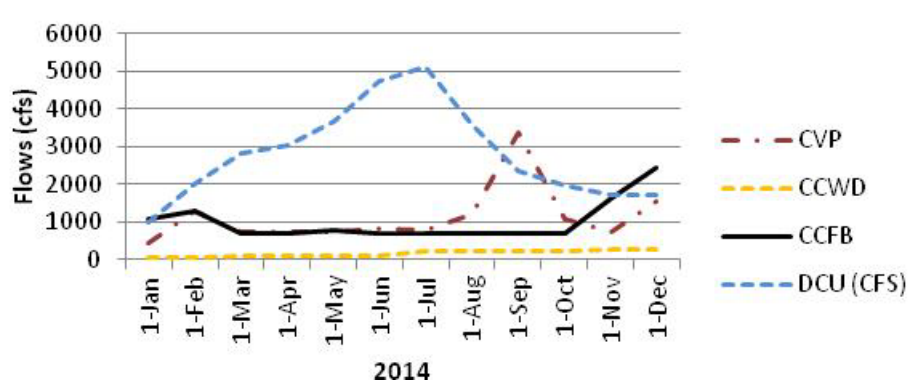
6.4.3.2 February 20 Forecast Results

Figures 6-13 and 6-14 show EC results for various emergency barrier installation times and the end of month reservoir storage for Oroville, Shasta, and Folsom. In Figure 6-13, there is a salinity increase at

Rio Vista, due to the emergency barriers. This is expected, due primarily to the flow moving through the north and central Delta because of barriers in Sutter and Steamboat Slough. In Figure 6-14, there is a decrease in salinity at Clifton Court Forebay due the emergency barriers. The barriers keep the EC below 1000 uS/cm for the minimum releases scenario for Clifton Court Forebay.

Figure 6-15 shows the same forecast plotted with 2013-2014 historical data and 1976-1977 historical data at Clifton Court Forebay. There are a few items to note from this graph.
- 2013 and 1976 were dry years leading into a dry year.
- DSM2 underpredicts historical EC at Clifton Court Forebay by more than 100 uS/cm.
- 2013- 2014 follows the salinity pattern of 1976-1977.
- Emergency barriers provide a significant reduction in salinity at Clifton Court Forebay.

Figure 6-16 shows EC results at Clifton Court Forebay with the assumption that water is released from reservoirs so that the D-1641 water quality objectives are met in the Delta through higher Sacramento River flow. When the reservoirs reach Power Pool, the reservoirs no longer release water. (DWR currently cannot release below the Power Pool level). Figure 6-17 also shows that when barriers are installed July 1, the EC at Clifton Court Forebay reduces but does not make it to less than 1000 uS/cm. This indicates that in order to meet a 1000 uS/cm EC at Clifton Court Forebay or a 250 Cl at Rock Slough, barriers would need to be installed earlier in the season with a reduced Sacramento inflow.

Figure 6-13 **February 20th, 2014 Forecasted Rio Vista Electrical Conductivity and End of Month Storage**
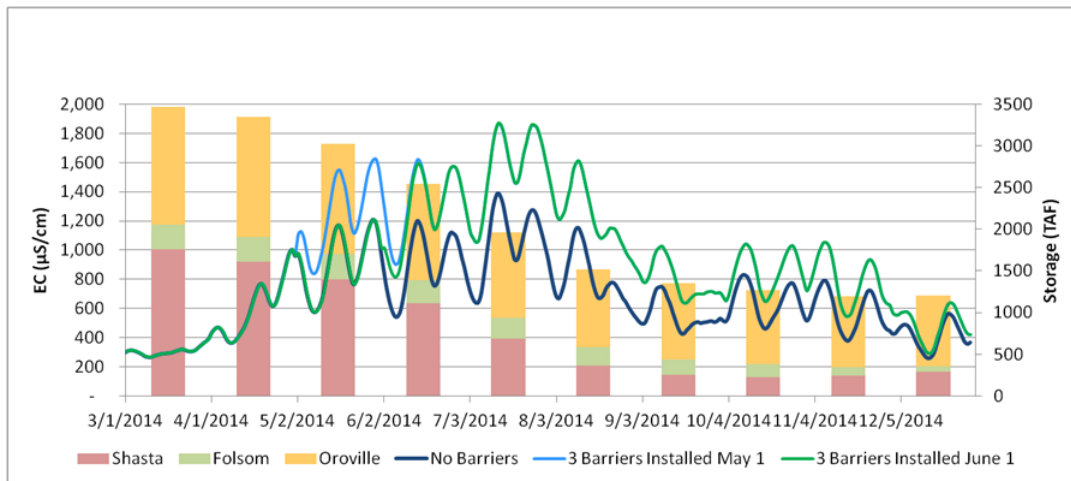
Figure 6-14 **February 20, 2014 Forecasted Clifton Court Forebay Electrical Conductivity and End of Month Storage**
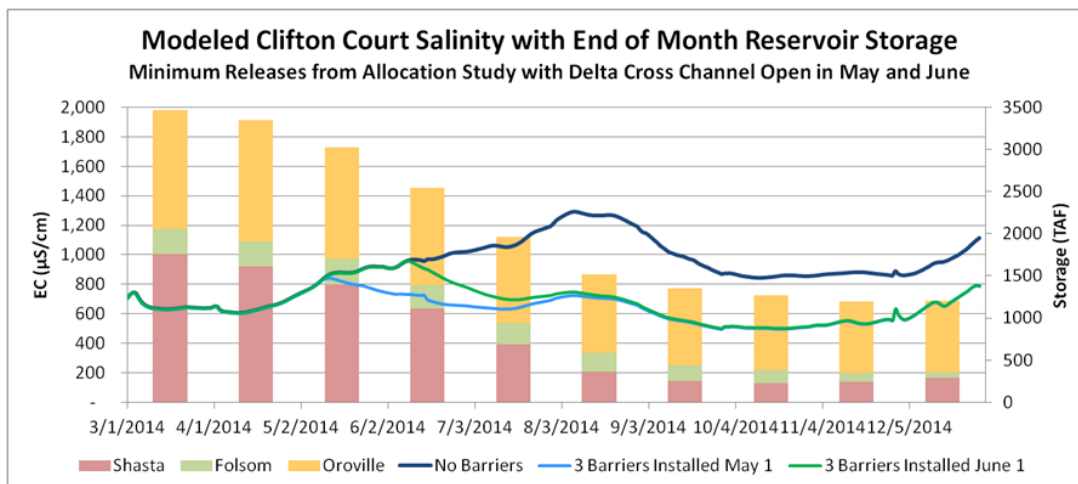
Figure 6-15 **DSM2 Historical and February 20, 2014 Forecasted Clifton Court Forebay Electrical Conductivity Shown with EC from 1976-1977**
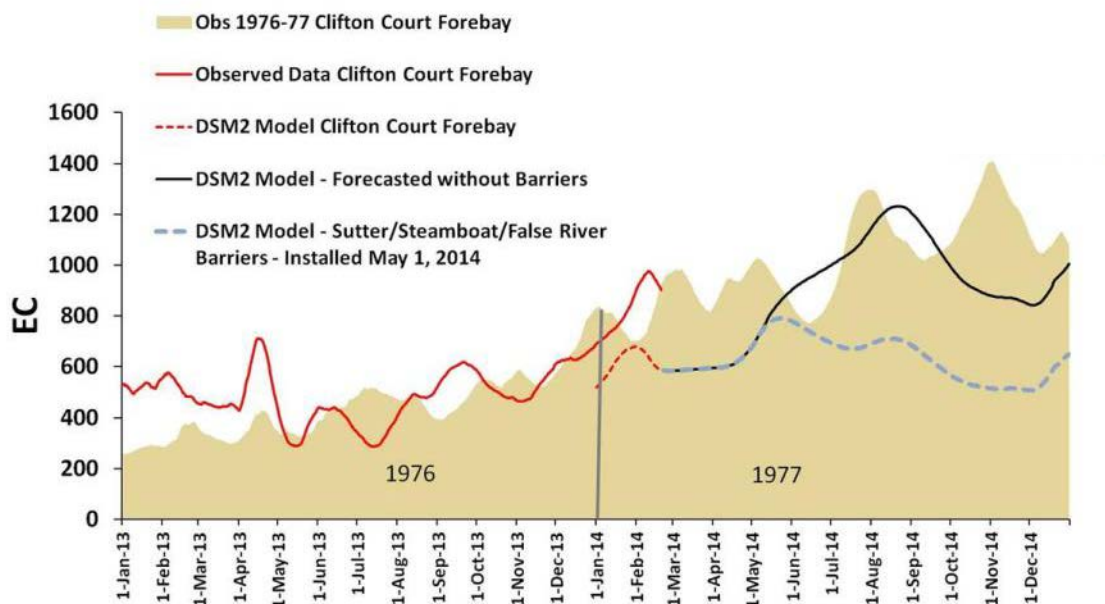
Figure 6-16 Modeled Clifton Court EC with End of Month Reservoir Storage February 20, 2014 Forecast
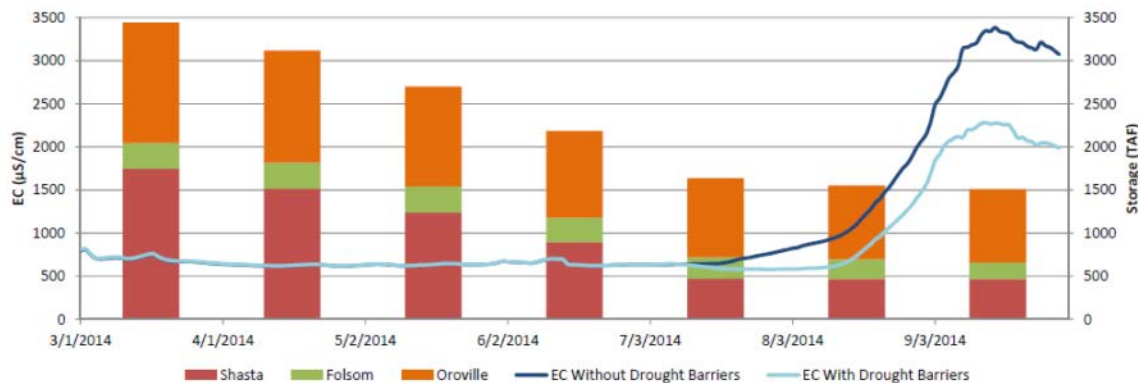
6.4.3.3 Discussion of Differences in Salinity Results between Different Delta Models

As part of the emergency barrier investigation, the State Water Contractors hired Resource Management Associates (RMA) to model different forecasted hydrologies with different barrier configurations using Water Allocation Model (WAM) and the RMA Bay-Delta Model. WAM is a one dimensional model that uses tidally averaged input and runs extremely fast so that many simulations can be made quickly. The RMA Bay-Delta Model is a combination 1-D/2-D model, representing the more complex western Delta and open water areas with a two dimensional grid. WAM has been calibrated to the RMA Bay-Delta Model.

One of the hydrologies that RMA used as boundary conditions was the same February 20 forecast that DSM2 used. There were some differences in how the boundary conditions were incorporated but after some investigation, those differences did not account fully for the large differences in model results between the two models. RMA's EC results were quite a bit higher than DSM2's EC results. For example, at Clifton Court Forebay, peak EC for the RMA Bay-Delta Model reached 2100 uS/cm EC for the minimum releases forecast, where DSM2 was closer to 1300 uS/cm. Differences at the Northbay Aqueduct were much larger still. SELFE was also run and resulted in EC values higher than either RMA or DSM2.

So which of the three models is "right?" There is no simple answer to that question given the uncertainty in consumptive use, net Delta outflow and the lack of catastrophic salinity intrusion in the last 70 years to serve as ground truth. Although the salinity results from different modeling studies seem vastly different, the differences were mostly due to one model passing just over a "tipping point" with no operational attempt to intervene and the other model not – in such cases a relatively small change in Delta outflow can have large salinity effects. Figure 6-17 shows the conceptual relationship between outflow and salinity intrusion at the brink of non-compliance when salinity intrusion is fully developed on the east-west axis and starts to move south. The equilibrium response to outflow and the speed of salinity intrusion is slightly different between models, a point that is exacerbated by the fact that this regime is well out of their calibration range on modern data.

For these simulations, consumptive use in the Delta is a major component of outflow (Figure 6-11 and Figure 6-12) and also has the greatest uncertainty of any input. Figure 6-10 shows different consumptive use estimates derived from different year types and assumptions, all proposed for use in this year's

drought modeling. The DICU estimate labeled Run 3 was used with DSM2, and has the highest consumptive use. With this consumptive use pattern DSM2 matches winter field data well. In contrast, SELFE, our 3-D model, over predicts runaway salinity intrusion with this level of consumptive use, but agrees well if the drought year average estimate shown in Figure 6-10 is used instead. The differences in outflow between the two estimates (800-1200 cfs) is substantial in terms of upstream storage depletion, but these estimates nonetheless represent the state of the art. Differences of 1000 cfs, coupled with a clear statement of operational intent, may be more palatable than allowing salinity to diverge without reason.

The differences between models also triggered an as-yet unresolved discussion as to the existence of equilibrium salinity ceiling at Martinez for low flow. Figure 6-18 was developed as part of the model investigation. The red and black lines are RMA forecasted EC and DSM2 boundary EC at Martinez for this year. The remaining lines are historical EC reconstructions at Martinez during severe drought years. The salinity data before 1991 were grab samples taken an hour and a half after high-high tide (roughly peak salinity), then converted to daily averages using historical relationships. Corresponding outflows are calculated using modern consumptive use estimates and do not account for agricultural response to high salinity.

Figure 6-17 **Conceptual Plot of Relationship between Net Delta Outflow and Salinity in the Delta**
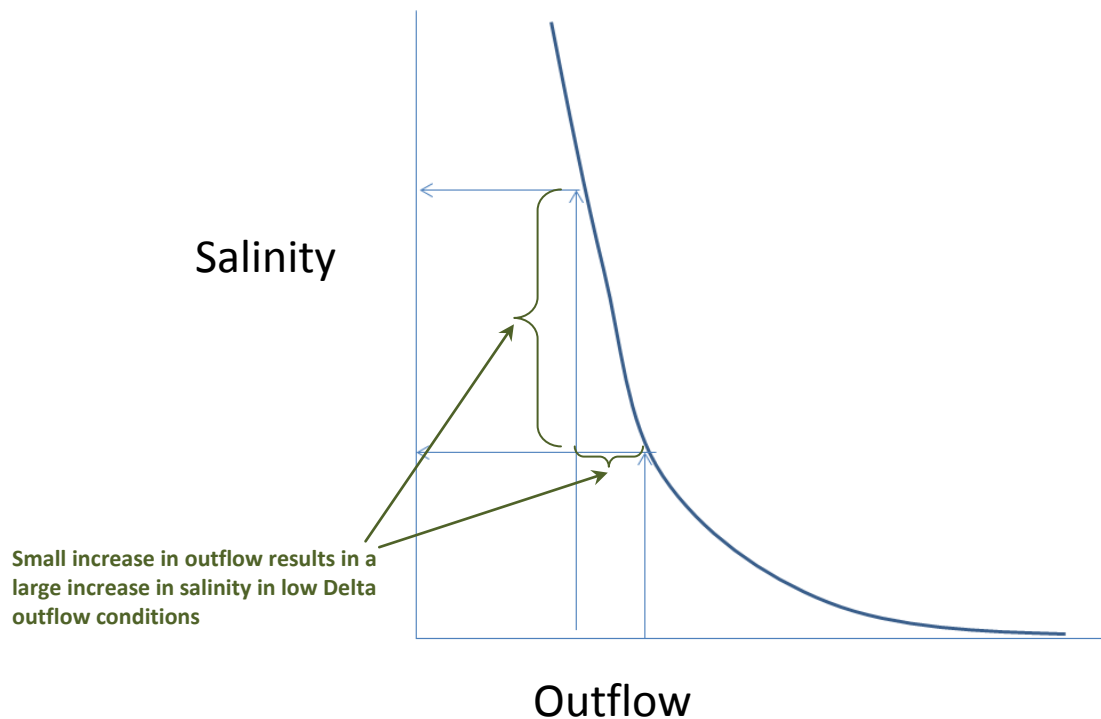
The processed grab sample data suggest, inconclusively, conductivity is bound from above at Martinez even in 1931, a year when outflow was probably less than zero and the 2 ppt chloride isohaline (roughly 3.5 ppt salinity) advanced within a few miles of Hood and the head of Old River. The existence of such a ceiling is consistent with data since the mid-1980s, when more modern monitoring began. However, for that part of the record the possibility of a physical maximum salinity is hard to confirm -- confounded by the regulatory maximum induced by upstream water quality standards

The existence of a near-ceiling to EC over a broad range of very low outflows has repercussions for modeling. An asymptotic limit is built into G-model, which is then carried over to the boundary estimation process for DSM2. Hence, DSM2 has no trouble reproducing this phenomenon, but our modeling workflow would need adjustments should the ceiling be disproved. Other models with boundaries much farther west do not reproduce the maximum. As shown in Figure 6-18, RMA predicts conditions at Martinez to be worse than 1931, 1977, and 1991, well outside its historical upper bound. The labels DSM2 1931 historical, DSM2 1977 historical, and DSM2 1991 historical are observed historical Martinez boundary condition data use for DSM2 and not G-Model determined values. SELFE had similar difficulties, although as previously mentioned the problems are resolved (and would, we think, be resolved in the RMA model also) by swapping consumptive use assumptions.

More investigation also needs to be made into how well the G-model represents the Martinez boundary condition in drought conditions. Given the estimated outflows, the G-model under-predicts the historical EC conditions at Martinez in 1991.

There is no resolution thus far on whether these differences arise from the models or the data, and a frustrating fraction of the data sources (including modern estimates of flow) have large, systematic sources of error and obvious historical non-stationarities. The Delta Modeling Section has begun an investigation into whether the current flow monitoring network can be used to better estimate historical outflow or consumptive use. This is difficult because net Delta outflow is a delicate residual phenomenon that is hard to accurately extract from instantaneous tidal flows that are 1-2 orders of magnitude larger.

Figure 6-18 February 20, 2014 Forecasted EC and Delta Ouflow as Compared to Historical Dry Years
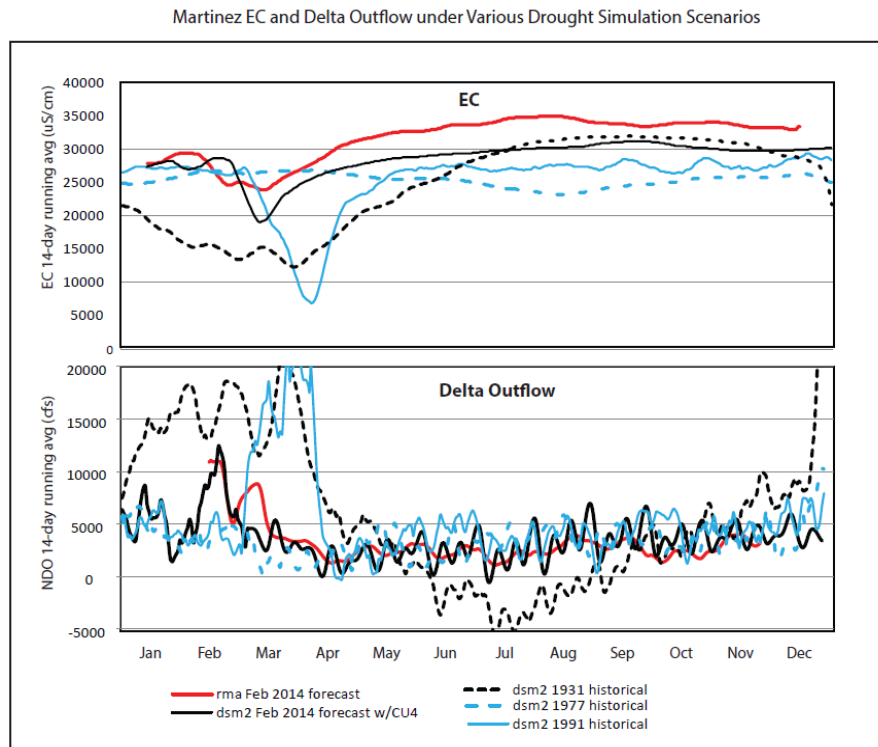
6.4.4 March 21 Forecast

6.4.4.1 DSM2 March 21 Forecast Assumptions

The assumptions for the March 21 forecast are the following:
- The forecast incorporates storms up to March 21 but not following.
- The DSM2 simulations used as their input, output from the March 21 DCO forecast from DWR's Operations and Maintenance. The forecast assumes a 90% historical hydrology. In this forecast, water was released to meet the D-1641 water quality objectives. There was enough water to not go below Power Pool levels in the reservoirs.
- Two different operations of the Delta Cross Channel were evaluated:
  - Delta Cross Channel operated to D-1641,
  - Delta Cross Channel kept open.
- A total Delta consumptive use value from the DCO forecast was used (Figure 6-10, DCO CU). The monthly value was distributed among the DSM2 nodes using the ADICU program.
- The temporary barriers in Grant Line Canal, Old River at Tracy, and at the head of Old River were installed at the end of March for the simulations.
- Separate simulations were made evaluating the salinity impacts of installing the emergency barriers on May 1 and June 1.
- Separate simulations were made investigating the effects of keeping the culverts open on the Sutter and Steamboat Slough locations.

Figures 6-19 and 6-20 show the forecasted inflows, net Delta outflow, exports, and the consumptive use values used as input to DSM2 for the March 21 forecast. Net Delta outflow values are at about 4000 cfs or above for this forecast. In contrast, the net Delta outflow went to 2000 cfs at times in the February 20 forecast.

Figure 6-19 March 21, 2014 Forecasted Inflows and Net Delta Outflow
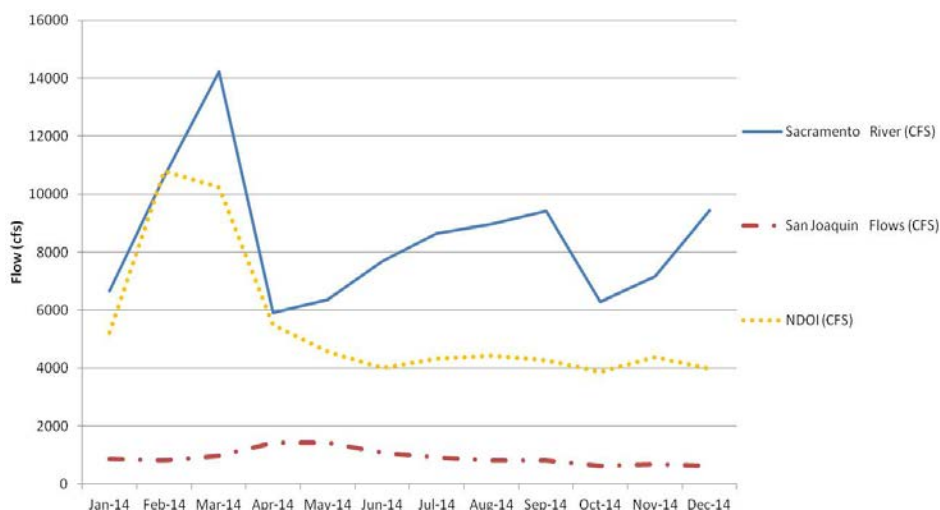
Figure 6-20 March 21, 2014 Forecasted Exports and Diversions
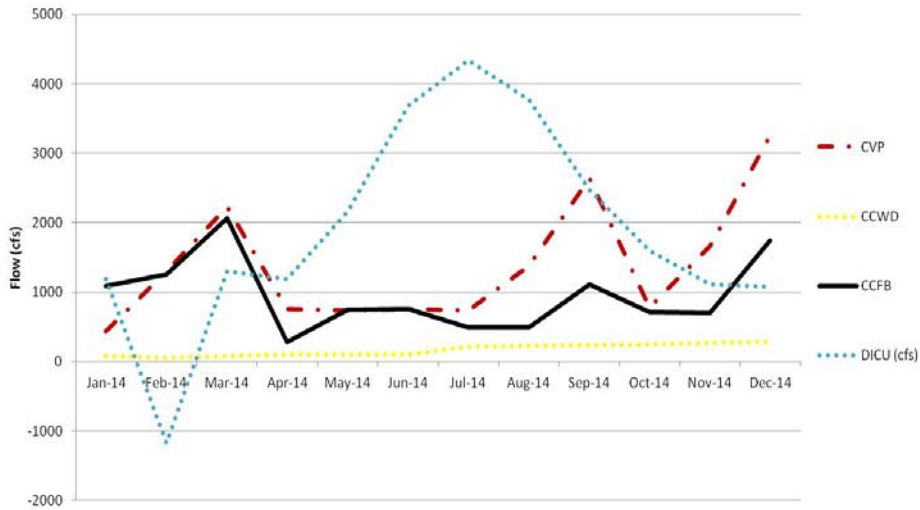
6.4.4.2 DSM2 March 21 Forecast Results

Figures 6-21 and 6-22 show the differences in results between the February 20 forecast and the March 21 forecast. Storms in late February and early March resulted in higher outflows which resulted in better water quality for the no-barrier simulations. EC starts to climb in the late fall due in part to increased exports beyond the health and safety levels (1500 cfs).

Figure 6-21 February 20 and March 21 Forecasted EC at Clifton Court Forebay
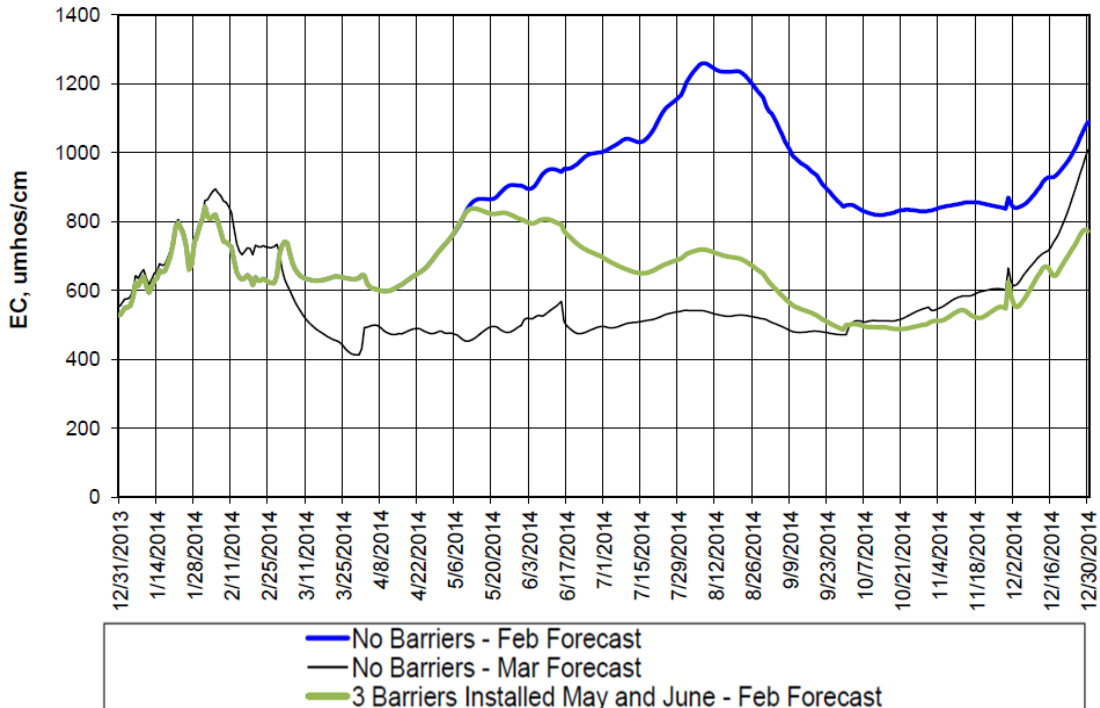
Figure 6-22 February 20 and March 21 Forecasted EC at Emmaton
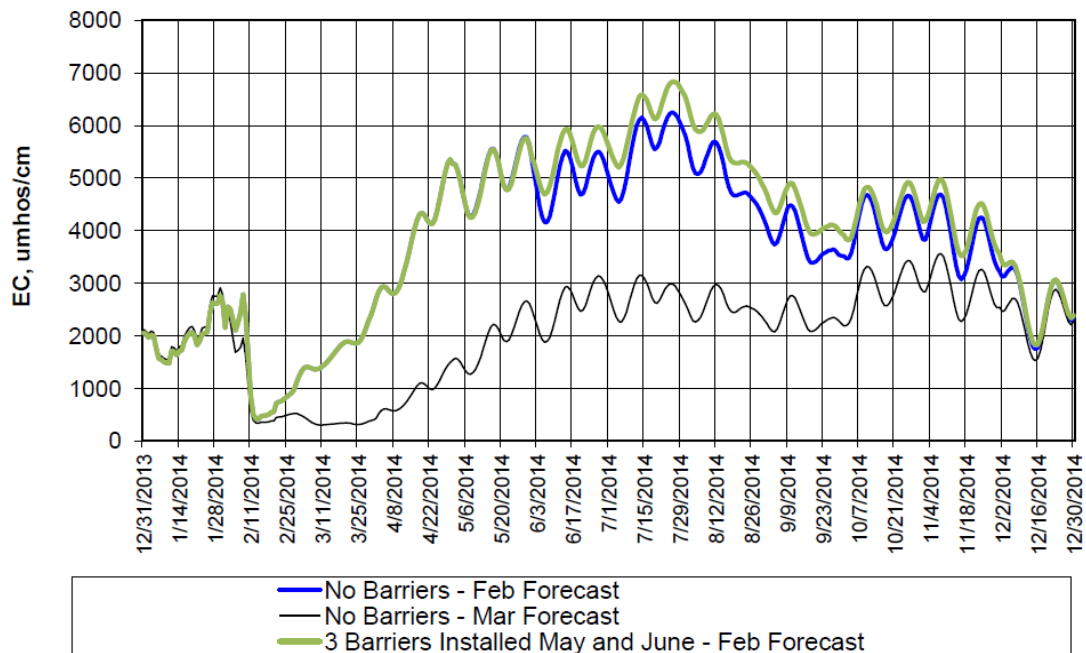
6.4.5 Analysis Tools and Providing Information to Stakeholders

Due to the number of stakeholders affected and the need to quickly analyze and distribute the results, a few tools were developed or modified to streamline the process. Figures 6-23 and 6-24 show a spatial salinity comparison plot and a screen shot of a visualization tool originally developed by CH2M Hill for the Bay Delta Conservation Plan to evaluate different alternatives. The excel spreadsheet tool creates various graphs on water level, velocity, flow, and water quality results for several locations in the Delta. The tool was modified to give results for the one-year forecast (as opposed to the 16 years used in planning studies). Additional locations were added as needed.

Figure 6-25 shows a screen shot of an Excel spreadsheet velocity tool used to plot water levels and water quality in the areas upstream and downstream of the different barrier sites. These graphs were used to help in determining if mitigation measures were necessary because of potential harm caused by the barriers to farmers and other Delta water users.

Figures 6-26 and 6-27 show spatial velocity plots for Dutch Slough and Fisherman's Cut. The results are from SELFE simulations and the plots, when animated over time, show where and when velocity hot spots occur. Higher velocities could cause scour, so these plots were used to aid in determining if the barriers would cause harm to the levees.

Figure 6-23 March 21 Forecast - Spatial Seasonal EC Comparison
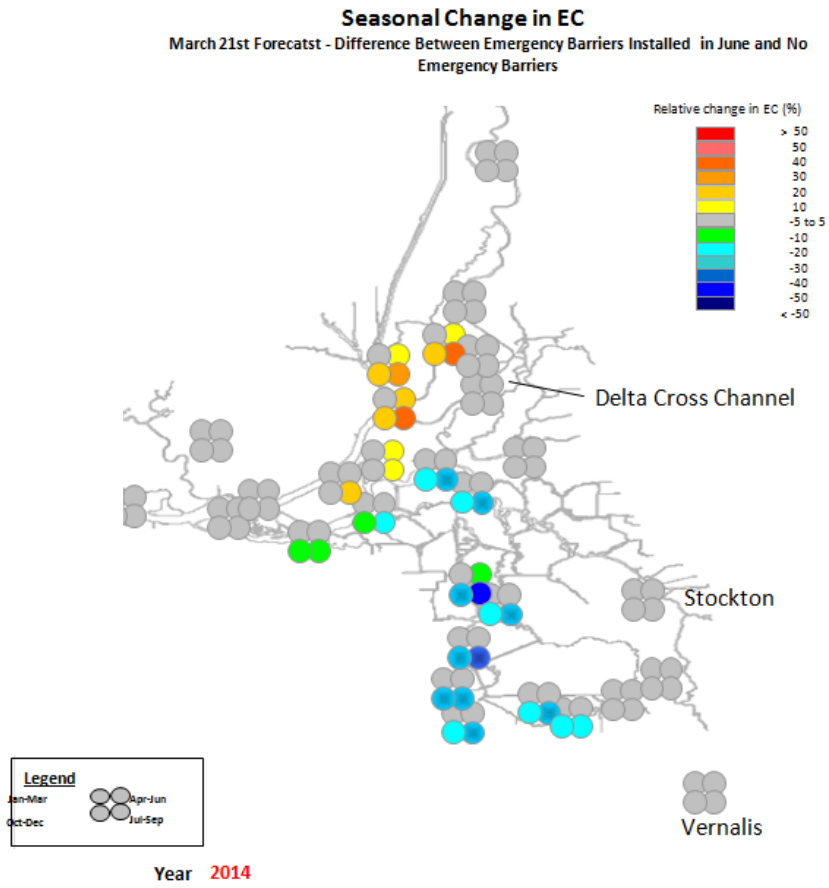
Figure 6-24 Modified BDCP Visualization Tool
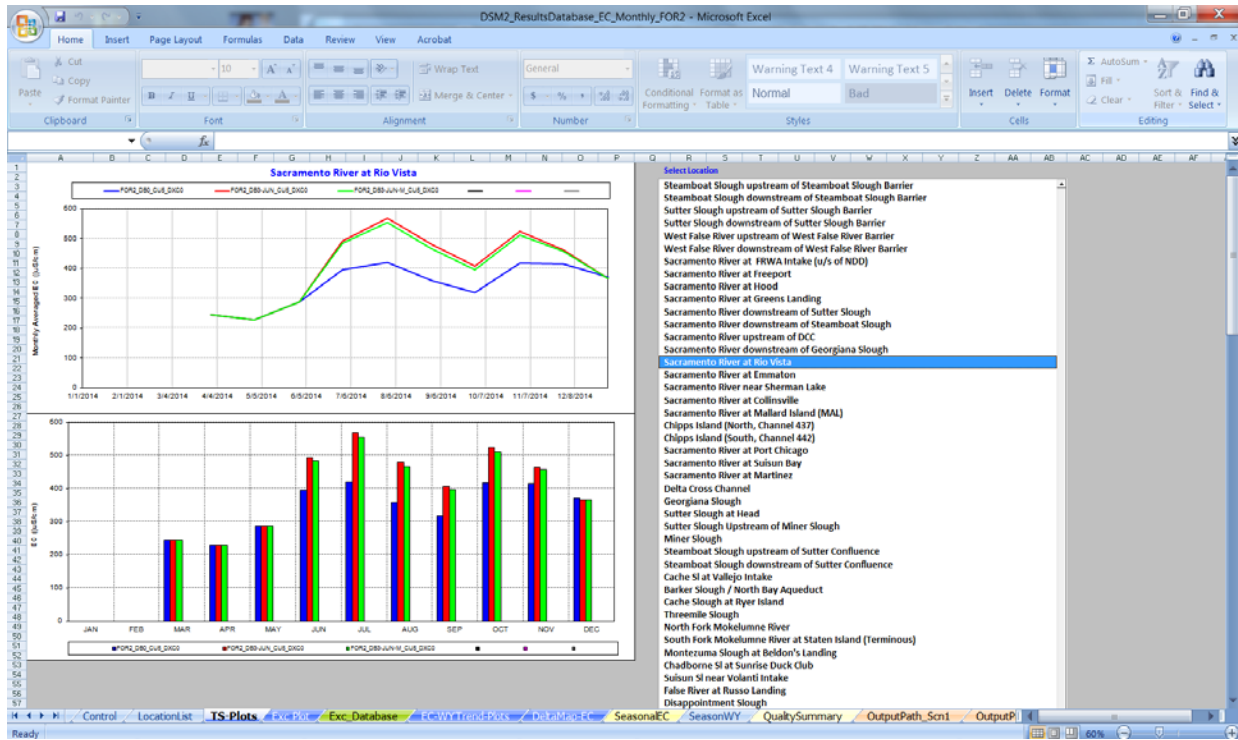
Figure 6-25 Stage and Velocity Tool for Locations Around the Barriers
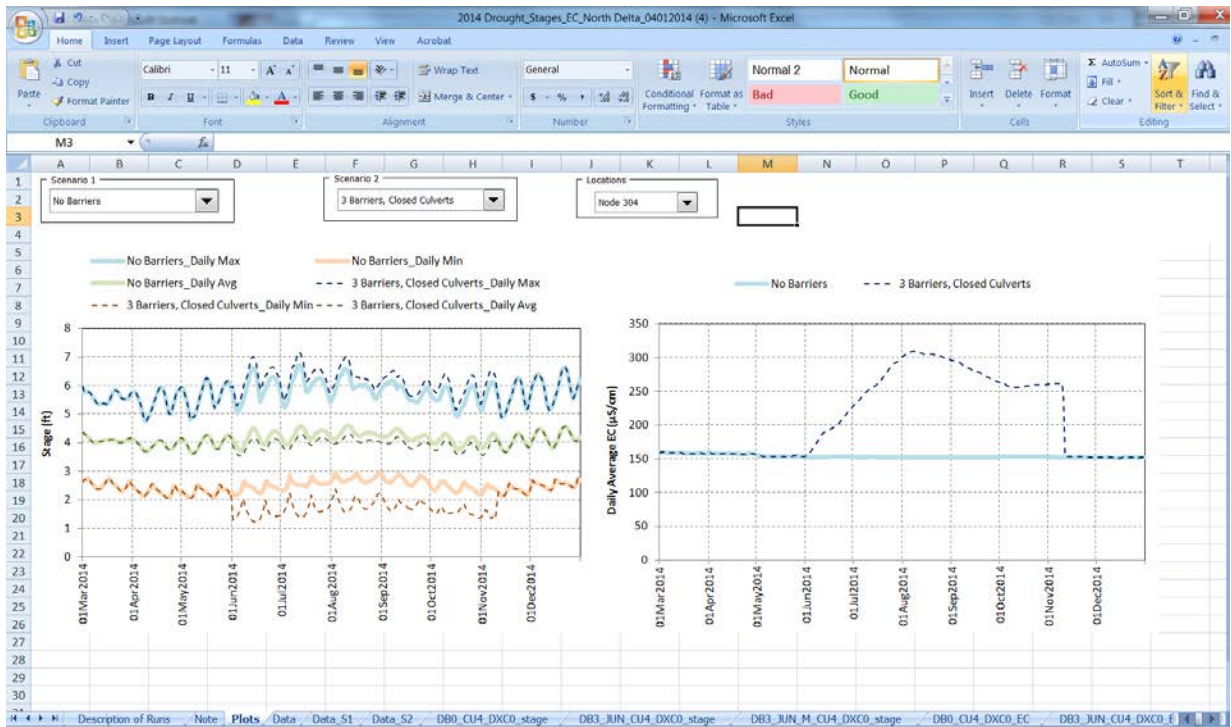
Figure 6-26 SELFE Spatial Velocity Distribution Plot for Dutch Slough
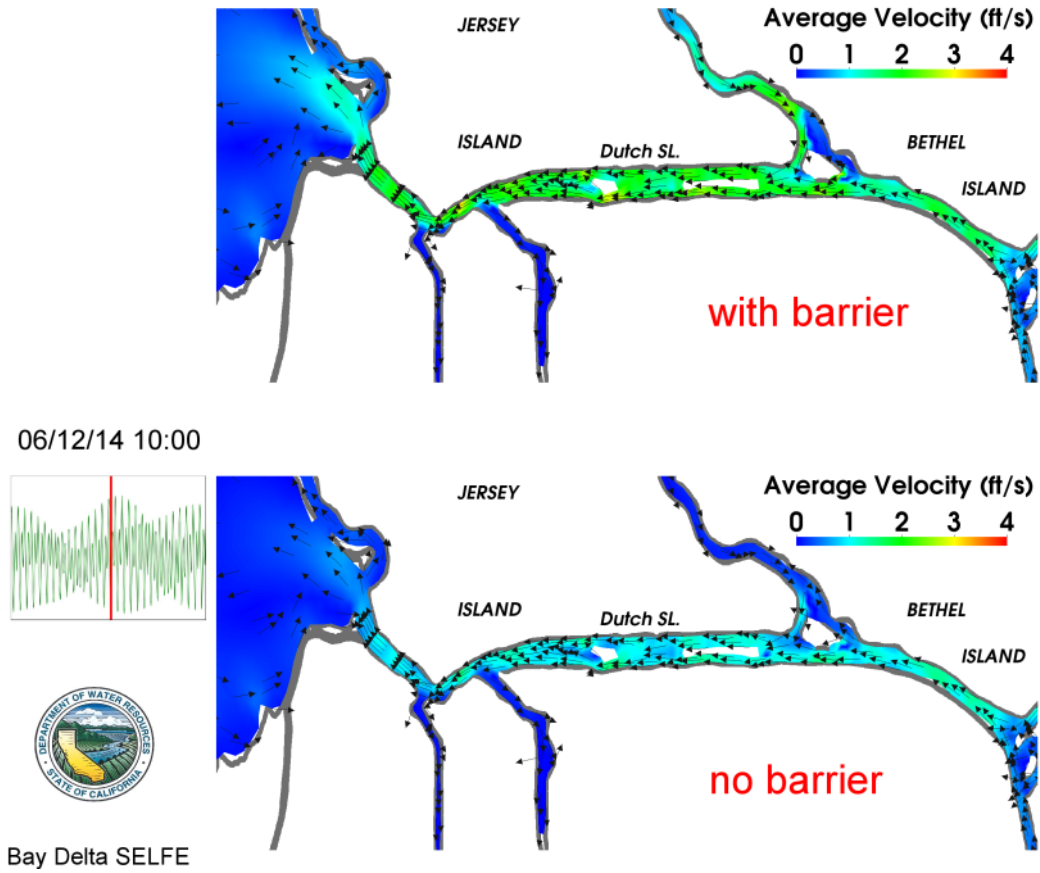
Figure 6-27 SELFE Spatial Velocity Distribution Plot for Fisherman's Cut
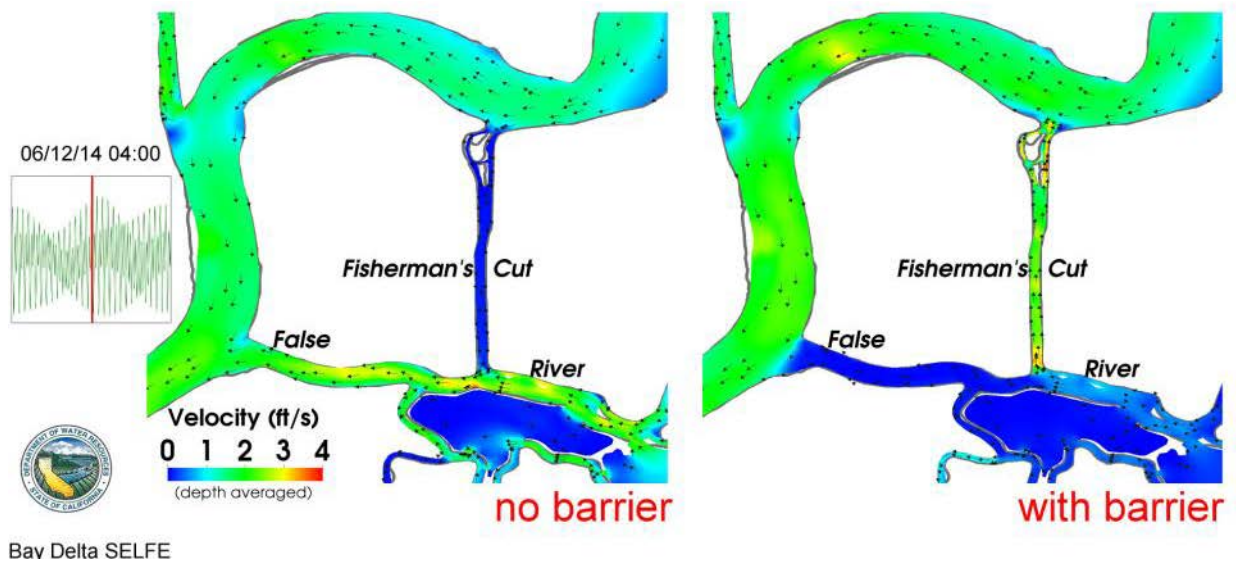
6.5 Water Cost Analysis Using the March 21, 2014 Forecast

In section 6.4.1, the evolving objectives of the studies were briefly discussed. When the March 21 forecast demonstrated that there would most likely be enough storage water to meet health and safety exports and keep salinity from intruding, further studies were done to determine if the emergency barriers could help in saving reservoir storage water for carry over storage, additional exports, or for environmental releases.

In order to determine water savings, DSM2 was run in an iterative process using a modified minimum water cost compliance problem tool (Ateljevich, 2002), http://modeling.water.ca.gov/delta/reports/annrpt/2002/2002Ch10.pdf.

In order to determine the water savings, the March 21 forecasted Sacramento flows are modified to change the net Delta outflow so that the salinity results for each alternative comply with the following D-1641 salinity objectives.
- Emmaton – 2.78 mmhos/cm
- San Joaquin at Jersey Point – 2.20 mmhos/cm
- South Fork at Terminous - 0.54 mmhos/cm
- San Joaquin at San Andreas Landing - 0.87 mmhos/cm
- West Canal at Mouth of CCFB – 1.0 mmhos/cm
- DMC at Tracy Pumping Plant – 1.0 mmhos/cm
- Rock Slough - 1.0 mmhos/cm (the assumption is that 1.0 mmhos/cm is approximately equal to 250 mg/l Cl)

Table 6-2 Net Delta Outflow Needed to Meet D-1641 Objectives for Various Alternatives

Objective	Without Emergency Barriers	Emergency Barriers	NDO Difference(positive indicates water savings with barriers)
Emmaton	3657 cfs	3893 cfs	-236 cfs
Relaxed	3045 cfs	2769 cfs	276 cfs
NDO Difference (positive indicates water savings with relaxed objectives)	612 cfs	1124 cfs	

The average net Delta outflow needed over a five month horizon from the time of forecast to meet the D-1641 objectives for the various alternatives are shown in Table 6-3. (These are not equilibrium outflow-salinity relationships). These results reflect optimal release schedules and show the following:
- Meeting the Emmaton objective and installing the emergency barriers would result in a season-averaged water cost of 236 cfs. This is expected because with the barriers, the water quality is degraded at Emmaton.
- Relaxing the Emmaton objective without emergency barriers results in a season-averaged water savings of approximately 612 cfs, as compared to an Emmaton objective without barriers.
- Relaxation of the Emmaton D-1641 objective results in a season-averaged water savings of 1124 cfs when emergency barriers are installed.

- If the Emmaton objective is relaxed, the three barriers provide an additional water savings of about 280 cfs.

In this study, initial expectations by some were that the water savings would be larger. Conclusions concerning the limited water savings of the barriers do not conflict with earlier findings that the barriers provide significant water quality benefits for a fixed release schedule. "Salinity improvement for a given water cost" and "water cost for a given salinity" are different goals. Figure 6-28 illustrates the relationship between salinity improvement for a fixed water supply and water savings for a given salinity target for dry hydrological conditions.

Figure 6-28 Water Cost Savings and Salinity Relationship

Large salinity change for fixed flow pattern

Small water cost savings for fixed salinity constraint
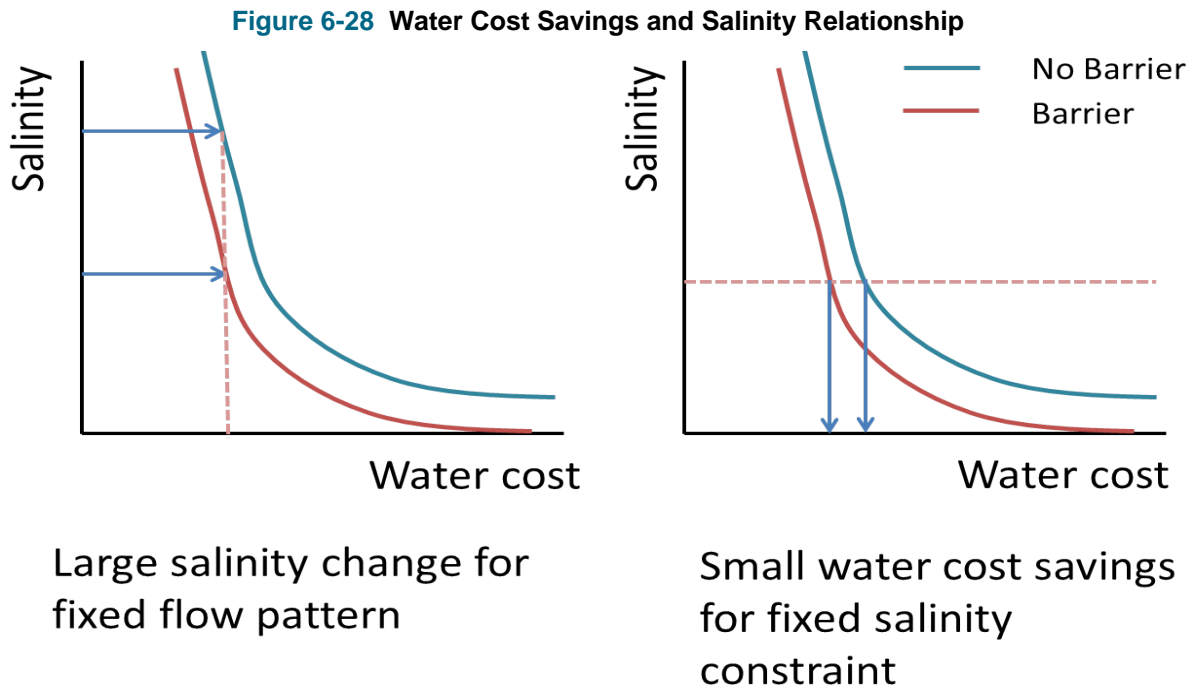
To get a better idea of the water savings in relation to reservoir storage, the water savings calculated above were converted to thousand acre-feet per month or thousand acre-feet per 5 months, and plotted with the reservoir storage from March 31. Figure 6-29 shows the results for one of the alternatives. The black horizontal line represents the Power Pool level for the three reservoirs (Folsom, Shasta, and Oroville). The dotted blue line is the historical average reservoir storage for March 31. The dashed red line is the capacity of all three reservoirs.

Figure 6-29 Relaxed Emmaton Objective Water Savings Plotted with March 31, 2014 Reservoir Storage
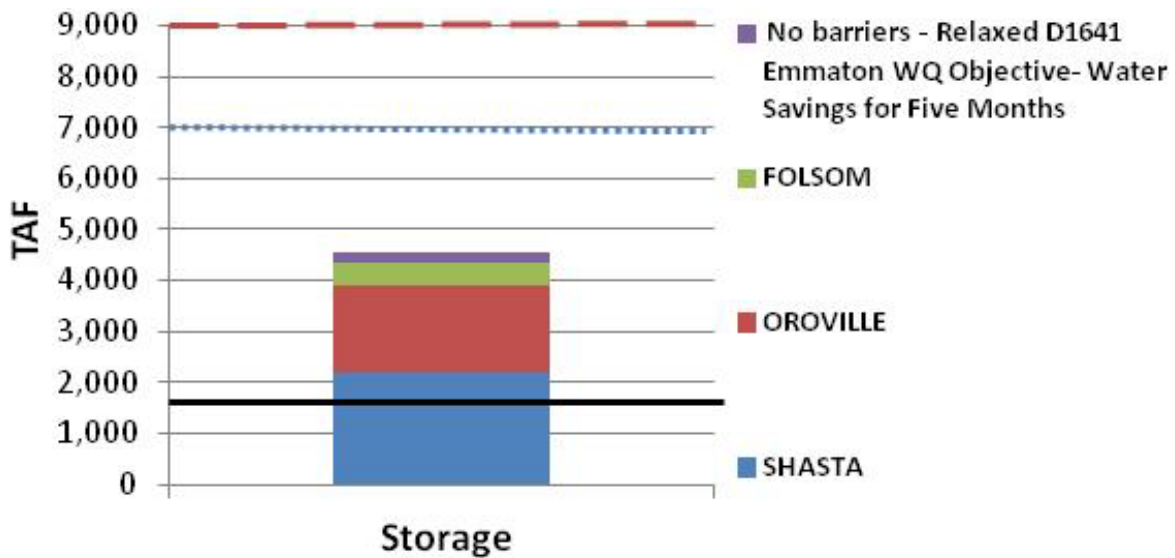
After looking at the water savings/costs for relaxation of the Emmaton standards and the emergency barriers, additional modeling studies were done to analyze the water costs or savings that would occur by moving the D-1641objective at Emmaton to Three Mile Slough. Table 6-4 shows the net Delta outflow needed for relaxed Emmaton objectives, meeting the D-1641 objective at Emmaton, and moving the objective to Three Mile Slough, with and without emergency barriers.

For the case without barriers, the relaxed objective and the objective that is moved to Three Mile Slough results in the same net Delta outflow. Without barriers, the Three Mile Slough objective is not the controlling water quality objective. When emergency barriers are in place, moving the objective to Three Mile Slough results in only 5 cubic feet per second difference over the Three Mile Slough objective without barriers.

Table 6-3 Net Delta Outflow Needed to Meet D-1641 Objectives When Moved to Three Mile Slough

Objective	Without Emergency Barriers	Emergency Barriers	NDO Difference(positive indicates water savings with barriers)
Emmaton	3657 cfs	3893 cfs	-236 cfs
Three Mile	3045 cfs	3050 cfs	-5 cfs
Relaxed	3045 cfs	2769 cfs	276 cfs

Figure 6-30 shows the EC at Clifton Court Forebay for the alternatives described in Table 6-5. The without barriers alternative with the relaxed objective or the objective moved to Three Mile Slough results in the highest salinity at Clifton Court Forebay. With emergency barriers and a relaxed objective results in salinity that is about equal to or less in salinity than maintaining the Emmaton objective without emergency barriers.

Table 6-4 **Description of Alternatives Shown in Figure 6-3**

no_barrier _emmaton
The 2.78 EC objective is met at Emmaton without barriers. This is the base condition. Net Delta Outflow is 3657 cfs.
barrier_emmaton
The 2.78 EC objective is met at Emmaton with barriers installed. Net Delta Outflow is 3893 cfs
barrier_relax
The water quality objectives are relaxed at Emmaton. Other locations still meet the water quality objectives. (Objectives that have number of days under 150 mg/l Cl have not been checked as part of this study). Net Delta outflow is 2769 cfs.
no_barrier_relax
The water quality objectives are relaxed at Emmaton without barriers. Net Delta outflow is 3045 cfs.
barrier_threemile
The water quality objective at Emmaton is shifted to Three Mile Slough (near Sacramento River). Barriers are installed. Net Delta outflow is 3050 cfs.
no_barrier_threemile
The water quality objective at Emmaton is shifted to Three Miles Slough without barriers. Net Delta outflow is 3045.

Figure 6-30 **Optimized DSM2 Forecasted EC at Clifton Court Forebay Using March 21 Forecast**
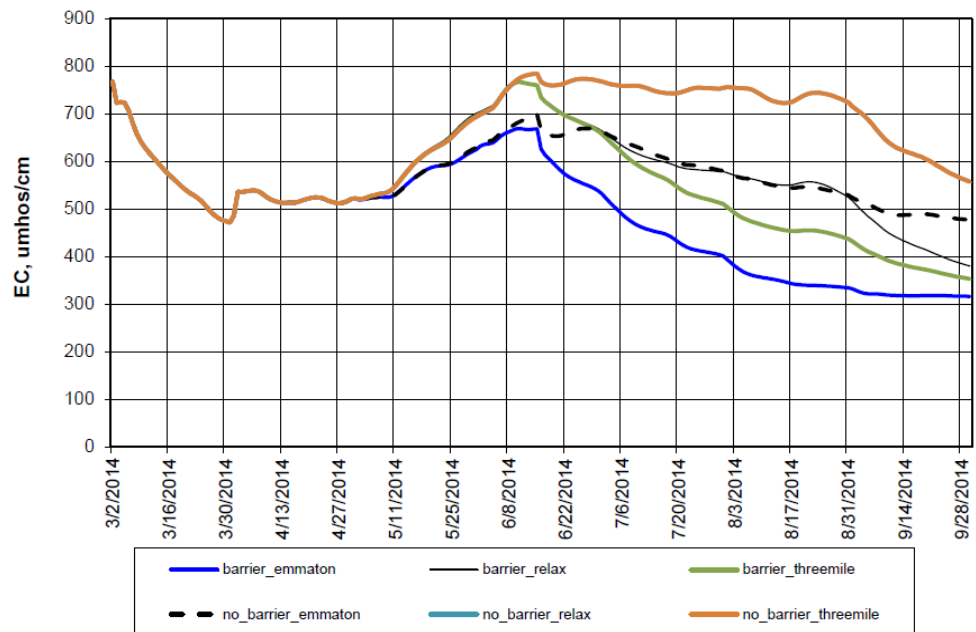
6.6 Summary

Through the late winter and spring, Delta modeling was performed using historical information and forecasts that represented very dry conditions. Each forecast fed into the decision making process of if, when, and/or where emergency barriers would be installed. In early February, with a dry conditions forecast, the outlook was grim in terms of having enough water for upstream releases, meeting water quality objectives in the Delta, and being able to export enough water for health and safety needs. This led to the analysis on how to best meet most of the water quality objectives in the Delta. As part of the

modeling output, potential negative impacts (and mitigation) for other stakeholders including western and northwestern Delta farmers/marinas, salmon migration, and smelt survival were considered. As precipitation occurred during the spring, the immediacy of installing the barriers started to diminish due to the likelihood that there was enough reservoir storage to make it through the summer. When this occurred, the objective of studies shifted to evaluate the water savings due to the installation of the barriers.

With the installation of the barriers, if all of the D-1641 water quality objectives are met, there is a water cost, not savings. The only water savings with barriers occur when the Emmaton objective is relaxed or moved. The largest water savings occurs with the relaxation or movement of the Emmaton objective. The barriers provide 1/4th of the water savings of relaxing the Emmaton objective alone. The barriers also improve water quality in the central and south Delta, and degrade water quality in the western and northwestern Delta.

At the writing of this chapter, additional studies are in process evaluating the impacts of relaxing or moving standards. Updated forecasts are being used to evaluate the effects of all three barriers and the False River barrier alone.

6.7 References

Ateljevich, E (2002). Optimal Control of Delta Salinity. Methodology for Flow and Salinity Estimates in the Sacramento-San Joaquin Delta and Suisun Marsh, 23rd Annual Progress Report. Chapter 10. State of California, Department of Water Resources

Ateljevich, E (2014). SELFE Development Status. Methodology for Flow and Salinity Estimates in the Sacramento-San Joaquin Delta and Suisun Marsh, 35th Annual Progress Report. Chapter 2. State of California, Department of Water Resources.

DWR, (2009). Delta Drought Emergency Barriers Administrative Draft, State of California, Department of Water Resources, Bay Delta Office

Mahadevan, N (1995) Estimation of Delta Island Diversion and Return Flows, State of California, Department of Water Resources Division of Planning.

Roy, Sujoy et al, (2014). Salinity Trends in Suisun Bay and the Western Delta: October 1921 – September 2012. Prepared for San Luis and Delta Mendota Water Authority and State Water Contractors. Paul Hutton Technical Representative.

Chapter 7. Bay-Delta SELFE Calibration Overview

7.1 Introduction

The Delta Modeling Section at DWR and Virginia Institute of Marine Sciences recently concluded a collaborative initial calibration of the 3-D semi-implicit Eulerian-Lagrangian finite element (SELFE) hydrodynamic model for the Bay-Delta (Figure 7-1). This chapter describes the scope of the calibration, assumptions, and additions made for the domain, preliminary calibration results, and discussion of suitability of the model for various types of studies. A more technically comprehensive calibration document is in preparation.

The goal of our project is to develop an open-source, cross-scale multidimensional model suitable to answer flow and water quality questions involving large extents on the Bay-Delta system over periods of several years. Target applications include:

- Habitat creation and conveyance options under BDCP alternatives
- Salinity intrusion changes under drought or sea level rise
- Velocity changes in nearby channels following the installation of barriers
- Fate of mercury produced in the Liberty Island complex in the north Delta
- Temperature, flow, and food production in the estuary as part of a 3-model full life cycle bioenergetic model of salmon (as participants in the NOAA SESAME project).

These applications vary a great deal in scope. Some can be studied with our base model as-is using a few quick adjustments, but the last two require focal regions of intense study, multi-disciplinary biogeochemistry, or more careful validation of a particular transport mechanism. In our collaboration with NOAA and NASA in the SESAME project, the flexibility and openness of SELFE allowed swift incorporation of CoSINE, an alternate nutrient model to the standard EcoSIM 2.0 in SELFE emphasizing the most important constituents for salmon in the system.

Our immediate goal has been to establish a foundation – to develop a sense of global accuracy, requiring that we resolve (or craftily under-resolve) the main mechanisms of hydrodynamics and transport up the estuary and in Delta channels. These include gravitational circulation and exchange flow, periodic stratification, tidal trapping, flood-ebb asymmetry of flow paths, shear dispersion, primary flow streamlines, and perhaps some secondary circulation in large channels. Although we expect our calibration to continue to improve, further work will be continue in project-dependent directions. Due to its flexible mesh, the model is easily re-usable in a near field/far field arrangement whereby the base model provides a pre-calibrated background grid for an extension or focal region of study.

Our base calibration focuses on hydrodynamics and salinity transport and on the North Bay and Delta. The reasons for concentrating on salt as a first step are well-known. Salinity intrusion is the most important water quality issue facing the water projects. Salinity (conductivity) is extensively monitored at stations throughout the estuary. Second, in the stratified part of the estuary, salt is essential to the vertical structure of flow through density – so modeling salinity is prerequisite to modeling the transport of other constituents such as sediment and organisms that are preferentially distributed vertically in the water

column. Finally, in much of the estuary and Delta, salt does behave much like any other diffuse, conservative tracer, and inasmuch as all conservative constituents are equivalent, a good salinity calibration is a good conservative tracer calibration.

7.2 SELFE Model

SELFE is a cross-scale 3-D (optionally 2-D) shallow water open source hydrodynamic model jointly developed by the Center for Coastal Margin Observation and Prediction (CMOP) and Virginia Institute of Marine Sciences. In the past, SELFE has been coupled to several ecological and water quality modules, two wind-wave interaction models, 2-D and 3-D sediment transport, data assimilation, and oil spill applications. A number of these are available as open source modules. In the current project, we have tackled some of the practicalities of Bay-Delta modeling, including the incorporation of subgrid hydraulic structures such as radial gates, weirs, and culverts.

The underlying computational engine in SELFE is a second-generation semi-implicit model sharing some of the algorithmic background of the UnTRIM family of models, which also includes UnTRIM and SUNTANS and emerging models from Deltares and FVCOM. The semi-implicit approach is robust, efficient, sufficiently accurate, and offers a natural treatment of wetting and drying. SELFE's predecessor, ELCIRC, was perhaps the first open source model of this class to receive wide distribution and that prior experience figured heavily into our model selection decision. SELFE shares some code with ELCIRC, but its discretization and solution scheme includes innovations to the algorithm that improves the depiction of bathymetry and salinity plume transport. SELFE has also been parallelized and used by groups all over the world on a diverse variety of high performance computers.

7.2.1 Formulation

The formulation of SELFE is based on classic expressions of mass and momentum conservation within a shallow fluid, as well as the transport equations for salt and heat. Flow is assumed to be *Reynolds averaged*, which means that small scale turbulent mixing of momentum and dissolved constituents is not resolved directly, but rather tied to mean flow properties using a turbulence closure. Pressure in the model is assumed to be hydrostatic in our application. SELFE has a non-hydrostatic module, but non-hydrostatic modeling requires higher resolution in space and time than an estuary-scale solution can typically provide in long-term simulations.

The main variables calculated by SELFE are the elevation of the free surface (stage), three-dimensional velocity and concentrations of salinity, temperature, and other scalar concentrations (only salinity is considered in this calibration), as well as turbulent quantities. Extensions in the SELFE suite use the flow field to calculate particle trajectories, sediment transport, and nutrient availability. The input required by SELFE includes the initial state of the system and boundary time series representing fluxes and/or water surfaces at all the open boundaries.

As with other semi-implicit layered models, SELFE can easily be applied in its single-layer 2-D form as well as in 3-D. Our preprocessing tools allow the domain to be cut at Martinez, above which the 2-D model can be used for model speedup; we are only beginning to explore this option.

Figure 7-1 Bay-Delta SELFE Domain, Boundaries and Agricultural Source/Sink (DICU) Locations
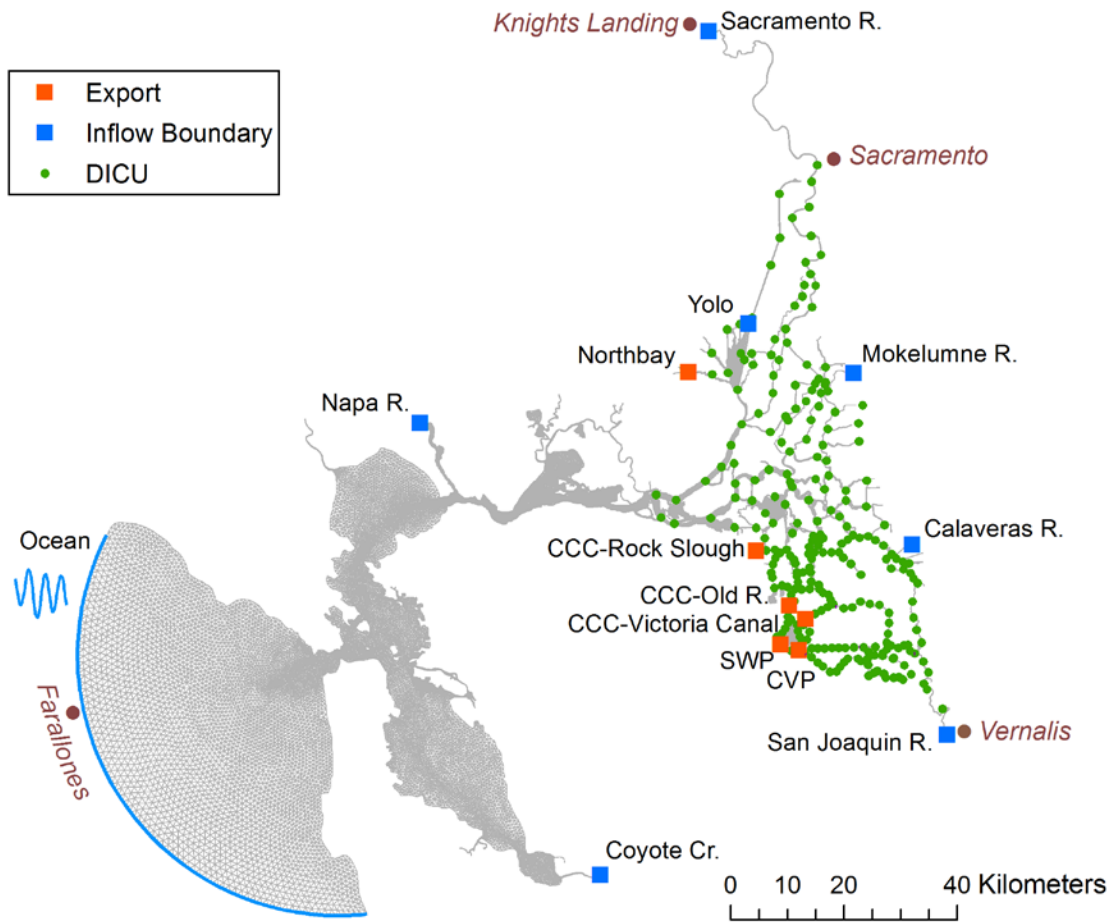
7.2.2 Roughness and Friction and Turbulence Closure

An important aspect of calibration is tuning the mechanism by which friction is imparted on flow. In SELFE, resistance is introduced into the water column through the combination of the bottom stress (drag) boundary condition felt just above the bed, and a vertical turbulent eddy viscosity that mixes the lower and higher velocity water (and salt) vertically. Figure 7-2 illustrates this process and also shows examples of how velocity and the eddy viscosity/diffusivity (mixing coefficient) might vary with depth.

Figure 7-2 **Typical Vertical Structure of Velocity (right) and Eddy Viscosity (left)**
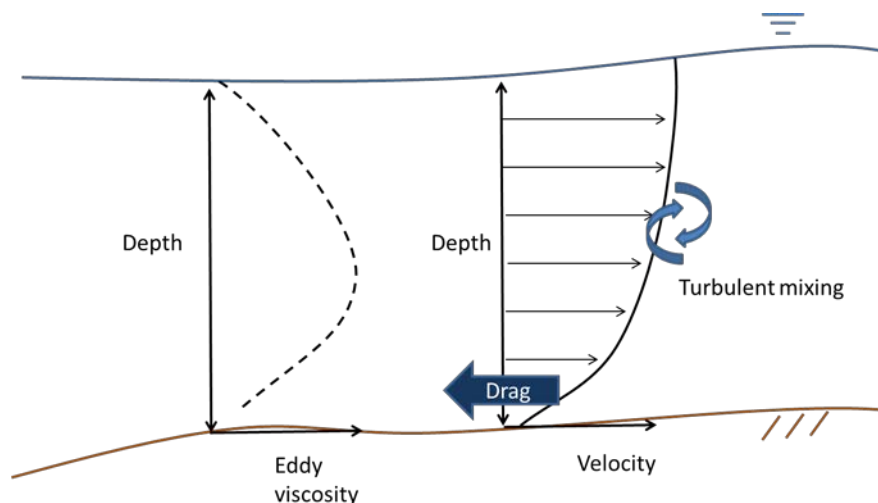
In calibrating the model, there are three options in the stipulation of the drag coefficient:
- C_d (drag) may be specified directly either as a constant or distributed over the mesh
- Roughness z_0 may be specified, and C_d will be calculated as a function of depth from a standard formula describing the bottom boundary layer. This was our ultimate choice.
- In 2-D, Mannings coefficients can be given directly.

The turbulent eddy viscosity (and diffusivity for salt) are not stipulated directly, but rather emerge from the turbulence closure. We use the vertical component of Umlauf and Burchard's generic length-scale model, and two auxilliary differential equations which are integrated off-line of the other equations based on values from the previous time step. We found the results to be relatively insensitive to turbulence closure choice, except Mellor-Yamada closure, which tended to eliminate stratification. Work here is presented based on $k - \varepsilon$.

7.2.3 Transport Equation

SELFE uses its transport module to track salt, temperature and sediment concentration, and water quality constituents. There are several algorithm choices in SELFE for constituent transport, and balancing these is critical for tuning model performance:
- First, order upwind finite volume method (FVM), which is faster but diffuses the vertical structure of salinity.
- Second, order total variation diminishing (TVD) upwind finite volume scheme, which is slower but preserves sharp gradients.
- Third, the Eulerian-Lagrangian Method (ELM) used for momentum advection, which combines (particle-like) backtracking along the velocity field with interpolation.

Because they are mass conservative, the two finite volume schemes are more commonly used than the ELM scheme. The two transport schemes can be mixed adaptively based on map and depth-based criteria. Specification of these criteria constitutes a calibration decision. Our use of the more expensive TVD method is limited to the region west of the confluence and to depths greater than 6m.

Horizontal diffusive mixing of constituent concentration is available, but not enabled. Velocity variation across the main flow field is directly resolved in most channels of importance, so modeling shear dispersion does not require a new term. Horizontal eddy diffusivity is very small compared to the other terms and enough is apparently introduced by the unavoidable horizontal numerical diffusion introduced in solving the equations.

7.2.4 Horizontal Meshes

The horizontal mesh is referred to as *unstructured* because the connectivity of the triangles is general and unconstrained. The benefit of unstructured meshes is that they are easy to represent complex natural domains with a fair amount of accuracy (see Figure 7-3).

Figure 7-3 Horizontal Mesh near Franks Tract
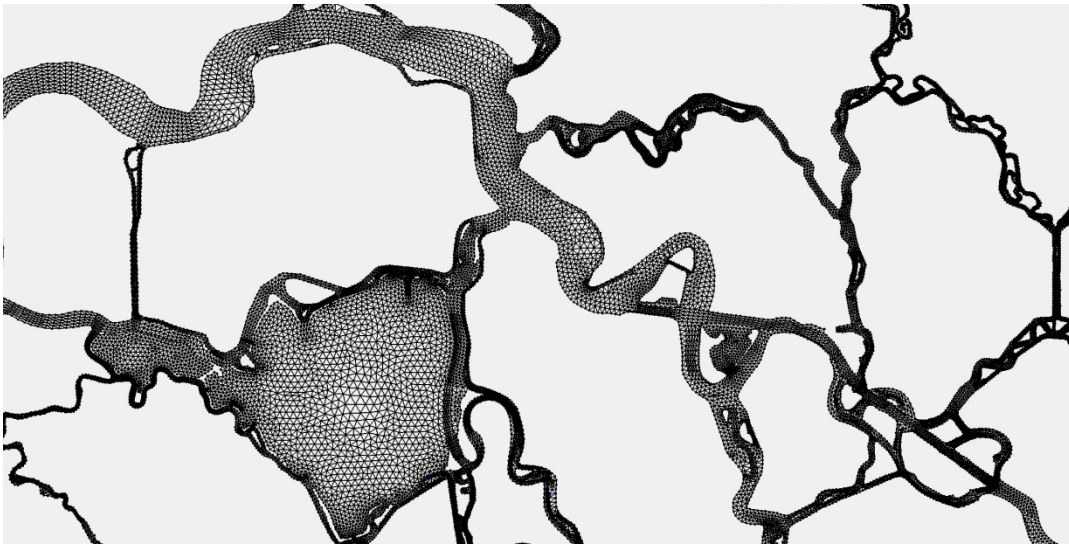
One additional distinguishing characteristic of the horizontal mesh used in SELFE compared to other semi-implicit models is that the mesh is not required to be *orthogonal* (Figure 7-4). In an orthogonal mesh, the edges of the mesh are perpendicular to the line between the "centers" (typically circumcenters) of the elements. For a triangular mesh, the orthogonality requirement leads to triangles that are nearly equilateral. While this shape is relatively efficient and accurate, generating such a mesh imposes tradeoffs with other desirable properties, such as conforming to the contours at the foot of a slope or thalwag of a channel.

Figure 7-4. (a) Orthogonal Triangular Mesh. (b) Non-orthogonal Mesh with some Skew

a.   b.
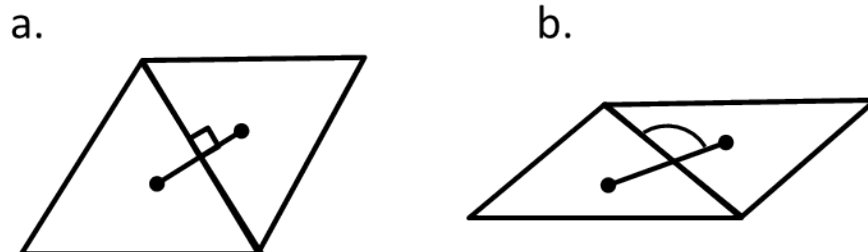
One efficiency disadvantage in SELFE is that the mesh is limited to triangles. UnTRIM uses quadralaterals. Newer versions of some other semi-implicit models (Deltares and SUNTANS) may allow more general element shapes, although, as far as we know, applications of these features are not ready. Some older models such as EFDC and the classic version of the Deltares 3-D model also have used quadrilaterals, but these are structured curvilinear quadrilaterals and are very restrictive when it comes to modeling natural systems.

The Bay-Delta mesh was constructed using the Aquaveo SMS model development software package (generic version), in which the user first specifies a skeleton mesh map comprised of discretized polygons each of which is then filled using automatic meshing algorithms. An advancing front algorithm ("paving") was used for large, well-resolved water bodies and some side embayments. Coons patches ("patching") were used in channelized areas, including internal channels in some bays and open water bodies. Figure 7-5 shows an example of the combination in preparation at San Pablo Bay, with Coons patches delineating the critical ship channel through Pinole Shoal Channel (the quadrilaterals will eventually be split into triangles) in an otherwise expansive embayment.

Figure 7-5 **Close-up of Mesh Preparation in San Pablo Bay with Coons Patches near Pinole Shoal**
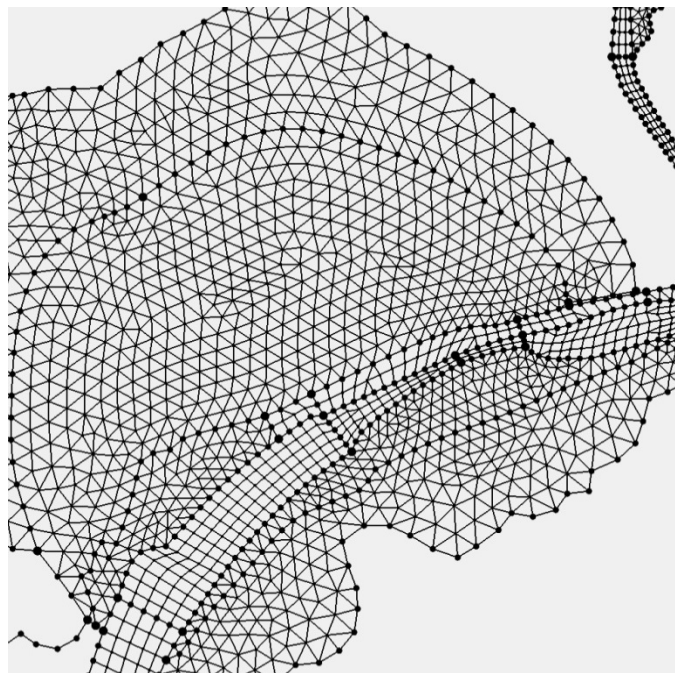
7.2.5 Vertical Mesh

SELFE has a flexible meshing system in the vertical direction, allowing a hybrid of Z layers below, and terrain-following S coordinates above, as shown in Figure 7-6. Z-layers are at fixed elevations, but the S-layers follow contours in the bed and allow the user to concentrate greater or less density in the lower or upper boundary layers. The original purpose of including the SZ hybrid was to avoid some of the pitfalls associated with topography-conforming meshes, particularly on very steep bathymetry in deep water. The Bay-Delta is generally shallow enough to avoid the Z layers entirely, so our mesh is defined by 23 vertical terrain-following S layers.

CMOP did extensive side-by-side testing of SELFE and ELCIRC, a Z-only model like UnTRIM and SUNTANS, and the terrain following mesh was one of the factors cited in the improved performance of SELFE for plume tracking. Although we are confident the pure-S approach is the best option available to us between S, Z, and SZ, we have also begun testing a vanishing quasi-sigma vertical coordinate system similar to that described by Dukhovskoy et al. (2009) in which layers disappear gradually in shallower water and therefore also have smaller gradients. Our implementation includes an enhancement to avoid the stairstepping noted by Dukhovskoy et al. (2009). This gridding system preserves the advantages of bathymetry conforming coordinates while reducing pressure errors, preserving stratification, and eliminating some practical issues associated with over-resolution in shallow water.

Figure 7-6 **(a) The Hybrid Coordinate System used in SELFE. S-Coordinates are used above the Threshold Depth, while Z (Stairstepping) Coordinates are used below. (b) Vertical Transect of an SZ Mesh**
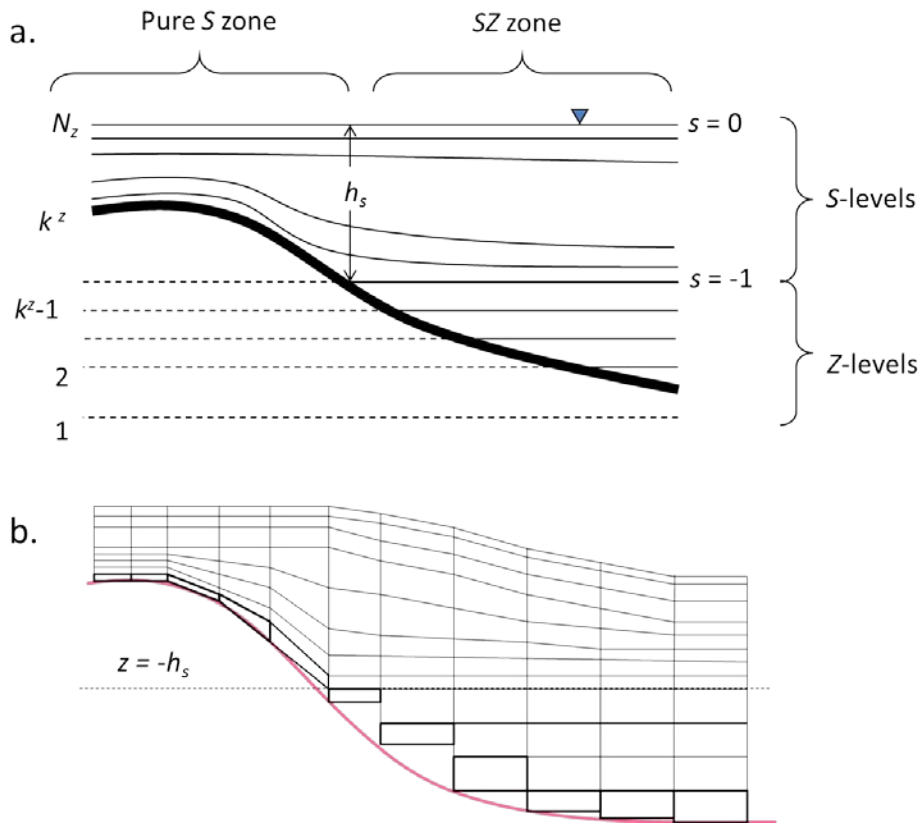
7.2.6 Hydraulic Structures and Mass Sources

As part of the Bay-Delta SELFE project we added two capabilities to SELFE that were not part of the original code base. The first was the abiltiy to model sub-grid hydraulic structures such as:

- Weirs, based on approximations in DSM2 and HEC-RAS,
- Culverts, based on simple orifice representations as in DSM2,
- Radial gates based on HEC-RAS,
- Direct transfers of water between subdomains.

Our implementation allows time series control of structures, as well as timed installation and full removal (in which case the location reverts to the usual hydrodynamic equations). In the near future we also plan to experiment with an energy-momentum approximation, for Clifton Court Forebay.

We also allowed a provision for mass sources and sinks, in order to accommodate Delta consumptive use (DICU). The mass addition is considered for purposes of continuity and transport but is not incorporated in the momentum equation.

7.3 Bay-Delta SELFE Application

7.3.1 Domain, Mesh, and Boundaries

The Bay-Delta domain encompasses a domain spanning from the Farallon Islands in the west, Knights Landing on the Sacramento River to the north, and Vernalis on the San Joaquin River to the south (Figure 7-1).

The ocean boundary of the Bay-SELFE model lies on a roughly 46 km radius arc from the Golden Gate, extending from Point Reyes to the Farallon Islands and south just past Half Moon Bay. The ocean boundary was chosen far enough offshore so that the dynamics inside the domain do not impact the boundary, including the discharge of sediment and fresh water plumes. For the simulations presented here, our boundary data is interpolated (inverse distance weighted) between Point Reyes and Monterey after which a fixed delay and scaling is applied everywhere along the boundary.

On the Sacramento River, the primary consideration was to model far enough upstream to avoid tidal reflection and facilitate a future extension to all of Yolo Bypass. To avoid complications and data shortages on the American and Feather rivers, flows on all three rivers are routed down the Sacramento. For flow data, we tidally filter U.S. Geological Survey (USGS) observations at Freeport and move the resulting time series upstream with a lead of 3 hours.

The other upstream boundaries and export sites are similar to those used by other community models including DSM2, data for which has been widely disseminated. The boundary data come from flow, pumping and conductance observations by USGS, DWR, and the U.S. Bureau of Reclamation (USBR). We made two additions for the Bay at Coyote Creek and Napa River.

The mesh comprises roughly 140,000 nodes and 238,000 triangles. Mesh resolution varies from approximately 1km in the ocean to 100-400m in the Bay and down to 20-60m in Delta channels, with the smallest element width less than 5m found near Middle River. Figure 7-7 shows a histogram of equivalent radii (i.e., radii of circles with equivalent area) of the elements, a measure of discretization length that tends to be on the small side – for anisotropic elements it tends to be smaller the width. The mesh sizing was chosen to:

- resolve bathymetric features and the deep sections of major channels, which is important for salinity intrusion,
- resolve lateral and vertical variations in velocity and shear dispersion,
- emphasize regions of policy importance or that have a greater effect on global accuracy,
- take good advantage of SELFE's ability to handle anisotropy and non-orthogonal elements.

- realistically introduce wetting and drying while keeping always-wet main channels open to flow, and
- otherwise minimize computation time.

7.3.2 Bathymetry

SELFE requires bathymetry data at every node in the mesh. A lot of our early effort was spent collating and improving bathymetry. We described the generation of seamless topography models for multidimensional modeling in a previous annual report chapter. Several models are now utilizing this product and recently we have begun a more active exchange with the USGS resulting in better review and reconcilliation of products.

Our bathymetry integrates elevation data from previous USGS maps, single and multibeam data collections into a set of mutually consistent 10m and 2m elevation DEMs. The data used in calibration is identical to the version 3 release of this bathymetry except that here we have incorporated recent improvements near the CVP intake and South Delta, and some additions in the north Sacramento River where we extended the bathymetry in response to boundary reflection.

Figure 7-7 Histogram of Element Size, using Equivalent Radius (Radius of the Circle with Equal Area)
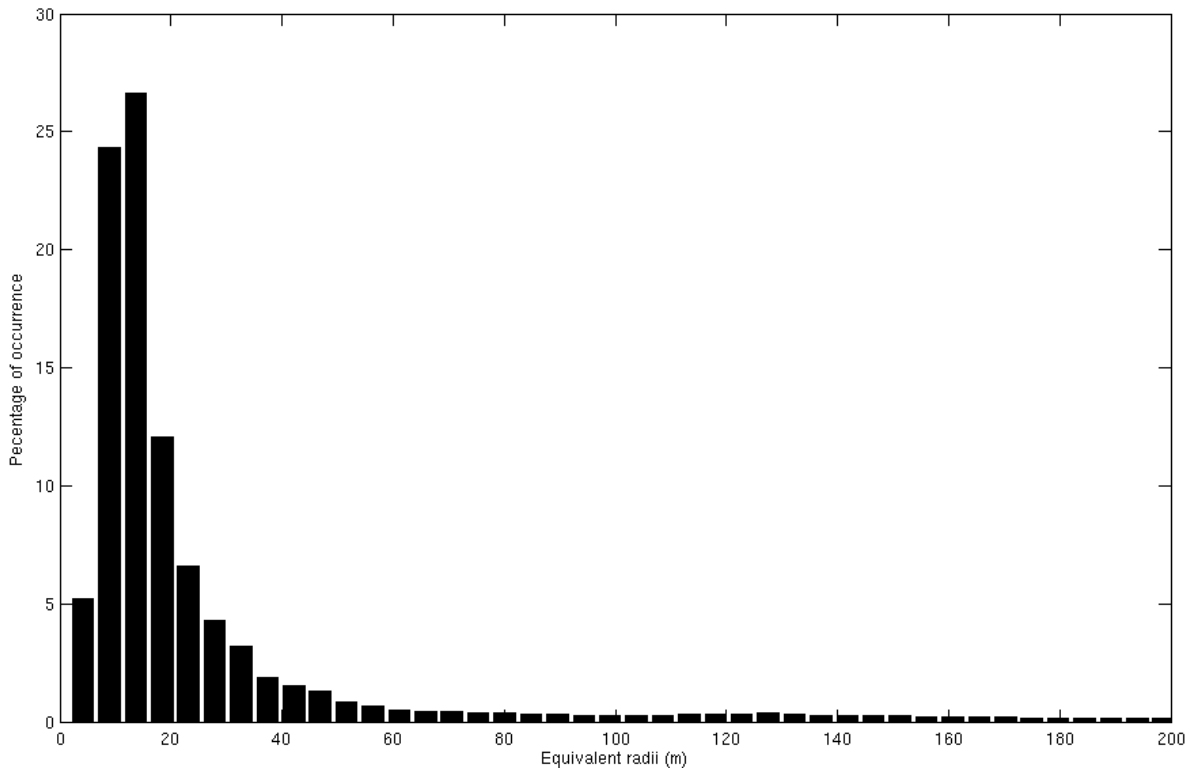
Note: For anisotropic elements, equivalent radius is typically smaller than width.

Some re-processing of bathymetry was performed in order to better represent volumetric quantities and moments (volume, vertical face area) over the areas covered by mesh elements. In addition, in several marshy areas, such as Sherman Lake, we used contour-based smoothing methods to "untangle" very twisted subgrid topography so that the storage areas represented by intricate tertiary channels could be

captured better by the model. These additional geometry processing steps will be covered in some detail in the main calibration document.

The vertical datum of the model is NAVD88.

7.3.3 Barriers and Gates

All the major gate and hydraulic structures in the Bay-Delta system are included in our model, including the Delta Cross Channel, Montezuma Salinity Control Structure, south Delta temporary barriers, and the gate at Tom Paine Slough. Up to now, we have omitted some small structures in the Morrow and Roaring River complexes in Suisun Marsh where the channels are much smaller than our local model scale or where we do not yet feel we have mastered the connectivity. The fish barrier at the head of Old River was not installed for either of our two calibration years; it was, however, included for subsequent drought modeling in 2013-2014.

Gate timing and coefficients were taken mostly from institutional logs for the south Delta barriers, Suisun Marsh Gate (DWR), and Delta Cross Channel (USBR). The south Delta barriers were installed and removed using time series. A schedule of operations for 2009 and 2010 can be found respectively in Figures 7-8 and 7-9.

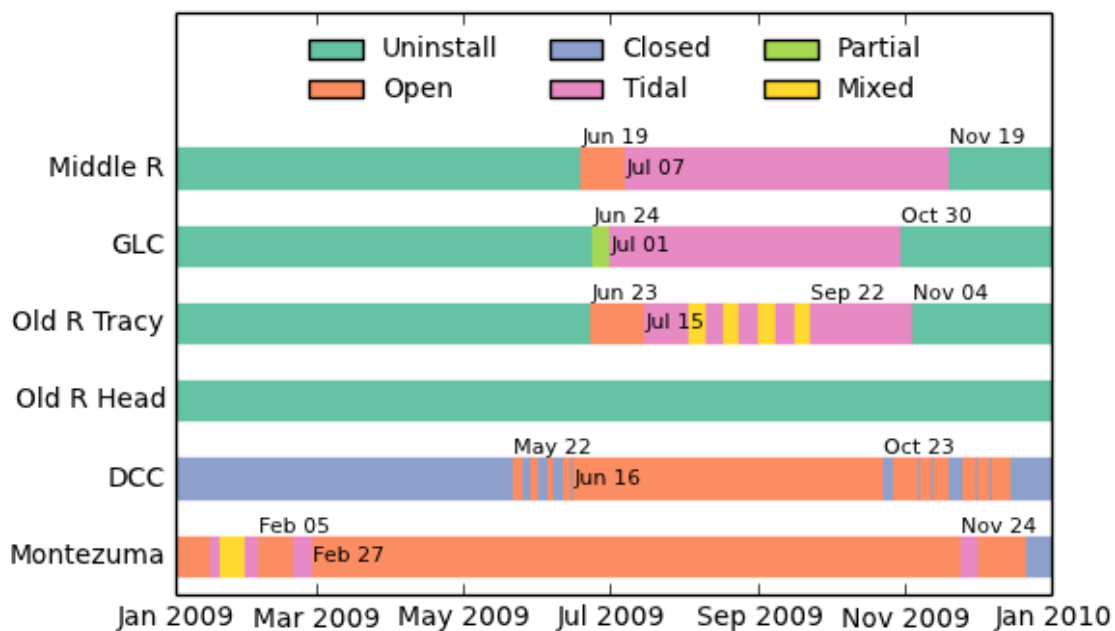**Figure 7-8** **Delta Hydraulic Structure Operations for 2009**

Figure 7-9 Delta Hydraulic Structure Operations for 2010
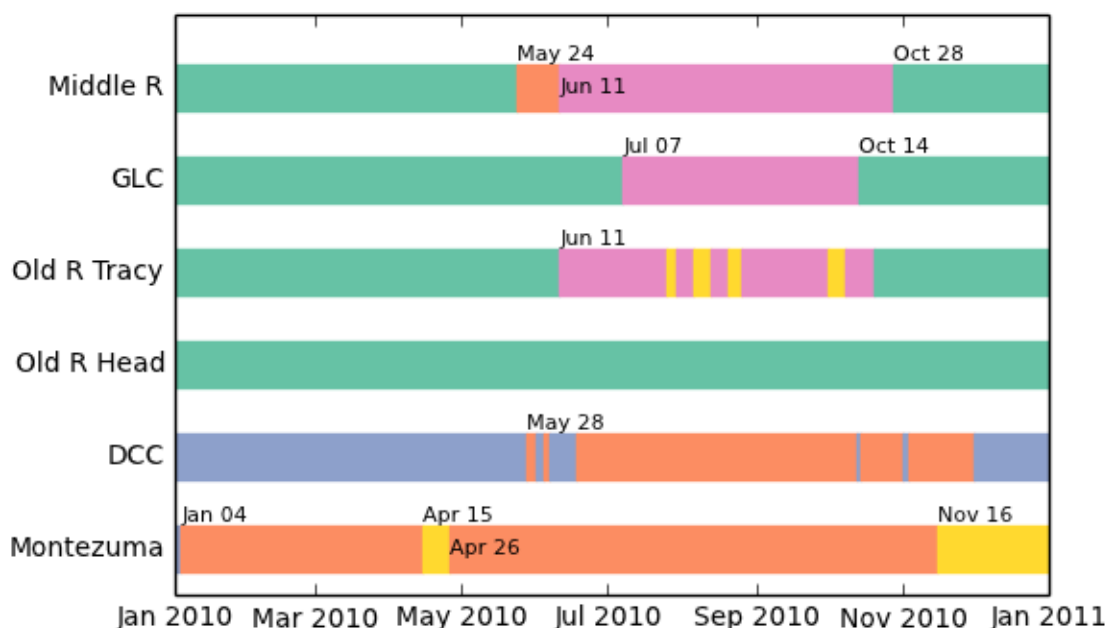
We modeled Clifton Court Forebay inflow using historical gate flows rather than as a radial gate. We were not confident that either the DSM2 rating or the Hills Equations used by Delta Field Division is sufficiently accurate to reproduce the water surface at Clifton Court or prevent gate flow errors from affecting the rest of the calibration. We have developed a rating for the gates based on several new data collections, and used it in the calibration to disaggregate daily gate flows in time as proposed by MacWilliams and Gross (2013). This solution works well for hindcast and calibration, though it has no analog in planning and small discrepancies between inflow and outflow can accumulate to unacceptable values over months. The new rating will be inserted inline in SELFE soon and used for long term historical and planning studies.

7.3.4 Atmospheric Inputs

The model accepts spatiotemporal atmospheric input representing surface wind, atmospheric pressure, and precipitation over the domain. The most significant of these is thought to be wind. There is no unified approach to modeling wind in the Bay-Delta region. Past work in the domain has either justified neglecting wind due to a short period of study or used atmospheric inputs from a small set of representative stations situated on the water.

The approach we adopted is to use climate or weather reanalysis products that combine a numerical model and data assimilation. Numerous reanalysis products are available for the region at both climate (coarser) and weather (finer) scales. For our calibration we used winds at 10m above ground from the NARR dataset from NOAA. This dataset is 32km in resolution, which is roughly the spacing of field stations used in and not fine enough to resolve the width of the Bay or local spatial patterns of wind at the Golden Gate, South Bay, San Pablo Bay, and Carquinez. Through our collaborators in the SESAME project, we have access to two much finer resolution wind fields from reanalysis products. The first is a 3km COAMPS model from the Central and Northern California Ocean Observing System (CenCOOS). The second is a 1km Weather Research and Forecasting (WRF) simulation from NASA unique to the

SESAME project. Preliminary results suggest high resolution data may not be required for global accuracy of salinity transport. This is a significant result because detailed wind data is not available in hypothetical situations, and will be particularly uncertain under climate change.

7.3.5 Initial Conditions

SELFE requires an initial condition for the entire model state, including velocity, water levels, and salinity. Initial conditions are quickly forgotten for water levels and velocities – and we use constants for these. The initial salinity field persists much longer, affecting the simulation for months.

We use an estimated salinity condition from data to reduce spinup time for the model. Our salinity initial condition is generated regionally:

- Ocean: A scalar value of 33.5 psu at all depths, which is typical of the shelf region at modest depth.
- Bay and Suisun: From the south Bay to the confluence the model is initialized using vertical salinity profiles from USGS Polaris water quality cruises, interpolating linearly between stations and extrapolating radially from the path of the cruise.
- Delta: A scalar constant value of 0.1 psu (215μS/cm EC) is used throughout the Delta. This value is typical for the north Delta but too fresh for the south Delta.

During 2013-2014 drought modeling, salinity spinup in the south Delta took 3-4 months and limited our agility doing realtime runs with new grids. We recently started to minimize spinup time by briefly (3-5 days) assimilating data from the many observation stations in the Delta through a simple 2-D scheme called Newtonian Relaxation, or *nudging*. This technique more rapidly brings the model state very close to observed values anywhere that is within a few tidal excursions of a monitoring station.

7.3.6 Delta Agricultural Sources and Sinks (Consumptive Use)

The Delta islands are agricultural, and diversions and returns of water from the islands significantly impact flow and water quality in the channels. The magnitude of the water quality impact varies with the seasons, as the balance between diversions, drainage, and seepage changes. During summer months (including 2009), it is not uncommon for consumptive use to be equal in magnitude to total Delta outflow (see Figure 7-10, note the units are in cfs). This means that consumptive use is not only a major driver of local water quality, but also a near-dominant component of the flow balance preventing salinity intrusion from the ocean.

Figure 7-10 **Net Delta Outflow and Delta Island Consumptive Use Estimates for 2009**
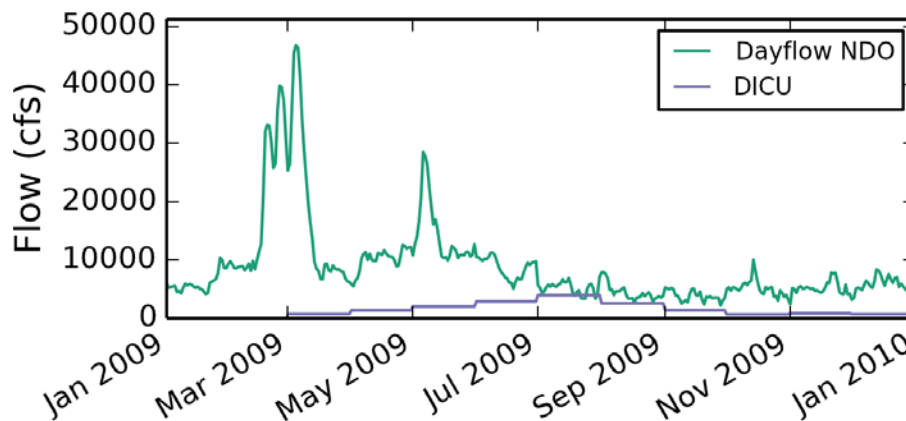
Historical flow and water quality data has not traditionally been available for the islands. In the absence of field data, we use estimates from the DWR Delta Island Consumptive Use model. The DICU model is centered on the islands (or regions), and performs a water balance that assumes land use and crop types and seeks to explain the resulting demand for water in terms of precipitation, soil moisture, seepage, and applied water. The inferred fluxes to and from the Delta channels are then assigned to discrete locations in a second step that is distinct from the water budget. Although the assignment of locations is based on survey locations, the original locations are aggregated and the final locations of the sources are influenced by the location of nodes in DSM2. The sites are shown in Figure 7-1.

In dry periods when salinity intrusion reaches the channelized Delta above the Sacramento-San Joaquin confluence, the uncertainty surrounding Delta outflow poses a confounding factor in any salinity calibration. Overall, we found the following two adjustments to DICU vastly improved agreement between model and data, including not only point observations but also vertical structure of salinity:

- For several days during big runoff events in 2009, we switched from DICU to DETAW, a beta-level daily consumptive use model being vetted to replace DICU. DICU, a monthly model, tends to undercalculate both the intensity and total volume of runoff from brief, intense storms (Figure 7-11). DETAW runoff data, Dayflow precipitation estimates and USGS outflow data all agree better.
- We scaled DICU so that outflow better matches seasonal fluctuations seen at the four USGS Net Delta Outflow gages (Sacramento River at Rio Vista, San Joaquin River at Jersey Point, Three Mile and Dutch sloughs).

Although these adjustments stem from observed data, they can still be problematic. Net flows at Jersey Point and Rio Vista are subject to substantial bias because they are extracted from tidal fluctuations orders of magnitude larger. The technique we used to correct outflow is limited to a short historical record and is brittle in some of those years including the winter 2013-2014. We are investigating newer methods that use the entire USGS and DWR flow observation network to better quantify Delta outflow.

Figure 7-11 Estimates of Agricultural Drainage from DICU and DETAW Around the Period of the Storm
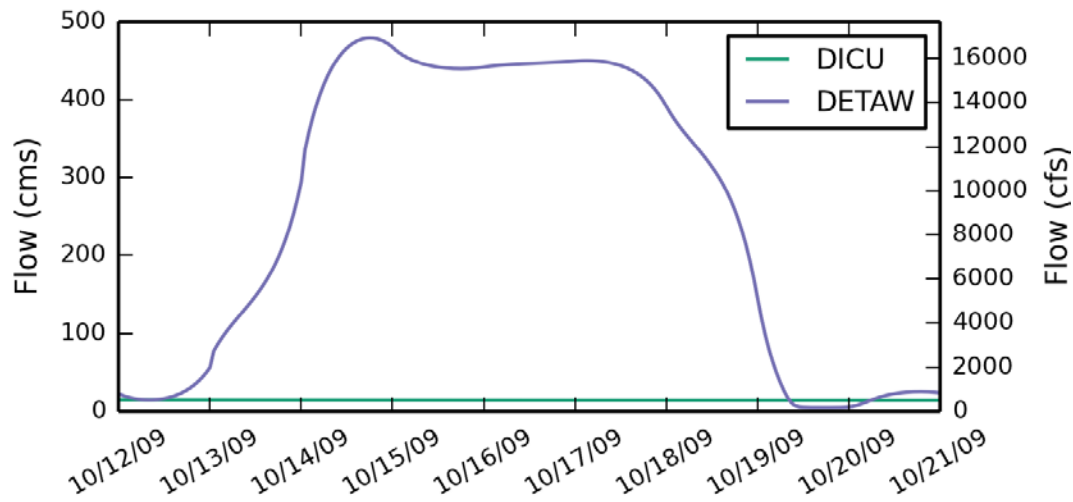
7.3.7 Description

The period of the the calibration is March 12, 2009 through October, 2010. The year 2009 is categorized as dry and 2010 is categorized as below normal. The period through summer 2009 was used to match elevation and flow and the period through the first freshet in 2010 was used as the basis of matching salinity. Most of the results here come from the remainder of 2010, which was modeled twice, once following the calibration, and once after incorporating some changes from emergency drought modeling.

The hydrodynamics time step is 120 seconds for all the simulations, in keeping with the minimum time step to avoid numerical diffusion in the the Eulerian-Lagrangian component of the algorithm. The scalar transport part of the code is constrained by a different time step restriction, this one a maximum rather than a minimum, and as a result the transport regularly subcycles the main hydrodynamic time step using steps typically less than 30 seconds.

7.4 Calibration

The Bay calibration covers hydrodynamic variables (water surface, velocities, and cross-sectional flows) as well as salinity. The main items that we manipulated in the calibration were:

- horizontal mesh configuration, and density
- vertical mesh selection, configuration and density
- roughness coefficients
- the selection of turbulence closure
- the order of ELM interpolation at the foot of characteristics (i.e., after backtracking)
- extent over which higher order TVD transport was used.

In keeping with the practice in other 3-D Bay-Delta models, we did not adjust roughness spatially. We experimented with several relationships between roughness or drag and depth, but always applied the same formulas over the entire domain. We may relax this assumption later to acknowledge the influence of channelization, bed forms, and vegetation.

7.4.1 Computational Performance

The simulations reported in this chapter were performed on a Linux cluster with 180 cores at a ratio of simulated to computational time of 110:1, meaning that it takes roughly 3 days of computer time to simulate a year. We are currently working with a refined, less optimized grid that is somewhat slower at 85:1.

7.4.2 Skill Metrics for Scalar Station Data

For station data, we evaluate model performance based on both visual assessments of tidal and subtidal time series plots and quantitative fitness scores. Here, only a representative sample of stations is given for each variable of interest, illustrating typical results. We will make results for many more stations available online with the release of the calibration document.

The following statistics are reported where appropriate:

- **RMSE:** Root mean square error, not phase-corrected.
- **Lag:** An estimation of lag in minutes between the observed and modeled signal based on cross-correlation analysis, as described in RMA (2005). The phase lag estimated here is used to shift the series for calculation of the remainder of the metrics.
- **Bias$_\varphi$**: The median bias of phase corrected error (modeled - observed)
- **NSE$_\varphi$** : The Nash-Sutcliffe efficiency for the phase-corrected error:
- $NSE\phi(f,r,x) = 1 - (MSE(f,x)/MSE(r,x))$
- where $MSE(f,x) = \dfrac{1}{n}\sum_{i=1}^{n}(f_i - x_i)^2$ is the mean squared error between a forecast or reference

  (f), and an observation (x); r represents the station time-average.
- **R$_\varphi$**: The correlation coefficient (the r in R^2 for the fit of the observations on the phase-corrected model values.

Our main criteria for these metrics were robustness and consistency of approach with other Bay-Delta published calibrations. Following RMA (2005), we first estimate phase error and then correct for phase (by shifting the model output in time) when generating the remaining statistics except for RMSE.

7.4.3 Elevation

7.4.3.1 Monitoring Stations

Continuous observations of elevation are available throughout the Bay-Delta, collected mainly by NOAA, DWR, and USGS. The instruments are precise, but there is considerable uncertainty concerning vertical datum – particularly in the Delta where subsidence is an issue.

Representative time series comparisons results and metrics are shown in Figures 7-12 through 7-14 on the Old River at Bacon Island, Sacramento River at Walnut Grove and I Street. Overall the fit is strong throughout the Bay and Delta. Subtidal fluctuations (changes slower than diurnal tides) are reproduced accurately over a variety of inflows, barometric fluctuation, and tidal energies. The tidal range at the

upstream sites on the Sacramento River and San Joaquin River illustrates a tendency towards under-dampening, with tidal range and phase lead growing with propagation distance.

We have omitted time series results for most of the Bay, although we will include them in our more comprehensive reports. As the tidal results below hint, elevation results in the Bay have small errors.

7.4.3.2 Tidal Phase and Amplitude

A system-wide view of tidal propagation is given in 7-15 and 7-16 , which map the amplitude and phase of the largest tidal constituent M2 (approximately 12.5 hour period) through the Bay-Delta system for both model and observations during April 2010. The amplitudes are in meters, phase is in minutes difference from arrival at the Golden Gate (not degrees).

The model reproduces tidal constituents very well through the Bay. Error is small and has no noticeable structure. Above the confluence, the model is underdamped, with model amplitude larger and phase earlier than observed. The amplitude error is modest mid-Delta, though it reaches 10% upstream on the Sacramento River and south Delta (but not along the Sacramento Ship Channel). Phase lead also begins above the confluence, with typical values of 15-30 minutes mid-Delta and higher values upstream. Despite some error, phase is gradual and regionally self-consistent – with care, the model does not create spurious potential differences between the main channels and side streams, a problem seen sometimes at Turner Cut with DSM2.

Figure 7-12 Stage Results at Old River at Bacon Island

RMSE=0.125 m   Lag=-20 min   Bias$_\phi$=-0.087   NSE$_\phi$=0.860   R$_\phi$=0.983
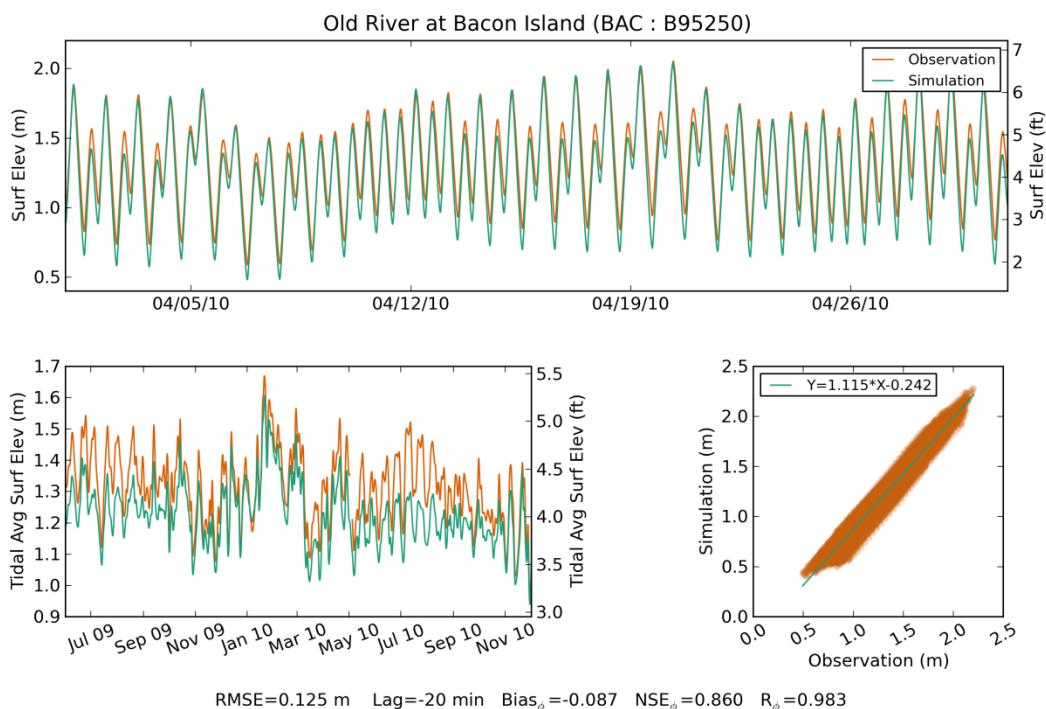
Figure 7-13 **Stage Results for Sacramento River at Walnut Grove**

RMSE=0.094 m   Lag=-25 min   Bias$_\phi$=-0.048   NSE$_\phi$=0.931   R$_\phi$=0.985
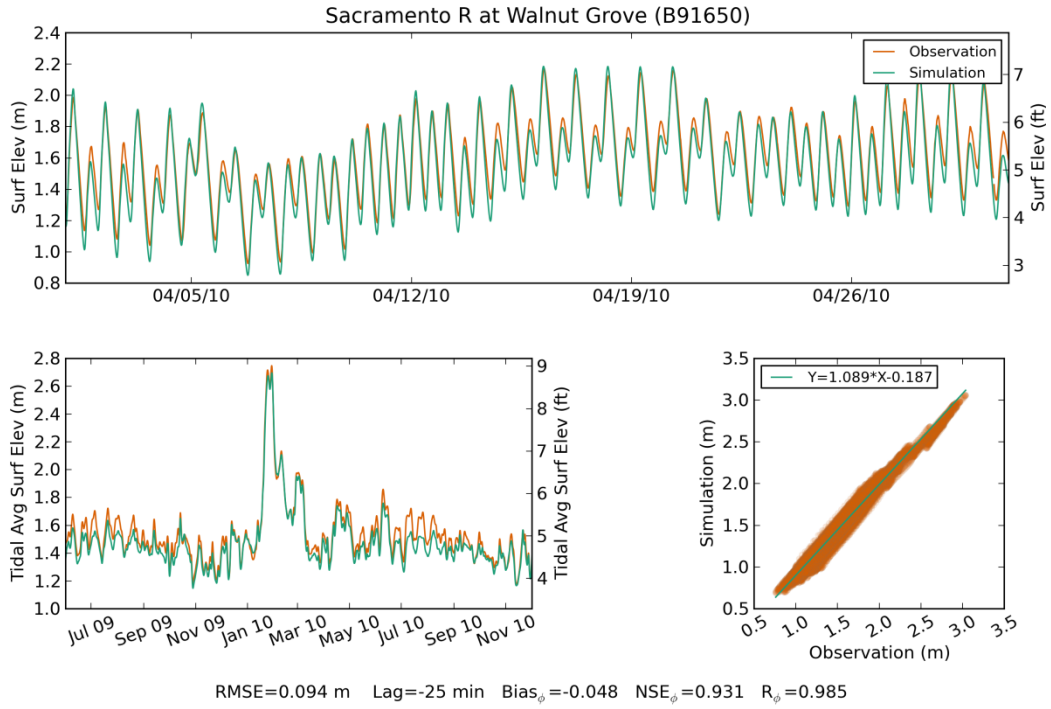
Figure 7-14 **Stage Results for Sacramento River at I Street**

RMSE=0.280 m   Lag=-64 min   Bias$_\phi$=-0.219   NSE$_\phi$=0.843   R$_\phi$=0.982

Figure 7-15 **Map of M2 Amplitude at Bay-Delta Stations, April 2010**

Figure 7-16 **Map of M2 Phase at Bay-Delta Stations, April 2010**

Note: The units are minutes of lag relative to San Francisco, not degrees.

7.4.4 Flow Results

Continuous flow monitoring stations are located throughout the Delta, operated primarily by the USGS and DWR. Flow observations are indirect, using surrogate *index velocity* measurements over part of the width of the river and relating them to total flow by a rating (linear or polynomial regression).

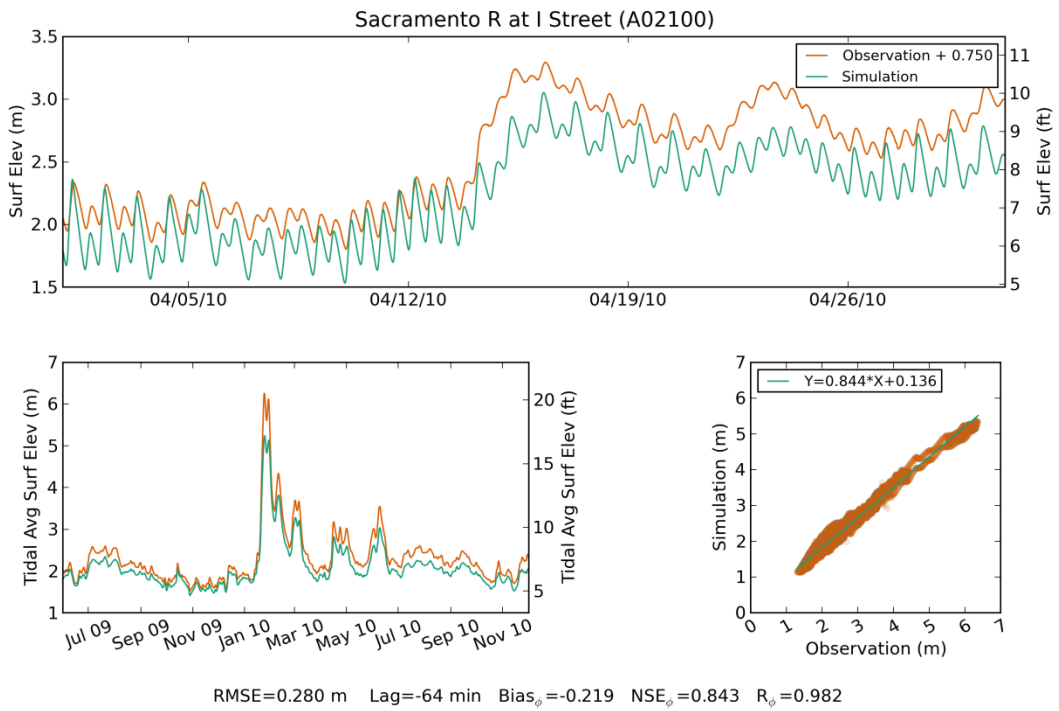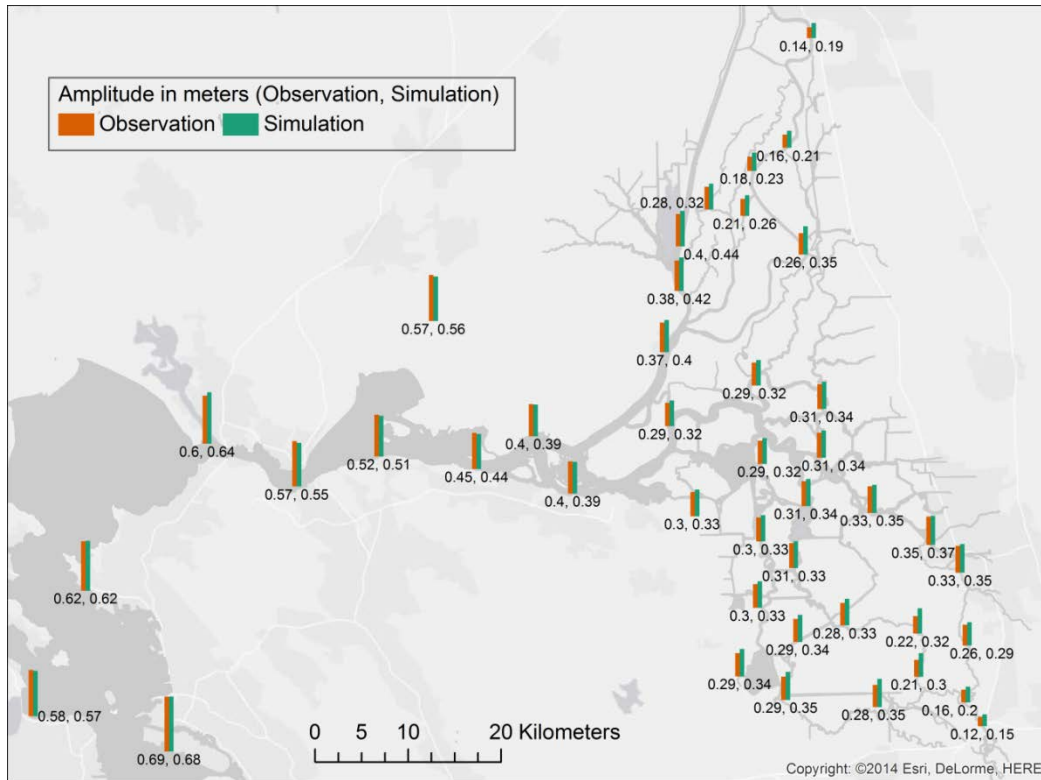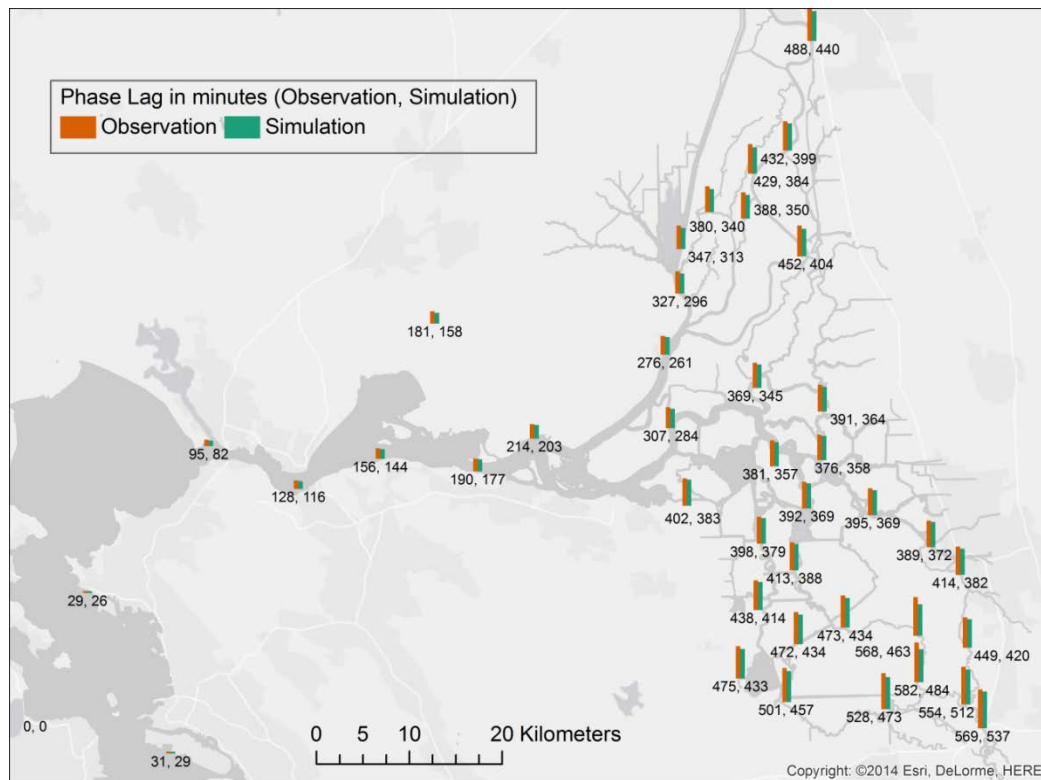Flow results for two sample stations are shown in 7-17 and 7-18. Tidal range for most stations in the Delta is very good. A particularly good result is obtained at Three Mile Slough, a traditional site of difficulty because it is driven by potential differences between the Sacramento and San Joaquin river systems.

Some stations have slightly attenuated or amplified tidal ranges, as in the case of Old River at Quimby Island. The errors in flow tend to be local in character. As with elevation, flow is subject to some phase lead; in this case we believe the lead is caused by a combination of model error and the techniques used to rate flow instruments, a point we will elaborate upon in the near future.

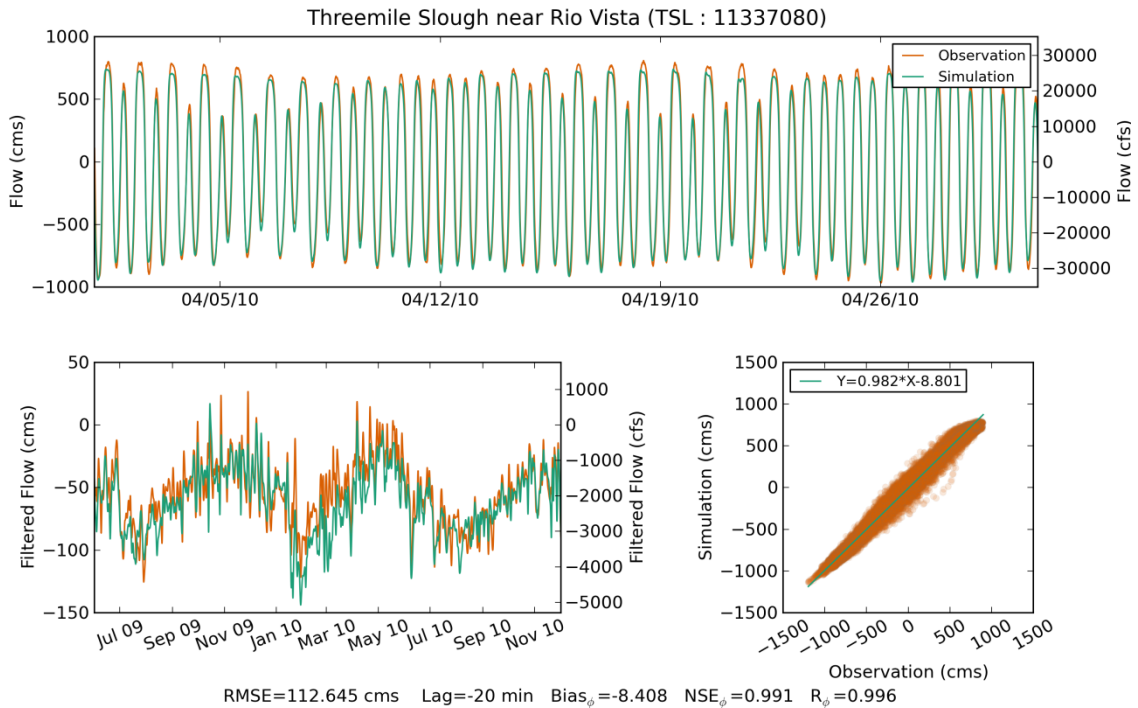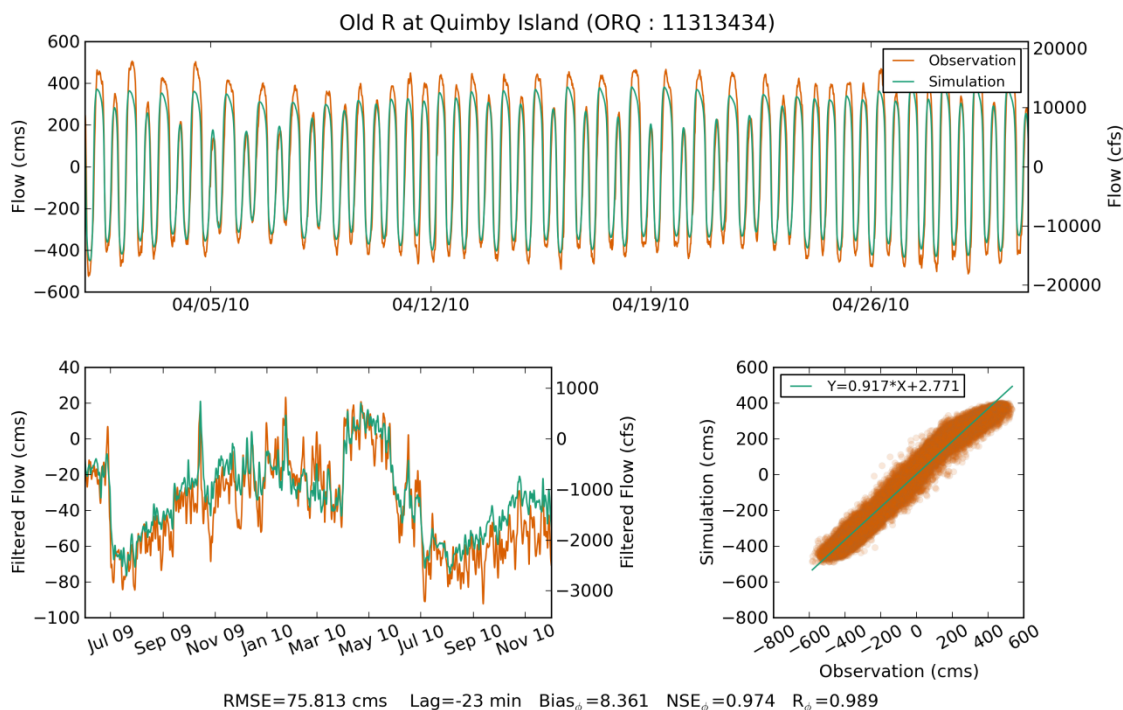**Figure 7-17 Flow Results at Three Mile Slough**

Figure 7-18 Flow Results at Old River at Quimby Island

RMSE=75.813 cms   Lag=-23 min   Bias$_\phi$=8.361   NSE$_\phi$=0.974   R$_\phi$=0.989

7.4.4.1 Net Flow Maps

Net flow maps were used by RMA in to give a synoptic view of mean circulation in the Delta. *Net flow* here refers to residual flows after filtering to eliminate tidal frequencies or spring-neap variation. Residual flow is of some direct interest because it contributes to transport and residence time in the Delta – though the importance of the mean flow contribution to transport is often overestimated. Residual flow is also a diagnostic of how well we can model the details of tidal processes, since residual flows often manifest as small systematic asymmetries in a much larger tidal pattern. Observed data share some of the same challenges when averaged to produce a net flow. Calculations from observations from wide stations such as Rio Vista or Jersey Point carry a particularly strong caveat, and it is not uncommon for small control volumes constructed from a few neighboring stations to exhibit net flow discrepancies of hundreds or even thousands of cubic feet per second.

Figures 7-18 through 7-20 compare modeled and observed mean flow in the north, central, and south Delta for the month of May 15 through June 15, 2010. Barriers are installed late in the period. The general agreement of model with observations is commensurate with the quality of the data, best in the north and south Delta. Rio Vista and Jersey Point are 10-20% off. The null velocity point near Prisoners Point where net flow reverses in orientation seems to be off by a few kilometers but otherwise is correctly captured by the model.

Figure 7-19 North Delta Monthly Residual Flow, May-June 2010
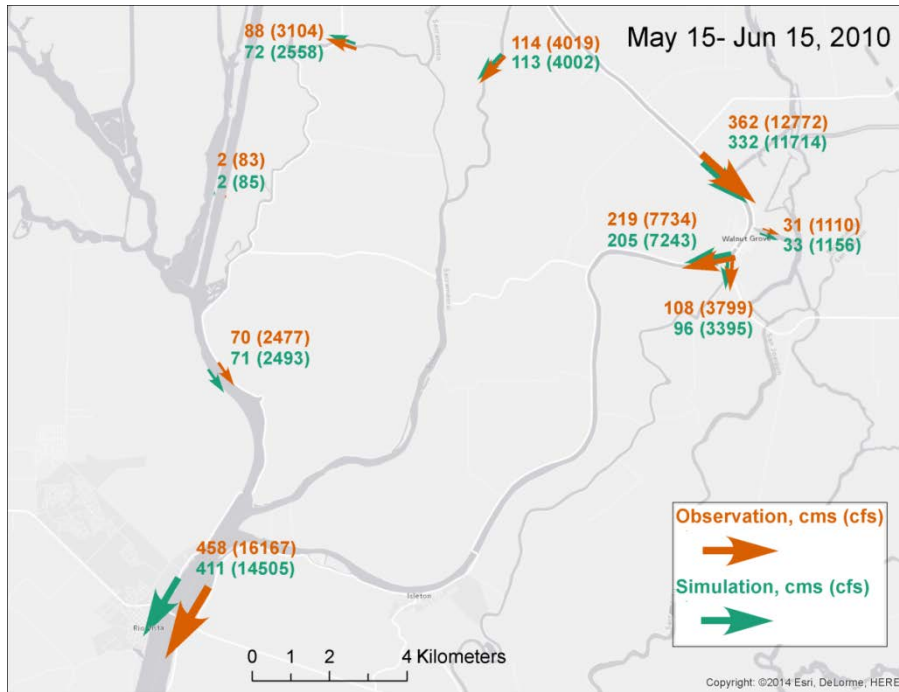
Note: Units are cms (cfs in parentheses)

Figure 7-20 Central Delta Monthly Residual Flow, May-June 2010
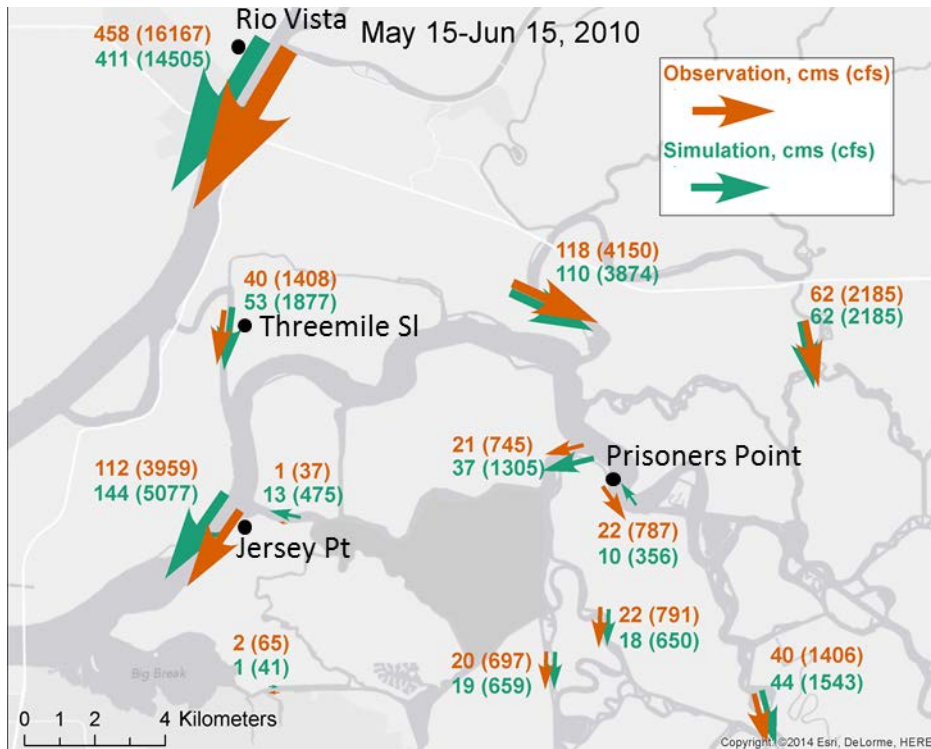
Note: Units are cms (cfs in parentheses)

Figure 7-21 South Delta Monthly Residual Flow, May-June 2010

Note: Units are cms (cfs in parentheses)

7.4.5 Salinity Results

7.4.5.1 Monitoring Stations

Salinity is mostly monitored in the form of electrical conductivity, (specific conductance) or EC, at more than 40 stations in channelized and open areas. Precision of the instruments is good, but observations of conductivity are noisy due to the high variability of salinity itself.

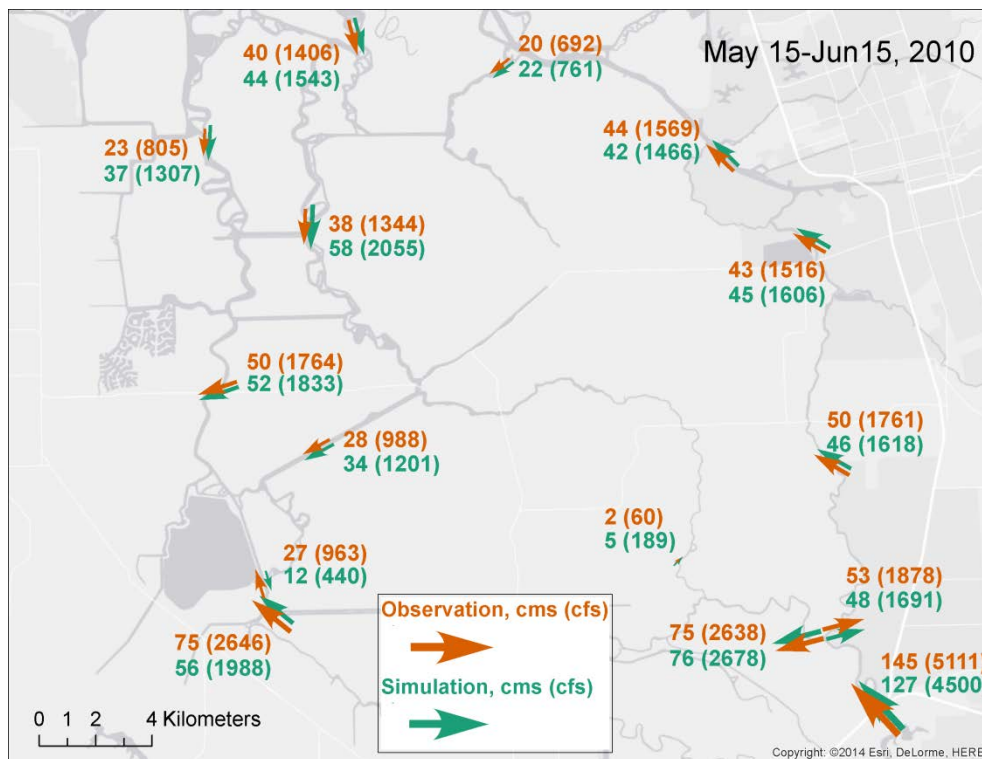Figures 7-21 through 7-23 show salinity results at three sites in the Delta in late October, and for a lengthier period in 2009-2010 at subtidal scale. It is difficult to show all the regimes of interest in a summary document. Our results here focus on salinity at Benicia, Rock Slough, and Clifton Court.

Benicia salinity is similar to that at Martinez, a site of interest to Delta modelers. The advantage of the Benicia location is that it is mid-stream and less affected by local bathymetry. Surface salinity plots at Benicia indicate the model reproduces salinity with a modest bias and RMSE error that is distributed fairly evenly between trend, tidal frequencies, and noise.

Rock Slough and Clifton Court follow seasonal trends well and have errors comparable to other models although the Nash skill metrics for Clifton Court are low. Stations between Antioch and Clifton Court were afflicted by an episode of over-intrusion of ocean salinity in late summer 2010, the recovery from which is evident in the beginning of the tidal-scale plots. This over-intrusion episode was timed almost exactly at the point when DICU becomes a dominant contributor to outflow error. The sensitivity – and

potential over-sensitivity – of the model to sustained periods of low outflows is still an area of active investigation for us.

Figure 7-22 Salinity Results at Benicia (Surface)
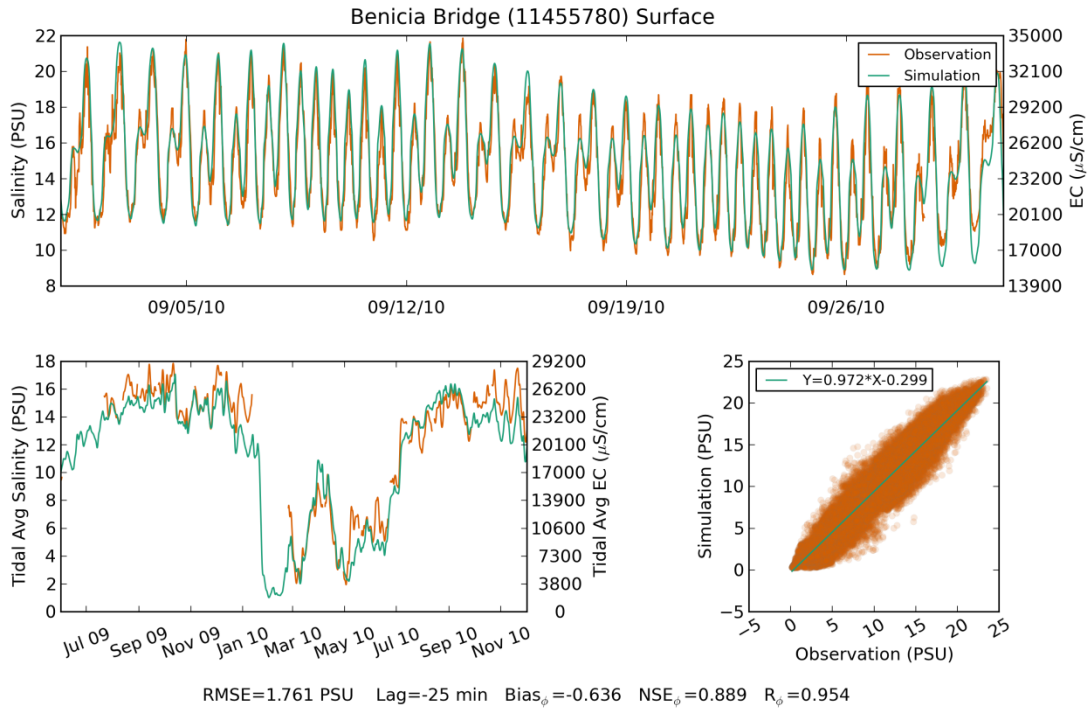

RMSE=1.761 PSU   Lag=-25 min   Bias$_\phi$=-0.636   NSE$_\phi$=0.889   R$_\phi$=0.954

Figure 7-23 Salinity Result at Rock Slough

RMSE=0.078 PSU   Lag=-93 min   Bias$_\phi$=-0.019   NSE$_\phi$=0.263   R$_\phi$=0.770
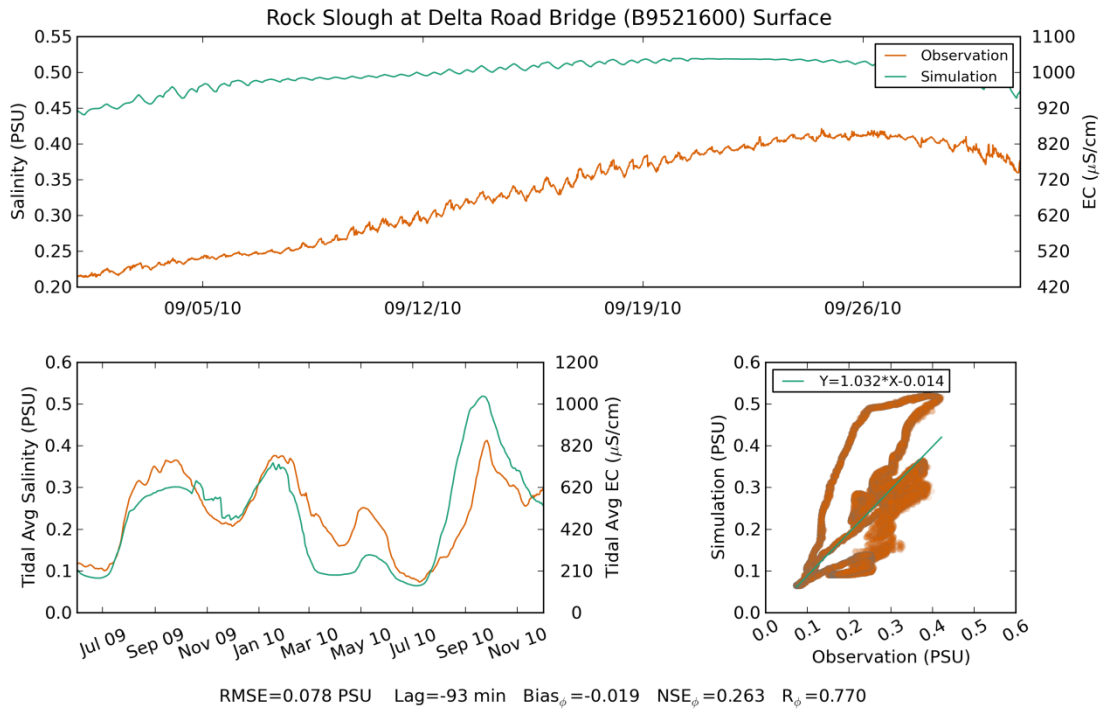
Figure 7-24 Salinity Result at Clifton Court
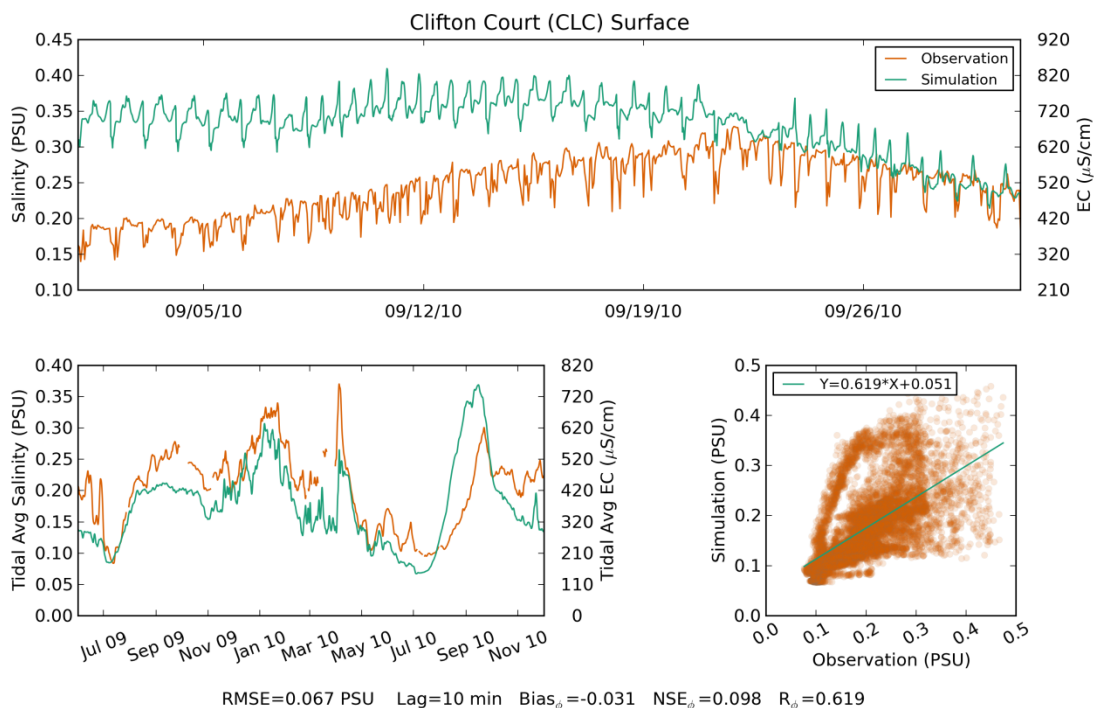
The USGS Polaris cruise (http://sfbay.wr.usgs.gov/access/wqdata) is a longitudinal profile of vertical conductivity-temperature-depth (CTD) casts from the south Bay to Rio Vista. Full or partial cruises are made once per month and have been used to validate the vertical or horizontal distribution of salinity in the Bay part of the domain, particularly for UnTRIM. The sites visited by the Polaris are shown in Figure 7-24. The northern leg of the cruise takes 6 hours; along its course it samples water at both extremes of a tidal excursion and therefore at minimum (typically zero) and maximum values of strain-induced stratification. So in terms of vertical structure the cruise is not a snapshot. There are also differences between observed and modeled bathymetry in the plots and these arise from slight deviations from scheduled locations along the cruise.

Figure 7-25 compares model and observed data between the Golden Gate and Rio Vista for a cruise in April 2010. Agreement is good for most isohalines of interest. Such stratification as exists in the observations (mostly in San Pablo Bay) is well reproduced down to 0.5 psu. At very low salinities (e.g. 0.25 psu or roughly 500 µmhos/cm EC), the sensitivity to outflow is higher.

Figure 7-25 USGS Polaris Cruise Sample Locations

Figure 7-26 USGS Observations and SELFE Model Output for the Northern Leg of an April 13, 2010 Cruise
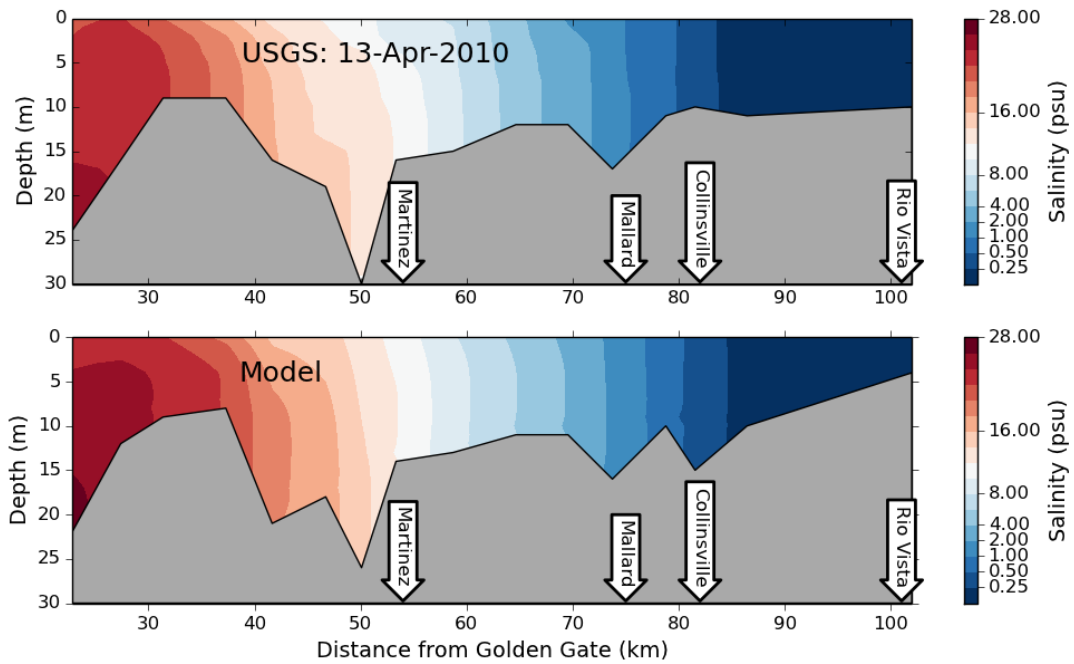
Note: Travel time for this leg is approximately 6 hours

7.4.5.2 Stratification Plots

The Polaris cruises give some indication of vertical structure, particularly persistent stratification in the lower estuary. Unfortunately, the cruises seldom coincide with major stratification events, particularly in the Carquinez Strait region. This can pose a challenge for calibration and validation. Even the stratification events categorized as large based on San Pablo Bay are only 2-3 psu on both sides of the strait, whereas stratification of 6 psu is a common peak in average neap tides and values of 10-12 psu are seen several times annually.

Another approach, fraught with different difficulties, is to look directly at time series of top and bottom salinity at mid-stream stations. SUNTANS stratification was compared to data from the upper and lower sensors on the Richmond and Benicia bridges and the authors were able to reproduce events of up to 8 psu on a short simulation with some success, although the accuracy varied regionally. This variation is to be expected as model forcing and horizontal transport problems cascade into stratification error.

Figure 7-26 through 7-28 shows results at Richmond and Benicia bridges for a 3-4 day stratification episode at neap tide in May 2009. Data have been low-passed with a cosine-Lanczos filter with cutoff frequency of 1/3 hour. The results are early in our calibration period, not from 2010, but seem to be somewhat typical. Provided the plume is located correctly horizontally, the model does a good job picking up very large stratification at Richmond. In contrast, the model under-predicts the largest events at Benicia, although it correctly identifies the transitions between periodic stratification and multi-day episodes.

We are still honing the model to reproduce the pycnocline better at Benicia. The error seems to be confounded by the placement of the sensor – something that we have not yet clarified. Figure 7-26 shows the high sensitivity of model stratification to the depth at which the bottom salinity is sampled – stratification nearly doubles between our original placement (-13.7m NAVD) and locations several meters deeper.

Figure 7-27 **Observed Top and Bottom Salinity and Stratification at Richmond Bridge**

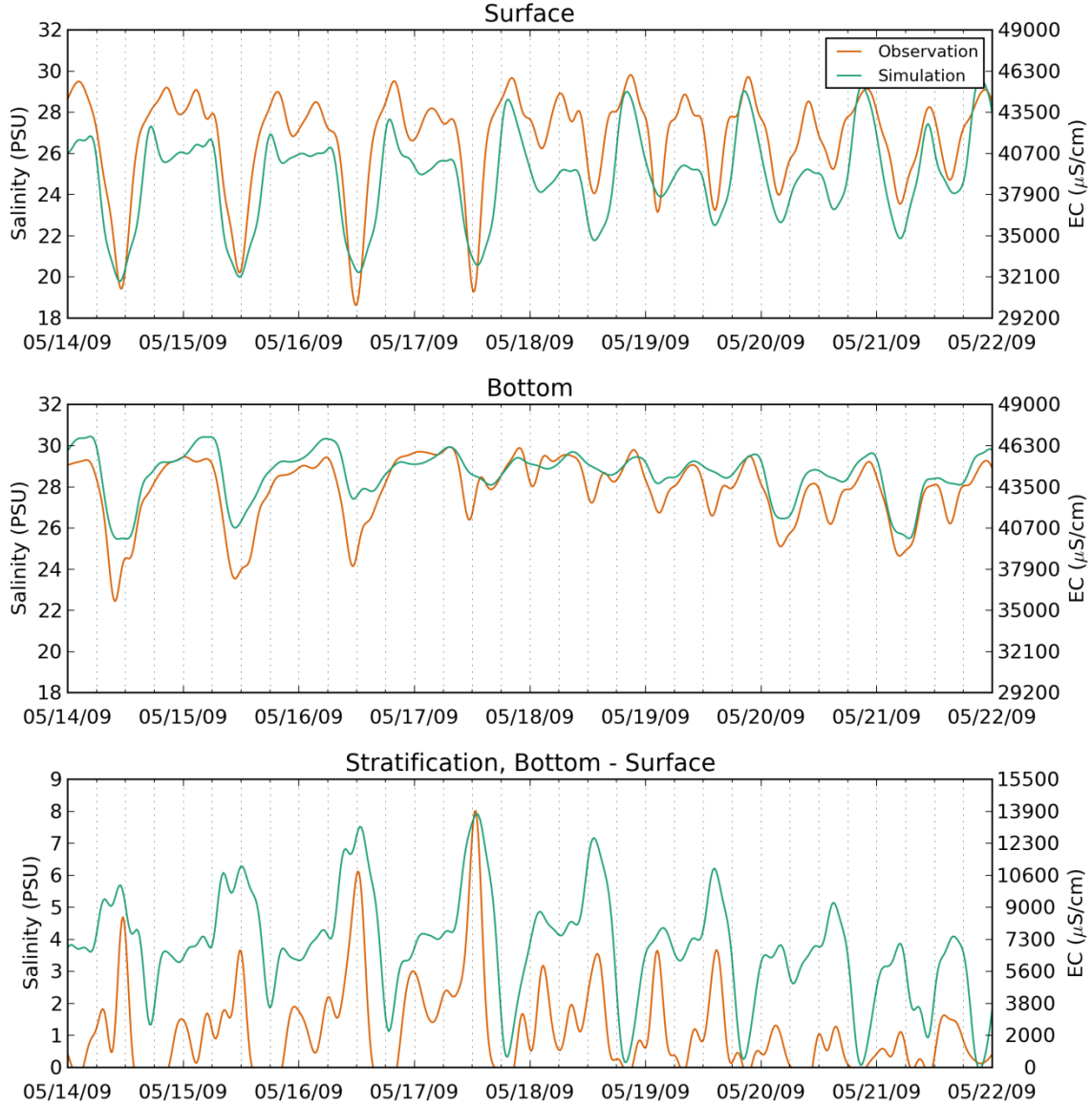Richmond-San Rafael Bridge (375607122264701)

Figure 7-28 Observed Top and Bottom Salinity and Stratification at Benicia Bridge
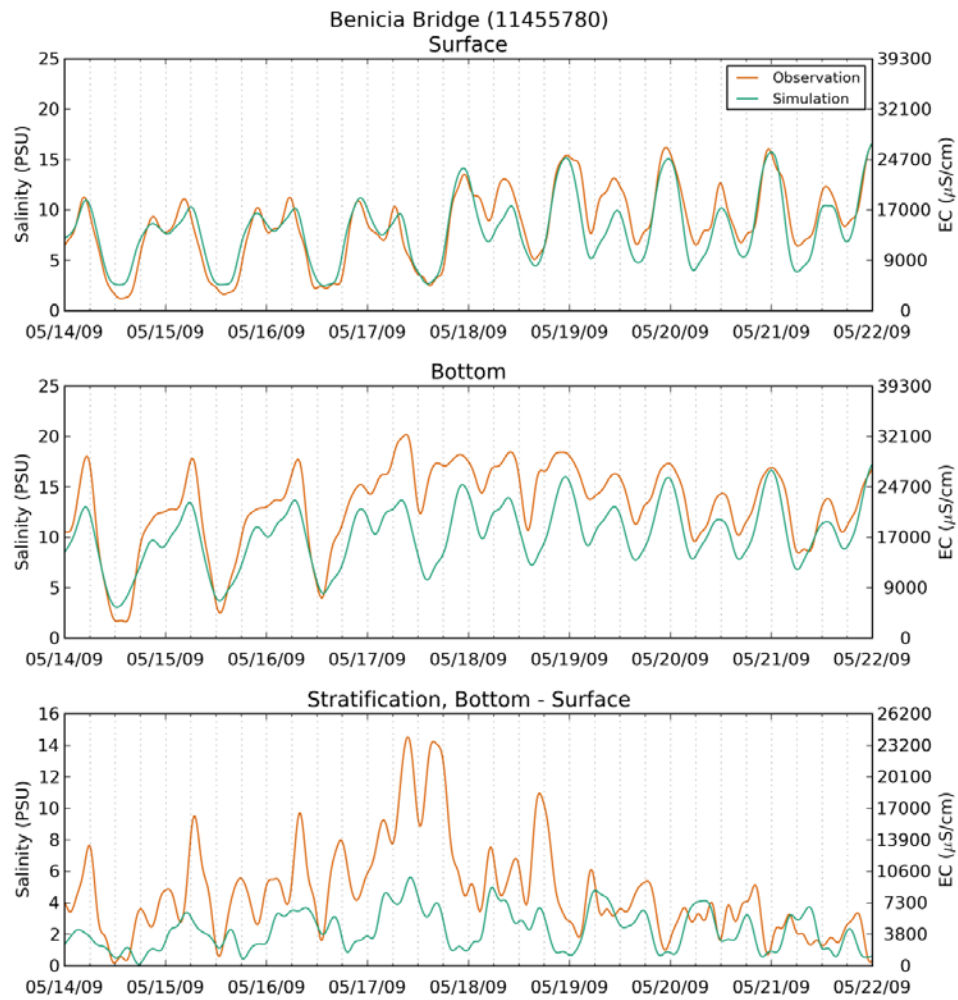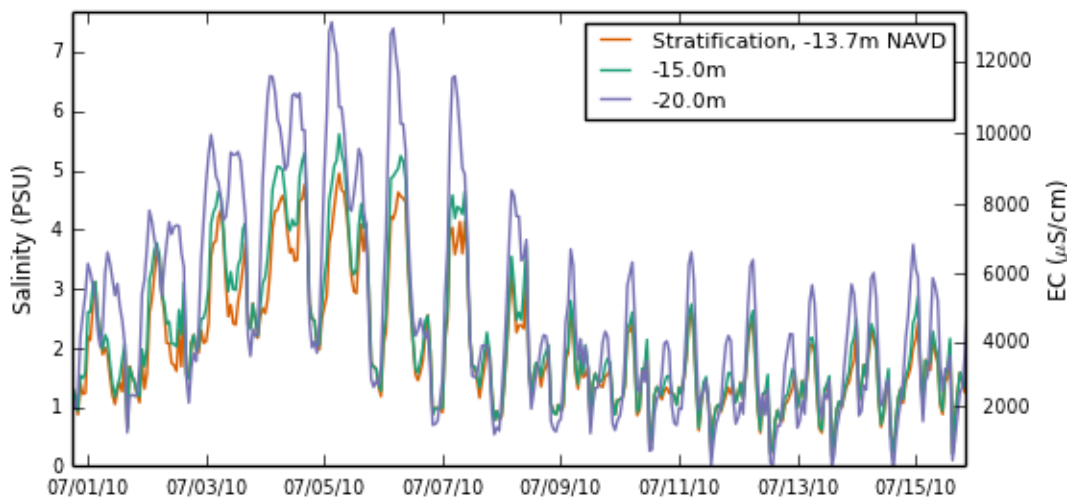

Figure 7-29 Sensitivity of Salinity Stratification to the Placement of the "Bottom" Sensor

Note: The timing of this plot does not coincide with that of Figure 7-27.

7.5 Conclusions

Our results suggest the suitability of the Bay-Delta SELFE model for use in multi-scale, system-wide estuary modeling, and as a far field background model for more focal studies. The model reproduces free surface elevation, flow, and salinity throughout the system with few standout issues. The model reproduces residual circulation in the Delta well. It reproduces vertical structure of salinity in the lower estuary where stratification plays its greatest role in transport; however, it underestimates the largest events at Benicia. Many of our target applications involving salinity, such as climate change analysis and flooded island studies, can be undertaken with the current model with little modification.

A calibration document is expected to be released soon after the publication of this chapter. It will contain additional detail about the formulation of the model and links to more comprehensive time series plots. We will also describe some qualitative features we have used to cross-check the model, including particle tracking evaluation of tidal excursion at Franks Tract and comparison with high frequency HF radar pictures of mean surface currents.

Additional validation materials will be developed in the next year covering the subjects of cross-sectional structure of salinity and velocity; horizontal variation of tidal phase and cross-stream velocity in tidal channels. Upcoming projects near Liberty Island and Yolo Bypass will also give us an opportunity to study the response of the model near breached levees and in overland flow. A temperature calibration is expected in the next year.

Some areas for further improvement are suggested by our results. These include a better or more conclusive understanding of equilibrium response to very low outflow, investigation of the onset of underdampening at the confluence, and improvement of bottom salinity at Benicia during large episodes of gravitational circulation.

Much of our focus in the coming few years will center on usability – things like the model interface, speed, and diversity of platforms. We have managed to double the speed for the Bay-Delta domain since beginning the project and hope to repeat this increase in performance. We have begun compiling the code on Windows with an aim to producing a 2-D model of the Delta.

7.6 References

[1] G. L. Bodhaine. *Measurement of peak discharge at culverts by indirect methods*, Chapter A3. USGS, 1968.

[2] P. R. Carlson and D. S. McCulloch. Aerial observations of suspended sediment plumes in San Francisco Bay and the adjacent Pacific Ocean. *U.S. Geological Survey, Journal of Research*, 2:519 – 526, 1974.

[3] V. Casulli and P. Zanolli. High resolution methods for multidimensional advection-diffusion problems in free-surface hydrodynamics. *Ocean Modelling*, 10(77):137 – 151, 2005.

[4] V. Casulli. A semi-implicit finite difference method for non-hydrostatic, free-surface flows. *Int. J. Numer. Methods Fluids*, 30:425 – 440, 1999.

[5] V. P. Chua and O. B. Fringer. Sensitivity analysis of three-dimensional salinity simulations in north san francisco bay using the unstructured-grid suntans model. *Ocean Modelling*, 39(3 - 4):332 – 350, 2011.

[6] A. Clemmens, T. Strelkoff, and J. Replogle. Calibration of submerged radial gates. *J. Hydraul. Eng.*, 129(9):680 – 687, 2003.

[7] S. Danilov. Ocean modeling on unstructured meshes. *Ocean Modelling*, 69:195 – 210, 2013.

[8] E. P. Dever and S. J. Lentz. Heat and salt balances over the northern California shelf in winter and spring. *Journal of Geophysical Research: Oceans*, 99(C8):16001 – 16017, 1994.

[9] D.S. Dukhovskoy, S. L. Morey, P. J. Martin, J. J. O. Brien, and C. Cooper. Application of a vanishing, quasi-sigma, vertical coordinate for simulation of high-speed, deep currents over the Sigsbee Escarpment in the Gulf of Mexico. *Ocean Modelling*, 28(4):250 – 265, 2009.

[10] R. L. Haney. On the Pressure Gradient Force over Steep Topography in Sigma Coordinate Ocean Models. *J. Phys. Oceanogr.*, 21:610 – 619, 1991.

[11] E. Hills. New flow equations for clifton court gates. Technical report, California Department of Water Resources, State Water Project Division of Operations and Maintenance, 1988.

[12] R. Holleman, O. Fringer, and M. Stacey. Numerical diffusion for flow aligned unstructured grids with application to estuarine modeling. *Int. J. Numer. Methods Fluids*, 72:1117–1145, 2013.

[13] M. P. Hurst and K. W. Bruland. The effects of the San Francisco Bay plume on trace metal and nutrient distributions in the Gulf of the Farallones. *Geochim. Cosmochim. Acta*, 72:395 – 411, 2008.

[14] M. Jung. Revision of Representative Delta Island Return Flow Quality for DSM2 and DICU Model Runs. Consultant Report to DWR MWQI-CR#3, 2000.

[15] M. L. MacWilliams and E. S. Gross. Hydrodynamic Simulation of Circulation and Residence Time in Clifton Court Forebay. *San Francisco Estuary and Watershed Science*, 11(2), 2013.

[16] M. L. MacWilliams, F. G. Salcedo, and E. S. Gross. San Francisco Bay-Delta UnTRIM Model Calibration Report, POD 3-D Particle Tracking Modeling Study. Technical report, Prepared for California Department of Water Resources, 2008.

[17] M. L. MacWilliams, F. G. Salcedo, and E. S. Gross. San Francisco Bay-Delta UnTRIM Model Calibration Report, Sacramento and Stockton Deep Water Ship Channel 3-D Hydrodynamic and Salinity Modeling Study. Technical report, Prepared for US. Army Corps of Engineers, San Francisco District, 2009.

[18] H.F. Matthias. *Measurement of Peak Discharge at With Contractions by Indirect Means*, Chap A4. Number 03-A4 in Techniques of Water-Resource Investigation. USGS, 1967.

[19] N. Mahadevan. *Estimation of Delta Island Diversions and Return Flows.* California Department of Water Resources, Division of Planning and Local Assistance. Sacramento, CA, 1995.

[20] M. Noble. Current patterns over the continental shelf and slope. Technical report, U.S. Geological Survey, 2001.

[21] J. Oliger and A. Sundström. Theoretical and practical aspects of some initial boundary value problems in fluid dynamics. *SIAM J. Appl. Math*, 35(3):419–446, 1978.

[22] P.-O. Persson and G. Strang. A simple mesh generator in matlab. *SIAM Review*, 46:329–345, 2004.

[23] P.-O. Persson. *Mesh Generation for Implicit Geometries*. PhD thesis, MIT, 2005.

[24] D. K. Ralston and M. T. Stacey. Shear and turbulence production across subtidal channels. *Journal of Marine Research*, 64:147 – 171, 2006.

[25] Saul Edward Rantz. Measurement and computation of streamflow: Volume 2, computation of discharge. TechReport 2175, USGS, 1982.

[26] RMA. Flooded islands pre-feasibility study rma delta model calibration report. Technical report, Prepared For: California Department of Water Resources For Submittal To California Bay-Delta Authority, 2005.

[27] C. A. Ruhl, D. H. Schoellhamer, R. P. Stumpf, and C. L. Lindsay. Combined Use of Remote Sensing and Continuous Monitoring to Analyse the Variability of Suspended-Sediment Concentrations in San Francisco Bay, California. *Estuarine, Coastal and Shelf Science*, 53:801 – 812, 2001.

[28] A. F. Shchepetkin and J. C. McWilliams. The regional oceanic modeling system (ROMS): A split-explicit, free-surface, topography-following-coordinate oceanic model. *Ocean Modelling*, 9:347 – 404, 2005.

[29] J. R. Siddorn. An analytical stretching function that combines the best attributes of geopotential and terrain-following vertical coordinates. *Ocean Modelling*, 66:1 – 13, 2013.

[30] Y. Song and D. Haidvogel. A Semi-implicit Ocean Circulation Model Using a Generalized Topography-Following Coordinate System. *J. Comput. Phys.*, 115(1):228 – 244, 1994.

[31] C. A. Stow, J. Jolliff, D. J. McGillicuddy Jr, S. C. Doney, J. I. Allen, M. A. M. Friedrichs, K. A. Rose, and P. Wallhead. Skill Assessment for Coupled Biological/Physical Models of Marine Systems. *Journal of Marine Systems*, 76:4–15, 2009.

[32] B. Suits. Calibrating dsm2-qual dispersion factors to practical salinity. In *Methodology for Flow and Salinity Estimates in the Sacramento-San Joaquin Delta and Suisun Marsh 23rd Annual Progress Report*, 2002.

[33] L. Umlauf and H. Burchard. A generic length-scale equation for geophysical turbulence models. *Journal of Marine Research*, 61:235 – 265, 2003.

[34] J. R. Villemonte. Submerged-weir discharge studies. *Engineering News Record*, pages 54–57, 1947.

[35] T. L. Wahl. Refined Energy Correction for Calibration of Submerged Radial Gates. *Journal of Hydraulic Engineering*, 131(6):457–466, 2005.

[36] R. Wang and E. Ateljevich. A Continuous Surface Elevation Map for Modeling. Technical report, California Department of Water Resources, Bay-Delta Office, Delta Modeling Section, 2012.

[37] C. J. Willmott, S. G. Ackleson, R. E. Davis, J. J. Feddema, K. M. Klink, D. R. Legates, J. O'Donnell, and C. M. Rowe. Statistics for the evaluation and comparison of models. *Journal of Geophysical Research: Oceans*, 90(C5):8995 – 9005, 1985.

[38] C. J. Willmott, S. M. Robeson, and K. Matsuura. A refined index of model performance. *International Journal of Climatology*, 32(13):2088 – 2094, 2012.

[39] C. J. Willmott. Some Comments on the Evaluation of Model Performance. *Bull. Amer. Meteor. Soc.*, 63:1309 – 1313, 1982.

[40] Y. Zhang, A. M. Baptista, and E. P. Myers. A cross-scale model for 3D baroclinic circulation in estuary-plume-shelf systems: I. Formulation and skill assessment. *Continental Shelf Research*, 24(18):2187 – 2214, 2004.

[41] Y. Zhang and A. M. Baptista. SELFE: A semi-implicit Eulerian-Lagrangian finite-element model for cross-scale ocean circulation. *Ocean Modelling*, 21:71–96, 2008.